Modelling lake ice cover under contemporary and future climate conditions

by

Laura C. Brown

A thesis
presented to the University of Waterloo
in fulfillment of the
thesis requirement for the degree of
Doctor of Philosophy
in
Geography

Waterloo, Ontario, Canada, 2012

AUTHOR'S DECLARATION

I hereby declare that I am the sole author of this thesis. This is a true copy of the thesis, including any required final revisions, as accepted by my examiners.

I understand that my thesis may be made electronically available to the public.

Abstract

Lakes comprise a large portion of the surface cover in northern North America, forming an important part of the cryosphere. Further alterations to the present day ice regime could result in major ecosystem changes, such as species shifts and the disappearance of perennial ice cover. Lake ice has been shown to both respond to, and play a role in the local/regional climate. The timing of lake ice phenological events (e.g. break-up/freeze-up) is a useful indicator of climate variability and change. Trends in ice phenology have typically been associated with variations in air temperatures while trends found in ice thickness tend to be associated more with changes in snow cover. The inclusion of lakes and lake ice in climate modelling is an area of increased attention in recent studies and the ability to accurately represent ice cover on lakes will be an important step in the improvement of global circulation models, regional climate models and numerical weather forecasting. This thesis aimed to further our understanding of lake ice and climate interactions, with an emphasis on ice cover modelling. The Canadian Lake Ice Model (CLIMo) was used throughout for lake ice simulations.

To validate and improve the model results, in situ measurements of the ice cover for two seasons in Churchill, MB were obtained using an upward-looking sonar device Shallow Water Ice Profiler (SWIP) installed on the bottom of the lake. The SWIP identified the ice-on/off dates as well as collected ice thickness measurements. In addition, a digital camera was installed on shore to capture images of the ice cover through the seasons and field measurements were obtained of snow depth on the ice, and both the thickness of snow ice (if present) and total ice cover. Altering the amounts of snow cover on the ice surface to represent potential snow redistribution affected simulated freeze-up dates by a maximum of 22 days and break-up dates by a maximum of 12 days, highlighting the importance of accurately representing the snowpack for lake ice modelling. The late season ice thickness tended to be under estimated by the simulations with break-up occurring too early, however, the evolution of the ice cover was simulated to fall between the range of the full snow and no snow scenario, with the thickness being dependent on the amount of snow cover on the ice surface.

CLIMo was then used to simulate lake ice phenology across the North American Arctic from 1961–2100 using two climate scenarios produced by the Canadian Regional Climate Model (CRCM). Results from the 1961–1990 time period were validated using 15 locations across the Canadian Arctic, with both in situ ice cover observations from the Canadian Ice Database as well as additional ice cover simulations using nearby weather station data. Projected changes to the ice cover using the

30-year mean data between 1961–1990 and 2041–2070 suggest a shift in break-up and freeze-up dates for most areas ranging from 10–25 days earlier (break-up) and 0–15 days later (freeze-up). The resulting ice cover durations show mainly a 10–25 day reduction for the shallower lakes (3 and 10 m) and 10–30 day reduction for the deeper lakes (30 m). More extreme reductions of up to 60 days (excluding the loss of perennial ice cover) were shown in the coastal regions compared to the interior continental areas. The mean maximum ice thickness was shown to decrease by 10–60 cm with no snow cover and 5–50 cm with snow cover on the ice. Snow ice was also shown to increase through most of the study area with the exception of the Alaskan coastal areas.

While the most suitable way to undertake wide scale lake ice modeling is to force the models with climate model output or reanalysis data, a variety of different lake morphometric conditions could exist within a given grid cell leading to different durations of ice cover within the grid cell. Both the daily IMS product (4 km) and the MODIS snow product (500 m) were assessed for their utility at determining lake ice phenology at the sub-grid cell level throughout the province of Quebec. Both products were useful for detecting ice-off, however, the MODIS product was advantageous for detecting ice-on, mainly due to the finer resolution and resulting spatial detail of the lake ice. The sub-grid cell variability was typically less than 2%, although it ranged as high as 10% for some grid cells. An indication of whether or not the simulated ice-on/off dates were within the sub-grid cell variability was determined and on average across the entire province, were found to be within the variability 62% of the time for ice-off and 80% of the time for ice-on. Forcing the model with the future climate scenarios from CRCM predicts ice cover durations throughout the region will decrease by up to 50 days from the current 1981-2010 means to the 2041-2070 means, and decrease from 15 to nearly 100 days shorter between the contemporary and 2071-2100 means.

Overall, this work examined the climate-lake-ice interactions under both contemporary and future climate conditions, as well as provided new insight into sub-grid cell variability of lake ice.

Acknowledgements

First and foremost, I would like to thank my advisor, Prof. Claude Duguay for all the opportunities, support and guidance throughout this research. It's been a fabulous four years as part of 'Team Duguay'!

I extend my appreciation to Dr. Chris Derksen (Environment Canada), Dr. Murray MacKay (Environment Canada) and Dr. Yulia Gel (Statistics and Actuarial Science) for serving as my committee members on this thesis. I would also like to thank to Dr. Jia Wang, Dr. Richard Kelly and Dr. Ellsworth LeDrew for being a part of the thesis examining committee. The Natural Sciences and Engineering Research Council of Canada (NSERC), the University of Waterloo and Ontario Graduate Scholarship (OGS) are also gratefully acknowledged for their financial support. Specific acknowledgements for each manuscript are located at the end of each chapter.

Throughout this thesis I have benefited from the friendships and collaborations of Stephen Howell, Kevin Kang and everyone in the UW 'Cryogroup'. I'd also like to thank Dr. Kathy Young and Dr. Ming-ko Woo for their support and encouragement over the years.

Finally, I'd like to thank Robin Thorne and my family for their support during the last four years, especially my parents, who have all helped me enormously to get to this point.

Table of Contents

List of Figures

List of Tables

List of Abbreviations

AO	Arctic Oscillation
AMSR-E	Advanced Microwave Scanning Radiometer for EOS
AWS	Automated Weather Station
CAA	Canadian Arctic Archipelago
CFO	Complete freeze over
CGCM	Canadian Global Climate Model
CID	Canadian Ice Database
CIS	Canadian Ice Service
CLASS	Canadian LAnd Surface Scheme
CLIMo	Canadian Lake Ice model
CRCM	Canadian Regional Climate Model
CORDEX	COordinated Regional climate Downscaling Experiment, regional climate change
CV	Coefficient of variation
ENSO	El Niño/Southern Oscillation
FLake	Freshwater Lake model
GCM	Global circulation models
ICD	Ice cover duration
IMS	Interactive Multisensor Snow and Ice Mapping System
MBE	Mean Bias Error
MD	Mean difference
MMT	Mean maximum ice thickness
MSC	Meteorological Service of Canada
MODIS	Moderate Resolution Imaging Spectrometer
NARR	North American Regional Reanalysis data
NAO	North Atlantic Oscillation
NP	North Pacific index
NWP	Numerical weather prediction model
PDO	Pacific Decadal Oscillation
PNA	Pacific North American pattern
RCM	Regional climate model
SWE	Snow water equivalent
SWIP	Shallow Water Ice Profiler
WCI	Water clear of ice
YD	Year day (or day of the year)

Preface

In addition to general introduction and conclusions, the thesis contains four journal articles that examine the interactions between lake ice and climate, focusing on modelling, supplemented by new technology and remote sensing. The first paper is published in *Progress in Physical Geography* and comprises of a literature review of lake-climate interactions. The second paper is published in *Hydrological Processes* and examines the use of new technology for validating the lake ice model, particularly for thickness. The third paper is published *in The Cryosphere* and presents a comparison of contemporary and future ice cover scenarios for the North American Arctic. The fourth paper is in preparation for submission to *Advances in Meteorology*, special issue: Large-Scale Modeling over Cold Climate Land Regions (planned submission, March 2012) and involves an investigation of the sub-grid cell variability present within a grid cell of forcing data for the lake ice model.

This work was all a result of direct collaboration with Professor Claude Duguay who aided a great deal with the initial proposal of the articles, and provided continuous advice and comments throughout the duration of the study. Assistance with the processing of the sonar data used in Chapter 3 was provided by ASL Environmental and the climate scenario data used in both Chapters 4 and 5 was generated and supplied by Consortium Ouranos (with assistance and advice from Ross Brown, Environment Canada at Ouranos, for the processing of the climate scenario data).

Chapter 1
General Introduction

1.1 Motivation

The majority of the lakes in the world are located in the Northern Hemisphere where snow and ice are prominent during the winter season (Figure 1.1). Within Canada, regions of the northern landscape are dominated by lakes, ranging in size from small tundra ponds to the large Northern (Great Slave Lake and Great Bear Lake) and Laurentian Great Lakes. With such a large spatial coverage, ice regimes of these lakes comprise an important part of the cryosphere.

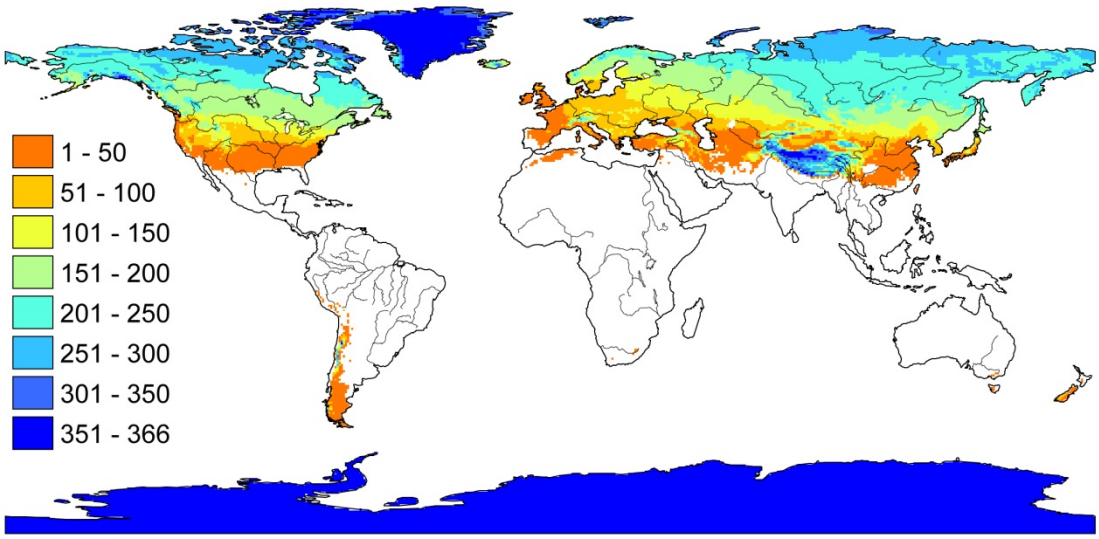

Figure 1.1. Average days of snow on the ground. Modified from: Woo, 2012.

Most lakes in Canada experience some duration of ice cover during the winter season (solid or partial/intermittent) and the presence or absence of ice cover is known to have an effect on both regional climate and weather events (e.g. thermal moderation and lake-effect snow) (Rouse et al., 2008). Future changes to lake ice regimes could have a substantial impact on the role of lakes on energy, water and biogeochemical processes in cold regions as well as socioeconomic impacts on northern transportation (ice roads) and recreation.

Typically, lake ice cover is more persistent and thicker progressing north (Figure 1.2), however this is not always the case as factors such as lake size and unique climate regions can override the general latitudinal pattern. For example, Stanwell-Fletcher Lake, a large lake on Somerset Island, NU (72°N), typical retains a summer ice cover while Lake Hazen, a large lake on Ellesmere Island, NU, (82°N) generally does not, due to the sheltered, warmer climate specific to that area (Woo, 2012). Figure 1.2 illustrates the effects of lake morphometry on ice cover, with more persistent and thicker ice cover on the much smaller Ennadai Lake with respect to Great Slave Lake even though Ennadai Lake is slightly further south.

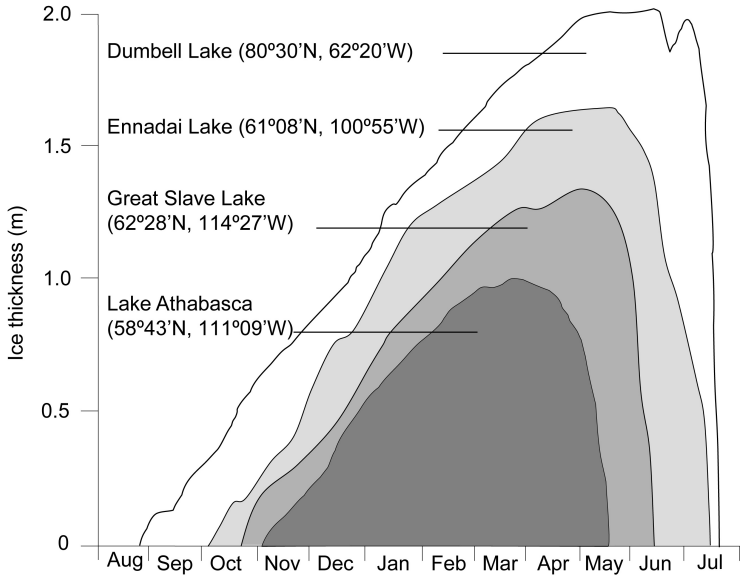

Figure 1.2. Average seasonal change in ice thickness on four lakes (of different sizes) along an approximate south-north transect in Central Canada. Modified from : Woo, 2012.

Lake ice has also been shown to respond to climate variability; particularly changes in air temperature and snow accumulation. Both long-term and short-term trends have been identified in ice phenology records and are typically associated with variations in air temperatures; while trends in ice thickness tend to be associated more with changes in snow cover (Brown and Duguay, 2010).

There has been a noted decline in in situ lake ice observation networks in recent years (e.g. Nagler et al., 2008). This is particularly poignant in Canada with data from only three remaining locations currently available from the Canadian Ice Service (as of 2012) (Figure 1.3). While the in situ network

has virtually disappeared, the Canadian Ice Service has been monitoring the fractional ice cover on 135 large lakes throughout Canada on a weekly basis using visual interpretation of satellite data for several years (Figure 1.3). With the loss of in situ networks, remote sensing and modelling of lake ice becomes increasingly important. Remote sensing products can provide information on ice phenology where no in situ data exists – however, the current products available are not suitable for many of the important lake ice parameters due to their spatial and temporal limitations (Nagler et al., 2008). Daily products that use a combination of different types of data, such as the Interactive Multisensor Snow and Ice Mapping System (IMS, 4 km), could provide the opportunity for automated extraction of daily ice cover extents across the entire northern hemisphere for larger lakes. The use of optical imagery is limited in the northern regions due frequent cloud cover and polar darkness (e.g. MODIS), although microwave data provides the potential for monitoring ice phenology in these regions (e.g. Howell et al., 2009).

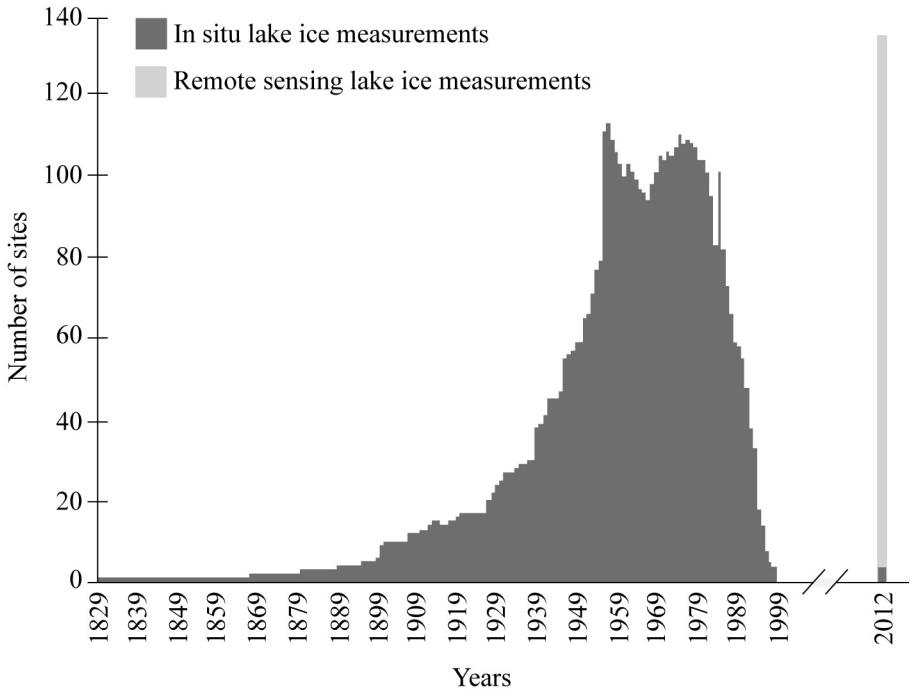

Figure 1.3. Evolution of the lake ice observation sites from the Canadian Ice Database (1829 – 1999). For comparison, the number of sites monitored in situ and by remote sensing are added for 2012. Modified from: Duguay et al. (2006).

Lake ice models are an ideal tool for examining ice cover regimes as they can provide valuable information, such as the timing of break-up/freeze-up, ice thickness and composition. While remote sensing can assist with the validation of modelled ice phenology where no in situ data is available, ice thickness is not yet easily obtained by satellite. Progress has been made in this area using passive microwave data to extract ice thickness on large lakes (Kang et al., 2010), however, lakes smaller than the large passive microwave footprints still present challenges for determining ice thickness. The incorporation of field-based technology, such as upward looking sonar, provides an excellent opportunity for model validation by collecting a continuous data set of the evolving ice cover on a lake.

The most suitable way to undertake wide scale lake ice modelling is to drive the models with either climate model output, or reanalysis data as meteorological stations are typically confined to relatively accessible areas of the mainland or coastal areas in the Arctic islands. While previous work has investigated modeling ice phenology using grid based climate data for hypothetical lakes of varying depths (e.g. Brown and Duguay, 2011; Dibike et al., 2011), one-dimensional models produce the same ice phenology for the entire grid cell of forcing data for lakes of a given depth. However, in reality, a variety of different lake morphometric conditions could exist within a given grid cell, leading to different ice on/off dates occurring within the grid cell. The incorporation of remote sensing data into modelling can contribute to advancements in the predictive abilities of lake ice models by providing possible improvements to input parameters and improving the ability to incorporate lakes at the sub grid cell scale.

1.2 Objectives

The overall goal of this research is to further the understanding of lake ice and climate interactions and expand the current lake ice modelling practices in order to provide ice phenology data in areas where no observations are recorded. Specifically, the three main objectives are to: 1) use a one-dimensional thermodynamic lake ice model in combination with new technology (upward looking sonar and a field-grade digital camera) to both examine how well the model performs in terms of ice thickness and also to assess the use of the new technology as an asset for supplementing the sparse in situ monitoring network across Canada; 2) extend the one-dimensional model to continental-scale modelling through the use of climate model output as forcing data, and to investigate the potential

change to the ice cover under future climate conditions; and 3) determine how well the one-dimensional model is able to represent the observed variability in lake ice-on/off dates present within a grid cell of forcing data as a result of various lake morphometry present in each grid cell.

1.3 Thesis Structure

This manuscript-based thesis consists of 6 chapters, where each chapter reflects the results of the specific objectives described in the previous section. This chapter outlines the rationale and objectives, while Chapter 2 presents a review of the literature pertaining to lake ice and climate interactions. This chapter has been published in the peer-reviewed journal *Progress in Physical Geography*:

> Brown, L.C., and Duguay, C.R. The response and role of ice cover in lake-climate interactions. *Progress in Physical Geography*, 34(5), 671-704, 2010. DOI: 10.1177/0309133310375653

Chapter three addresses the first objective and examines the use of a Shallow Water Ice Profiler (SWIP) to measure ice thickness and assess the performance of the lake ice model CLIMo (Canadian Lake Ice Model), in the Churchill region of Manitoba, with respect to ice on/off dates and ice thickness. This chapter has been published in the peer-reviewed journal *Hydrological Processes*:

> Brown, L.C. and Duguay, C.R. A comparison of simulated and measured lake ice thickness using a Shallow Water Ice Profiler. *Hydrological Processes* 25 (19), 2932-2941, 2011. DOI: 10.1002/hyp.8087

Chapter four addresses the second objective and applies the lake ice model CLIMo to the entire North American Arctic, forced with climate model output from the Canadian Regional Climate Model (CRMC), to examine lake ice phenology, thickness and composition under both contemporary and future climate conditions. This paper has been published in the peer-reviewed journal *The Cryosphere*:

> Brown, L.C. and Duguay, C.R. The fate of lake in in the North American Arctic, *The Cryosphere*, 5, 869-892, 2011, www.the-cryosphere.net/5/869/2011/, doi:10.5194/tc-5-869-2011

Selections of this work have also contributed towards a summary paper of change in the Canadian Cryosphere:

> C. Derksen, S.L. Smith, M. Sharp, S. Howell, L. Brown, C. Fletcher, D. Mueller, L. Copland, Y. Gauthier, M. Bernier, R. Brown, C.R. Burn, C. Duguay, A. Langlois, A. Walker, A.G. Lewkowicz, J. Bourgeois. Variability and Change in the Canadian Cryosphere. *Climatic Change* – in review.

Chapter five furthers the concept of using grid based climate data to force the lake ice model CLIMo, and examines the sub grid cell variability in ice phenology, addressing the third objective. This chapter also explores the use of daily remote sensing products for ice phenology monitoring. This paper is in preparation for submission to a special issue of *Advances in Meteorology* involving large scale modelling of cold climate land regions:

> Brown, L.C. and Duguay, C.R. Modelling lake ice phenology with sub-grid cell variability. *Advances in Meteorology*, submitted March 2012.

Chapter 6 presents a summary of this research and suggests further research directions. As Chapters 2, 3 and 4 have been published and are subject to copyright, the manuscripts are presented in their entirety, which results in some duplication between chapters in terms of equations and methodologies.

Chapter 2
The response and role of ice cover in lake-climate interactions

2.1 Introduction

Lakes cover approximately 2% of the Earth's land surface, with the majority of lakes located in the Northern Hemisphere. Many lakes are located in the northern boreal and tundra areas with an estimated coverage in the Arctic and Subarctic regions of North America reaching up to 15 - 40% depending on the location (Duguay et al., 2003). With such a large spatial coverage, ice regimes of these lakes comprise an important part of the cryosphere.

Understanding the processes and interactions of lake ice with climate is essential for climate modelling and weather forecasting, as many models either to date do not incorporate lakes into the landscape, or can only resolve large lakes. The presence (or absence) of ice cover on lakes during the winter months is also known to have an effect on both regional climate and weather events (e.g. thermal moderation and lake-effect snow) (Rouse et al., 2008b). Climate warming at northern latitudes for the 21st century, as projected by global climate models, will likely have drastic impacts on lake ice phenology, and with the potential of further increasing the role of lakes in the regional energy and water balance

This paper reviews the current state of knowledge pertaining to the interactions of lake ice and climate. Part 2 presents a review of the dominant controls and processes of lake ice cover; part 3 examines the response of lake ice phenology and thickness to climate in the northern hemisphere; part 4 explores the role of lake ice in weather and climate; and part 5 draws conclusions and discusses future directions.

2.2 The formation and decay of ice cover

Lake ice formation, growth and decay are the result of an energy surplus or deficit in the energy balance of the ice cover. The first law of thermodynamics governs the interactions occurring between atmosphere-water-ice interfaces, whereby the conservation of energy is accounted for by the transfer of energy from one form to another. The surplus or deficit in energy available for ice growth/decay is determined by heat exchange with the atmosphere, heat stored in the water and heat input from inflows of water (Williams, 1965). The exchanges with the atmosphere are mainly determined by air

temperature, precipitation, wind and radiation, while heat storage in the lake is determined additionally by morphometry (depth, area, volume).

Along with ice phenology, the thickness and composition of an ice cover can also be affected by changes in the climatic and non-climatic controls that determine ice cover formation/decay. However, the role and importance of these controls on the ice cover vary by stages of the ice – the following stages will be used to describe the ice-climate interactions: freeze-up, ice growth and break-up.

2.2.1 Climatic controls

The relationship between air temperature and ice phenology is well established (e.g. Williams, 1965; Bilello, 1980; Paleki and Barry, 1986; Stewart and Magnuson, 2009) whereby the preceding air temperature, for weeks to months depending on the location, can be used as a predictor of freeze/break-up, although recent studies have suggested this relationship with temperature is non-linear with latitude (Weyhenmeyer et al., 2004, 2010). For the Northern Hemisphere from 1846 to 1995, Magnuson et al. (2000) estimated that an increase in air temperatures of 1.2°C would have been necessary to result in the shift of freeze-up and break-up dates that they identified (5.7 days/100 years later and 6.3 day/100 years earlier respectively). Relationships such as this have been developed for various regions and specific lakes, some recent examples being Lake Baikal, Russia (Kouraev et al., 2007), Polish Lowland lakes (Marszelewski and Skowron, 2006) and relationships between trends in ice covers and 0°C isotherms for Canada (Duguay et al., 2006).

In the northern hemisphere, freeze-up in northern areas (e.g. Lake Kallavesi, Finland) was reported by Magnuson et al. (2000) to reflect the climate conditions around October and November, while freeze-up in areas further south (e.g. Grand Traverse Bay, Lake Michigan) reflect the climate from January to February. Break-up dates have been shown to be affected by the February-March climate for Lake Mendota (Wisconsin) (Magnuson et al. 2000) and April climate for Alaskan ponds (Jeffries and Morris, 2007).

Duguay et al. (2006) showed a strong relationship between ice phenology and the arrival date of the spring and fall 0°C isotherm, with freeze-up/break-up lagging the 0°C isotherm date by a few days to about 1 month. They found that trends in air temperature (both winter and spring) were generally consistent with the break-up trends identified for most of Canada (except for north eastern Canada and Newfoundland). Freeze-up was shown to be highly variable and hence difficult to establish a clear trend, however, the few sites examined that showed statistically significant freeze-up

trends, were located in areas of Canada where trends in the fall isotherm generally followed the same direction (positive or negative).

Snow accumulation can affect the growth and thaw rates of the ice cover by adding insulation, influence the composition of the ice by promoting snow ice development, and hence influence the thickness of the ice cover. Snowcover on a lake ice surface is affected by both wind redistribution and snowpack metamorphism (Adams, 1976a). The steep temperature gradient found in snowcover on lake ice is mainly responsible for the metamorphism that takes place at the bottom of the snowpack, where large grains with lower densities develop, increasing the insulative properties of the snowpack (Adams, 1976a). Jensen et al. (2007) found that break-up for lakes in the Great Lakes region was best predicted by trends in snow days using regression models based on water body characteristic and meteorological variables, similar to Duguay et al. (2003) who showed through modelling that much of the variability in ice thickness and break-up dates were driven by snowfall.

Another climatic variable that affects ice phenology is wind, affecting both freeze-up and break-up (Liston and Hall, 1995; Duguay et al., 2006). During freeze-up wind speed can break the skim ice that first forms, preventing a solid ice cover from forming. When the ice cover does form, wind can promote the growth of ice by increasing the 'freezing exposure' of the surface, effectively cooling the ice surface further (Adams, 1976a). During break-up, the heat gained from the atmosphere is usually the dominant factor, however, the mechanical action of wind can be more important in some cases than heat gained by the atmosphere (Williams, 1965).

The seasonal changes in solar radiation are the main influence for the overall energy available to form/decay lake ice cover. The seasonal timing of ice phenology events will depend on the latitudinal location of the lake as the amount of shortwave radiation received at the surface varies by latitude.

2.2.2 Non-climatic controls

Lake morphometry is also a determinant of ice cover as this affects the wind fetch, water circulation and temperature as well as heat storage (Jeffries and Morris, 2007). The most important morphologic aspect of a lake is the depth (Korhonen, 2006), since this will determine the amount of heat storage in the water and hence the time needed for the lake to cool and ultimately freeze. Lake morphometry, while an important factor for freeze-up, was found to be less important for predicting break-up when compared to air temperature, latitude and elevation (Williams and Stefan, 2006), but shown to be an important determinant in break-up dates for shallow lakes at high latitudes (Duguay et al. 2003) and

to have a slightly stronger influence on freeze-up than break-up for high latitude ponds (Jeffries and Morris, 2007). Lake elevation has also been shown to affect ice phenology, generally with higher elevation lakes having longer ice-cover seasons (see Livingstone et al., 2009)

In addition to the morphometry and elevation, inflow from streams or land runoff can also affect the formation and decay of ice cover, adding heat inputs and/or creating currents within the lake, affecting the phenology (Williams, 1965). MODIS satellite imagery over Great Slave Lake, Northwest Territories, Canada from 2004-2006 (Figure 2.1) shows a crack forming in the ice cover during break-up in the vicinity of the Slave River inflow, where the water becomes clear of ice first (Howell et al., 2009).

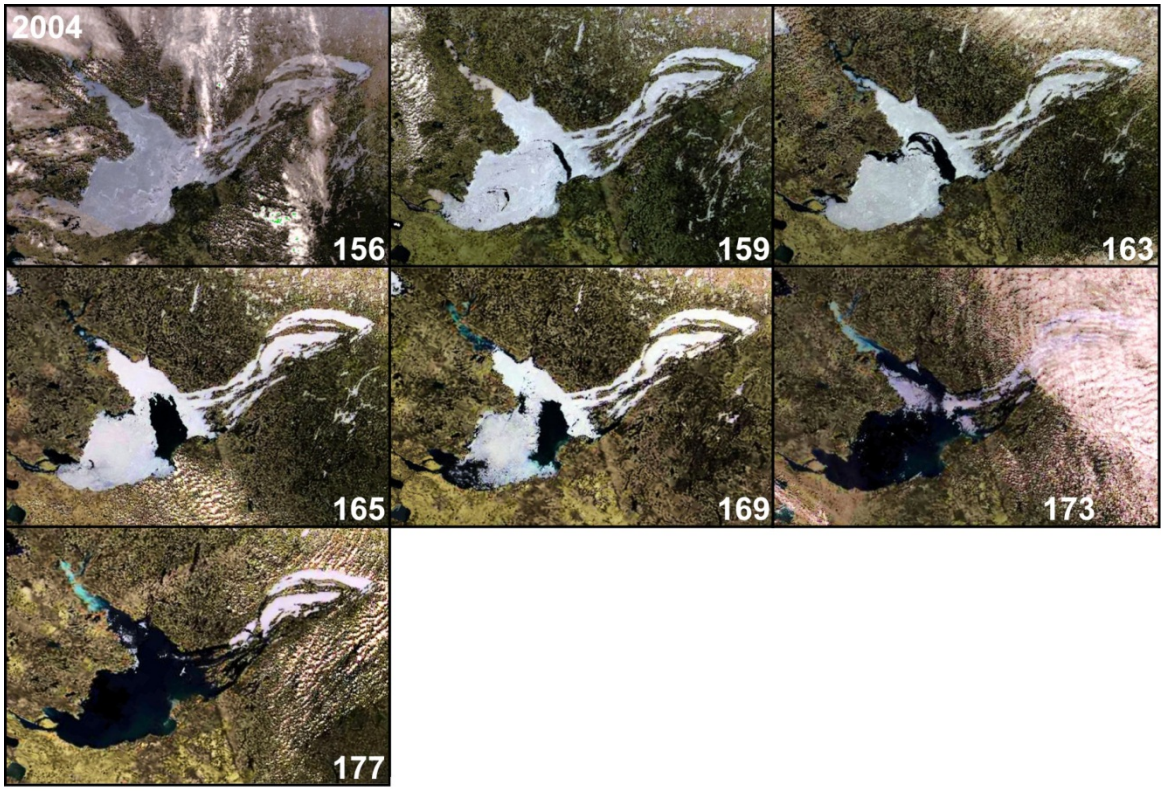

Figure 2.1. MODIS imagery from 2004 showing the break-up of Great Slave Lake (Day of year in lower right of each frame), with a crack and initial melt forming near the Slave River inflow. Source: Howell et al. (2009).

2.2.3 Freeze-up

The dominant climatic controls on lake ice freeze-up are the summer and fall temperatures and the amount of radiation absorbed from heating during the ice-free months (with the amount of heat

storage being affected primarily by latitude and lake depth/volume). With the ice cover absent from the lake during the summer season, turbulent fluxes increase and heat storage in the lake takes place, with the amount of storage depending on the size/depth of the lake and the strength of the influencing climatic factors. Rouse et al. (2000) provide a physical example of how anomalous climatic conditions affect freeze-up on Great Slave Lake (Northwest Territories, Canada). During 1998, an abnormally strong El Niño event occurred with average air temperature in Yellowknife reaching 4°C higher than the 30 year mean. The previous winter and early spring were warm, resulting in an early ice break–up and the very warm summer and fall conditions resulted in delayed ice freeze-up until January 9, 1999. During this extended ice-free season evaporation rates from the lake reached nearly those of the Laurentian Great Lakes, Southern Ontario/North Eastern United States.

As heat is lost at the surface the cooler denser water sinks to the lower portion of the lake with warmer water surfacing in its place. Fresh-water reaches its maximum density at 4°C and further cooling reduces convective overturning allowing ice to form on the surface. During freeze-up, wind can break the skim ice that first forms delaying a solid ice cover from forming. This process can happen several times until solid ice cover forms. The formation of the ice crystals, and the differences resulting from the different types and orientations, are detailed in Jeffries et al. (2005b).

The relatively clear ice that typically forms first is known as black ice, or congelation ice. When cracks form in the ice cover, whether due to weight or temperature fluctuations, the surface and overlying snow will be flooded forming a bubble-filled slush layer which then freezes, forming snow ice (Adams, 1976a; Bengtsson, 1986). Snow ice can also be formed by water percolating through the snow to the ice surface (liquid precipitation, or mid-season melt); or from snow occurring during initial freeze-up. Formation of ice tends to be non-uniform across lakes, with shallow enclosed areas usually freezing first, and freeze-up then progressing to the main body of the lake (e.g. Ashton, 1986; Bengtsson, 1986; Howell et al., 2009). Black ice tends to be found more extensively in the central parts of lakes, with snow ice forming more commonly around the shore lines due to wind drifting of snow (Bengtsson, 1986). The spatial pattern of snow ice development compared to black ice tends to be related to the persistent snow distribution (Adams and Roulet, 1980).

2.2.4 Ice Growth

During the ice growth season, the dominant factors that affect lake ice are temperature and precipitation. The ice continues to thicken as the lake continues to lose heat through the upper ice surface due to the gradient from the relatively warmer water below and the colder air above (Adams,

1976a). Adams (1976b) outlines how the occurrence of snowfall can advance the timing of freeze-up, and affect the form of the first ice present on the lake. However, once the ice has formed, the snow cover then slows the growth of ice below due to the insulating properties as a result of the lower thermal conductivity (thermal conductivity of snow, 0.08 - 0.54 $Wm^{-2}K^{-1}$ versus 2.24 $Wm^{-2}K^{-1}$ for ice, (Sturm et al., 1997)) and can result in changes to the composition of the ice by promoting snow ice development (Adams, 1976a).

The growth of ice can also be affected by the presence of clouds (Maykut and Untersteiner, 1971). With little to no turbulent fluxes, and limited solar radiation (particularly in high latitude area), longwave radiation plays an important role in the growth/melt of ice cover in the winter. Clouds can both reflect solar energy away from the ice (cooling effect) and trap emitted longwave radiation (warming effect), with their overall effect determined by whichever process is dominant (Wang and Key, 2005). In the high latitudes when polar darkness occurs, the energy balance for ice is controlled by the longwave fluxes, where in the absence of clouds increasing longwave losses and increasing ice growth result (and vice versa)(Curry et al., 1993).

2.2.5 Break-up

Ice decay and break-up is controlled by the heat gain from the atmosphere, the snow and ice conditions, as discussed in the previous section, wind and currents, and inputs of warmer water from inflowing rivers or runoff (Williams, 1965). Ice decay can take place at the surface, bottom and lateral edges of the ice pack due to internal melting and mechanical disintegration (Figure 2. 2) (Woo and Heron, 1989). The internal crystal structure of the ice crystals changes during melt and is then easily broken by radiative or mechanical processes (Ashton, 1986). The albedo of the snowcover on the ice (if present) and the underlying ice when it becomes exposed, determines the amount of solar radiation absorbed and available for melt as the radiative inputs increase during the melt season. The presence of snow ice tends to delay break-up due to the higher albedo compared to black ice (Michel et al., 1986).

Variations in albedo over the season can result from changes both at the ice surface and internally. Internal melt in ice cover affects the albedo through changes in density and the hydrostatic water level. Heron and Woo (1994) found that ice albedo peaked with minimum ice density and lowest hydrostatic water levels, and decreased along with the porosity of the ice cover. The orientation of the c-axis of the ice crystals also affects the albedo of the ice (Knight, 1962, Heron and Woo, 1994). For ice cover on a High Arctic lake, a decrease in albedo from 0.45 to 0.2 occurred after the overlying

layers of vertically orientated c-axis ice crystals had melted, revealing darker, denser horizontally oriented c-axis crystals below, where internal melting had not yet taken place (Heron and Woo, 1994). Albedo peaks when fresh snow cover is present on the lake ice (typical ranges 0.7 - 0.9), decreases as the presence of water increases during the melt season (e.g. melting snow, ponding water) (>0.6 - <0.25) and decreases further to the end of the season (<0.1 - 0.2 range) before ice is completely melted (Heron and Woo, 1994; Petrov et al., 2005; Rouse, et al., 2008, Howell et al., 2009, Jakkila et al., 2009).

The break-up process of lake ice with respect to different types of ice (snow ice, black ice) is detailed in Jeffries et al. (2005b). As temperatures increase and the albedo drops due to increasing water content, the absorption of solar radiation then increases adding additional heat inputs and increasing the melt rate of the ice cover. This process is known as the classic ice-albedo feedback originally recognized by Croll (1875). The solar radiation penetration through the ice can result in heating the water below the ice cover contributing both to the melt at the underside of the ice as well as convective mixing in the lake (e.g. Jakkila et al. (2009) found water temperatures of 3°C below the ice cover before break-up).

Ice break-up has been found to be more dependent on air temperature than freeze-up (e.g. Jeffries and Morris, 2007). For example, break-up dates for Alaskan ponds were most strongly determined by the April air temperatures, with a ±1°C change in air temperature resulting in a ±1.86 day change in break-up dates (Jeffries and Morris, 2007). The heat gained from the atmosphere is usually the dominant factor in ice break-up, however, the mechanical action of wind can be more important in some cases than heat gained by the atmosphere (Williams, 1965). Additionally, inflow from streams or runoff can affect break up as discussed previously.

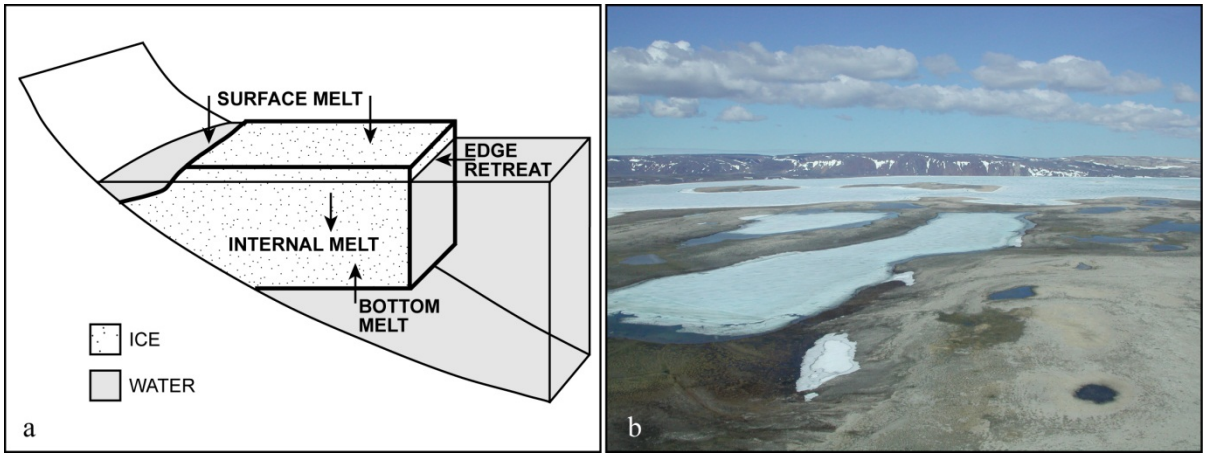

Figure 2.2. a) Ice melt components. Modified from: Woo and Heron (1989) b) Ice conditions on Somerset Island, Nunavut (July 11, 2003), showing ponds ice free, while larger lakes remain partially ice covered. Melt visible around edges of larger lakes particularly in areas of water inflow (Photo courtesy of Dr. K. Young).

2.3 The response of lake ice to climate

Freeze-up and break-up of lake ice are transitional processes that can occur over days, weeks, or months, and therefore long term changes in these processes can be useful indicators of climate variability and change (e.g. Palecki and Barry, 1986; Assel and Robertson, 1995; Livingstone, 1997; Magnuson et al., 2000; Assel et al., 2003). Future changes in lake ice cover conditions due to changing climate conditions could impact on the role of lakes on energy, water and biogeochemical processes in cold regions as well as socio-economic impacts in terms of transportation (ice roads) and recreation. Several timing events are noted for ice phenology studies: e.g. freeze onset, date of final ice cover, melt onset, and water clear of ice. However, there are inter-country and even inter-agency differences in ground-based freeze-up and break-up records. For example, some document the initiation of break-up, while others register the date when the water body becomes completely ice-free. This is an important distinction when examining variability and trends in ice records from different sources, given that the entire break-up process can last for up to four weeks at a single site (Prowse et al., 2007).

Another potential issue with reported changes in lake ice phenology is that ice cover records have largely been determined by point in situ observations and are typically observed on only one part of the lake and are not spatially representative. While some recent studies have used remote sensing for

phenology studies (e.g. Wynne and Lillesand, 1993; Wynne et al., 1996; Latifovic and Pouliot, 2007; Howell et al., 2009), another viable solution is the use of lake ice models to supplement observational networks for studying the effect of climate on ice phenology (Duguay et al., 2003). Lake ice models can also be used to investigate the response of lake ice to changes in climate variables to better understand the large-scale forcing factors.

2.3.1 Observations of lake ice response to climate

The time extent used for the trend analysis is an important factor, as results have been shown to be dependent on this time window. For example, long term records dating back the late 1800's will be affected by the end of the Little Ice Age, a cooler period lasting from the 16th to 19th century, leading towards increasing temperature trends from the late 1800's to present time – reflected in a shift towards earlier break-up dates found from the late 1880's (e.g. Finnish lakes, Korhonen, 2006; Lake Michigan, Assel and Roberston, 1995). In contrast, recent records examining shorter time scales, for example the last 30 years in North America, will reflect the warming period since the mid-1970's.

In addition to the time scale of the trends examined, other factors that affect the interpretation of trends include large-scale atmospheric and oceanic circulation patterns, or teleconnections. The teleconnections that can influence the Northern Hemisphere are primarily the Pacific Decadal Oscillation (PDO), the Pacific North American (PNA) pattern, the North Pacific (NP) index, and El Niño/Southern Oscillation (ENSO), North Atlantic Oscillation (NAO) and the Arctic Oscillation (AO). As outlined in Bonsal et al. (2006), oscillations account for a significant portion of the observed variability in 20th century temperature trends and variability, especially in the winter (Hurrell, 1996).

The shift to a deeper Aleutian low in 1976 has been associated with a trend toward warmer winter and spring temperatures across western Canada; in addition, late autumn to early spring temperatures have been linked to ENSO, PNA (positive phase) and PDO (positive phase) (Bonsal et al., 2006). Eastern Canada and Europe are affected primarily by the NAO, with positive phases resulting in winter and spring cooling in northeastern Canada and warmer milder winters in Europe (Bonsal et al., 2006; George, 2007). With ice phenology closely related to air temperatures, several studies have related trends in break-up and freeze-up dates to patterns in the oscillations (e.g. Benson et al., 2000; Blenckner, 2004; Magnuson et al., 2004; Bonsal et al. 2006; George, 2007; Ghanbari et al., 2009). However, as Blenckner (2004) outlines, atmospheric indices are usually more related to the timing of

break-up rather than freeze-up since break-up is more temperature/wind dependant, while freeze-up is also dependant on morphometry (Palecki and Barry, 1986).

Indirect methods of determining lake ice changes have also been examined by using biological and physical proxies. Diatom records have been used in many studies as indicators of changes in ice cover duration associated with different climate conditions (Smol et al., 2005). Cooler conditions result in persistent ice cover, which limits the amount of light penetration and hence reduces algae habitat and primary production (with the opposite occurring during warmer conditions) (Smol, 1983; Smol, 1988; Douglas and Smol, 1999; Keatley et al., 2008). Sediment records from lakes can also be used to reconstruct past climate conditions (e.g. Besonen et al., 2008; Francus et al., 2008) and hence infer changes to the ice cover on the lake (Tomkins et al., 2009). Tomkins et al. (2009) created ice cover records on a perennially frozen lake using sediment pellets found in the sediment record, likely deposited from ice rafting in high-melt years. Their results suggest that during the past 1000 years the most reduced ice cover occurred from ca. 1891 to present, with more persistent ice cover before 1582 AD, reduced ice cover from ca. 1582 - 1774 AD and more persistent ice cover again during the 1800's.

Changes in the ice regimes of typically perennially ice-covered lakes on northern Ellesmere Island (Nunavut, Canada) have been related to rapid threshold dependant shifts in climate regimes in that area (Mueller et al., 2009). Prior to 1988 a colder climate was prevalent and perennial ice-cover was observed for the five lakes examined. In 1988 a regime shift in the air temperatures was reflected in the ice records, which show infrequent ice loss occurring after this time. A second regime shift in temperature further changed the ice regimes from infrequent to frequent ice loss on these lakes after 1997-98.

2.3.1.1 Ice Phenology and Thickness Trends - Europe

For 21 lakes and bays of large lakes spread around the Northern Hemisphere, Magnuson et al. (2000) showed freeze-up dates (13 lakes) shifted 5.7 ys/100 years later and break-up (20 lakes) 6.3 days/100 years earlier from 1846 to 1995. Relationships such as these have been developed for various regions and specific lakes. The main trend findings of several lake ice studies in the Northern Hemisphere are summarized in Table 2.1. The statistically significant trends identified in Table 2.1 have been mapped in Figure 2.3.

Table 2.1. Summary of ice phenology trends found from various studies.

Location	Author	Years Analyzed	Freeze-up Trends	Break-up Trends	Other
Northern Hemisphere	Magnuson *et al.*(2000)	1846 - 1995	Later: 5.7 days/100 years	Earlier: 6.3 days/100 years	21 lakes (5 rivers)
Finland	Korhonen (2006)	1800's - 2002	Later: 5-8 days/100 years	Earlier: 6-9 days/100 years	87 lakes studies (32 for thickness). No trends found for Lapland. Some trends towards thicker maximum ice in north and central Finland, some lakes thinner in southern Finland
		1961 - 2000 (thickness)			
		1885 - 1930s	Later		
		1930s - 1960s	Earlier		
		1960's - 2002	Slightly delayed		
		1885 - 2002	Later: 5.4 days/100 years	Earlier: 7.6 days/100 years	Average for all 16 lakes
			Later: 7.9 days/100 years	*Earlier: 8.6 days/100 years*	*Southern Finland (5 lakes)*
			Later: 3.6 days/100 years	*Earlier: 6.6 days/100 years*	*Central Finland (7 lakes)*
			Later: 4.6 days/100 years	*Earlier: 7.5 days/100 years*	*Northern Finland (4 lakes)*
Finland/Sweden	Bleckner (2004)	1961 - 2002	None	Earlier breakup in southern Swedish and Finnish lakes. Strong trend toward earlier break-up for all areas >1995	50 lakes studied
Poland	Marszelewski and Skowron (2006)	1961-2000	Varying	Earlier: 6 - 8 days/10 years	6 lakes studied. Decreasing ice thickness found
Russia (Lake Baikal)	Kouraev *et al.* (2007)	1992 - 2004	Earlier	Later	used satellite altimetry and radiometry
Russia (Southern Lake Baikal)	Livingstone (1999)	1869 - 1996	*NA*	Earlier: 1 day / 19.3 years (5.2 days/100 years)	Long-term trend not characteristic of data series.
		1869 - 1920	*NA*	Earlier: 1 day/ 3.3 years (30 days/100years)	Trend shift identified in 1920
		1920 - 1996	*NA*	None	
Russia (Lake Ladoga)	Karetnikov and Naumekno (2008)	1943 - 2006	Earlier: 14 days/100 years	None	Ice duration increasing 0.06 days/year
England (Lake Windermere)	George (2007)	1933 - 1962	Increasing number of ice days		Examined number of ice covered days
		1964 - 1990	Decreasing number of ice days		
		1990 - 2000	Very few ice days		
Canada	Duguay *et al.* (2006)	1951 - 1980	Later: Western Canada, earlier: Central and Eastern Canada	Earlier: west of Hudson Bay, later: eastern Canada	Break-up trends were found to be more spatially coherent than freeze-up trends
		1961 - 1990	Later: Coastal mainland Arctic region, Quebec/South eastern Ontario, Earlier: far eastern Canada	Earlier: Canada-wide	
		1971 - 2000	Later: Great Lakes region, earlier: Boreal Ontario/Manitoba, Atlantic region	Earlier: most lakes, however later in some northern areas	
		1966 - 1995	Mainly similar to 1961-1990	Mainly similar to 1961-1990	

Location	Author	Years Analyzed	Freeze-up Trends	Break-up Trends	Other
Canada	Latifovic and Pouliot (2007)	~1950 - 2004	Later: 0.12 days/year	Earlier: 0.18 days/year	36 lakes, combination of observations and satellite data.
		1970 - 2004	Later: 0.16 days/year	Earlier: 0.23 days/year	Average trends for lakes across the country
Canadian Arctic	Latifovic and Pouliot (2007)	1985 - 2004	Later: 0.76 days/year	Earlier: 0.99 days/year	6 lakes, satellite data only
Southern Ontario	Futter (2003)	1853 - 1995		Earlier	46 lakes with break-up data, 15 lakes freeze-up and break-up
		1853 - 1899		Earlier	
		1900 - 1948		Later	
		1958 - 1995		Earlier	
		1853 - 1994			Longer ice free season
		1853 - 1899			Longer ice free season
		1900 - 1947			Shorter ice free season
		1963 - 1994			Longer ice free season
Western Ontario (Lake 239, Experimental Lakes Area)	Schindler *et al.* (1990)	1969 - 1988	Ice free season increase by about 20 days over studied time frame		
Great Lakes Region	Jensen *et al.* (2007)	1975 - 2004	Later: 3.3 days/decade	Earlier: 2.1 days/decade	65 water bodies in Michigan, Minnesota, New York, Ontario and Wisconsin
Great Lakes	Assel *et al.* (2003)	1963 - 1976	Lower ice cover regime		Annual maximum ice concentration. Ice regimes are relative to each other
		1977 - 1982	Higher ice cover regime		
		1983 - 2001	Lower ice cover regime		
Grand Traverse Bay (Lake Michigan)	Assel and Robertson (1995)	1851 - 1888			Change in average dates after break in trends
		1889 - 1993	Later: 12.2 days		
		1851 - 1864			
		1865 - 1888		Later: 16.4 days	
		1889 - 1939		Earlier: 11.26 days	
		1940 - 1993		Earlier: 8.32 days	
Lake Mendota, Wisconsin	Assel and Robertson (1995)	1856 - 1888			Change in average dates after break in trends
		1889 - 1993	Later: 8.3 days		
		1889 - 1979		Earlier: 7.26 days	
		1980 - 1993		Earlier: 7.2 days	
Wisconsin (and Lake 239, Experimental Lakes Area, Ontario)	Anderson *et al.* (1996)	1968 - 1988	*NA*	Earlier: 0.82 days/year for southern lakes Earlier: 0.45 days/year for northern lakes	20 lakes studied
Minnesota	Johnson and Stefan (2006)	1965 - 2002		Earlier: 0.13 days/year	Noted reversing trends in 10 year averages
		1979 - 2002	Later: 0.75 days/year		

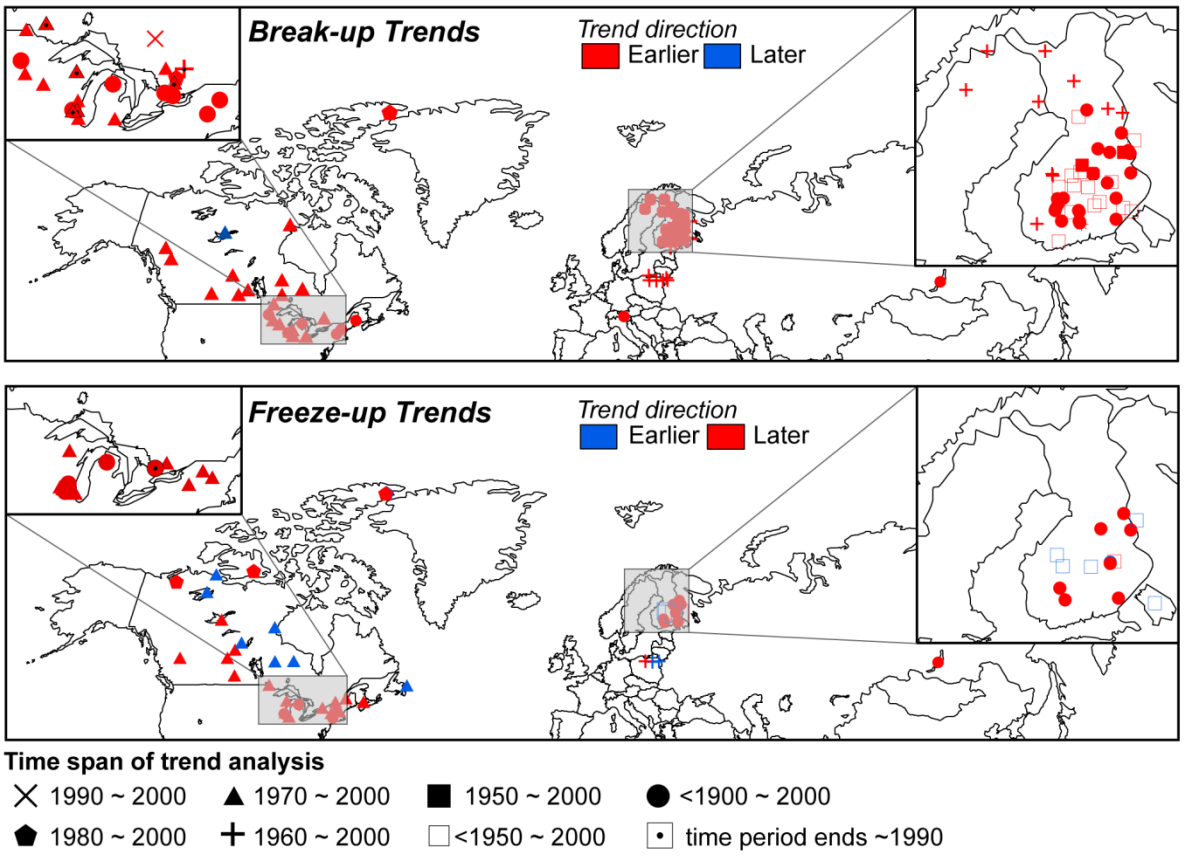

Figure 2.3. Lake ice trends (identified as statistically significant) for the Northern Hemisphere based on studies presented in Table 2.1.

Several studies have examined lakes in Finland, where a long series of ice records exists. (e.g. Palecki and Barry, 1986; Magnuson et al., 2000, Blenckner, 2004; Korhonen, 2006). Ice records have shown significant trends towards earlier break-up from the late 19th century, with the exception of the very northern lakes, as well as significant trends towards later freeze-up. However, lakes with records existing only after 1900 showed few significant trends (Korhonen, 2006). Korhonen (2006) analyzed ice phenology for 87 Finnish lakes (32 for thickness) and presents a detailed breakdown of trends for each lake. A shift in earlier freeze-up dates and later break-up dates in the long-term ice records (since early 19thC) were comparable to those found by Magnuson et al. (2000) (see Table 2.1). The maximum ice thickness has tended to decrease or have relatively no change in southern Finland,

increasing or no change in central and northern Finland, with the increase attributed to an increase in snow ice (Korhonen, 2006). Examining the shorter time scale of 1961-2002, trends towards earlier break-up were found in southern Swedish and Finnish lakes, with no trends in freeze-up dates (Blenckner et al., 2004).

Marszelewski and Skowron (2006) examining lakes in the Polish Lowland from 1961-2000, found varying trends for freeze-up but 0.6 – 0.8 days per year earlier for break-up, a ten-fold increase from the long term trends in the Northern Hemisphere found by Magnuson et al. (2000). Ice thickness was shown to decrease, with the ice regime reflecting the warmer winter air temperatures associated with the NAO during this time.

In a more temperate region, George (2007) identified some trends in the number of days with ice cover in a bay of Lake Windermere, England. The results showed three main ice periods – increasing ice cover from 1933-1962, decreasing ice cover from 1964-1990, and very little ice cover formed from 1990-2000. A shift in the Finnish lake ice cover (Korhonen, 2006) was also detected for those time spans - earlier freeze-up trend from 1930s to 1960's, shifting to a later freeze-up trends after 1960's.

While most studies use ice records from a point to represent the lake ice cover, Karetnikov and Naumenko (2008) used percentage ice cover determined from aircraft and satellite for Lake Ladoga, Russia, to examine trends from 1943-2006. These results showed a small but significant trend for longer ice duration as a result of the earlier freeze-up trends. No significant trends were found for break-up.

Looking at long term records of ice break-up (1869 – 1996) from southern Lake Baikal (eastern Siberia), Livingstone (1999) found that for the entire time series a trend of 1 day per 19.3 years (5.2 days /100 years, similar to Magnuson et al. (2000) for southern Lake Baikal at 5.1 days /100 years) was evident, however not characteristic of the entire data series. Two segments were separated from this time series, from 1869 to 1920 a trend towards earlier break-up at 1 day per 3.3 years was significant (30 days/100 years), but no significant long-term trend was found after 1920. Magnuson et al. (2000), using 1868-1995 time scale, found trends of 11 days/100 years later for freeze-up for southern Lake Baikal. While most studies have looked at longer-term trends, Kouraev et al. (2008) used satellite imagery to examine ice phenology on Lake Baikal during recent years, 1992-2004 (southern, central and northern Lake Baikal). Their results showed later break-up and earlier freeze-up – in contrast to longer and earlier time frame studies. The authors note that this corresponds well

with known 20-30 year cycles in air temperatures for Lake Baikal, with a warming period from the mid 70's and a cooling period since the 1990's.

Wehenmeyer et al. (2004) examined the response of ice break-up in two different climatic regions in Sweden – a section of northern Sweden with mean annual temperatures of 0-3°C and the other from southern Sweden with 5-7°C. The response of ice break-up was found to be non-linear (an arc cosine function) under the same temperature change (0.8 warmer from 1991-2002, than from 1961-1990) resulting in a different response between the two climate regions – with a 17 day earlier shift in break-up in the warmer region versus 4 days earlier in the cooler region. This non-linearity in response to temperature changes with latitude has also been noted by others (e.g. Palecki and Barry, 1986; Blenckner, 2004).

2.3.1.2 Ice Phenology Trends – North America

In Canada, from 1951-2000, trends toward earlier water-clear-of-ice dates have been observed for many lakes during the latter part of the 20th century, but complete freeze over dates have shown few significant trends over the same period (Duguay et al., 2006; Latifovic and Pouliot, 2007). Duguay et al. (2006) determined trends for Canadian lake ice phenology using the Canadian Ice Database records, breaking the 1951-2000 time span into 30 years segments, as well as 1966-1995 to facilitate comparison between other trend studies. Trends for ice freeze-up were not spatially coherent, and many were not significant. The freeze-up trends that were significant tended to be located in regions where the autumn isotherm reflected a similar trend, and the trends towards later freeze-up corresponded with areas of increasing fall snow cover (Duguay et al., 2006). Trends in break-up however became increasingly earlier for most of the country, with strong spatial coherence and strong relation to the 0°C isotherm dates. Western Canada showed the strongest trends towards earlier break-up, consistent with changes in the spring snow cover duration.

Significant long-term trends have been shown in South-Central Ontario, using ice records dating back to 1853 (collected largely by volunteer monitoring efforts), as well as in a time series 30 years prior to the study (Futter, 2003). Earlier break-ups and longer ice-free seasons were observed with a high degree of synchrony, with closer lakes being more coherent (a similar finding to Magnuson et al. (2005) from the Laurentian Great Lakes region). The long term trend found by Futter (2003) can be attributed to the end of the Little Ice Age, while an alternating trend of warming and cooling periods was shown depending on the blocks of years analyzed. Lake Simcoe, Ontario, for example, showed a warming trend from 1853 – 2001, however only 1853 – 1899 was statistically significant, while 1900

– 1949 actually showed a cooling trend, and 1950 – 1995 showed a slight warming trend. Alternating trends have been also been noted in long term phenology records by Magnuson et al. (2001) when data is split into blocks of years from 20 – 50 years, clearly outlining the importance of the length of the time series used when interpreting trend analyses (see also Magnuson et al., 2006).

Looking at small inland lakes in the Laurentian Great Lakes region (Minnesota, Wisconsin, Michigan, Ontario and New York) using the time span from 1975 – 2004, Jensen et al. (2007) found trends for advance in break-up date, and delay in freeze-up date, with rates that were 5.8 (freeze-up) and 3.3 (break-up) times faster than the trends found by Magnuson et al. (2000) for the Northern Hemisphere from 1846 – 2000; again, illustrating the importance of different record lengths in calculating trends. While Jensen et al. (2007) identified that trends in the break-up dates are correlated with trends in temperature, snow depth and snow days, they found that although there was a stronger trend in large, low-elevation lakes for later freeze-up; no geographical patterns or relation to meteorological variables were found for freeze-up. The non-linear relationship identified by Weyhenmeyer et al. (2004) between ice break-up and air temperature was also shown in the Laurentian Great Lakes Region by Jensen et al. (2007). Their study found that the greatest rate of change in break-up dates was occurring in the south western region of their study area rather than in the more northern latitudes – likely attributed to the small temperature rise needed to change from freezing to non-freezing temperatures in this region versus more northerly regions. This concept of greater sensitivity with respect to latitude was furthered by Weyhenmeyer et al. (2010) who, based on interannual variability of ice cover durations in the Northern Hemisphere, suggest that 3.7% of the world's lakes located towards the southern reaches of winter ice cover are at risk of transitioning from ice-covered systems to open water systems in the near future if air temperatures continue to rise.

Anderson et al. (1996) found trends in Wisconsin ice cover from 1968-1988 towards earlier break-up (0.82 days/year in southern Wisconsin and 0.45 days/year in northern Wisconsin). Johnson and Stefan (2006), however, determined trends for break-up (and freeze-up) of nearby Minnesota Lakes from 1965-2002 at 0.13 days/year earlier for break-up (and 0.75 days/year later for freeze-up: 1979-2002), pointing out that the trends identified are different when looking at different year spans within their data, with 1990-2002 nearly double the rate for break-up and freeze-up. The northern Wisconsin lakes used by Anderson et al. (1996) are at comparable latitudes to most of the lakes used in Minnesota (Johnson and Stefan, 2006), (the Wisconsin lakes are in closer proximity to Lake Superior and Lake Michigan) with both Minnesota and Wisconsin being included in Jensen et al. (2007) (some

overlapping lakes used). Johnson and Stefan (2006) have a trend of 0.24 days/year earlier break-up from 1970-2002, (comparable to Jensen et al., 2007, for southern Minnesota from 1975-2004 at 0.25 days/year), but not as fast as those reported from 1968-1988.

Schindler et al. (1990) examining trends from 1969-1988 at Lake 239 in the Experimental Lakes Area (approx. 100 km north of two lakes at the Minnesota/Ontario border used by Jensen et al. 2007 examining trends from 1975 - 2004) found a longer ice free season of 20 days over the 20 years time span due to earlier break-up, which they attributed to warmer spring temperatures and less snow fall during that time. Lake 239 is much smaller than the Minnesota lakes, where a non-significant trend towards earlier break-up of 0.57 days / decade for Rainy Lake and 0.70 days / decade for Kabetogama Lake was found (Jensen et al., 2007). The differing time spans used and different lake morphometry make comparing trends between individual lakes difficult. Since overall climate patterns change over time, examining only partial sections of a time series can show very different results from another time series. Comparing ice phenology trends to teleconnections has provided some insight and furthered the understanding of the linkages between lake ice and climate.

2.3.1.3 Ice phenology and Teleconnections

Many European studies have compared ice phenology trends to large scale oscillations – particularly the North Atlantic Oscillation (NAO), and found strong relationships to exist (e.g. Lake Ladoga, Russia – Karetnikov and Naumeko, 2008; Lake Baikal, Russia – Kouraev et al., 2007, Livingstone, 1999; Lake Windemere, UK - George, 2007; Scandinavian Lakes - Blenckner et al., 2004).

George (2007) found a relationship between ice cover for Lake Windemere to the NAO and was able subsequently to hindcast the times series of number of ice days back to 1864, which compared well to written weather records from that time. However, Livingstone (1999) using a similar time series (1869-1996) showed a strong relationship between NAO and ice cover break-up on Lake Baikal in the later portion of the time series (>1920) – but the trend for earlier break-up dates prior to 1920 was influenced by the end of the Little Ice Age rather than influences of the NAO. Karetnikov and Naumeko (2008) found, through correlation of an ice cover index with NAO, that while the NAO is correlated with ice cover in Lake Ladoga (north-western region of Russia), the NAO does not correlate well for extreme years of ice cover, showing the ice cover is not only influenced by the NAO. While most studies found strong relationships between the NAO variations and ice cover trends, Blenckner et al. (2004) discuss that for northern Finland (above 65°N) the influence of the

NAO was less pronounced in the local climate than southern Finland – suggesting a different circulation pattern affecting that area as outlined by Busuioc et al. (2001).

The observed changes in Canada's lake ice cover have also been influenced by large-scale atmospheric forcing indices such as the PDO, PNA, NP, ENSO (Bonsal et al., 2006). Ice phenology was shown to be more responsive to the extreme phases of the teleconnections, with the Pacific indices (PNA, PDO, SOI and NP) having the strongest correlation to ice cover - with the exception of the extreme eastern areas which were more affected by NAO (Bonsal et al., 2006). For most of the country, positive phases on PNA, PDO/negative phases of SOI, NP result in earlier break-up and later freeze-up of the ice cover, while in the eastern areas positive phases of NAO were shown to produce later break-up.

Looking at the Laurentian Great Lakes, using annual mean ice concentrations derived from ice charts rather than near-shore observations, Assel et al. (2003) suggest three ice regimes between 1963-1990: lower ice concentrations from 1963-1976, higher ice concentrations from 1977-1982, and lower concentrations from 1983-1990. They related the shift in the Aleutian Low in 1976 to the change in the ice regime from 1977 and noted a lack of El Niño or La Niña events during these years. Significantly lower ice concentrations were found to occur in the winters following strong El Niño events (Assel, 1998; Rodinov and Assel, 2000), however a much weaker relationship was found for La Niña events. Looking at cold winters, Rodinov and Assel (2000) found relationships between lesser-known indices, the Polar/Eurasian Low (POL) and Tropical/Northern Hemisphere (TNH), in combination with the NAO. Typically, the years with above mean ice concentration for the Great Lakes were found to be associated with a strengthening of the Hudson Bay Low (HBL), allowing cold air from the Arctic to reach the Great Lakes regions (Assel et al. 2003), with a weakening of the HBL resulting in an inflow of milder Pacific air during the below average ice concentration years (Assel et al., 2003).

Livingstone (2000) found the NAO signal in the ice phenology records from Lake Mendota was present and strong from the "latter half of the 19th century to the first half of the 20th century" but had weakened since then. Recent work by Ghanbari et al. (2009) found that the ice cover on Lake Mendota was affected at the inter-annual and inter-decadal scale by teleconnections; most prominently by the effects of PDO (through snow fall/snow depth) and SOI (through temperature) at the inter-annual scale and by the PDO (though air temperature) and NAO (through snowfall) at the inter-decadal scale. For the same lake, Anderson et al. (1996) report that the ice break-up variability

from 1968-1988 was associated with El Niño episodes. Interactions and moderations of the indices by each other can also occur, for example the effects of ENSO on winter air temperature were found to be modulated by the PDO in Great Lakes regions (Rodinov and Assel, 2003) and western Canada (Bonsal et al., 2001). The strength and relationship of the indices to ice phenology has also been shown to change. Robertson et al. (2000) show how El Niño episodes in North America affect the ice records differently before and after 1940. They found later freeze-up and break-up dates during El Niño episodes prior to 1940 but earlier break-up dates during El Niño episodes after 1940.

2.3.2 Lake ice modelling

Modelling provides an opportunity to further understand the interactions between lake ice and climate, which is key for future anticipated changes. Altering the input variables independently (via sensitivity analysis) can assist in understanding the effects of each variable on the ice cover. They can also be a useful complement to observations. Various types of models have been used to investigate the response of lake ice to external forcing(s), with varying degrees of complexity. Several studies have developed regression models or empirical models for specific lake phenology records with respect to air temperature (e.g. Palecki and Barry, 1986; Livingstone and Adrian, 2009) or morphometry and geographic position (Williams and Stefan, 2006). In terms of energy exchanges, some studies have created energy balance models to investigate the response of the ice cover (e.g. Heron and Woo, 1994; Liston and Hall, 1995b).

Thermodynamic lake ice models, frequently based on sea-ice models, have also been modified/created for use in lake ice studies. Maykut and Untersteiner (1971) developed a popular model that has been modified and enhanced for lake ice by many studies (e.g. Ebert and Curry, 1993; Flato and Brown, 1996; Vavrus et al., 1996; Launiainen and Chang, 1998; Duguay et al., 2003). The Flato and Brown (1996) model for land fast sea ice has since been modified to become the Canadian Lake Ice Model (CLIMo) and is a well tested model used for freshwater ice cover studies (e.g. Ménard et al., 2002; Duguay et al., 2003; Morris et al., 2005). In addition to ice-specific models, several models have been developed for lakes that include sub-models for ice cover. Some examples of these are Gu and Stefan (1990) who created a model based on the ice model by Maykut and Untersteiner (1971), modified by Fang et al. (1996)(MINLAKE 96); PROBE model e.g. Elo and Vavrus (2000), Elo (2006); LIMNOS model e.g. Vavrus et al. (1996), Elo and Vavrus (2000); DYRESM (e.g. Hamilton et al. 2002; Perroud et al., 2009), Hostetler Lake Model (Hostetler et al., 1993) and FLake model e.g. Mironov (2007). Several of the above mentioned models are described

and compared in Perroud et al. (2009) and Stepanenko et al. (2010). In addition to statistical and process-type models, artificial neural networks have been developed to model lake ice growth and have been shown to be a viable alternative to complex thermodynamic models for modelling ice thickness, (Seidou et al., 2006; Zaier et al., 2010). The following section discusses studies that have used modelling to examine changes in phenology (break-up, freeze-up, ice cover duration), thickness and composition of the ice cover.

2.3.2.1 Modelling Lake Ice Phenology

Sensitivity analysis has shown that ice phenology is most sensitive to changes in air temperatures (e.g. Gao and Stefan, 2004; Morris et al., 2005). This relationship has been the basis of empirical models for many years and is used to predict changes in ice cover based on temperatures changes, and vice versa (e.g. Paleki and Barry, 1986; Assel and Robertson, 1995). Several studies in the Laurentian Great Lakes region have examined the sensitivity of lake ice cover with respect to air temperature. A synthesis of their findings is reported in Table 2.2, showing the range of responses from the lakes examined. Models developed by Assel and Robertson (1995) and Robertson et al. (1992) for Lake Mendota (Wisconsin) used mean temperatures from the months most strongly correlated with the ice phenology: November to December for freeze-up and January to March for break-up.

Vavrus et al. (1996) noted an increased sensitivity to warming air temperatures rather than cooling in their simulations as a result of the ice-albedo feedback. Since albedo is a function of surface temperature and thickness of the ice or snow slab in their model (LIMNOS – a physically based numerical model), the warmer (cooler) air temperatures result in lower (higher) albedo and therefore more (less) solar absorption into the snow/ice affecting the bottom melt.

Comparing the ice phenology produced by altering the albedo values in both FLake and the Hostetler model (both process-type models), Martynov et al. (2010) showed that the ice albedo had no effect on freeze-up dates, but the ice break-up dates became increasingly later as the albedo values were increased.

Table 2.2. Summary of the projected effect of 1°C rise in air temperature on freeze-up and break-up dates in the western Laurentian Great Lakes region, and North America. Modified from Williams and Stefan (2006) and Williams et al. (2004).

Authors	Lakes	Type of model	ΔFreeze-up/ΔT (days/1°C)	ΔBreak-up/ΔT (days/1°C)
Robertson *et al.* (1992)	Lake Mendota, Wisconsin	Sensible heat transfer	4.9	-6.4
Assel and Robertson (1995)	Lake Michigan (Grand Traverse Bay)	Fixed-period regression	2.0	-2.8
		Dynamic sensible heat transfer	8.4	-7.1
Assel and Robertson (1995)	Lake Mendota, Wisconsin	Fixed-period regression	4.0	-3.9
		Dynamic sensible heat transfer	5.3	-6.4
Vavrus *et al.* (1996)	Wisconsin Lakes	LIMNOS	3.9	-5.6
Williams *et al.* (2004)	North American Lakes	Single variable regression	3.3	-4.4
		Multivariable regression	4.7 – 5.3	-6.0 - -6.5
Gao and Stefan (2004)	Kenora (ELA), Ontario	MINLAKE 96	2.7	4.2
Williams and Stefan (2006)	North American Lakes	Regression (Linear)	1.7	-3.8
		Regression (Log)	3.4	-2.5
		Regression (Hybrid)	1	0.3

Accurate albedo values are needed for modelling, however since albedo changes daily and seasonally based on snow/ice conditions it is difficult to parameterize accurately. Henneman and Stefan (1999) noted a lack of clarity on which existing albedo decay models were best suited for use for snow/ice cover on freshwater lakes. They collected albedo values for a season to develop models that separated melt from non-melt conditions, which performed better than other existing albedo models when tested for their study lake. Difficulties in albedo parameterization have also been noted by Jeffries et al. (2005), whose simulated albedo was lower than those found from field measurements.

Paleki and Barry (1986) examined the relationship between ice phenology and air temperature for two regions of Finland (northern and southern). They found that in southern Finland, a 5 day change in freeze-up (break-up) dates would result in a 1.1°C change in November temperature (1°C change in April temperature) and that an equivalent shift of dates in the northern region would result in a larger magnitude shift of temperatures for that region. Weyhenmeyer et al. (2004) also showed changes in the break-up dates across a latitudinal gradient with a 0.8°C change in temperature, resulting in earlier break-up by 4 days in a colder (mean air temperature 0-3°C) region of Sweden, versus 17 days in the warmer (mean air temperature 5-7°C) region of Sweden. Looking at Great Slave

Lake near Yellowknife, Ménard et al. (2003) determined through sensitivity analysis using a physically based thermodynamic model (CLIMo) that altering the normal daily air temperature by 1°C resulted in a nearly linear increase or decrease of 6 days in ice cover duration.

Sensitivity analysis was done on Alaskan lake ice cover also using CLIMo. Morris et al. (2005) showed that for these lakes, freeze-up was affected by monthly air temperature changes in September and October, with October (±6 days) more prominent than September (±1day). Break-up was affected by air temperature in April (±6 days) and May (±2 days) with only minor changes from September to March (Morris et al., 1995).

Using the LIMNOS model, Walsh et al. (1998) simulated ice phenology for the northern hemisphere for 5 and 20 m deep lakes and compared the results to in situ data for 30 lakes. They found the model simulations to be within 2 - 4 days of the long term averages from the observation data, with the exception of some identified lakes that were located in extreme climate conditions (e.g. atypical amounts of snowfall for the region) or that had considerably dissimilar morphometry from the 'small, round-bottomed lake' type that the model was developed for (e.g. extremely deep or large surface areas).

Snow cover changes have been shown to have a stronger effect on the timing of break-up, rather than freeze-up (Morris et al., 2005; Vavrus et al., 1996). For Alaskan lakes, changes in the annual snow cover, or changes in the snow cover from October to April, were shown to have a small effect on break-up, but not to the extent of air temperature; with the exception of simulating the results with snow-free conditions on the lake surface. Under the snow-free conditions, break-up was delayed by 19 days due to the thick ice that developed as a result of the lack of insulating snow on top of the ice (Morris et al., 2005). For Lake Mendota (Wisconsin), Vavrus et al. (1996) showed simulation results from increasing and decreasing snow cover, with an increase in snow cover almost linearly delaying break-up. For decreasing snow simulations, break-up dates were earlier for the 75% and 50% snow case due to the reduction in insulating properties of the snow, but became delayed again for 25% and the no-snow scenario as a result of the increasing conductive heat loss from the ice surface, resulting in only a one day difference between no-snow and 100% snow. In the Mackenzie River Basin (MRB), Rouse et al. (2008a) showed simulations for the changes of ice duration under full-snow and no-snow scenarios using the CLIMo model (Figure 2.4). Their result showed that reducing the snow cover to 0 (for hypothetical 3 m or 30 m lakes in the MRB) resulted in a change of ice cover duration of up to 10 days. Modelling ice cover for lakes located at the same latitude (Rouse, 2008a) showed

that shallow lakes (3m) remained ice covered 40-50 days longer than deeper lakes (30m), mainly due to the added heat storage in the deeper lakes resulting in later freeze-up times (Figure 2.4). This was also shown by Elo (2006) with deeper lakes in Finland freezing about one month later than shallower lakes.

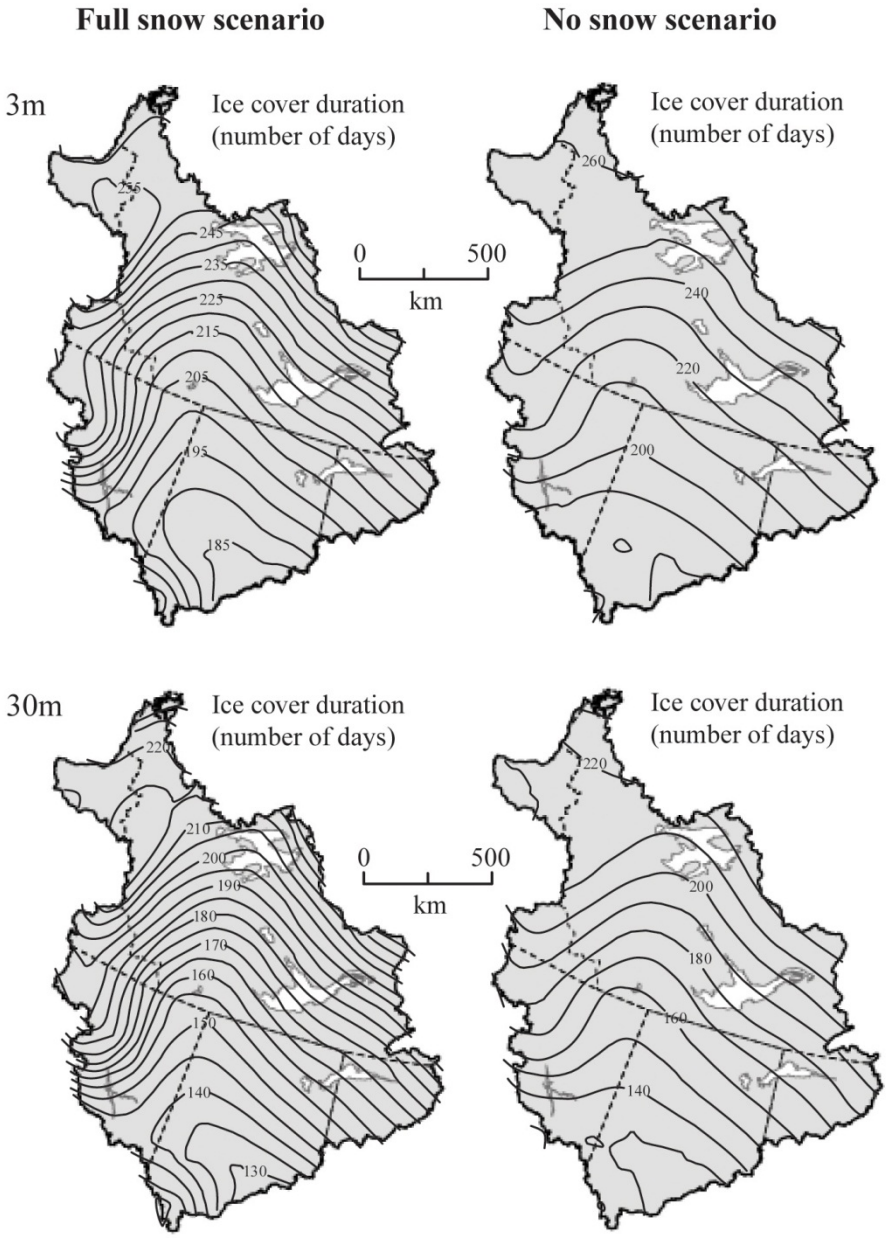

Figure 2.4. Ice cover duration for 1980-1996 for hypothetical 3m and 30m deep lakes across the Mackenzie River Basin as modelled for full snow and no snow scenarios using the CLIMo model. Modified from: Rouse et al. (2008a).

Using two process-type models (FLake and the Hostetler model) to examine the changes to ice phenology by altering lake depth, Martynov et al. (2010) showed that increasing the depth of the lake resulted in shorter ice cover durations, with the magnitudes of these duration shifts depending on the physical formulations of the models (see Perroud et al. (2009) for a detailed comparison of the two models). As lake depth increased, ice break-up was shifted from 4 to 19 days earlier (Hostetler and FLake model results, respectively) and ice freeze-up was shifted 15 to 99 days later (Hostetler and FLake results respectively). The depth only affected the phenology simulations up to 20 m using the Hostetler model, and no ice was formed when depths of 56 m were reached using the FLake model.

2.3.2.2 Modeling lake ice thickness

Several studies have examined the effects of altering the air temperatures and snow depths on lake ice thickness by sensitivity analysis (e.g. Vavrus et al., 1996, Ménard et al., 2002, Morris et al., 2005). Overall, changes to snow depths had more effect on ice thickness than changes to air temperatures, and decreasing the amount of snow cover resulted in thicker ice formation. Morris et al. (2005), found that annual and monthly changes in snow depth (±100%) resulted in changes to the thickness and composition of the ice cover on Alaskan ponds. Changing the amount of snow cover was more effective in altering the ice thickness than changing the air temperature. Reducing the snow cover by 75% to 100% resulted in the total ice thickness doubling due to the lack of insulating snow cover and altering the snow cover from -50% to +100% increased thickness due to an eight to ten fold increase in snow ice (with less black ice formed). Ménard et al. 2003 showed similar findings with respect to increased ice thickness with decreased snow cover, with a more prominent effect on thickness by altering snow cover rather than air temperature changes (Figure 2.5). Reducing the snow cover resulted in the maximum ice thickness becoming 17 cm thicker for each 25% reduction from the normal snow depth amounts.

Vavrus et al. 1996 showed the response of simulating ice cover thickness with no-snow and double-snow scenario (Lake Mendota, Wisconsin). Initial rapid ice growth slows during the frozen season and decays rapidly due to positive feedbacks (Ice-albedo feedback). With no-snow cover for insulation, the simulated ice cover in the no-snow scenario is thick early in the season, but decay begins earlier resulting in the same time frame as the scenario using snow measurements. In the scenario with simulated doubled snow, the ice remained thicker longer as a result of the higher reflectance of the thicker snow/ice cover prolonging the breakup by two weeks.

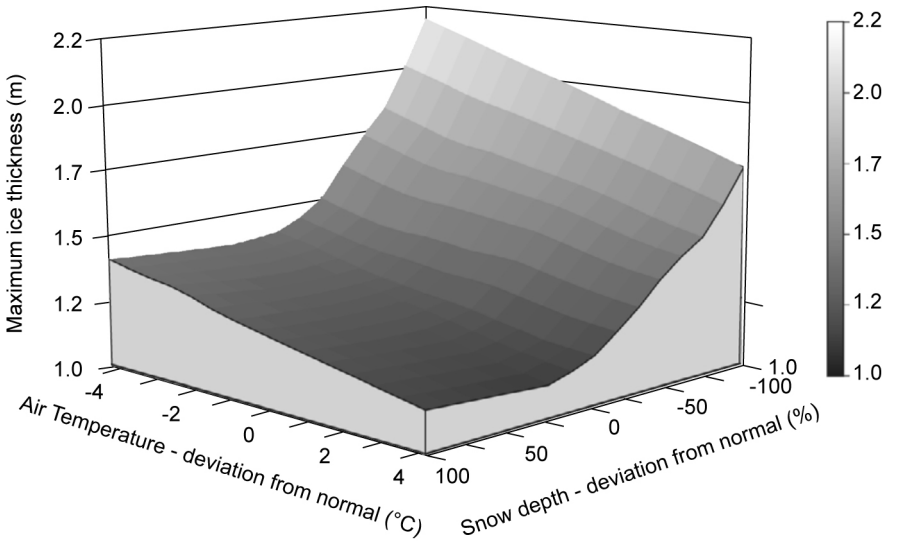

Figure 2.5. Impact of changes in air temperature and snow depth on maximum ice thickness, Back Bay (Great Slave Lake). Source: Ménard et al. (2003).

Contrary to the previously mentioned studies, Gao and Stefan (2004) found air temperature to have a greater effect on ice thickness than snowfall, however they acknowledge this might be as a result of the high snowfall found in their area (the Experimental Lakes Area, near Kenora, Ontario) as altering the snowfall by ± 20% did not produce any significant changes.

Similar to the ice duration modelling shown previously, Rouse et al. (2008a) used CLIMo to simulate changes to ice thickness with full-snow and no-snow scenarios. They showed a maximum ice thickness difference of 10 – 20 cm for 3 versus 30 m deep lakes (with deep lakes being thinner due to a later freeze-up date). The range of ice thicknesses showed a potential for 50-60 cm difference in the northern area between full-snow and no-snow (Rouse et al., 2008a). The changes in the spatial pattern of ice thickness are also evident between full-snow and no-scenarios.

2.3.2.3 Modelling lake ice composition

While changes to air temperatures and snow amounts alter the phenology and thickness of ice cover, they also influence the type of ice formed. Looking at how changes in monthly air temperatures affect ice composition for Alaskan lakes, Morris et al. (2005) found that changes in October and November most strongly affected the ice composition. Changing the October temperature from -4°C to +4°C resulted in a decrease in total thickness due to less snow ice, while changes in November resulted in decrease of black ice only (no change to snow ice amounts). The change in snow ice is a result of

later freeze-up dates with the warmer air temperatures, resulting in less snow accumulation on the ice cover, and hence less snow load to depress the ice. In winter, changing temperatures affect mostly the growth rate and thickness of black ice rather than snow ice (Morris et al., 2005).

Liston and Hall (1995b) found through simulations that wind speed affects both the surface temperatures (through energy balance components) and the type of ice formation via snow accumulation. Snow accumulation was an important factor in the formation of ice types; with lower wind speeds allowing more snow accumulation on the ice surface, promoting the growth of snow ice, rather than black ice (as the higher wind speeds inhibited snow accumulation).

Looking at how snow cover has been shown to affect ice composition, Morris et al. (2005) found that decreasing the snow depth on an ice cover resulted in a decrease in snow ice thickness; an increase of black ice thickness at the ice/water interface (due to reduced thermal resistance from the snow cover); and a decrease in total thickness overall (and vice versa). This increase in snow ice with a corresponding decrease of black ice was also shown in field samples from Finland in an area with increased snowfall (Korhonen, 2006). This is important since projected changes in high latitude areas suggest an increase in precipitation accompanying warmer temperatures (Serreze, 2000) and these changes are expected to be reflected in the ice cover composition.

2.4 The role of lake ice on weather and climate

While the previous section examined the response of lake ice to climate, this section will examine the lesser-known role that lake ice plays in the weather and climate systems. Increased evaporation from longer open water seasons can lead to downwind fog or precipitation into the winter season (i.e. lake-effect snow), and lakes have been shown to exert a thermal moderation on their local or regional climate depending on the size of the lake. The coupling of lake/lake-ice models to atmospheric models can provide more accurate simulations particularly with respect to feedbacks as climate variables, such as surface temperature, are passed to and from each model. Coupling of lake models (with or without lake ice components) to regional climate models (RCMs) can provide more accurate simulations of the regional climate by incorporating the effects of lakes (e.g. Hostetler et al., 1993; Goyette et al., 2000; León et al., 2005). The parameterization of lakes in global circulation models (GCMs), with the inclusion of lake-ice sub-models, can improve the predictive abilities of the overall models.

2.4.1 Lake-effect snow

With lakes that form a solid ice cover in the winter, the ice essentially forms a 'lid' on the lake, effectively stopping the turbulent fluxes, leaving only radiative or conductive energy exchanges to take place. However, with larger lakes that do not form a complete ice cover, interactions with the water-atmosphere continue throughout the winter. The Laurentian Great Lakes do not usually freeze over completely in the winter (with the exception of the shallowest, Lake Erie) although extensive areas of ice cover do form (Cordeira and Laird, 2008). Cordeira and Laird (2008) analyzed two large lake-effect snow events downwind of Lake Erie that occurred when the lake was largely frozen over (ice charts showing 90 to 100% ice coverage for most areas of the lake). At that concentration of ice, Gerbush et al. (2008) showed the latent heat flux to be at approximately 13% of the open-water value and the sensible heat flux between 23-58% that of the open-water value (with that value rising to 100% with 70% ice concentration) (Cordeira and Laird, 2008). Their study showed that lake-effect snow does not have to develop in an area of low ice concentration or over 'fractures' and suggests the relationship between surface heat fluxes and ice concentration needs to be further examined. Conditions in northern Great Lakes (Great Slave, Great Bear) are similar to Laurentian Great Lakes in the winter, where evaporation from the lake water continues into the fall/winter season after the surrounding land has frozen. This can trigger downwind snow squalls in the fall and early winter, as seen in satellite images over the northern Great Lakes region (Rouse, 2008a), and increased snow water equivalent downwind from larger lakes in the Mackenzie River Basin (Rouse, 2008b).

Recent work by Kunkel et al., (2009a) in the Laurentian Great Lakes area examined lake-effect snowfall trends using a newly created temporally homogenous data set of station snowfall records (created by Kunkel et al. 2009b). Using the new dataset, they found similar trends to previous studies with increasing lake-effect snow (e.g. Norton and Bolsegna, 1993; Ellis and Johnson, 2004) however with less magnitude in the identified trends than previous work using the uncorrected dataset of station snowfall records. They suggest that the trends shown in the lake-effect snowfall are related not only to the warming surface water and decreasing ice cover on the lakes (identified by Assel, 2003) but also to changes in the large-scale synoptic patterns that affect the cold-air outbreaks - an area which they identify to need further research.

2.4.2 The role of lake ice on gas exchanges with the atmosphere

Accurate atmospheric green house gas budgets are important for any future projections of climate, and lakes are an important source of the atmospheric green house gasses such as carbon dioxide

(CO_2), methane (CH_4), and nitrous oxide (N_2O) (e.g. Walter et al., 2006). These gases can accumulate under the ice cover throughout the winter and result in a pulse of emissions upon ice melt that is not generally considered in surface-atmosphere flux estimates (Striegl et al., 2001). Large releases of CO_2 (Cole et al., 1994; Huttunen et al., 2004) and CH_4 (Huttunen et al., 2001) to the atmosphere after ice-melt have been observed. CH_4 emissions were found to be related to the amount of O_2 present in the water, with eutrophied lakes in Finland releasing large amount of CH_4 after ice melt and oligotrophic-mesotrophic lakes in Finland not releasing a substantial amount of CH_4 (Huttunen et al., 2001, 2004). While the trophic state of the lakes was shown to affect the CH_4 emissions, all of the lakes measured had large CO_2 emissions at spring melt (Huttunen et al., 2001, 2004).

Ebullition can be responsible for more than 95% of CH_4 released from northern lakes, but it is not usually measured due to the patchy nature of bubble formation (Walter et al., 2008). Bubbles trapped in the ice cover as it forms across a lake can be used to determine the amount of CH_4 released from the lake sediments during the ice-covered season (Walter et al., 2006). Current estimates of northern wetland CH_4 emissions were increased by up to 63% when ebullition amounts from Siberian thermokarst lakes were included (Walter et al., 2008). Walter et al. (2008) show how early season Synthetic Aperture Radar imagery can be used to achieve lake-wide estimates of CH_4 released from ebullition in Alaskan lakes by mapping bubble clusters. They also suggest that this method could be used to determine regional and pan-arctic estimates of CH_4 released from ebullition (Walter et al., 2008). Walter et al. (2007) determined that tens of thousands of teragrams of CH_4 will be released from thermokarst lakes as the permafrost thaws in the future, but emissions will be reduced after the permafrost is gone due to a predicted reduction in total lake area (as a result of the changes to the thawed permafrost).

2.4.3 Thermal moderation and energy exchange

In addition to being affected by regional climate, lake ice can also play a role in the surrounding regional climate. During the early open water season, lakes can cool the surrounding land with lake breezes (Rouse, 2008a), however, as the air temperatures drops in the fall/early winter, the lakes can become a source of heat to the atmosphere with increased evaporation and downwind snow squalls (lake-effect snow). With the ice cover removed, turbulent fluxes increase and net radiation, no longer contributing to ice melt, increases the heat storage in the lake, with the amount of heating depending on the size/depth of the lake. Rouse et al. (2008a) outline the response of different sized lakes to the

energy balance after ice cover has melted. Small lakes heat rapidly and evaporation begins early in the season, with the lakes reaching their maximum storage in mid-summer and cooling quickly in the fall. Surface heating takes longer for medium sized lakes, delaying the increase in latent heat flux and sensible heat flux after ice melt, but the heat storage possible in the medium sized lakes then prolongs the latent heat flux and sensible heat flux until fall/early winter. In the case of large lakes, net radiation is the primary means of heating in the spring (Schertzer et al., 2000) and due to the deep thermal mixing and large volume of water, turbulent fluxes from large lakes do not typically begin until the summer, reaching a maximum in the fall/early winter (Rouse et al., 2003; Rouse et al. 2008b) until cooling is sufficient to allow ice formation to occur (Rouse, 2008a).

An example of the effect that lakes can assert on their surroundings can be found in Rouse et al. (2008b), who compared the measured energy balance between a landscape with lakes and without lakes. They have shown that the average evaporation lasts three months longer (fall/early winter) in a landscape with lakes versus one without (Figure 2.6). Although the turbulent fluxes from lakes stop with the formation of ice cover, conductive heat flow continues through the snow and ice. Heat flow through the ice decreases as the thickness of snow and ice increases (Jeffries and Morris, 2006). Jeffries and Morris (2006) showed that the heat flow through snow/ice-covered lakes reflects different weather conditions across Alaska, in particular air temperature and wind, and the wind effects on snow density and depth. Their estimated value of conductive heat loss through the winter for Great Slave Lake was 7 ± 1 x10^{11}MJ, showing that this heat transfer mechanism through snow and ice deserves more attention, especially in areas with large ice covered lakes (Jeffries and Morris, 2006).

2.4.4 Representation of lake ice in regional climate and weather prediction models

Lakes are an important part of the climate system, as seen in the previous sections, and should be accounted for in climate models. At present, most numerical weather prediction (NWP) models do not include lakes, or crudely represent lakes since many lakes are small at the sub-grid scale (Mironov, 2008). As resolution in Global Circulation Models (GCMs) and Regional Climate Models (RCMs) increases with computer processing advances, there is a need to parameterize lakes/lake ice in order to correctly capture the effects of the climate-lake interactions. A detailed review of the how lakes have been incorporated into climate modelling and how models have been used to explore the effects of climate on lakes can be found in MacKay et al. (2009).

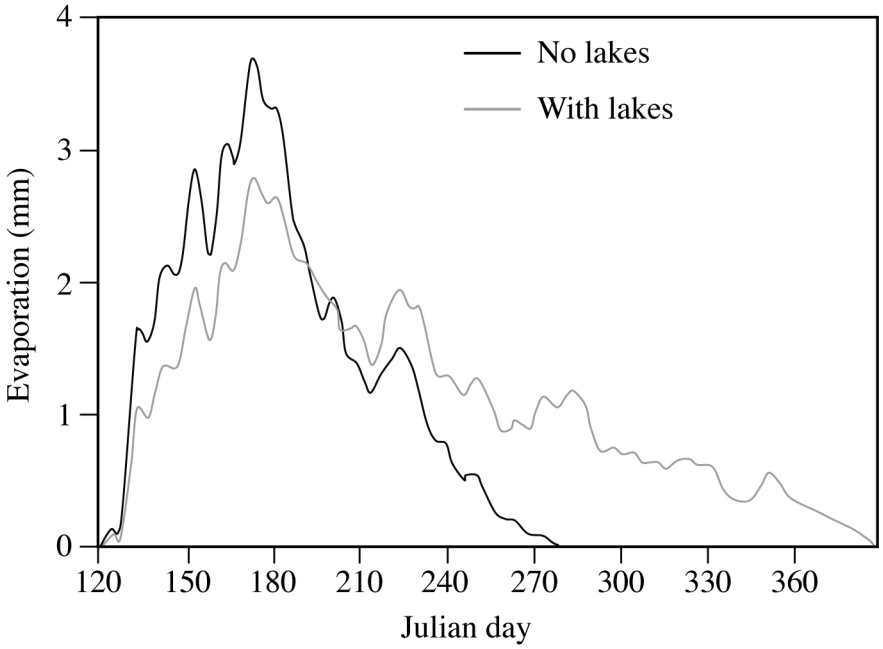

Figure 2.6. Average evaporation patterns for a region with no lakes and a region with lakes Source: Rouse et al. (2008b).

Lake representation in GCMs is particularly challenging as most lakes would be at the sub-grid scale and hence, not resolved. Lofgren (1997) examined the effects of including an idealized representation of the Laurentian Great Lakes into a GCM using a lake model calibrated by Croley and Assel (1994), which includes a lake ice component. The results showed a temperature difference between the land and water, with water surface temperatures cooler in spring and summer (up to 5°C lower in May), but higher in the fall/winter (up to 17°C warmer in December). Looking at the energy balance determined from the model with and without lakes, the extended evaporation period in the fall with lakes included is evident in the GCM simulations.

Simulations using the Canadian GEM-LAM (Global Environmental Multiscale – Limited Area Model) model (a one-way nested version, 2.5 km grid, of the GEM model used operationally by the Canadian Meteorological Service) clearly show the importance of including lake ice in climate models (ESA, 2008). The simulations compare the effects on surface air temperature between including lake ice cover and no lake ice cover (Figure 2.7) and show temperature anomalies covering regions beyond the extent of the lakes in the mean winter surface air temperatures exceeding 5-10°C in Manitoba, Northern Saskatchewan and the Northwest Territories, Canada, and parts of Eurasia.

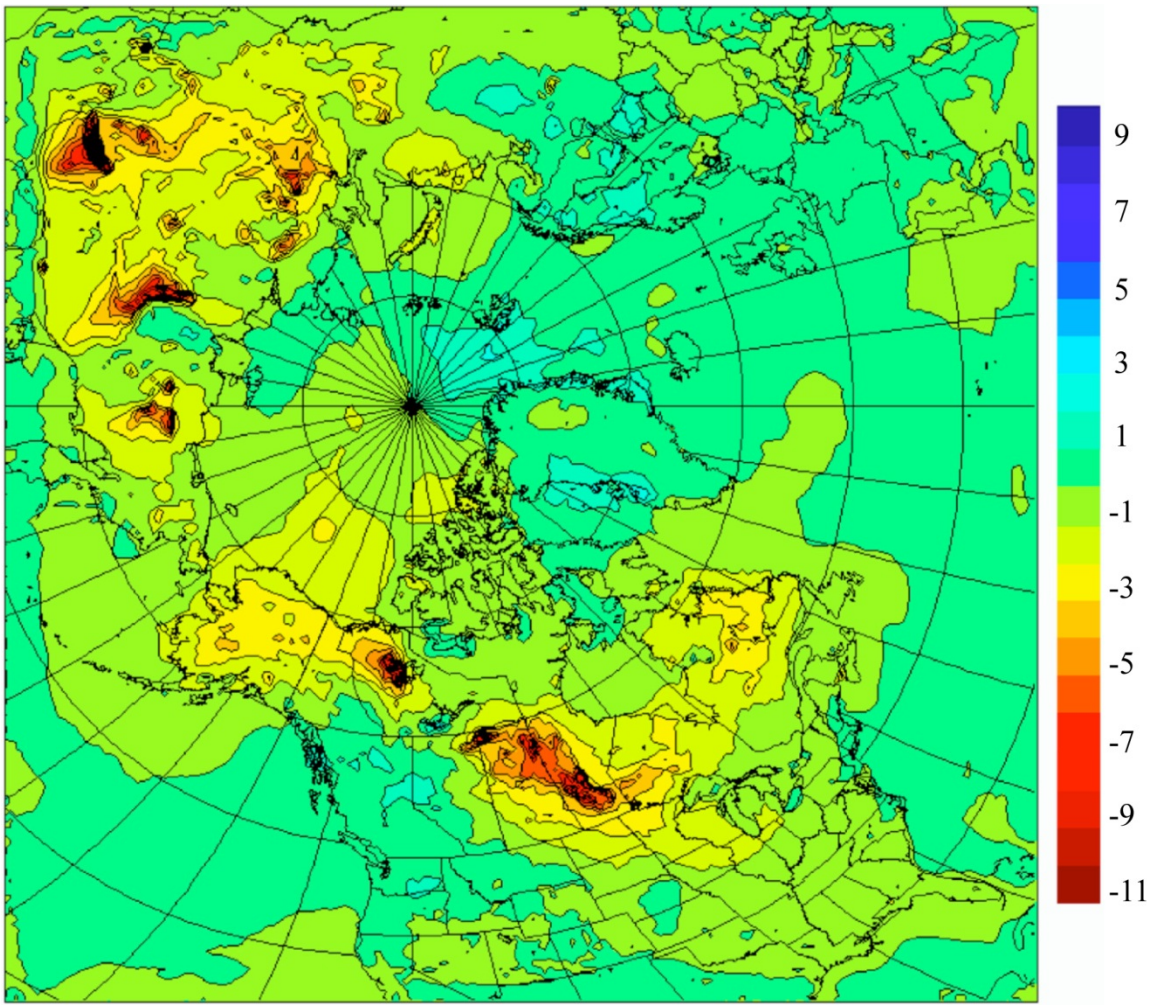

Figure 2.7. Map showing differences (°C) in mean winter air temperature obtained with the Canadian GEM- LAM model (with-ice minus without-ice on lakes). The largest differences (negative values in the legend) are found over large lakes such as Lake Winnipeg, Great Bear Lake, Lake Baikal, and surrounding areas.: ESA (2008).

Using RCMs is one method for downscaling GCM output to the regional scale, as well as for regional weather forecasting. By coupling lake models with atmospheric models, ice cover can be included; temperatures at the water/air interface can be better accounted for; as well as feedbacks between the atmosphere, lake/lake ice and surrounding land. The Canadian Regional Climate Model (CRCM, 45 km resolution) currently includes a lake model for the Laurentian Great Lakes (Goyette et al., 2000; de Elía, 2008). The lake model is a mixed layer model that is able to properly simulate the thermal cycle in the Great Lakes, include ice leads, and allows for redistribution of ice. Lake-effect snow and the seasonal evolution of ice cover are simulated realistically; however, the model

underestimated the monthly mean ice concentrations (Goyette et al., 2000). Simulations without the lake model over the Great Lakes region reduced precipitation downwind by 1mm d^{-1} on average and accumulation 3-7 kgm^{-2} less than simulations with the lakes included (Goyette et al., 2000). Several other studies have examined the effects of including the Laurentian Great Lakes in RCMs, also finding better simulation results (e.g. Bates 1993, Bates 1995).

Looking at western Canada, MacKay et al. (2009) provide an example of the representation of the numerous lakes in the Boreal region in the CRCM (Figure 2.8) and discuss the need to develop a suitable atmosphere-land surface-lake model that represents both the energy and mass flows between lakes and their surroundings.

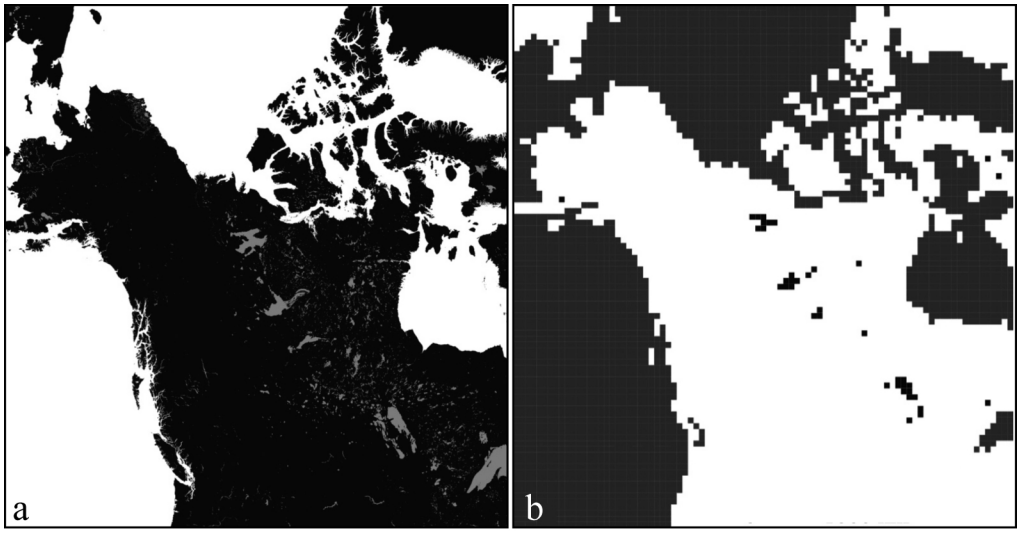

Figure 2.8. Distribution of North American Lake: (a) on the basis of satellite remote sensing; (b) as resolved by a typical simulation of the Canadian Regional Climate Model. Modified from: MacKay et al. (2009).

Long et al. (2007) coupled the CRCM with the Princeton Ocean Model (POM) for the Mackenzie River Basin to simulate the effects of Great Bear Lake and Great Slave Lake on regional climate. Coupling the models provided better surface temperature estimates than uncoupled simulations. Results suggest that Great Bear and Great Slave Lake reduce the amount of snow on the ground in the areas around the lake as a result of the heat source provided by the lakes. The coupled model also improved estimates of heat fluxes from lakes and water temperatures, however Long et al. (2007) note that the representation of ice is simplified, with the surface temperature holding at 0°C until the lake is ice free. FLake, a model that is intended for lake parameterization in weather forecasting

models or climate models and includes a lake ice cover component (Mironov et al., 2007; Mironov, 2008; Mironov et al., 2010), is under consideration for coupling with the CRCM (Nagler et al., 2008). To date is has been implemented in several RCMs and NWP models and is also used as a lake parameterization module in several surface schemes. Mironov et al. (2007, 2010) described how FLake improved the lake surface temperatures when included in the NWP COSMO (Consortium for Small-scale Modelling) by allowing for interactions with the climate and as a result COSMO was better able to simulate temperatures and ice phenology of lakes with FLake incorporated than without (Mironov et al., 2007) and incorporating FLake was found to correct a significant overestimation of lake surface temperatures typically encountered with the COSMO sea surface temperature analysis (used to represent lake surface temperatures) (Mironov et al., 2010). FLake is also being implemented as a parameterization scheme for lake surface temperature / ice cover in the NWP High Resolution Limited Area Model (HIRLAM) (Eerola et al., 2010).

A comparison of lake surface temperatures simulated by eight one-dimensional models suitable for coupling with RCM's was done by Stepanenko et al. (2010) as part of the Lake Model Intercomparison Project (Including: DYRESM, Hostetler's model, MINLAKE 96, FLake, Goyette's model, and three others). All performed well on the small lake tested, but good agreement was not shown for simulations of surface temperatures for Lake Michigan suggesting that the three dimensional processes involved in large lakes need better parameterization in the models compared (Stepanenko et al., 2010).

2.5 Summary and future directions

Lake ice has been shown to respond to climate variability; particularly changes in air temperature and snow accumulation. Both long-term and short-term trends have been identified in ice phenology records and are typically associated with variations in air temperatures; while trends in ice thickness tend to be associated more with changes in snow cover. Variability in the ice cover has also been related to teleconnections as they affect the overall circulation patterns and hence influence local climate, offering further explanation for the observed inter-annual variances in ice cover. Varying the years analyzed results in differing trends, highlighting the importance of the extent of the time series for interpreting trend data. Specific months correlate best to phenological events depending on location, with November/December affecting the Laurentian Great Lakes region versus September/October in Alaska for freeze-up, and January to March in the Great Lakes region versus April/May in Alaska. Increased snow fall results in thicker ice cover, mainly due to an increase in

snow-ice formation, while reducing the snow cover below a certain point will also result in thickening of the ice cover due to less thermal resistance.

The role of ice cover in the regional climate is less documented, however several studies have noted the effects of increased evaporation and downwind precipitation (lake-effect snow) in the fall and winter seasons from partially ice covered or ice free lakes. During the break-up season, ice cover remaining on the lake after the surrounding land has warmed can have a cooling influence on the local/regional climate, while in the freeze-up season, the formation of an ice cover will stop the heating of the local/regional climate by stopping the turbulent fluxes between the water and the atmosphere (while conductive heat transfer through the ice and snow continues through the ice covered season).

Including lakes and lake ice in climate modelling is an area of increased attention in recent studies. Not all GCM/RCM/NWP models parameterize lakes; however, simulations that include parameterized lakes when coupled to lake models (including ice cover) have presented results that are closer to observed values. The incorporation of remote sensing data into modelling can contribute to advancements in the predictive abilities of lake/lake-ice models by providing possible improvements to input parameters and improving the ability to incorporate lakes at the sub-grid cell scale. If temperatures rise as predicted for the Northern Hemisphere, lakes will have longer open water seasons, resulting in increased evaporation. This example highlights the importance of correctly simulating climate variables that are directly affected by lakes.

There has been a noted decline in in situ lake ice observation networks in recent years (e.g. Nagler et al., 2008). Remote sensing products can provide some ice observations where no in situ data exists – however the current products available are not suitable for many of the important lake ice parameters due to their spatial and temporal limitations (Nagler et al., 2008). Another method to address the lack of surface-based networks is to use ice observations collected by volunteers, for example Futter (2003) using data from the 'IceWatch' program – Canadian lake ice observations by citizens; Jeffries and Morris (2006) using data collected by teachers and students as part of the Alaska Lake Ice and Snow Observatory Network (ALISON); and Dyck (2007) discussing long term monitoring of Crazy Lake, Nunavut by Nunavut Arctic College students.

An important step in improving predictions of ice conditions in models is the assimilation of remote sensing data in areas where in situ data is lacking, or non-representative of the lake conditions. For example, Jeffries et al. (2005) noted that local data for air temperature (and snow on ground)

resulted in better ice cover simulations than data from the nearest weather station, which may be some distance from the site. In the data-sparse northern regions, this discrepancy between weather stations and local climate is particularly pronounced, as the nearest weather station may not be representative of the local climate. Improving the albedo parameterizations in lake ice models is also an important step for improved simulations. Since the surface albedo will change depending on the snow cover or ice type, a parameterization method that accounts for ice composition could result in a more realistic albedo (Jeffries et al., 2005a; Morris et al., 2005), and incorporating remote sensing albedo data into ice cover simulations for larger lakes could be beneficial to capture daily changes. Accurate snow depth measurements may be difficult to attain, and using snow data from remote weather stations as input to lake ice models can be unrealistic at the local scale. Using snowfall records to represent depth of snow on the ground is sometimes necessary; but weather station records have a tendency for snow undercatch (Goodison, 1981). The ability to obtain variables such as on-ice snow depths at fine spatial resolutions, such as that presented by the upcoming satellite mission CoReH20 (Nagler et al., 2000) will be extremely beneficial for accurate modelling, leading to improvements in climate simulations using RCMs and GCMs with the inclusion of lake ice components.

One of the most important aspects for improving the parameterization of lakes in climate modelling is to accurately represent the surface temperature of the water (or ice). The ability to incorporate satellite-based or in-situ observations of lake surface temperatures into models coupled with NWPs would be expected to produce better results (Eerola et al., 2010). Climate simulations which included lake models found improved results as the interactions between the water/ice and atmosphere were better represented. Coupling lake/lake ice models with an RCM or GCM will be increasingly important as resolution of climate models increase (Mironov, 2008) and more of the smaller lakes are resolved.

2.6 Acknowledgements

The authors wish to acknowledge funding support from NSERC (Canada Graduate Scholarship to Brown and NSERC Discovery Grant to Duguay). The constructive comments and suggestions from the reviewers were greatly appreciated, in particular from Drs. Magnuson and Benson.

Chapter 3
A comparison of simulated and measured lake ice thickness using a Shallow Water Profiler

3.1 Introduction

Lakes comprise a large portion of the surface cover in the northern boreal and tundra areas of Northern Canada forming an important part of the cryosphere, with the ice cover both playing a role in and responding to climate variability. The presence (or absence) of ice cover on lakes during the winter months is known to have an effect on both regional climate and weather events (e.g. thermal moderation and lake-effect snow) (Rouse et al., 2008b). Lake ice has also been shown to respond to climate variability; particularly changes in air temperature and snow accumulation. Both long-term and short-term trends have been identified in ice phenology records and are typically associated with variations in air temperatures; while trends in ice thickness tend to be associated more with changes in snow cover (Brown and Duguay, 2010).

During the ice growth season, the dominant factors that affect lake ice are temperature and precipitation. However, once the ice has formed, snow accumulation on the ice surface then slows the growth of ice below due to the insulating properties as a result of the lower thermal conductivity (thermal conductivity of snow, 0.08 - 0.54 $Wm^{-1}K^{-1}$ versus 2.24 $Wm^{-1}K^{-1}$ for ice, (Sturm et al., 1997)). Snow mass can change the composition of the ice by promoting snow ice development, and hence influence the thickness of the ice cover (Brown and Duguay, 2010).

In northern regions where observational data is sparse, lake ice models are ideal for studying ice cover regimes as they can provide valuable information including timing of break-up/freeze-up, ice thickness and composition. Several different types of models have been used to investigate the response of lake ice to external forcing(s), with varying degrees of complexity such as regression or empirical models (e.g. Palecki and Barry, 1986; Livingstone and Adrian, 2009); energy balance models (e.g. Heron and Woo, 1994; Liston and Hall, 1995b) and thermodynamic lake ice models (e.g. Vavrus et al., 1996; Launiainen and Chang, 1998; Duguay et al., 2003). Application of these models has been effective in examining the effects of altering the air temperatures and snow depths on lake ice thickness by sensitivity analysis (e.g. Vavrus et al., 1996, Ménard et al., 2002, Morris et al., 2005). Overall, changes in snow depths had more of an impact on ice thickness than changes to air temperatures. Decreasing the amount of snow cover tended to result in thicker ice formation (Brown

and Duguay, 2010). However, snow with higher snow water equivalent accumulating on the ice surface can also lead to an increase of ice thickness as a result of increased snow ice formation (Korhonen, 2006).

Modelling provides an opportunity to further understand the interactions between lake ice and climate, which is important for examining potential changes in northern ice regimes under future anticipated changes in the climate system. However, before future conditions can be explored, models need to be validated against current conditions to improve predictions. Validation of modelled ice thickness in northern Canada presents unique difficulties as frequent sampling is not logistically feasible in remote locations and ice thickness on small lakes is not easily obtainable from remote sensing imagery. A useful tool for validation of the ice thickness is the Shallow Water Ice Profiler (SWIP) manufactured by ASL Environmental Sciences Inc. This upward-looking sonar device was developed for shallow water studies based from the well established IPS (Ice Profiling Sonar) that has been used for more than a decade to examine sea ice drafts in the polar and sub polar oceans (e.g. Melling et al., 1995; Jasek et al., 2005; Marko and Fissel, 2006). The SWIP has primarily been used to study river ice drafts to date (e.g. Jasek et al., 2005; Marko et al., 2006) and this study represents the first application of a SWIP for comparing measured ice thickness to model simulations in a shallow lake.

The objective of this study is to examine the effectiveness of the Canadian Lake Ice Model (CLIMo) at simulating ice thickness compared to in situ ice thickness measurements using an upward-looking ice profiling sonar, complemented by traditional manual measurements and digital camera imagery.

3.2 Study Area and Methodology

The selected lake for this study, Malcolm Ramsay Lake (previously known as Lake 58), is situated within the Hudson Bay Lowlands in a forest-tundra transition zone near Churchill, Manitoba (58.72°N, 93.78°W) (Figure 3.1). The lake covers an area of 2 km^2 with a mean depth of 2.4 m (maximum depth of 3.2 m) (Duguay et al., 2003). The mean annual temperature in Churchill is -6.9°C with only June to September temperatures reaching above 0°C. Total precipitation is 432 mm, with an annual snowfall of 191 cm.

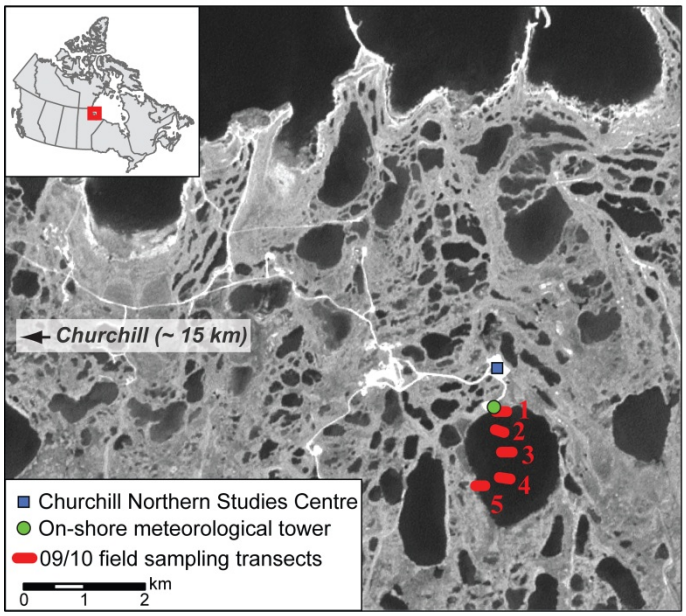

Figure 3.1. Location of Malcolm Ramsay Lake, near Churchill, Manitoba. Sampling transects shown with identifying numbers.

The model used is the Canadian Lake Ice Model (CLIMo), a one-dimensional thermodynamic model used for freshwater ice cover studies (e.g. Ménard et al., 2002; Duguay et al., 2003; Jeffries et al., 2005a, Morris et al., 2005) capable of simulating ice on and off, thickness and composition of the ice cover (clear or snow ice). CLIMo has been modified from the one-dimensional sea ice model of Flato and Brown (1996), which was based on the one-dimensional unsteady heat conduction equation, with penetrating solar radiation, of Maykut and Untersteiner (1971), i.e.

$$\rho C_p \frac{\partial T}{\partial t} = \frac{\partial}{\partial z} k \frac{\partial T}{\partial z} + F_{sw} I_o (1-\alpha) K e^{-Kz} \qquad \textbf{(1)}$$

where ρ (kg m^{-3}) is the density, Cp (J kg^{-1} K^{-1}) is the specific heat capacity, T (K) is the temperature, t (s) is the time, k (Wm^{-1} K^{-1}) is the thermal conductivity, z (m) is the vertical coordinate, positive downward, F_{sw} (Wm^{-2}) is the downwelling shortwave radiative energy flux, I_o is the fraction of shortwave radiation flux that penetrates the surface (a fixed value dependent on snow depth), α is the surface albedo, and K is the bulk extinction coefficient for penetrating shortwave radiation (m^{-1}).

The surface energy budget can then be calculated:

$$F_o = F_{lw} - \varepsilon\sigma T^4(0,t) + (1-\alpha)(1-I_0)F_{sw} + F_{lat} + F_{sens} \qquad \textbf{(2)}$$

where F_o (Wm^{-2}) is the net downward heat flux absorbed at the surface, ε is the surface emissivity, σ is the Stefan–Boltzmann constant (5.67×10^{-8} Wm^{-2} K^{-4}), F_{lw} (Wm^{-2}) is the downwelling longwave radiative energy flux, F_{lat} (Wm^{-2}) and F_{sens} (Wm^{-2}) are the latent heat flux and sensible heat flux respectively (both positive downward) (Ménard et al., 2002, Jeffries et al., 2005a).

CLIMo includes a fixed-depth mixed layer in order to represent an annual cycle. When ice is present, the mixed layer is fixed at the freezing point and when ice is absent, the mixed layer temperature is computed from the surface energy budget and hence represents a measure of the heat storage in the lake. The water column of shallow lakes is typically well-mixed and isothermal from top to bottom during the ice-free period, permitting the mixed layer depth to be a good approximation of the effect of lake depth leading to autumn freeze-up (Duguay et al., 2003).

Melt at the upper surface of the ice is determined by the difference between the conductive flux and the net surface flux; the snow (if any) on the ice surface is melted first and the remaining heat is used to melt the ice. The growth and melt of the ice cover at the underside is determined by the difference between the conductive heat flux into the ice and the heat flux out of the upper surface of the mixed layer. The shortwave radiation that penetrates through the bottom of the ice cover is assumed to be absorbed by the mixed layer and returned to the ice underside in order to keep the temperature of the mixed layer at the freezing point (Duguay et al., 2003). The current version of the model includes a simplified heat exchange between the water column and the lake sediments in the form of a constant heat flux, rather than a varying heat flux that fully captures the annual cycle; this is an area that will be addressed in a future version of the model.

Snow ice is created by the model if there is a sufficient amount of snow to depress the ice surface below the water level. The added mass of the water filled snow pores (slush) is added to the ice thickness as snow ice. The amount of snow ice formed (if any) is not taken into account when melting the ice slab. The albedo parameterization in CLIMo is based mainly on surface type (ice, snow, or open water), surface temperatures (melting versus frozen), and ice thickness, with no distinction regarding ice composition. A more detailed description of CLIMo can be found in Duguay et al. (2003).

The model was driven by daily on-shore meteorological data from an Automated Weather Station (AWS) using Campbell Scientific equipment. Input data for the model included air temperature and relative humidity (HC-SC-XT Temperature and Relative Humidity probe), wind speed (RM Young Wind Monitor), and snow depth (SR50A Sonic Ranging Sensor). In addition to the AWS data, cloud

cover data was obtained from the Meteorological Service of Canada's Churchill weather station, located approximately 16 km to the west. A modification to CLIMo was made for this study to incorporate measured incoming solar radiation at the AWS (CNR-1 Net Radiometer) rather than the model's internal calculations for solar radiation based on latitude and cloud cover. A second modification to CLIMo was made wherein measured snow density values from on-ice measurements (ranging from 171.1 kgm^{-3} to 364.3 kgm^{-3} over the season) were used rather than a fixed value for cold and warm snow. All model simulations used the weekly snow measurements made on-ice during the 2009/10 season. A Campbell Scientific digital camera (CC640 Digital Camera) was installed on the AWS, capturing hourly images of the lake to allow for on-site observations of the ice processes. In order to account for snow redistribution across the lake ice surface, the ice cover for two seasons (2008/09 and 2009/10) was simulated using a series of snow cover scenarios (0%, 5%, 10%, 25%, 50% and 100% of the on-shore snow cover depths).

In order to validate and improve the model results, in situ measurements of the ice cover formation and decay were obtained using a Shallow Water Ice Profiler (SWIP) - an upward-looking sonar device installed on the bottom of the lake within the field of view of the digital camera. The SWIP consists of a 546 kHz acoustic transducer, pressure transducer, thermometer, two axis tilt sensors and a battery pack capable of long deployments (Figure 3.2). The SWIP was programmed for target detection, collecting target data (scanning the water column for acoustic backscatter returns from a target e.g. ice, water-air interface) every 1 second (10 seconds from January to March) and measuring instrument temperature, pressure, and tilt data every 60 seconds. On-shore barometric pressure at the AWS (61205V Barometric Pressure Sensor) was used in combination with the pressure transducer on-board the SWIP to determine local water levels over the seasons. The acoustic ranges to the bottom of the ice cover measured by the SWIP were corrected for the instrument tilt, variations to the speed of sound in water (based on temperature) and subtracted from the local water levels to determine the thickness of the ice (see Marko and Fissel, 2006; Melling et al., 1995).

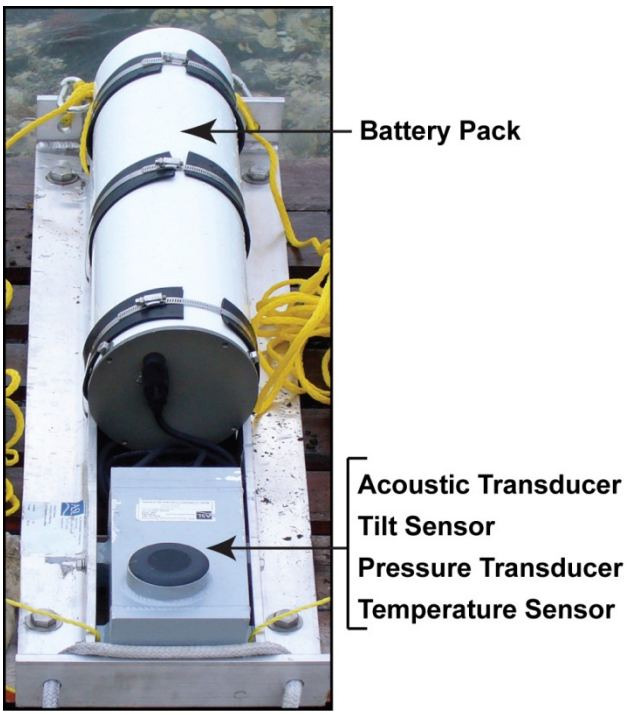

Figure 3.2. Shallow Water Ice Profiler.

During the spring of 2009 (April 13 to June 27), weekly measurements of on-ice snow depth, thickness of the snow ice layer (if present) and total ice thickness were obtained (approximately four samples averaged for each per sampling date). Throughout the ice covered season of 2009/10 (November 15, 2009 to April 6, 2010) five transects were used for sampling (see Figure 3.1), weekly measurements were taken of on-ice snow depth (100 depth samples from each of the five transects); on-ice snow density (ten samples for each of the five transects); thickness of the snow ice layer (if present) and total ice cover thickness (five samples for each of the five transects). The sampling transect closest to the location of the SWIP was used for comparison between the SWIP, simulated ice thickness and on-shore snow depths.

One challenge in comparing simulations to observations of ice cover is the differing definitions used. Freeze-up and break-up are observable processes occurring over time and space, whereas the SWIP data is at a single point in the lake and the simulated freeze-up and break-up dates from the model are an instantaneous, one-dimensional, event based on ice thickness (Jeffries et al., 2005a). In order to minimize discrepancies in terminology, the date at which the simulations formed a permanent cover for the season is referred to as complete freeze over, while the first day of open water simulated

is referred to as water clear of ice. The SWIP freeze-up and break-up dates are defined as the first date when ice/open water is detected above the sensor. The camera imagery is more subjective, and freeze-up is defined as the time between first visible ice in the camera view (freeze-onset) until a solid ice cover is formed (complete freeze over). Surface ice decay is defined as the time from when a portion of ice is visibly beginning to melt (snow free, wet/slushy surface) and break-up is defined as the date from the first appearance of open water until the water is free of ice (water clear of ice). The ice season referred to throughout the paper is defined as the time from ice formation in the autumn to water clear of ice in the following summer.

3.3 Results and Discussion

3.3.1 Field measurements and observations of the ice cover

3.3.1.1 2008/09 season

Ice formation was visible periodically in the camera imagery starting on October 20 and formed a solid cover by October 27. The SWIP detected the ice formation on October 26 (Figure 3.3a, Figure 3.4). The ice thickened throughout the season until March 22, 2009 (143 cm) at which point it exceeded the lower limit of the detection ranges programmed into the SWIP. However, field measurements provided the ice thicknesses during the time the SWIP was unable to record the lower levels of the ice cover (maximum ice thickness sampled was 165 cm on June 5). Visible ponding, shushing and surface melt were seen in the camera imagery from approximately June 11 – July 9, with the first open water visible on June 26 (Figure 3.3c). Field measurements of on-ice snow thickness showed the absence of snow cover on the lake ice by June 11, with the SWIP detecting water levels rising after this date. An interesting event was noted in the SWIP readings during the ice cover decay. The tilt data from the sensor showed it being slowly tilted on both on the vertical and horizontal axes for a number of days beginning on June 14, tilting as far as 20° on the horizontal axis before returning to a steady near-level by June 27. This event is likely attributed to the ropes that were attached to the back-end of the SWIP frame for retrieval purposes being frozen into the ice, pulling the sensor and frame upwards as the ice cover rose with the influx of snowmelt before melting/breaking free of the ice draft. The SWIP detected open water by July 7, resulting in an ice cover duration for the 2008/09 season of 252 days. While the camera images also show open water in the approximate location of the SWIP on this date, floating ice continues to drift through the camera field of view until July 9 (Figure 3.3d).

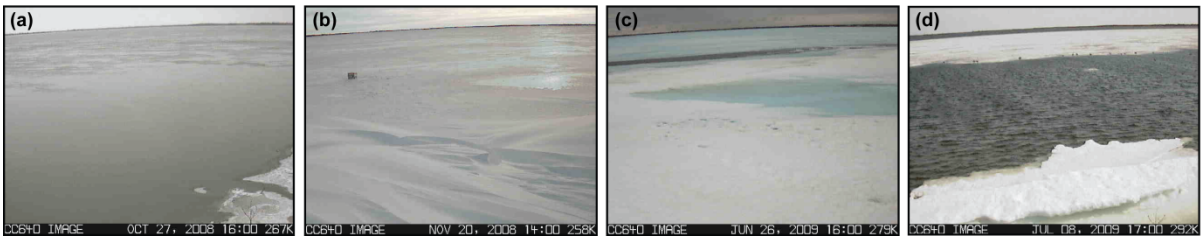

Figure 3.3. (a) Ice cover formation (Oct. 27, 2008), (b) snow redistribution on the ice surface (Nov. 20, 2008), (c) ice break-up in progress with open water and slush visible on the ice surface (Jun. 26, 2009), and (d) redistribution of floating ice pans just prior to the end of break-up (Jul. 8, 2009).

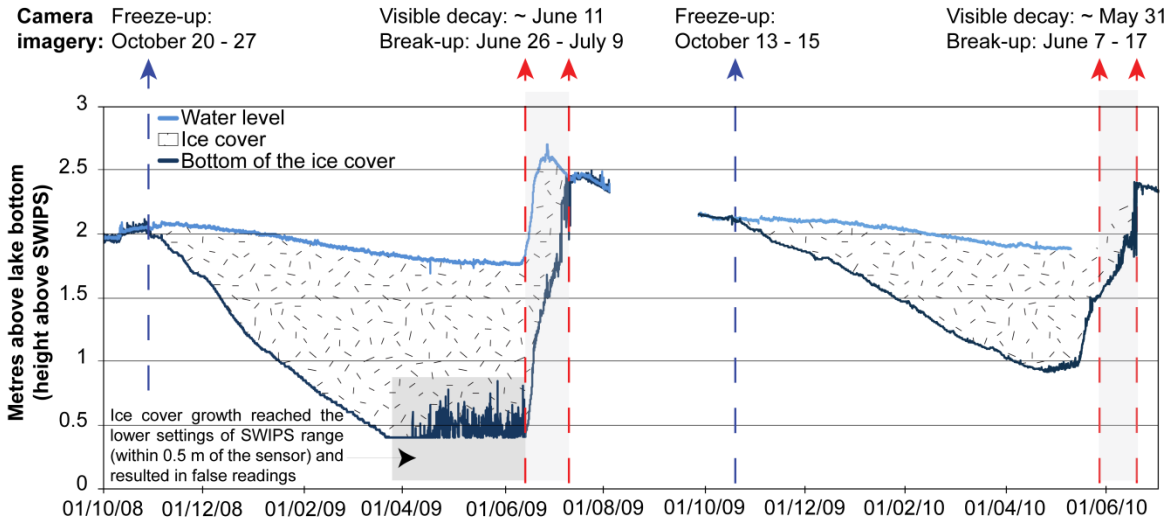

Figure 3.4. Water level and ice cover ranges measured by the Shallow Water Ice Profiler. Coinciding dates of events observed from the digital camera noted above graph.

3.3.1.2 2009/10 season

During the 2009/10 ice cover season, ice formation was detected by the SWIP on October 14 and seen from the camera imagery on October 13, with a solid cover formed by October 15. Snow began accumulating on the ice surface by early November, with brief snow cover on October 20 - 22. Thickening of the ice cover occurred until the maximum depth was reached on April 15 (98 cm) based on the SWIP and measured manually at 94 cm (as of March 29 at the sampling location nearest the SWIP). The camera imagery showed a section of the ice to be snow free on May 10, snow

covered again from May 21 - 30, visibly melting from May 31 and open water appearing by June 7. Water levels from the SWIP were not available during the melt season due to a power supply issue, which prevented the calculation of the ice thickness after May. Both the SWIP and the camera imagery detected open water on June 13, followed by moving ice floes on June 14, and returning to open water by June 15 (with the exception of near shore ice seen in the imagery, which was fully melted by June 17). The 2009/10 ice season was on average 4°C warmer than 2008/09 season (Table 3.1). This resulted in a thinner ice cover forming, allowing for a complete season of ice readings from the SWIP, with an ice cover duration of 243 days.

Table 3.1. Comparison of monthly average air temperatures (°C) between the two ice seasons.

	Oct	Nov	Dec	Jan	Feb	Mar	Apr	May	Jun	Jul
2008/09	1.09	-8.48	-26.11	-23.21	-23.02	-21.42	-8.17	-6.65	2.46	7.93
2009/10	-0.46	-6.57	-20.59	-21.27	-19.52	-10.04	-3.48	-1.81	6.97	13.88

3.3.2 Snow cover variability on the lake ice surface

Snow cover is known to be an important determinant for lake ice thickness. Snow redistribution by wind and associated changes in depth and density of the snow pack contribute to variations in ice thickness (Brown and Duguay, 2010). Weekly snow depth and density measurements during the 2009/10 season highlight the variability present in the snow cover across the lake surface both spatially and temporally (Figure 3.5). The snow density and depth measurements fluctuate throughout the season differently at each of the transects (for locations, see Figure 3.1), with the most variability found at one of the central lake locations (Transect 4). Seasonal average density increases with distance from shore for Transects 1 through 3, with the highest densities found at Transect 4; while Transect 5, which was situated along a shallower shoreline, had densities in the mid-range of the others. Expectedly, snow depth tended to be slightly higher towards the shore overall (e.g. Adams and Roulet, 1984), however the highest snow depths measured were from a central lake transect (Transect 4) on April 6 (30 cm), a 12.1 cm increase from the previous measurement. An increase of only 5 cm was measured on the same date at the near-shore transect (Transect 5), while on-shore snow accumulation during this time was 18 cm during the snowfall events on April 5 and 6 - again highlighting the variability present in the snow cover across the lake. The thickest ice was measured in March at Transect 3 (111 cm), however no April measurements were available.

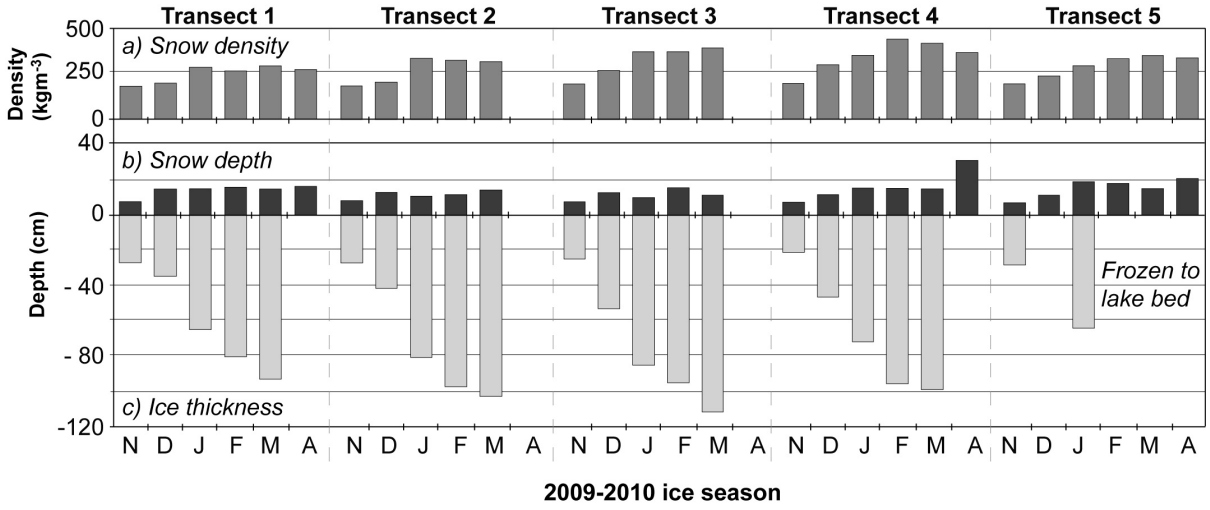

Figure 3.5. (a) Monthly average density (kgm-3), (b) snow depth (cm) and (c) ice thickness (cm) from sampling transects on the lake ice surface 2009/10. Location of the transects shown in Figure 3.1.

A monthly summary of the 2009/10 snow measurements and ice thickness can be found in Table 3.2. Snow depth had little variation from December - March, with spring snowfalls increasing the depth (no on-ice measurements from May were available). Snow density increases throughout the season, with the exception of the April measurements, which consisted of only one date. Comparing the snow depths measured at Transect 1 (the nearest transect to the location of the SWIP) to the snow depths on shore at the AWS shows a ratio of 25% snow-on-ice to show-on-shore (Figure 3.6). Seasonal variations are noted in early 2009 with a ratio of 10% and 23% before and after the spring snowfall events. The large difference between the measured snow depth on the ice and at the AWS is due to a combination of redistribution by wind over the lake ice surface, and drifting and trapping of snow by the shrubs beside the AWS on shore.

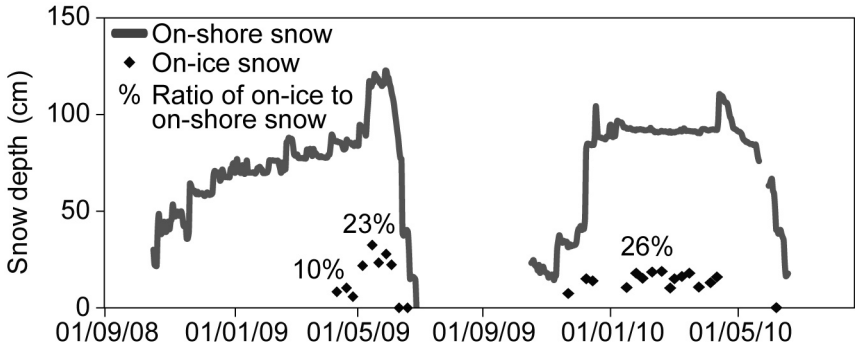

Figure 3.6. Comparison of the measured snow depth on shore at the AWS and on the ice from field sampling and the ratio between them.

Table 3.2. Monthly average of the mean and standard deviation of lake-wide snow and ice measurements (2009/10).

	Snow depth (cm)		Snow density (kgm^{-3})		Ice thickness (cm)	
	mean	Stdev	mean	Stdev	mean	Stdev
Nov.	7.2	0.5	195.3	5.7	25.7	2.8
Dec.	12.2	1.3	248.0	42.7	43.9	7.9
Jan.	13.4	3.7	335.3	34.9	72.0	8.4
Feb.	14.7	2.2	355.4	63.6	92.0	7.8
Mar.	13.5	1.6	362.1	49.4	101.7	7.5
Apr.	21.9	7.5	334.4	43.5		

Previous work by Duguay et al. (2003) showed through modelling that much of the variability in ice thickness and break-up dates were driven by snowfall. Several studies have examined the effects on lake ice thickness through altering snow depths; finding overall, that decreasing the amount of snow cover resulted in thicker ice formation (Vavrus et al., 1996; Ménard et al., 2002; Morris et al., 2005). In order to determine the best snowfall representation for the on-ice snow depths, several simulations were generated with varying percentages of the on-shore snow depth.

3.3.3 Model simulations

Ice thickness was simulated using the following snow cover scenarios: 0%, 5%, 10%, 25%, 50% and 100% of the on-shore snow depths at the AWS (Figure 3.7). During the first season (2008/09), all simulations had complete freeze over on October 26 (Table 3.3). The ice thickened throughout the season at different rates based on the snow cover scenarios. A 0% to 25% snow cover resulted in progressively more ice growth as snow cover decreased (with little to no snow ice formation), while

50% snow cover resulted in slightly thicker ice cover than the 25%. The full snow scenario was similar to the 10% scenario until early April, at which point the formation of snow ice in the full snow scenario continued to increase the total thickness of the ice for the remainder of the season. While the 25% to 100% snow cover scenarios had fairly similar ice thickness for the first half of the ice season (< 10 cm difference between them until late February) the ratio of snow ice to clear ice differed between them (progressively more snow ice formed with increase of snow cover scenario). The maximum ice thicknesses varied between the scenarios (Table 3.4) with the least from the 25% scenario (128 cm) and maximum from the 0% scenario (176 cm). Melt began first in the 0% snow cover, briefly in mid-April then continued in late May, at which point the rest of the scenarios began melt - resulting in a variation of 13 days between the scenarios to reach water clear of ice.

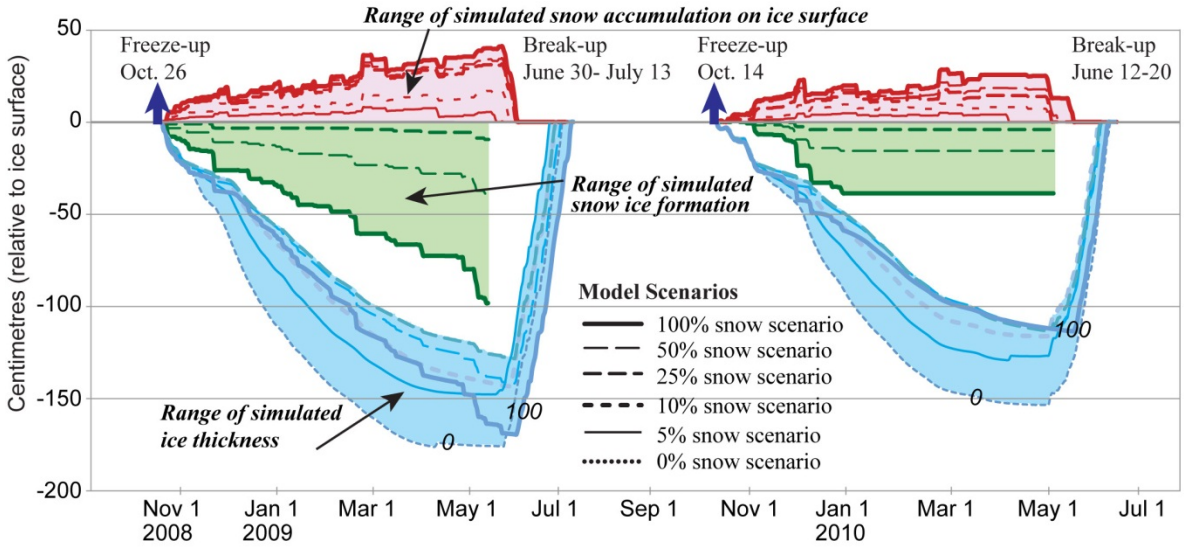

Figure 3.7. Model simulations of snow on ice, depths of snow ice and total ice thickness for each snow cover scenario (0, 5, 10, 25, 50, 100% accumulation) to represent potential snow redistribution on the ice surface. Melt is not shown for the simulated snow ice as CLIMo does not distinguish between ice compositions during melt

Table 3.3. Complete freeze over, water clear of ice and ice cover duration simulated by CLIMo for various snow cover scenarios.

Snow cover scenario (%)	2008-2009 Complete freeze over (2008)	Water clear of ice (2009)	Ice cover duration (days)	2009-2010 Complete freeze over (2009)	Water clear of ice (2010)	Ice cover duration (days)
100	Oct. 26	Jul. 13	260	Oct. 14	Jun. 18	248
50	Oct. 26	Jul. 7	254	Oct. 14	Jun. 14	244
25	Oct. 26	Jul. 3	250	Oct. 14	Jun. 13	243
10	Oct. 26	Jul. 3	250	Oct. 14	Jun. 12	242
5	Oct. 26	Jun. 30	247	Oct. 14	Jun. 13	243
0	Oct. 26	Jul. 9	256	Oct. 14	Jun. 20	250

Table 3.4. Maximum ice thickness simulated by CLIMo for various snow cover scenario simulations.

Snow cover scenario (%)	2008-2009 Maximum ice thickness (cm)	Date	2009-2010 Maximum ice thickness (cm)	Date
100	170	Jun. 8	114	May 26
50	142	Jun. 7	112	May 12
25	128	Jun. 6	114	May 11
10	143	Jun. 3	116	May 5
5	148	May 23	127	May 3
0	176	Jun. 1	154	May 6

During the second season (2009/10), the ice cover formed on October 14 for all scenarios (Table 3.3). Ice growth followed the same pattern as the 2008/09 season, with the thickest ice forming from the 0% snow cover scenario followed by the 5% and 10% scenarios, with the 25% and 50% scenarios forming slightly thinner or equal amounts as the 100% snow cover scenario. After two substantial snowfalls in December, the remaining snow accumulation during 2010 recorded by the on-shore snow sensor increased gradually (rarely more than 1 cm at a time). While snow did continue to accumulate, the weight of the additional snow was not enough to depress the ice to cause slushing and form any addition snow ice. This resulted in the 2009/10 season having less than half as much snow ice as 2008/09 for the 100% snow cover scenario (39 cm versus 103 cm). With little accumulation in the early 2010 months, the differences between the snow cover scenarios were small, resulting in similar ice thicknesses for the 25% to 100% snow cover scenarios, albeit with different ratios of snow ice to clear ice. These similar scenarios diverged during the melt season due to the differing amounts of snow on the surface that was required to melt. Maximum ice thickness did not vary as much for the 2009/10 season with 0% snow cover scenario reaching 154 cm, 5% scenario reaching 127 cm and

the rest of the scenarios ranging between 111-116 cm (Table 3.4). The removal of the ice cover was simulated between June 12 and 20 in 2010, resulting in a variation of 8 days between simulations for water clear of ice.

Despite the differing snow covers on the ice, the 25 and 50% (2008/09) and 25% to 100% (2009/10) scenarios formed similar ice thicknesses within their respective years. The ratio of snow ice to clear ice within the scenarios is, however, different. The 100% scenario for 2008/09, while similar to the 25% and 50% scenarios for the first half of the ice season, showed that the dominant means of ice growth from February to April was the addition of snow ice, indicated by the similar increases in ice thickness on dates when snow ice was formed. With less than 25% snow cover the conductive heat loss through the ice/snow exceeded the insulating properties of the thinner snow pack and thicker clear ice was formed with little to no snow ice. Previous work by Ménard et al. (2003) found the maximum ice thickness simulated became 17 cm greater for each 25% reduction in snow cover in the Back Bay area of Great Slave Lake, NWT, Canada, while Morris et al. (2005) found that the reduction of the snow cover by 100% resulted in a doubling of the total ice thickness for shallow lakes in central Alaska. Reduction of the snow cover to 50% of full snow for the Alaskan lakes resulted in slightly thinner ice as was also observed in this study. Reduction of the snow to 25% of the full snow scenario for the Alaskan lakes resulted in slightly larger maximum ice thickness than the full snow scenario whereas the present study showed slightly thinner or the same ice thicknesses from the 25% and 100% snow scenarios (with the exception of the increase as a result of snow ice in 2008/09). This pattern of reducing snow cover resulting in thinner ice to a certain threshold was also identified by Vavrus et al. (1996) for Lake Mendota (Wisconsin), where decreasing snow simulations resulted in break-up dates earlier for the 75% and 50% snow scenarios due to the reduction in insulating properties of the snow, but became delayed again for 25% and the no snow scenario as a result of the increasing conductive heat loss from the ice surface. By contrast, simulations for Barrow, Alaska (Duguay et al., 2003) show continuing increase of ice thickness with decreasing snow cover - however the differing snow cover conditions between Barrow and Churchill (mean density used for simulations in Barrow was 350 kgm^{-3}, versus 276 kgm^{-3} mean density for Churchill in this study) and lack of snow ice formed in Barrow are the expected reasons for the difference.

3.3.4 Observed versus simulated ice covers

3.3.4.1 2008/09

All of the snow cover scenarios simulated the initial ice thickening well until mid-November, at which point the simulations diverge, with the 10% - 100% snow cover scenarios thickening more gradually than the measured ice thickness (Figure 3.8). After this divergence, the 5% snow cover scenario most closely matched the measured ice thickness. This shift in the ice thickness regime is likely related to the substantial redistribution of the initial snow cover that occurred just prior to November 20 (Figure 3.3b). While the 5% snow cover scenario simulated the measured SWIP data through the winter to the loss of the SWIPS record (end of March), field measurements indicate the ice to be thicker than that produced by the 5% simulation. Throughout May, several snowfall events occurred which increased the snow depth on the ice beyond that simulated in the 5% snow cover scenario (Figures 3.7 and 3.8), with depths on ice closer to those from the 25% snow cover simulation. Virtually no snow-ice was generated by the 5% and 10% snow scenarios (approximately 1 cm), however, nearly 30 cm was measured at the onset of melt (approximately June 10), which falls between the 25% and 50% snow cover simulations. Slushing caused by the additional weight of the snow in the spring resulted in an increase of snow ice that was not captured by the reduced snow cover simulations. The full snow scenario did capture the continued formation of snow ice through the spring, resulting in the 100% scenario reaching the maximum depth of the field measurements just prior to melt – albeit with three times more snow ice simulated than measured. With less ice thickening in the spring, the reduced snow cover scenarios under-represented the total ice thickness.

Snow melt on the ice surface was simulated well for the 25% to 100% snow covers (within 2 days of observations) however, even though the 25% and 50% simulations under-represented the ice thickness, break-up occurred within 3 days of observations for those scenarios. As well, since the 0% to 10% snow cover scenarios did not correctly represent the amount of snow on the ice in the spring, they became snow free too early and hence began ice melt too early. The full snow scenario shows similar melt to the SWIP measurements until just prior to the observed water clear of ice, at which point the measurements show the remaining 50 cm of ice cover to decay fully in two days, while the full snow scenario ice cover persists a further six days. This is likely due to the one-dimensional aspect of the model not capturing any lateral heat inputs from the open water visible in the camera imagery, which would have accelerated the final decay. The discrepancy between the pre-melt thicknesses of the reduced snow cover scenarios and the measured ice thickness resulted in water

clear of ice being simulated up to seven days early, while the full snow scenario that did reach the maximum ice thickness simulated water clear of ice six days too late.

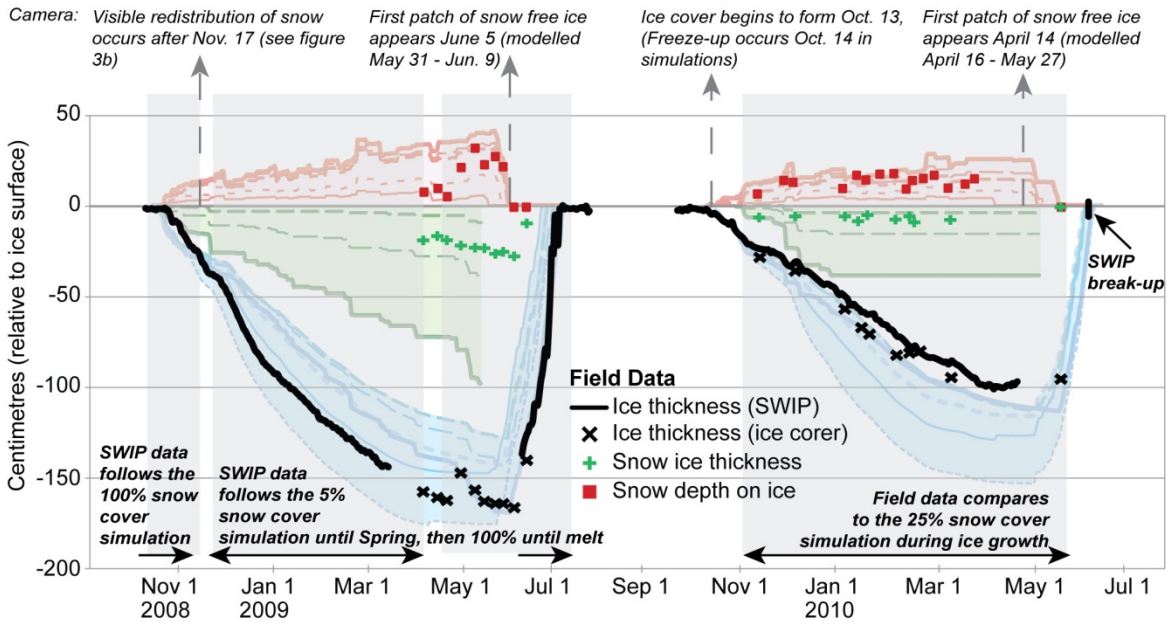

Figure 3.8. SWIP ice thickness data and field measurements of ice thickness, type and snow depth, superimposed on Figure 3.7.

3.3.4.2 2009/10

Field measurements during the 2009/10 field season show different ice conditions than those from the previous year. The first visible formation of ice was detected in the camera imagery on October 13 and by the SWIP on October 14, which coincided with the formation of ice in the simulations (October 14). Other than trace amounts of drifting near the shore, snow cover did not begin to accumulate on the ice surface until early November, with the exception of a brief snow cover from October 20 to 22. The simulated ice cover thickened similarly to the SWIPS measurements until early November, while field measurements (commencing on November 15) closely followed the patterns from the 25% to 100% snow cover simulations. Measurements show the on-ice snow depths to range between the 25% to 100% snow cover scenarios as well until February at which point measurements were closer to the 25 % snow cover scenarios. Throughout the winter season the simulations and field measurements are quite similar, however the SWIPS measurements show the ice to be slightly thinner. This discrepancy is likely a result of local variations in the ice cover, as the field

measurements were not taken directly over the SWIPS in order to avoid contaminating the sensor view. An ice thickness measurement from May 30 shows the ice decay to be within the range of the simulations. Water clear of ice ranged from June 12 to June 20 in the simulations (with the 10% to 50% scenarios all between June 12-14), compared to June 7 - 13 from the camera imagery and June 13 from the SWIP (excluding the pieces of floating ice on the 14th).

Simulations from the Fairbanks, Alaska, area done by Duguay et al. (2003) using a constant snow density for the season found that while CLIMo simulated the total thickness well, the results underestimated the snow ice thickness and they suggested that a better account of the density changes over the season might improve upon these results. Using a variable density over the season measured on-ice for this study showed the snow ice thickness simulated by CLIMo was within 1cm of the mean measurements for the season (6 cm) based on the 25% snow cover scenario which fit the snow-on-ice and total ice thickness adequately as well. This suggests that the slushing events early in the season were well represented by the model when the on-ice snow conditions were correctly represented.

3.4 Conclusions

The Shallow Water Ice Profiler is an excellent tool for monitoring lake ice growth and was able to identify areas of the model simulations that require improvements with respect to timing and thickness of the ice cover. Formation of the ice cover was well simulated for 2008/09, and the evolution of the ice cover depended on the snow cover scenario. For 2009/10 the 25% snow cover scenario simulated the ice thickness most suitably with respect to the SWIP and field data - as the ratio of snow-on-ice to snow-on-shore did not deviate greatly from 25% over the season. As well, changes to the overlying snow pack create changes in the ice thickness regimes within the season, e.g. the redistribution event in November 2008 changing the ice thickness from the 100% to 5% snow cover scenario, and snowfall on the ice May 2009 creating more snow ice than the reduced cover scenarios can represent. Changing the snow cover scenarios to represent the snow redistribution did not affect the simulated freeze-up dates but did affect the break-up dates by 13 and 8 days (2008/09 and 2009/10 respectively), highlighting the importance of snow cover on the ice.

An accurate representation of the snow conditions on the ice (depth and density) is important for attaining the correct ice thickness. Allowing the density to vary throughout the season for the simulations provided the most consistent results from the 2009/10 season - the time span when the density measurements were made; simulations were most similar to the 25% scenario for freeze-up

and break-up, snow depth on ice, snow ice and total thickness. Using those densities to represent density for other years might not be representative of the snow conditions in those years. Since no field measurements were available prior to April 2009, the percentage of the AWS snow actually on the ice surface, and its density, are unknown. As of April 2009, 10% of the snow received at the AWS is present on the ice surface, and while that ratio may have prevailed during the winter the simulations based on the 2009/10 densities suggest that a 5% snow cover scenario was present.

The maximum ice thickness for 2008/09 was captured in the simulations, although one single snow cover scenario was not able to represent the entire season. The early half of the season was similar to the 5% snow cover scenario and the latter half of the season more resembled the full snow cover scenario after the addition of the snow ice in the spring. The simulations for 2009/10 however, were able to capture the ice evolution fairly well throughout the season with the 25% snow cover scenario. The ice formed from the 25% snow cover scenario in 2009/10 was too thin compared to the one available field measurement during the melt season suggesting that melt may be occurring too quickly in the early stages of decay. The current method for albedo parameterization in CLIMo does not take snow ice into account during melt. The higher albedo from the more reflective snow ice would slow the melt rate of the ice compared to an ice cover composed of purely clear ice with a lower albedo, so the observed melt rate at this point in the season is likely slower than that from the simulations. As seen in 2008/09, the observed ice decay from the SWIPS shows accelerated melt in the final days before water clear of ice compared to the simulations, this would likely have occurred in 2009/10 as well (based on similar melt patterns on the lake from the camera imagery) and may have compensated for the early melt – resulting in break-up simulated correctly with the 25% snow cover scenario even though the melt rates may not have been captured correctly.

This suggests two separate areas of the model need to be addressed: the ratio of snow ice formation to clear ice and the albedo parameter during melt. Measurements collected on the ice surface (e.g. snow depth, snow density, snow/ice albedo) would be particularly valuable to address these issues rather than on-shore measurements, as no adjustments for snow redistribution on the ice would be required, leading to more accurate representation of snow ice/clear ice amounts. Currently, the parameterization of the albedo in CLIMo is based on measurements from High Arctic lake ice (Heron and Woo, 1994) where snow ice is less prevalent than clear ice (Woo and Heron, 1989). The use of an albedo decay model (see Henneman and Stefan, 1999) or on-ice albedo measurements within CLIMo would be advantageous for capturing the seasonal changes to albedo - especially during the melt

season when the higher albedo from snow ice (if present) would reflect more incoming radiation, slowing the absorption of solar radiation into the ice cover and reducing the melt rate.

Also, using a higher resolution setting on the camera imagery is possible and would facilitate the identification of melt onset as differentiating between snow-free and melting/slush was difficult at times. This study has illustrated how these techniques can be beneficial, not only for model validation, but also for the monitoring of ice cover on lakes since very little remains of the lake ice observation network in Canada (see Lenormand et al., 2002). While other methods of monitoring ice cover are possible (e.g. volunteer monitoring programs such as IceWatch (see Futter, 2003) or the use of remote sensing) a fully automated observing system can reduce discrepancies introduced by multiple observers, provide continuous monitoring of the ice cover, and presents another viable option for rebuilding the lost network of ice monitoring stations in Canada.

3.5 Acknowledgements

The authors would like to thank David Fissel and Adam Bard of ASL Environmental Sciences Inc. for their assistance with the configuration and processing of the SWIP data. We would also like to acknowledge Arvids Sillis and all of those who assisted in the collection of field data used in this study: Chris Derksen, Stephen Howell, Kevin Kang, Andrew Kasurak, Josh King, Merrin Macrae, Jason Oldham, Nicolas Svacina, Aiman Soliman, Peter Toose; as well as Ross Brown for providing the cloud cover data. Support for data collection from the Churchill Northern Studies Centre (CNSC) staff and Scientific Coordinator LeeAnn Fishback was appreciated. Financial support for this project was provided by NSERC to C. Duguay and CFI grants to C. Duguay and R. Kelly.

Chapter 4
The fate of lake ice in the North American Arctic

4.1 Introduction

Lakes are a major feature across northern North America, forming an important part of the cryosphere, with their ice cover both playing a role in and responding to climate variability. Future changes in ice cover conditions due to changing climate conditions could impact the role of lakes on energy, water and biogeochemical processes in cold regions as well as socio-economic impacts in terms of transportation (ice roads) and recreation.

Both long-term and short-term trends have been identified in ice phenology records and are typically associated with variations in air temperatures, while trends in ice thickness tend to be associated more with changes in snow cover (Brown and Duguay, 2010). Generally, lake ice records show trends towards earlier break-up, and later freeze-up (Northern Hemisphere: Magnuson et al., 2000; Europe: e.g. Blenckner et al., 2004; Korhonen, 2006; Palecki and Barry, 1986; Weyhenmeyer et al., 2004; Livingstone, 1999); North American Laurentian Great Lakes region: e.g. Jensen et al., 2007; Johnson and Stefan, 2006; Anderson et al., 1996). However, the statistical significance and magnitude of the trends varies by location and time scale examined (see Brown and Duguay, 2010).

Throughout Canada, from 1951-2000, trends toward earlier water-clear-of-ice dates have been observed for many lakes during the latter part of the 20th century, but complete freeze over dates have shown few significant trends over the same period (Duguay et al., 2006; Latifovic and Pouliot, 2007). Changes in the ice regimes of typically perennially ice-covered lakes on northern Ellesmere Island (Nunavut, Canada) have been related to shifts in the climate regimes in that area and shown to have changed from infrequent to more frequent summer ice loss (Mueller et al., 2009). Past changes to lake ice regimes have also been inferred in the arctic using proxy methods such as diatoms (Smol, 1983; Smol, 1988; Douglas and Smol, 1999; Smol et al., 2005; Keatley et al., 2008) and sediment records (Tomkins et al., 2009).

Snow is a very important influencing factor for lake ice. Once the ice has formed, snow accumulation on the ice surface slows the growth of ice below due to the insulating properties as a result of the lower thermal conductivity (thermal conductivity of snow, 0.08 - 0.54 $Wm^{-1}K^{-1}$ versus 2.24 $Wm^{-1}K^{-1}$ for ice, Sturm et al., 1997). Conversely, the mass of the snow can also change the

composition of the ice by promoting snow ice development, and hence influence the thickness of the ice cover (Korhonen, 2006; Brown and Duguay, 2011a).

Recent work using a combination of several datasets by Brown et al., (2010) showed a reduction of the spring snow cover extent throughout the pan-arctic from 1967 – 2008. Specifically for the North American Arctic, they found a 12% reduction of mean snow cover extent in May and a 31% reduction in June. Additionally, Tedesco et al. (2009) using passive microwave data, found that the melt season for arctic snow has decreased by 0.6 days yr^{-1} from 1978-2008. Future climate predictions using the Arctic Climate Impact Assessment (ACIA) model ensemble also suggests the greatest changes to the arctic snow cover will occur during the spring (ACIA, 2005). Increasing temperatures reduce the amount of snow in a region by decreasing the fraction of precipitation that falls as snow and also by increasing snowmelt, however, increasing precipitation could counteract this (Räisänen, 2007). The complex interactions between increasing temperatures and increasing precipitation vary by region but climate model predictions for the 21st century tend to show shorter snow cover durations, with increased amounts of snow water equivalent in the colder northern regions of North America (Räisänen, 2007; Brown and Mote, 2009). Several studies have examined the trends in the climate of the North American Arctic, typically showing warming temperatures and increased precipitation (e.g. Zhang et al., 2007; Kaufmann et al., 2009) and those trends are predicted to continue with future climate scenarios (e.g., ACIA, 2005; Bonsal and Kochtubajda, 2009). From a hydrological perspective little work has been done for this region examining future changes, however, GCMs have been used in combination with hydrological models to predict changes within a small headwater basin (Pohl et al., 2007) and the larger Liard Basin (Woo et al., 2008; Thorne, 2011). River ice duration by 2050 for most of Canada is estimated to be approximately 20 days shorter than 1961-1990, based on projected changes to the 0° isotherm (Prowse et al., 2007). In the Peace-Athabasca Delta (western end of Lake Athabasca) the ice cover is estimated to be up to 20% thinner and with a reduced duration of 2 - 4 weeks by 2071-2099, with most of the reduction being attributed to changes in break-up (Beltaos et al., 2006). Sea ice extent is also predicted to decrease with future climates (Holland et al., 2006). Changes to the sea ice within the Canadian Arctic Archipelago (CAA) for 2041–60 are predicted to show little change in wintertime ice concentrations, with summer ice concentrations decreasing by 45% and the thickness decreasing by 17% in the winter and by 36% in summer (Sou and Flato, 2009).

Many studies have examined how lake ice might respond to changes in both temperature and precipitation, and sensitivity analysis has shown that ice phenology is most sensitive to changes in air temperatures while ice thickness is more sensitive to snow cover (eg., Vavrus et al., 1996; Ménard et al., 2002; Duguay et al., 2003; Gao and Stefan, 2004; Williams et al., 2004; Morris et al., 2005) (see Brown and Duguay 2010 for a detailed comparison). While most work involving ice cover changes has been done for specific locations, Walsh et al. (1998) produced gridded ice phenology for the entire Northern Hemisphere using historical 1931-1960 mean climate data to create the first wide-scale examination of lake ice phenology. A recent study using climate model output examining possible changes to the lake ice regime in North America from 40°N to 75°N under future climates suggests break-up will advance by 10-20 days, while freeze-up will be delayed by 5-15 days, resulting in a reduction of the ice cover duration by 15-35 days (Dibike et al., 2011).

In situ data is very sparse throughout northern North America and the majority of the climate stations in the Arctic are typically confined to relatively accessible areas of the mainland or coastal areas in the islands. The use of reanalysis data or climate model output data to drive numerical lake ice models provides the ability for wide-scale assessments of ice cover, as well as the ability to produce predictions of future ice conditions (Duguay et al., 2007; Dibike et al., 2011). The aim of this paper is to create gridded ice phenology data for North America (greater than 58°N) using input data from the Canadian Regional Climate Model (CRMC) both for present day climate as well as future simulation, while highlighting the importance of snow cover on the potential changes to the lake ice regimes.

4.2 Study Area and Methodology

4.2.1 Study Area

Canada and Alaska (USA), north of 58° latitude are dominated by discontinuous or continuous permafrost except at the southern reaches of the Yukon and Northwest Territories (NWT), and northern part of the provinces of British Columbia and Alberta (Figure 4.1). The area encompasses mainly subarctic and arctic climate, where the temperatures can reach up to 25°C in the summer in the interior continental areas (e.g. Yellowknife, NWT) to below -40°C in the winter throughout most of the area. Mean annual temperatures range from 4°C in the coastal areas of Alaska, to -18°C on Ellesmere Island. Precipitation varies greatly across the continent with over 3000 mm near the northern coast of the Gulf of Alaska; the interior regions receiving 200 – 400 mm (higher amounts in

the Yukon and NWT mountain areas); decreasing to less than 200 mm per year in the Canadian Arctic Archipelago (CAA). Snow cover amounts through most of the region range from 30 – 50 cm (higher in the mountains) with less than 30 cm in the western parts of the CAA.

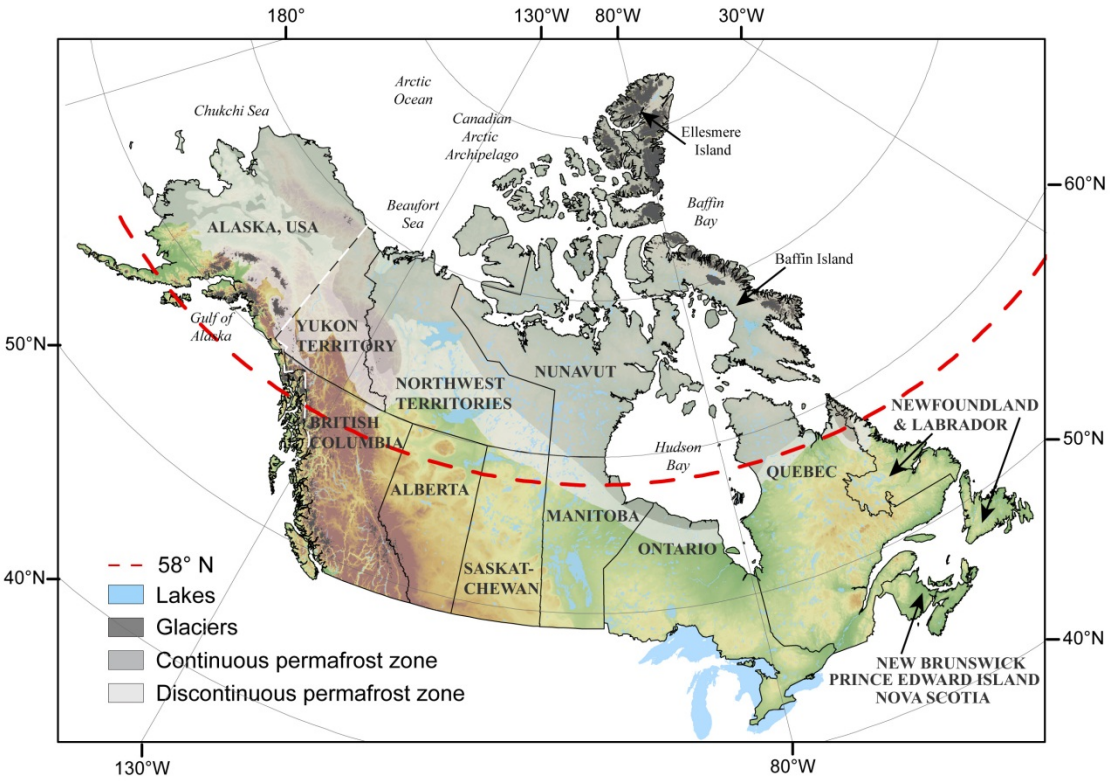

Figure 4.1. Canada with provincial and territorial boundaries and the state of Alaska (USA), highlighting the area above 58°N used for this study. Also shown are areas of permafrost and glacier.

Many mountainous areas are present in the study region: The Western Cordillera extending up the west coast through British Columbia and Alaska with the Alaska Range and the Brooks Range to the north; and the Arctic Cordillera spanning most of the northern areas of the CAA. Across the interior plains and the northern parts of the Canadian Shield is the boreal forest while tundra extends to the north of the tree line.

Many large lakes (>400 km^2) are situated north of 58°N (e.g. Nettelling Lake, Amadjuak Lake, Baker Lake) as well as the Northern Great Lakes (Great Bear Lake and Great Slave Lake). Lakes in the northern boreal and tundra areas are numerous, with an estimated coverage in the Arctic and

Subarctic regions of North America reaching up to 15 – 40% depending on the location (Duguay et al., 2003).

4.2.2 Lake ice model

The model used is the Canadian Lake Ice Model (CLIMo), a one-dimensional thermodynamic model used for freshwater ice cover studies (e.g. Ménard et al., 2002; Duguay et al., 2003; Jeffries et al., 2005a, Morris et al., 2005) capable of simulating ice on and off, thickness and composition of the ice cover (clear or snow ice). CLIMo has been shown to perform very well at simulating lake ice phenology when using input data that well represents the climate for the lake, for example from nearby meteorological towers (Duguay et al., 2003; Jeffries et al., 2005a; Brown and Duguay, 2011a). CLIMo has been modified from the one-dimensional sea ice model of Flato and Brown (1996), which was based on the one-dimensional unsteady heat conduction equation, with penetrating solar radiation, of Maykut and Untersteiner (1971):

$$\rho C_p \frac{\partial T}{\partial t} = \frac{\partial}{\partial z} k \frac{\partial T}{\partial z} + F_{sw} I_o (1-\alpha) K e^{-Kz} \qquad (1)$$

where ρ (kg m^{-3}) is the density, Cp (J kg^{-1} K^{-1}) is the specific heat capacity, T (K) is the temperature, t (s) is the time, k (Wm^{-1}K^{-1}) is the thermal conductivity, z (m) is the vertical coordinate, positive downward, F_{sw} (Wm^{-2}) is the downwelling shortwave radiative energy flux, I_o (Wm^{-2}) is the fraction of shortwave radiation flux that penetrates the surface, α is the surface albedo, and K is the bulk extinction coefficient for penetrating shortwave radiation.

From this, the surface energy budget can then be calculated:

$$F_o = F_{lw} - \varepsilon\sigma T^4(0,t) + (1-\alpha)(1-I_0)F_{sw} + F_{lat} + F_{sens} \qquad (2)$$

where F_o (Wm^{-2}) is the net downward heat flux absorbed at the surface, ε is the surface emissivity, σ is the Stefan–Boltzmann constant (5.67 x 10^{-8} Wm^{-2} K^{-4}), F_{lw} (Wm^{-2}) is the downwelling longwave

radiative energy flux, F_{lat} (Wm^{-2}) is the downward latent heat flux, and F_{sens} (Wm^{-2}) is the downward sensible heat flux (Ménard et al., 2002, Jeffries et al., 2005a).

CLIMo includes a fixed-depth mixed layer in order to represent an annual cycle. When ice is present, the mixed layer is fixed at the freezing point and when ice is absent, the mixed layer temperature is computed from the surface energy budget and hence represents a measure of the heat storage in the lake. The water column of shallow lakes is typically well-mixed and isothermal from top to bottom during the ice-free period, permitting the mixed layer depth to be a good approximation of the effect of lake depth leading to autumn freeze-up (Duguay et al., 2003). While warming lake temperatures from longer ice free seasons could alter the lake stratification (e.g. Kvambekk and Melvold, 2010; Mueller et al., 2009) an assumption was made that the mixed layer remained constant in the future simulations. In order to represent potential changes to the mixed layer a lake model such as the Fresh-water Lake model (FLake: Mironov, 2008) could be used to provide mixed layer information for CLIMo (Kheyrollah Pour et al., 2012).

The snow layer (if present) is represented as a single layer in CLIMo. While recent work has highlighted some advantages to multi-layer snow models (e.g. Chung et al., 2010 who coupled a snow model (SNTHRM) to a sea ice model) when provided realistic on-ice snow densities, CLIMo has been shown to simulate the on-ice snowpack depth and melt well compared to observations (Brown and Duguay, 2011a). Snow ice is created by the model if there is a sufficient amount of snow to depress the ice surface below the water level. The added mass of the water filled snow pores (slush) is added to the ice thickness as snow ice.

The albedo parameterization in CLIMo is based mainly on surface type (ice, snow or open water), surface temperatures (melting vs frozen) and ice thickness, with no distinction regarding ice composition. A more detailed description of CLIMo can be found in Duguay et al. (2003).

4.2.3 Forcing data

CLIMo was driven by climate model output from the Canadian Regional Climate Model (CRCM 4.2.0) (45km true at 60°N) provided by Consortium Ouranos. CRCM is a limited-area model, originally developed at Université du Québec à Montréal (UQAM), driven at the boundaries by GCMs or reanalysis data. CRCM uses the Canadian LAnd Surface Scheme (CLASS 2.7; Verseghy, 1991; Verseghy et al., 1993) to describe the water and energy exchanges between land surface and

atmosphere (Music and Caya, 2007). For a detailed description of CRCM see Caya and Laprise (1999) and Laprise (2008).

Two CRCM scenarios were used, both spanning from 1961 – 2100, driven at the boundaries with the Canadian Global Climate Model (CGCM 3.1/T47 member 4 (scenario 1) and member 5 (scenario 2)) following the IPCC Special Report on Emission Scenarios A2 green-house-gas scenario, of continually increasing CO_2 emissions. The two scenarios are the same except with a slight perturbation to the initial GCM conditions which allows the climate to evolve slightly differently, providing some insight into the interannual variability in the climate simulations. CGCM data is produced by the Canadian Centre for Modelling and Analysis (CCCma). Daily data from each scenario consisted of 2 m screen temperature, humidity (specific humidity converted to relative humidity using a calculated saturated vapour pressure as a function of temperature (Beljaars et al., 1989) and a fixed air pressure of 1015 mb), wind speed, water equivalent of snow, snow density and cloud cover amounts.

A temperature bias has been previously identified in the CRCM data (Plummer et al., 2006; Gagnon et al., 2009) and was an average of 4°C below the observed station temperatures, varying seasonally up to 14°C too cold during the spring in some areas. The use of reanalysis data (e.g. NCEP-NCAR, ECMWF) is limited in this region as previous studies have found these data sets to have cold biases as a result of the large grid cells representing the glaciated and mountainous areas more-so than the channels between the islands (Sou and Flato, 2009) and hence not representative of the low-lying or coastal areas where lakes would more likely be situated. Instead, a bias correction was done using temperature data from the Adjusted and Homogenized Canadian Climate Data (AHCCD) available from Environment Canada, which is a database of homogenized and long-term temperature time series specifically designed for climate change analysis over Canada (Vincent and Gullet,1999; Vincent, 1998; Vincent et al., 2002). 47 stations were available across the Canadian north and an additional 15 weather stations from Alaska were added for the bias correction (Figure 4.2). While this method of bias correction is adequate for the majority of the study area, correcting the large bias in the mountainous Ellesmere Island areas using coastal station data (Alert) could potentially introduce a warm bias over the glaciated mountains. Conversely, since this study aims to examine changes in the lake ice cover, the adjusted temperature data would be suitable to represent the areas where lakes would be more likely to be situated (e.g. lowland areas, valleys, rather than in high altitude glaciated areas). The mean monthly bias was determined from the 1961-1990 data and

then adjusted accordingly. Snow amounts from the CRCM scenarios were compared to station data (see section 4.3.1) and were found to be suitably comparable. Other variables play a lesser role in the model and no bias correction was undertaken. An assumption was made that the bias present from 1961-1990 is consistent into the future.

Figure 4.2. Locations of stations used for CRCM temperature adjustment; 15 stations within Alaska and 47 stations within Canada.

4.2.4 In situ data

Fifteen lakes were selected as validation sites for the CRCM simulations (Figure 4.3, Table 4.1). Each lake chosen has observation data available for ice break-up and freeze-up in the Canadian Ice Database (CID) during the contemporary climate (1961-1990). The 1961-1990 climate mean was chosen rather than the more recent 1979 - 2000 climate mean as the earlier set coincides with the peak years of in situ lake ice observations. The CID is a national historical database of in situ ice cover (lake ice, river ice, landfast sea ice) from 1822 for 757 sites across Canada (259 Lakes) (Lenormand et al., 2002). For clarity, the two unnamed lakes will be referred to by their nearest communities (Mould Bay and Sachs Harbour). To assess the performance of the CRCM simulations of freeze/break-up, simulations were also run for each of the validation sites using data from nearby weather stations operated by the Meteorological Service of Canada (MSC) (air temperature, relative humidity, wind speed, and cloud cover). Snow depth and density were obtained from the Canada Snow CD (MSC, 2000), a database of quality controlled and reconstructed snow data from

Meteorological Service of Canada stations throughout Canada (Brown and Braaten, 1998). Snow density was obtained as a seasonal average from bi-weekly gridded snow density normals, created from snow course data and interpolated to a 200 km grid (MSC, 2000). Six of the selected validation sites had on-ice snow depths measurements recorded by the Canadian Ice Service (CIS) as part of the Canadian Ice Thickness Program (http://www.ec.gc.ca/glaces-ice/default.asp?lang=En&n=E1B3129D-1). Ice thickness and snow depths are available for 195 Lake/River/Sea ice sites throughout Canada from 1947 to present, with varying completeness of years. Snow depths on the lake ice surface were compared with snow depths at the MSC stations and the corresponding CRCM tile in order to examine the effects of snow depth on the ice cover simulations.

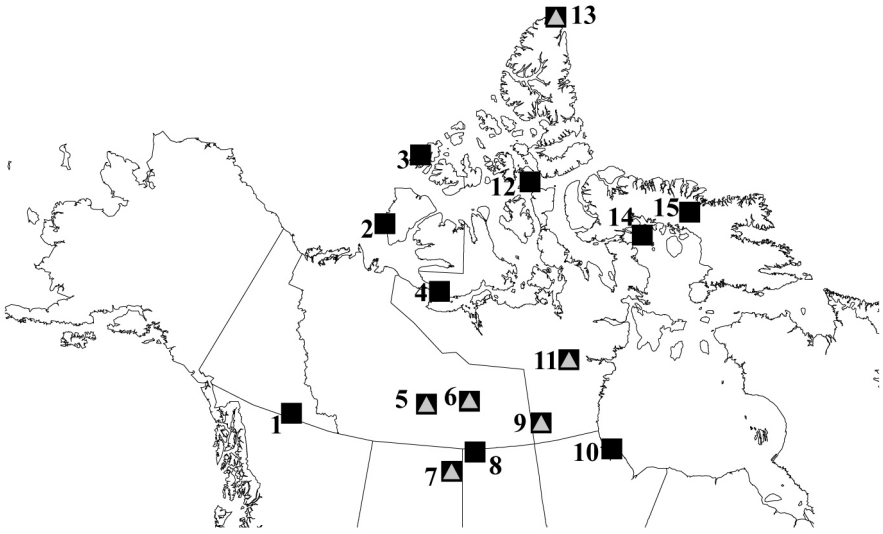

1. Watson Lake
2. Unnamed Lake (Sachs Harbour)
3. Unnamed Lake (Mould Bay)
4. Module Lake
5. Back Bay, Great Slave Lake
6. Charlton Bay, Great Slave Lake
7. Lake Athabasca
8. Beaverlodge Lake
9. Ennadai Lake
10. Farnworth Lake
11. Baker Lake
12. Resolute Lake
13. Upper Dumbell Lake
14. Fenor Lake
15. Dewar Lakes

Figure 4.3. Lakes used as validation sites for the model simulations. Squares represent the lakes used for ice phenology validation, triangles represent the lakes where snow depth on ice and ice thickness data was also available.

Table 4.1 provides a summary of the available observation data from the validation lakes, along with the years of available meteorological data and on-ice snow depths where available. A statistical

comparison was done for the validation results using the Mean Bias Error (MBE) or Absolute Error (AE).

Table 4.1. Summary of the lake ice observation data, corresponding climate station and the years used.

Lake Observations (CID)	Nearby Climate Station (MSC)	Years	Years of ice observations Break-up/ Freeze-up	Years of Snow Depth on ice
Watson Lake	Watson Lake	1961-1990	28/25	
Unnamed Lake	Sachs Harbour	1961-1986	18/18	
Unnamed Lake	Mould Bay	1961-1990	18/21	
Module Lake	Kugluktuk	1980-1990	7/9	
Back Bay	Yellowknife	1961-1990	28/27	1961-1990
Charlton Bay	Fort Reliance	1961-1990	26/29	1961-1990
Lake Athabasca	Fort Chipewyan	1968-1990	20/17	1962-1990
Beaverlodge Lake	Uranium City	1963-1982	20/16	
Ennadai Lake	Ennadai Lake	1961-1979	19/19	1961-1979
Farnworth Lake	Churchill	1961-1990	22/22	
Baker Lake	Baker Lake	1961-1990	29/29	1961-1990
Resolute Lake	Resolute	1961-1990	10/18	
Upper Dumbell Lake	Alert	1961-1990	3/24	1961-1990
Fenor Lake	Hall Beach	1961-1990	4/6	
Dewar Lakes	Dewar Lakes	1961-1990	21/23	

4.2.5 Simulations

In order to account for redistribution of snow across the ice surface, simulations for the North American Arctic were run using the CRCM data with both a full snow cover and no snow cover (see Section 4.3.1 for details). Three sets of simulations were run with respect to mixing depth: 3 m (to represent shallow lakes, e.g. in the North Slope area of Alaska; the Hudson Bay Lowlands), 10 m (to represent medium deep lakes, near-shore areas where observations would be taken on larger lakes, or lakes of unknown depth following Samuelsson et al. 2010) and 30 m (to represent large, deep lakes).

While the pan-arctic simulations were run with two possible snow covers (full snow cover or no snow cover), the validation lakes were each simulated separately in order to obtain the best representation possible. The percentage of snow-on-ice to snow-on-land was determined when possible from the CIS data, or was estimated based on best fit to observations when no measurements were available. To compare how well the CRCM data performed for the in situ lakes, the CRCM snow data was adjusted in the same manner for the tiles over each validation lake and additional simulations were run.

4.3 Results

4.3.1 Comparison of snow cover on the lakes

Realistic representation of snow cover on a lake ice surface is important for accurate simulation of ice evolution (Brown and Duguay, 2011a) because of snow's important insulating role and contribution to snow ice growth. Redistribution of the snow across the lake ice surface can result in a non-uniform snow cover, typically less than what would be measured nearby on-land. For example, in northern Alaska, the ratio of snow-on-ice over the lakes to snow-on-land was found to be and average of 56% (Sturm and Liston, 2003). In order to represent the range of potential snow conditions on the lake ice surface, simulations are run with a 'full snow cover' to represent 100% of the snowfall accumulating on the ice, as well as a 'no snow cover' simulation to represent the opposite conditions. Table 4.2 presents the comparison of the snow cover between the CRCM data sets with respect to the measured snow at the MSC stations nearest to the lakes where on-ice snow measurements were available. Although it is not advised to compare a CRCM tile with a weather station (Gagnon et al., 2009) an assessment of the amounts of snow in each data set is important to determine the ability of the CRCM tile to represent the snow cover of the lakes within it.

The ratio of on-ice snow depth to on-shore snow depth at the MSC stations were all less than 1 (Table 4.2). The lakes have an average of 41 – 82% of the snow measured at the MSC stations on their surface, with the exception of Baker Lake, which had only 9% of the recorded snow measured on the ice surface. The CRCM tiles over these lakes had fairly comparable ratios between them, and were within 80 – 122% of the snow amounts measured at the MSC stations, excluding Upper Dumbell Lake. CRCM snow cover in the region near Upper Dumbell Lake is consistently overestimated due to perpetual snow cover in the CRCM data after the snow has melted at the station.

The CRCM tile over Upper Dumbell Lake covers both land and ocean; however, the climate in this tile is more likely representative of the surrounding high altitude regions.

Table 4.2. Ratio of snow depths measured on-ice and snow depth from the CRCM data with respect to the amounts measured at the MSC weather stations.

Lake (MSC Station)	Ratio of on-ice snow depth to MSC station	Ratio of CRCM snow depth to nearest MSC station	
		S 1	S 2
Back Bay, GSL (Yellowknife)	0.68	0.89	1.04
Charlton Bay, GSL (Fort Reliance)	0.48	0.80	0.88
Lake Athabasca (Fort Chipewyan)	0.41	0.83	0.83
Ennadai Lake	0.67	1.21	1.22
Baker Lake	0.09	0.85	0.81
Upper Dumbell Lake	0.82	2.34	2.35

4.3.2 Ice cover during 1961 – 1990 climate

The two CRCM scenarios are similar for the contemporary climate years (1961-1990). The similar input data results in similar simulated ice cover patterns with the primary difference between them occurring in the areas predicted to have perennial ice cover. The ice cover figures produced for the 1961 – 1990 climate use scenario 1 and are meant to represent hypothetical lakes at the given depths (3, 10 and 30 m), since many different lakes sizes and shape could exist within a given grid cell.

4.3.2.1 Ice cover duration 1961 – 1990

Break-up of the ice cover ranges from March in the Gulf of Alaska coastal areas to August in the High Arctic (yd 102 - yd 241), with perennial ice cover on Ellesmere Island and other regions of the CAA; as well as northern Baffin Island with the no snow scenarios (Figure 4.4). Mean break-up dates for the entire study region range from yd 162 – 165 for all simulations with snow cover (mean yd 163) and yd 171-174 (mean yd 172) for no snow. Both climate scenarios show break-up to be similar for all depth simulations (not shown), however changes are evident based on snow cover (mean difference of 9 days between snow and no snow cover) and are more pronounced in the high latitude areas of perennial ice cover. Freeze-up however, is dependent on the depth of the lake rather than the snow cover scenario (Figure 4.5). Freeze-up ranges from September to December (yd 245 – yd 358),

with a mean freeze-up date for 3 m lakes of yd 281, 10 m lakes freezing an average of 11 days later (yd 292), and 30 m lakes freezing an average of a further 20 days after the 10 m lakes (yd 313). The resulting ice cover durations vary for both depth and snow cover, ranging from 90 to 365 days (Figure 4.6), with the longest ice cover duration (ICD) on shallow snow-free lakes (average of 255 days) and shortest for large snow-covered lakes (average 215 days).

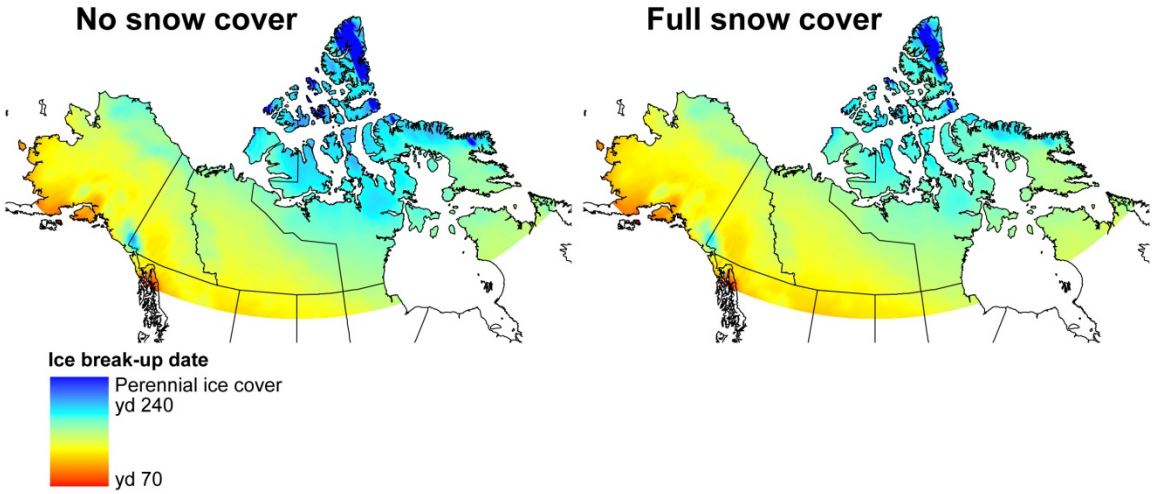

Figure 4.4. Mean simulated break-up dates for 1961-1990 for hypothetical 10 m lakes, for both no snow and full snow scenarios.

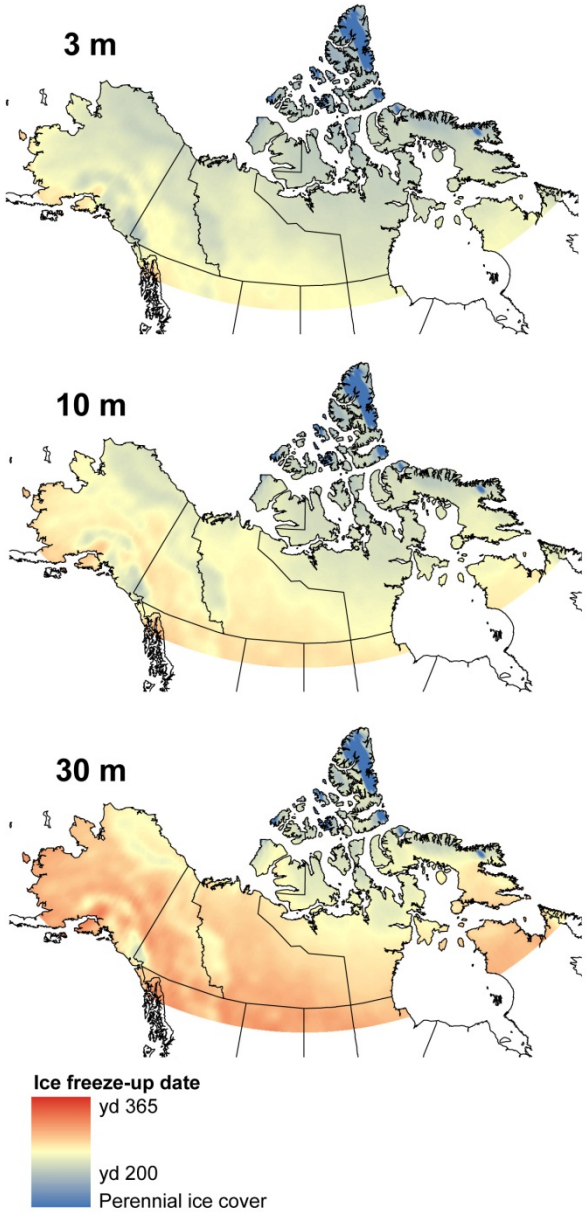

Figure 4.5. Mean freeze-up dates for 1961-1990 for the three depth simulations, highlighting the effect of depth on freeze-up dates.

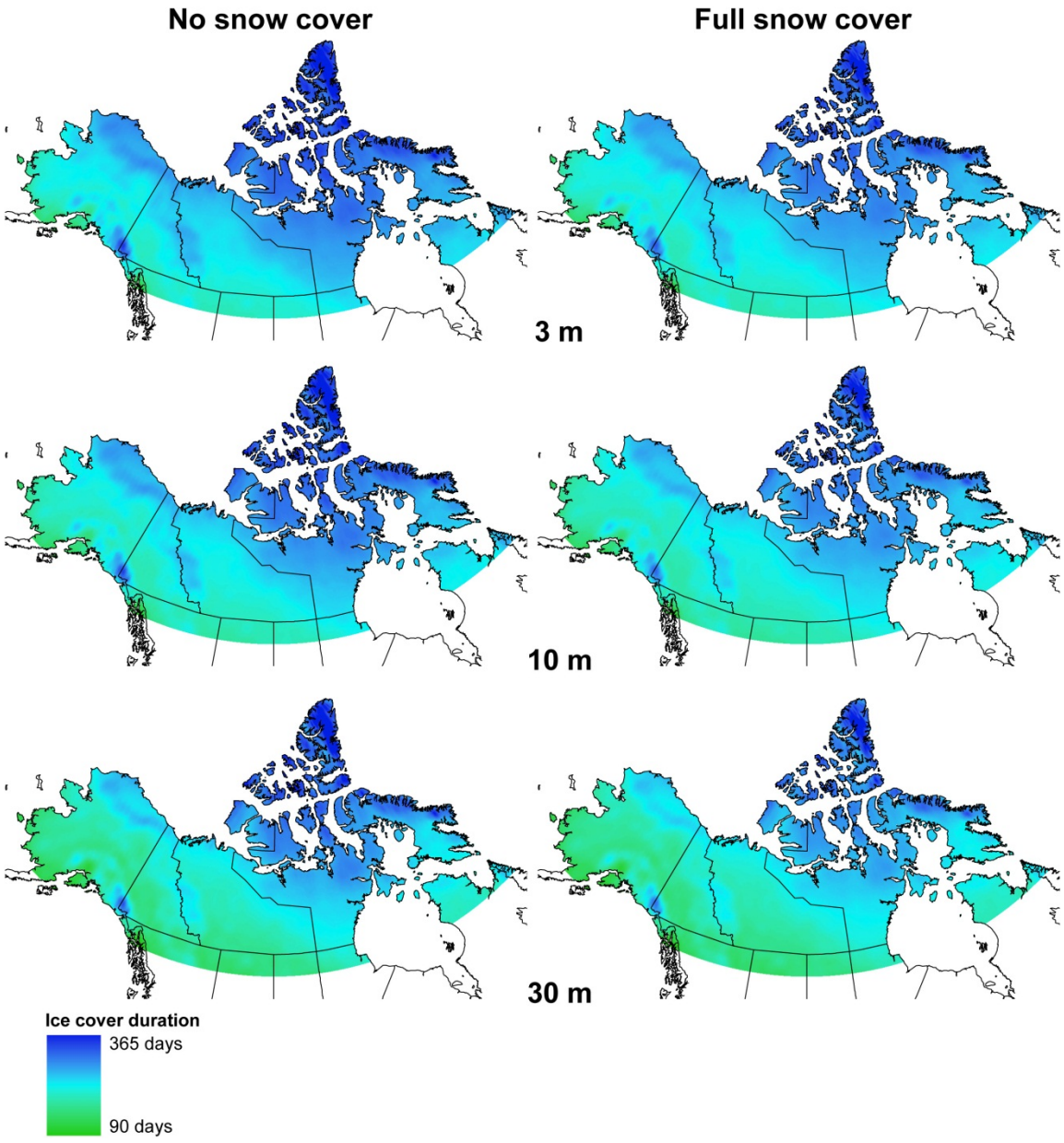

Figure 4.6. Mean ice cover duration for 1961-1990 for the three depth simulations, for both the no snow and full snow scenarios.

In the far northern areas, break-up does not always occur on an annual basis resulting in occasional summer ice cover. All simulations encountered occasional summer ice cover on the lakes in the far northern areas, however only grid cells where no break-up occurred during the 30 year mean were

designated as ‘perennial ice cover’. Perennial ice cover is simulated the same regardless of lake depth but is slightly different between the two climate scenarios. Scenario 1 produces 40 grid cells (81000 km^2) where perennial ice is simulated on snow-free lakes (versus 33 (66825 km^2) for scenario 2) and 19 grid cells (38475 km^2) for snow-covered lakes (versus 10 (20250 km^2) for scenario 2).

4.3.2.2 Ice cover thickness 1961 – 1990

Lake ice thickness is known to be influenced by snow cover on the ice (e.g. Ménard et al., 2003; Morris et al., 2005; Brown and Duguay, 2011a) as shown in Figure 4.7, with a substantial difference between the thickness in snow-free versus snow-covered lakes. Since CLIMo uses the mixing depth rather than absolute lake depth the areas where perennial ice cover occurs continue to thicken each year and are hence, capped at 3 m to avoid unrealistically thick ice. Both CRCM scenarios produce similar mean maximum ice thickness (MMT) (within 2 cm of each other) ranging from an average of 1.91 m to 2.03 m for the snow-free scenarios, and 1.44 m to 1.51 m for the snow-covered scenarios for all depths. The difference in MMT between the snow-free and snow-covered scenarios differs by depth, with an average of 58 cm thicker ice for snow free 3 m lakes, 53 cm thicker ice for snow free 10 m lakes and 42 cm thicker for snow free 30 m lakes.

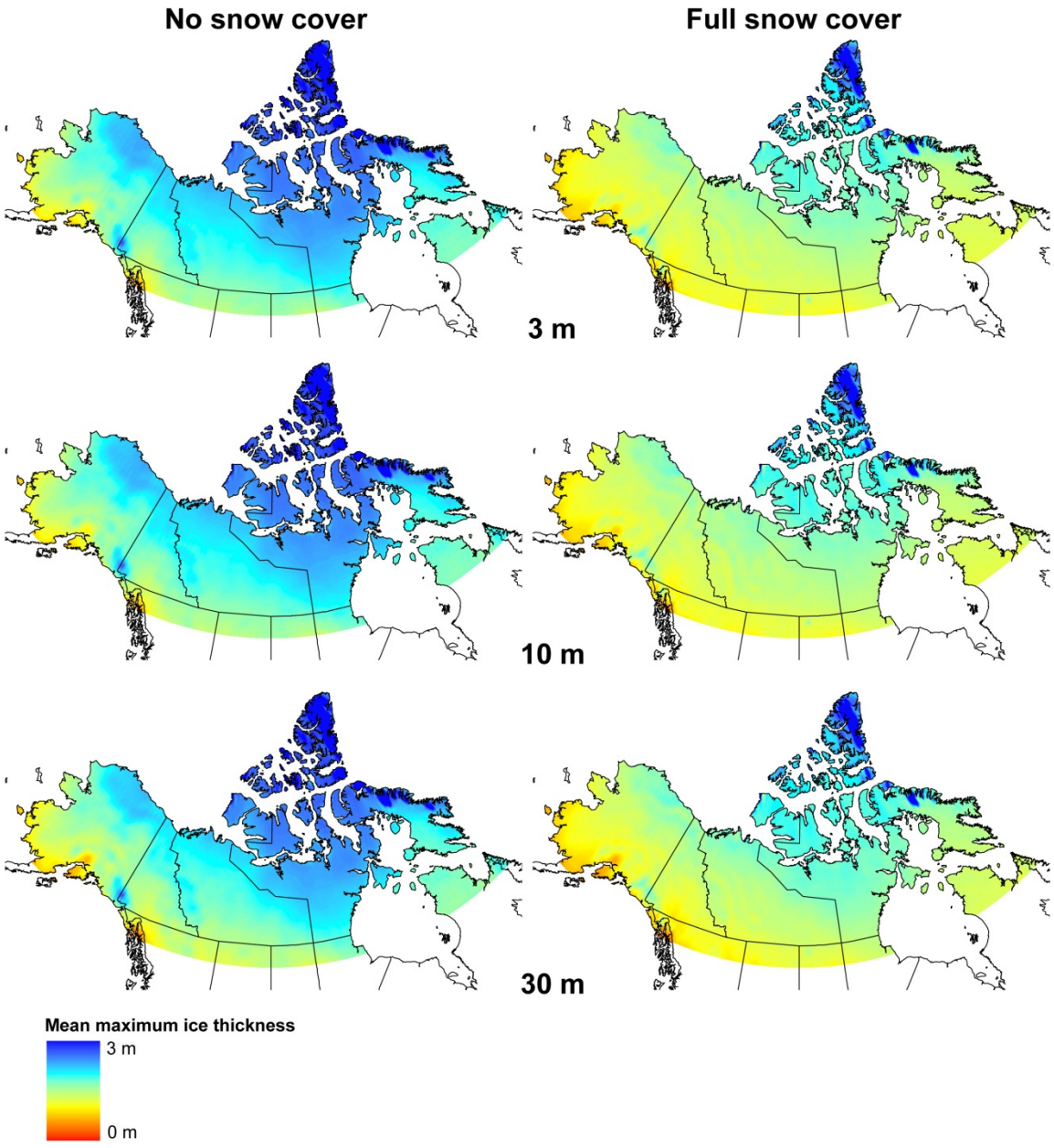

Figure 4.7. Mean maximum ice thickness for 1961-1990, for three depth simulations, and both the no snow and full snow scenarios. Ice thickness capped at 3m in areas where perennial ice cover growth continued due to the model structure of CLIMo.

The composition of the ice (snow ice/clear ice) can affect the strength of the ice as well as the melt rates due to albedo differences between the snow versus clear ice. Figure 4.8 shows the distribution of

snow ice (as a ratio to total ice thickness), highlighting the areas where enough snowfall is received to depress the ice cover enough for snow ice to form. Cold temperatures and low snowfall amounts through most of the Arctic limit the amount of snow ice that forms, however throughout the mountainous areas and northern Quebec/southern Baffin Island some snow ice is simulated.

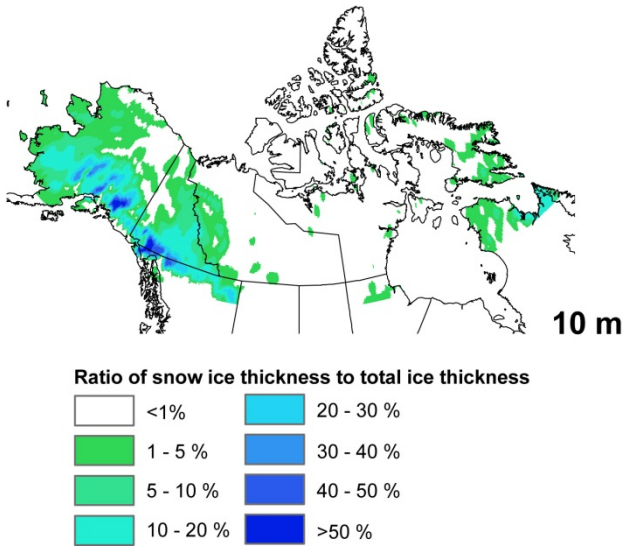

Figure 4.8. Ratio of mean snow ice thickness to mean maximum ice thickness for 1961-1990.

4.3.3 Validation of ice phenology and thickness

Validation of modelled ice phenology and thickness in Northern Canada and Alaska presents challenges as the observational network for lake ice is very sparse. Simulations using CLIMo typically compare well to observation data when run using climate data that adequately represents the lake observed (i.e. nearby weather stations) (e.g., Duguay et al., 2003; Brown and Duguay, 2010; Jefferies et al., 2005). To examine how representative the CRCM simulations are compared to observations, simulation results from the containing CRCM tiles were compared to 15 locations that had both observation data and MSC station data available. If CLIMo is not able to accurately capture the break-up/freeze-up dates using nearby MSC station data, then the same would be expected of the CRCM data. This allows for distinguishing between limitations with the model rather than the CRCM data.

Table 4.3 presents the Mean Bias Error (MBE) for the simulations compared to observations. Looking at the MSC simulations results for the validation sites, all but six had a MBE of less than one

week for the simulations compared to observations, with most being slightly early. Break-up for Mould Bay was simulated 13 days late compared to the observations, suggesting either the snow conditions are not well represented or a factor not captured by the 1D model. Break-up for Dewar Lakes was simulated 20 days too late, again suggesting other factors that are not captured by the 1D model – in this case likely a result of the morphometry as this locations is part of a long narrow series of lakes. Break-up at Charlton Bay and Ennadai Lake was two weeks early, however the dates vary in phase. This same early tendency for break-up was also found at Charlton Bay by Ménard et al. (2002), who suggested that this might in part be due to the sheltered location creating a favourable environment for a longer ice cover. Lake Athabasca was the only lake where freeze-up could not be adequately simulated, being 38 days too early compared to observations. The in situ data for this lake is from Fort Chipewyan, situated beside the Peace-Athabasca Delta (PAD), in a very shallow area of Lake Athabasca. The mean depth of the lake is 20 m however the lake is 3 m or shallower at the western end near the PAD. The PAD is a hydrologically complicated area, where reversal of flow is known to occur (Peters and Buttle, 2010), and the additional heat inputs to the lake from the PAD and surrounding rivers in this area likely contributed to the discrepancy between the observed and simulated freeze-up. Since CLIMo usually represents freeze-up quite well a test was run adjusting the mixing depth in the simulations in order to match the observations. A mixing depth of 30 m was required for simulations for Lake Athabasca to match observations – suggesting that the heat added from the surround inputs to this area has the equivalent heat storage of an extra 27 m of water.

The CRCM simulations were within 1 week of observations for 6 of the 15 lakes simulated (Table 4.3). As expected from the MSC simulations, the CRCM simulations for break-up at Mould Bay and Dewar lakes were too late, and freeze-up at Lake Athabasca was too early. The five lakes with the greatest MBE for early break-up (Charleton Bay (GSL), Lake Athabasca, Ennadai Lake, Baker Lake and Resolute Lake: 10 – 18 days, with the exception of Resolute Lake for scenario 2, which matched observations) also had early break-up seen in the MSC simulations (5-14 days). The only anomaly between the CRCM and MSC simulations occurred at Upper Dumbell Lake for freeze-up, while the station data resulted in freeze-up being captured within 3 days of observations, CRCM simulations for scenario 1 and 2 were both over a week late.

Table 4.3. Mean bias error (MBE) in break-up and freeze-up dates from simulations using Meteorological Service of Canada (MSC) data, CRCM scenario 1 (S1) and scenario 2 (S2) for the validation sites along with the mean observed break-up and freeze-up from the Canadian Ice Database (CID)(dates as indicated in Table 4.1).

Lake	Snow cover (%)	Mixing Depth (m)	Break-up				Freeze-up			
			CID yd	MSC (MBE days)	S 1	S 2	CID yd	MSC (MBE days)	S 1	S 2
Watson Lake*	0+	10	141	5	0	-2	314	1	1	2
Unnamed Lake - Sachs Harbour*	100+	3	188	1	5	4	269	1	-5	-6
Unnamed Lake - Mould Bay*	100+	2	191	13	13	16	247	2	6	2
Module Lake *	100+	3	181	-4	-2	-6	278	-5	1	-2
Back Bay	68	10	151	-2	-3	-3	302	3	5	4
Charlton Bay	48	20	172	-14	-16	-15	321	-2	-3	-4
Lake Athabasca**	41	3	145	-9	-11	-6	339	-38	-37	-38
Beaverlodge Lake*	0+	20	151	-4	-8	-8	329	-2	-2	-4
Ennadai Lake*	62	10	183	-14	-18	-15	295	0	6	4
Farnworth Lake	0+	2	171	0.5	-7	-4	291	-1	2	4
Baker Lake	9	20	200	-9	-14	-13	297	0	4	1
Resolute Lake	50+	10	212	-6	-10	0	262	-2	5	3
Upper Dumbell Lake	82	15	218++				251	-3	9	12
Fenor Lake*	50+	10	203	-5	-3	-5	280	-3	4	-1
Dewar Lakes*	0	10	185	20	10	10	275	-3	1	2

Overall, the absolute error compared to observations for all fifteen lakes combined was 8 days for break-up and 6 days for freeze-up (4 days excluding Lake Athabasca), indicating that CLIMo produces satisfactory simulations for break/freeze-up using CRCM climate data.

A comparison of mean maximum thickness (MMT) was possible at five of the validation lakes (Table 4.4). Simulating the ice thickness correctly is dependent on accurately representing the snow cover depth and density on the lake ice surface where the measurements were taken. Also, since the in situ thickness measurements are generally taken weekly (but not always) there is a small possibility of missing the maximum thickness during the sampling. For Back Bay (GSL) the MSC simulations had a MBE of 10 cm too thin, while the CRCM simulations here were 20 cm too thick. Ennadai Lake was also too thin with MSC (12 cm) however in this instance the CRCM simulations were closer to the observations (< 4 cm MBE). MMT was underestimated at Baker Lake as well with the MSC simulations 14 cm too thin, and the CRCM simulations 11 cm too thin. Break-up was not simulated

well at Charlton Bay (GSL) so the likelihood of representing the thickness well here is reduced with all simulations being too thick. The large discrepancy for the thickness of Upper Dumbell Lake for the CRCM simulations is due to the snow cover being poorly represented here (MSC simulations captured the thickness well with a MBE of 6 cm)

Table 4.4. Mean bias error in mean maximum thickness for the validation sites along with the mean maximum thicknesses (dates as indicated in Table 4.1).

Lake	Snow cover (%)	Mean Maximum Ice Thickness (m)				MBE (m)		
		CIS	MSC	S1	S2	MSC	S1	S2
Back Bay (GSL)	68	1.32	1.23	1.54	1.50	-0.10	0.22	0.18
Charlton Bay (GSL)	48	1.28	1.36	1.60	1.62	0.09	0.32	0.35
Ennadai Lake	62	1.68	1.56	1.64	1.68	-0.12	-0.04	-0.00
Baker Lake	9	2.27	2.13	2.16	2.16	-0.14	-0.11	-0.11
Upper Dumbell Lake	82	1.96	1.90	2.51	2.48	-0.06	0.55	0.52

The average absolute error for the simulated MMT compared to observations is 10 cm for the MSC simulations and 25/23 cm for the CRCM simulations using the best estimate for snow cover amounts. Excluding Charlton Bay where the MSC simulations did not capture the observations well (and hence CRCM would not be expected to either), and Upper Dumbell Lake where snow cover amounts are inaccurate, the average absolute error for the remaining three lakes is within 12 cm of observations for both scenarios.

Snow ice measurements are not recorded in the historical archives, however a study on Baffin Island near Iqaluit, Nunavut, found a 7% ratio of snow ice to maximum ice thickness during the 2005-2006 winter (Dyck, 2007). The 1961-90 mean ratio in this area was ~ 6%.

4.3.4 Ice cover during future climate

The dominant climatic variables in terms of ice cover changes are air temperature and the snow conditions (both depth and density). The future scenario data from CRCM is driven by CGCM3 which was one of the models used in the IPCC AR4 (CMIP3) model ensemble. CGCM3 showed a greater increase in precipitation than the ensemble mean, but was near the mean in terms of temperature increase overall (Meehl et al., 2007). Spatially, comparison figures provided on the IPCC website (IPCC, 2007) suggest CGCM3 has a larger increase in surface air temperature (1980-99 to 2046-65) than the ensemble mean through the Gulf of Alaska region.

Although the two CRCM scenarios begin with similar conditions and both show warming throughout (Figure 4.9), by the 2041-2070 mean they have evolved different temperature patterns. Temperatures in scenario 1 show the greatest change in the winter seasons (December, January, February) ranging from 5 - 9°C warmer over the land areas. Spring (March, April, May) shows an increase mainly in the 3 - 5°C degree range; summer (June, July, August) only 1 - 3°C, and fall (September, October, November) a 2 - 6°C change. Temperatures in scenario 2 however are cooler and show less warming to 2041-2070. Winter in scenario 2 does not have warming in the Alaskan area seen in scenario 1, and the bulk of the NWT shows less warming in the spring. Summer is quite similar for both, while fall shows less warming in Alaska.

Precipitation is expected to increase throughout the northern regions in future climate scenarios (see figures available on the NARCCAP website using similar scenario data: http://www.narccap.ucar.edu/results/crcm-cgcm3-results.html) however, in terms of snow water equivalent (SWE) the CRCM data show spatially varying changes in the future (Figure 4.10). The majority of the northern areas show an increase of SWE consistent with increasing precipitation, however the Alaskan coastal regions and the tip of Labrador show a decrease in SWE – which would be attributed to changes from snowfall to rainfall in these areas. The two scenarios are more similar in terms of SWE than temperature, and the amount of change is mainly in the range of ± 10%, with some winter SWE increases up to 30%. Snow depths compared at the lake validation sites tend to increase, however based on a sensitivity study for Back Bay (GSL) by Ménard et al., (2003) increasing the snow depth on the ice does little to affect the ice cover duration and only slightly affect the thickness as compared to the effects of reducing the snow cover on the ice. While increased snow depth on the ice surface may not have a large impact on the duration, the ice composition is likely to be affected by the increased formation of snow-ice in the areas where the mass of the snow (or SWE) on the ice increases.

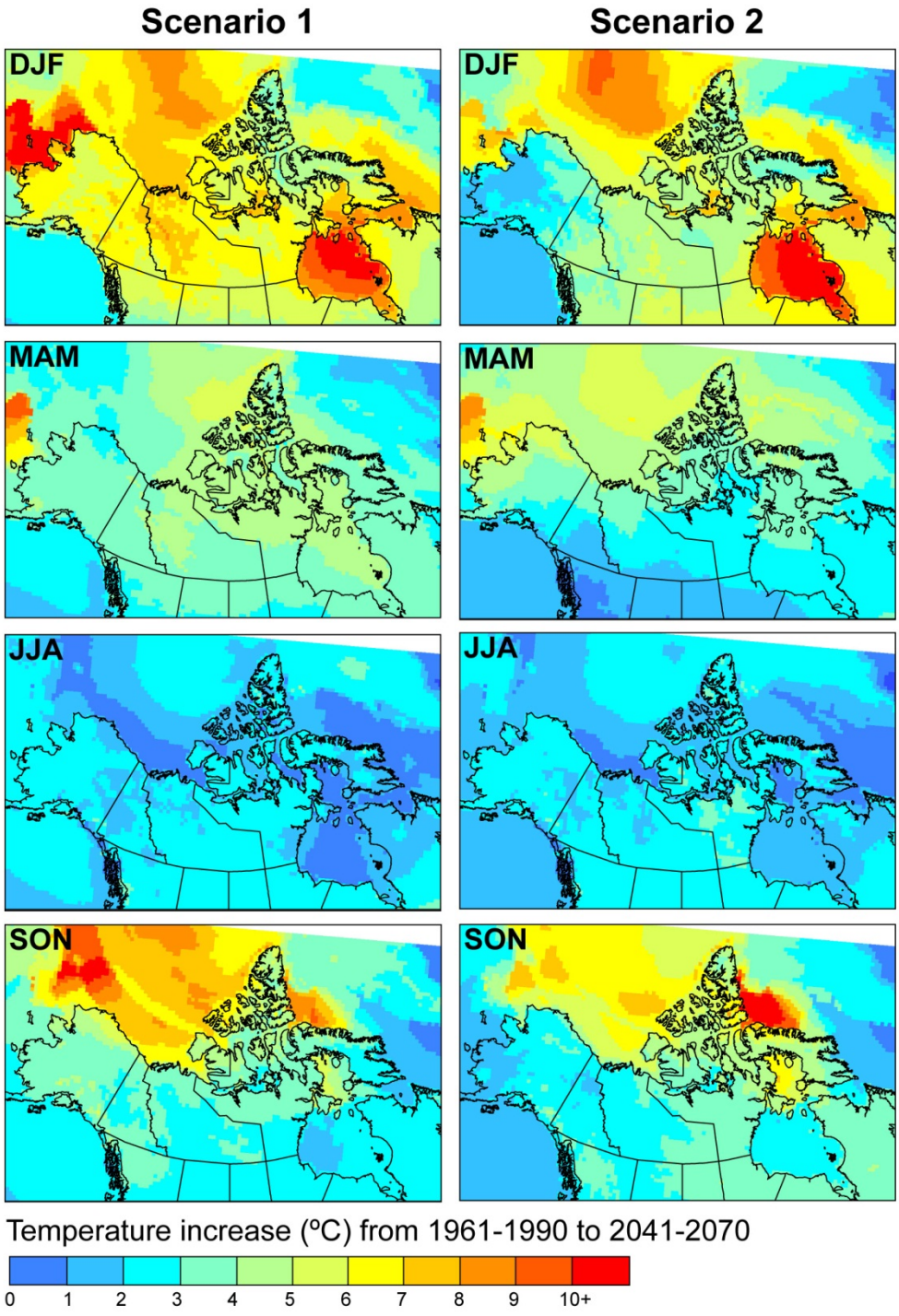

Figure 4.9. Increase in air temperature from 1961-1990 mean to 2041-2070 mean from the CRCM data displayed by season Winter (Dec., Jan., Feb.), Spring (Mar., Apr., May), Summer (Jun., Jul., Aug.) and Fall (Sep., Oct., Nov.).

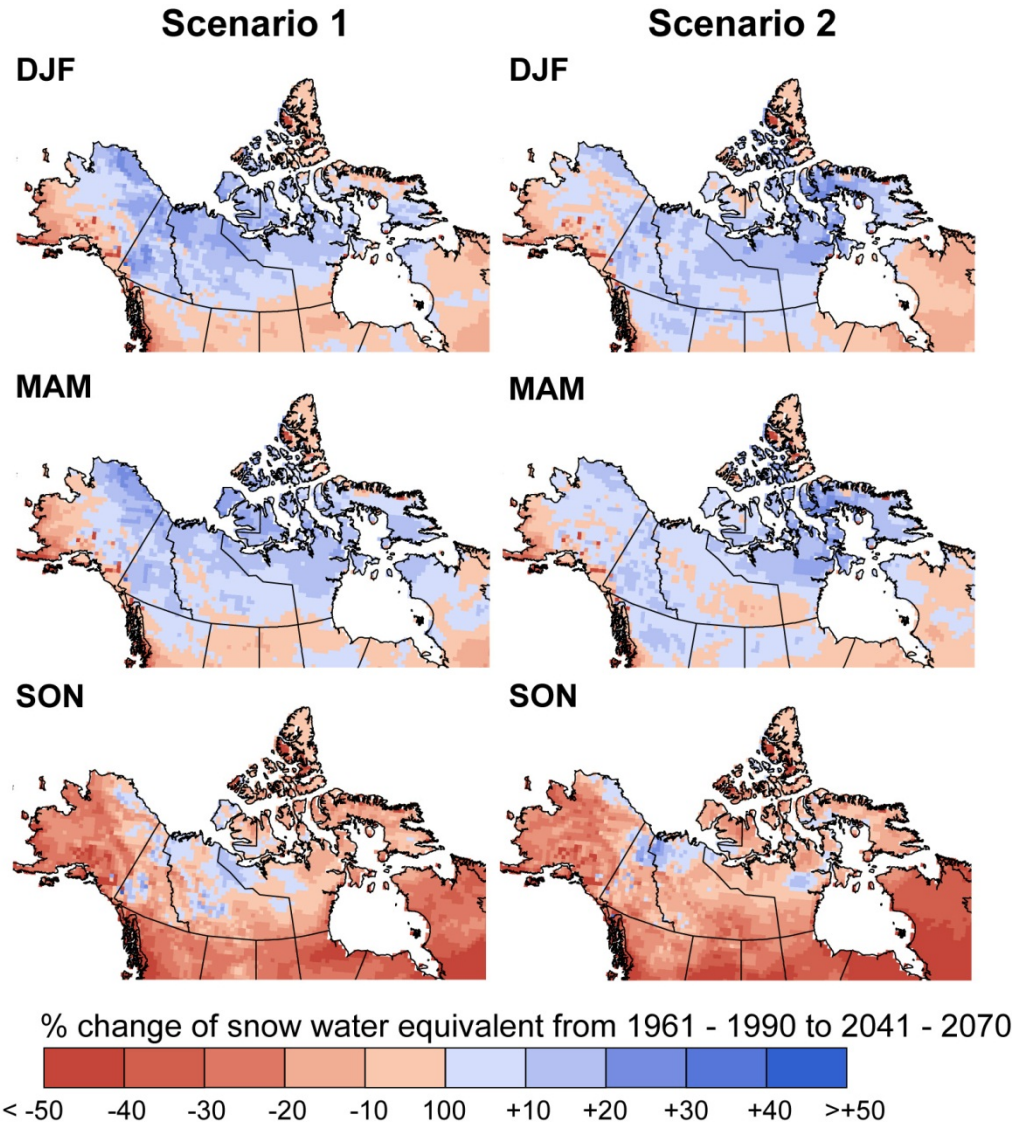

Figure 4.10. Change in snow water equivalent from 1961-1990 mean to 2041-2070 mean from the CRCM data displayed by season Winter (Dec., Jan., Feb.), Spring (Mar., Apr., May) and Fall (Sept., Oct., Nov.).

4.3.4.1 Ice cover duration 2041 – 2070

Comparing the mean break-up dates for 2041-2070 to the mean 1961-1990 dates show later break-up across the entire study area (Figures 4.11a, 4.11b) with the exception of 1 small area on Baffin Island in the snow free scenario 1 simulation where the increased frequency of summer break-up resulted in a slightly earlier date. Break-up ranges from late February to mid-August (yd 51 – yd 232) for all

simulations, with the mean break-up date now yd 150 (151 for scenario 2) for full snow scenarios and 156 (157 for scenario 2) for no snow scenarios - a shift of mean break-up date 7 days earlier for the snow scenario and 14 days earlier for no snow scenario. No perennial ice cover remains in scenario 2 and only 5 grid cells remain in scenario 1 for the no snow scenarios (compared to 19 and 40 for snow/no snow in 1961-1990). Although in most areas scenario 2 is cooler than scenario 1, the far northern parts of Ellesmere and Baffin Islands where the perennial ice was located, experience warmer temperatures than scenario 1 during the winter and spring, likely contributing to the differences in the perennial ice cover.

Comparing the results from the two future scenarios can provide some insight on the possible range of dates predicted by this CRCM scenario data (Figure 4.11c). Examining the snow-free scenarios, the majority of the study area has mean 2041-2070 break-up dates for both CRCM scenarios within 5 days of each other. Scenario 2 is mainly 0 - 5 days later than scenario 1; not unexpected as slightly cooler temperatures persist in most areas of scenario 2. Only a few areas show a difference of more than 5 days between the scenarios, with a few smaller areas dispersed around the southern reaches of the study area showing 5-10 days later break-up. The northwestern coastal and southern coastal areas of Alaska (and northern British Columbia) show 10-30 days earlier break up with scenario 2. The northern and eastern parts of the CAA show earlier break-up for scenario 2, again the result of warmer temperatures in this area. The areas with greater than 30 days differences in break-up dates on Ellesmere Island result from the lack of any remaining perennial ice cover in scenario 2. For the snow-covered scenarios, break-up for the two CRCM scenarios is still mainly within 5 days, with a larger portion of the study area shifting to 0 - 5 days earlier break-up, particularly in the north eastern areas.

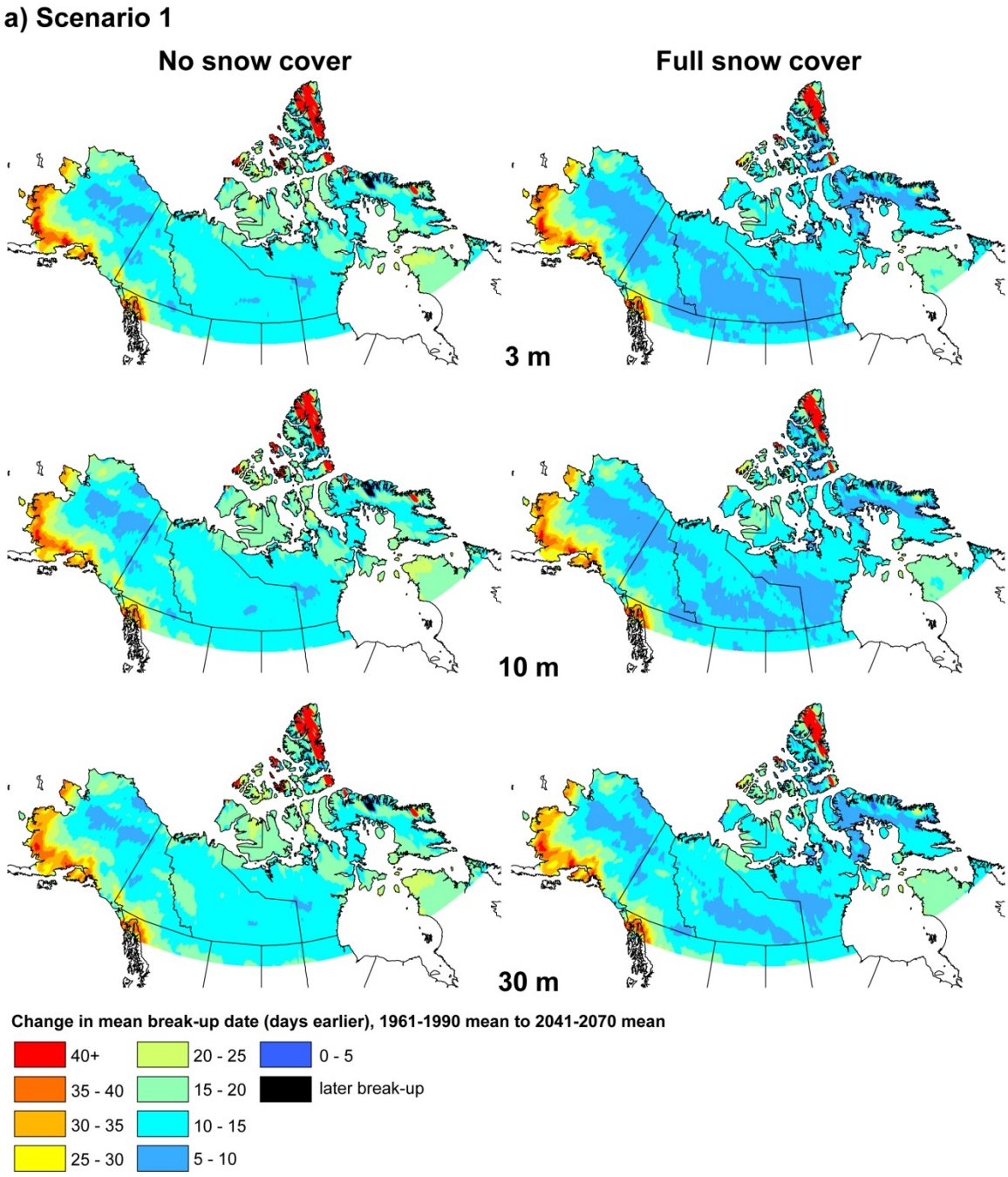

Figure 4.11. Change in mean break-up date from 1961-1990 to 2041-2070 for a) scenario 1; b) scenario 2; c) the difference between the scenarios for the 2041-2070 mean break-up dates.

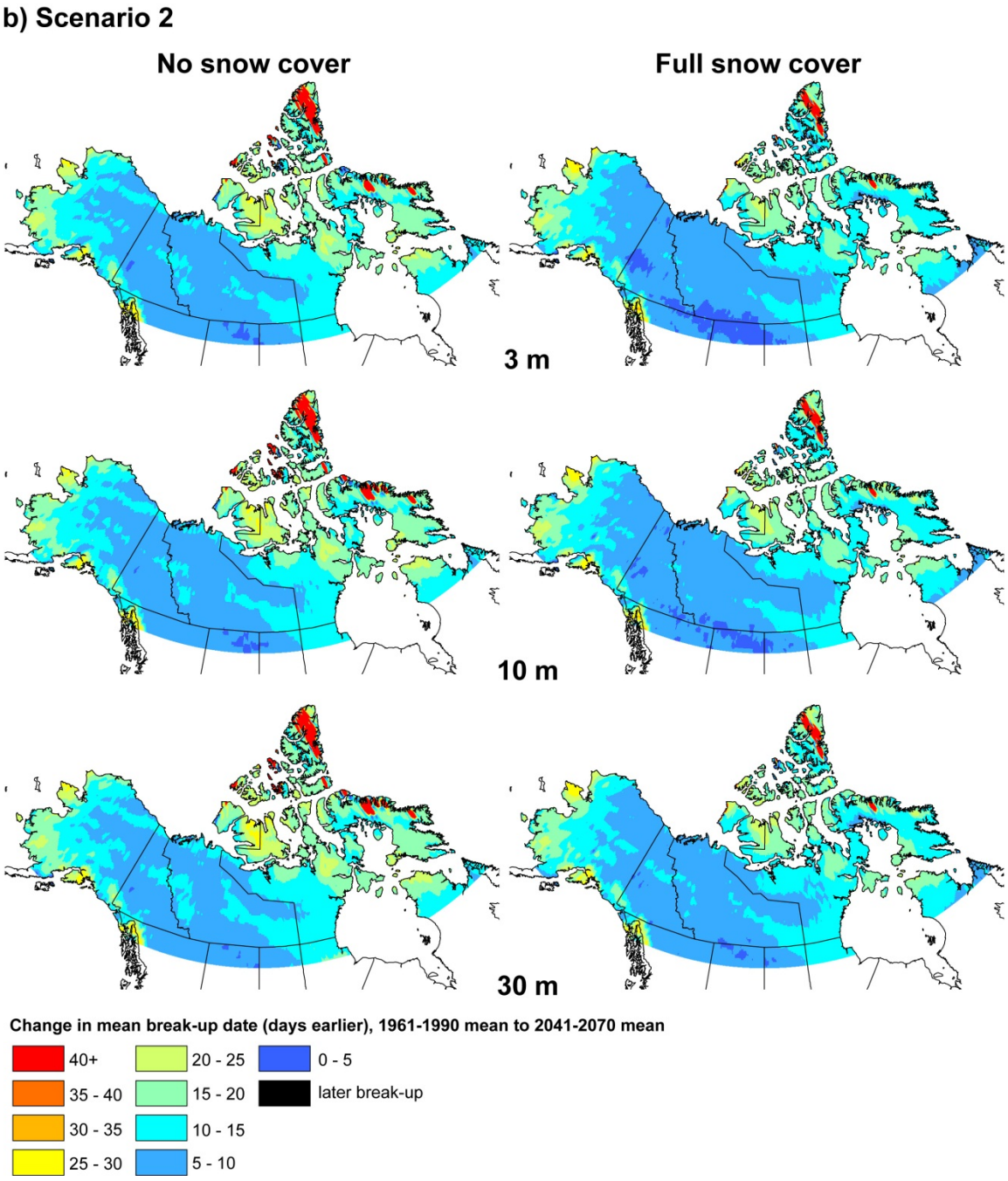

Figure 4.11. Continued.

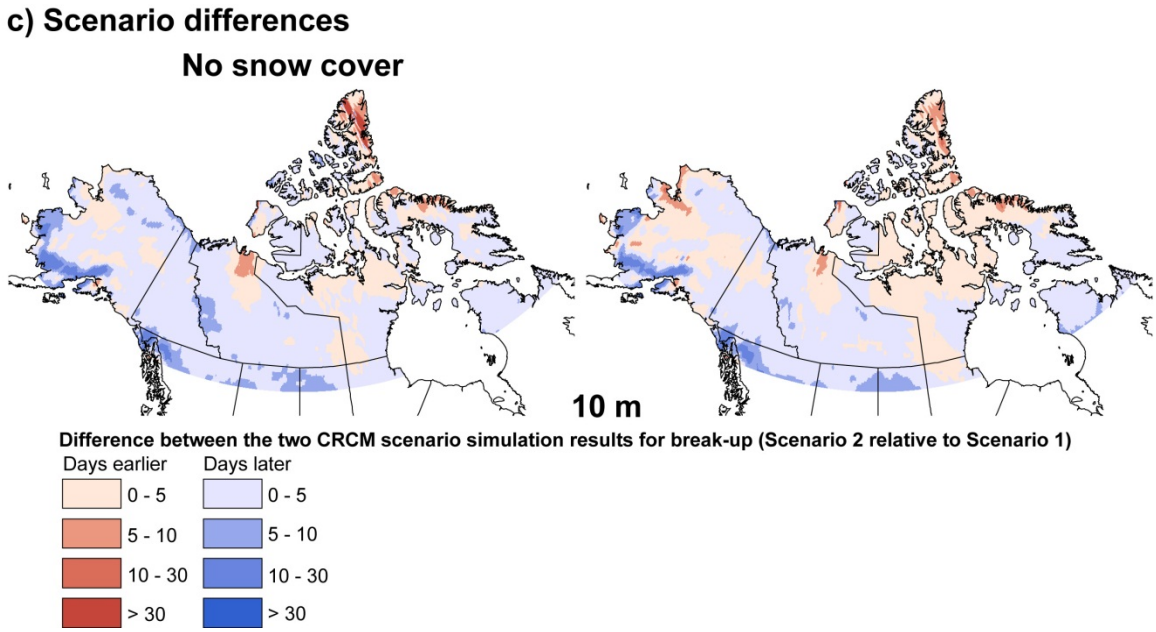

Figure 4.11. Continued.

Freeze-up for 2041-2070 now ranges from late August until the end of December (yd 240 - yd 365 for scenario1 and yd 245 – yd 364 for scenario 2), with mean freeze-up dates the same for both scenarios: 289 (3 m), 301(10 m) and 325 (30 m). Mean freeze-up dates show a shift of 6 -11 days later than those from 1961-1990, less of a change than break-up. Figures 4.12a and 4.12b present the changes in freeze-up dates from 1961-1990 to 2041-2070. Scenario 1 has the greatest changes for freeze-up in Alaska and the High Arctic while scenario 2 has the greatest changes in the High Arctic and eastern areas (Baffin Island and northern Quebec). The areas with greater than 40 days change in freeze-up on Ellesmere Island are the areas where the perennial ice cover changed to seasonal ice cover. There are more pronounced differences between the scenarios for freeze-up than break-up (Figure 4.12c). The central section of the study area is still ± 5 days between the scenarios, however northern Quebec and Baffin Island show 5-20 days later freeze-up with scenario 2, while freeze-up in Alaska is 5-10 days earlier with some section in the shallower lakes >10 days earlier (not shown).

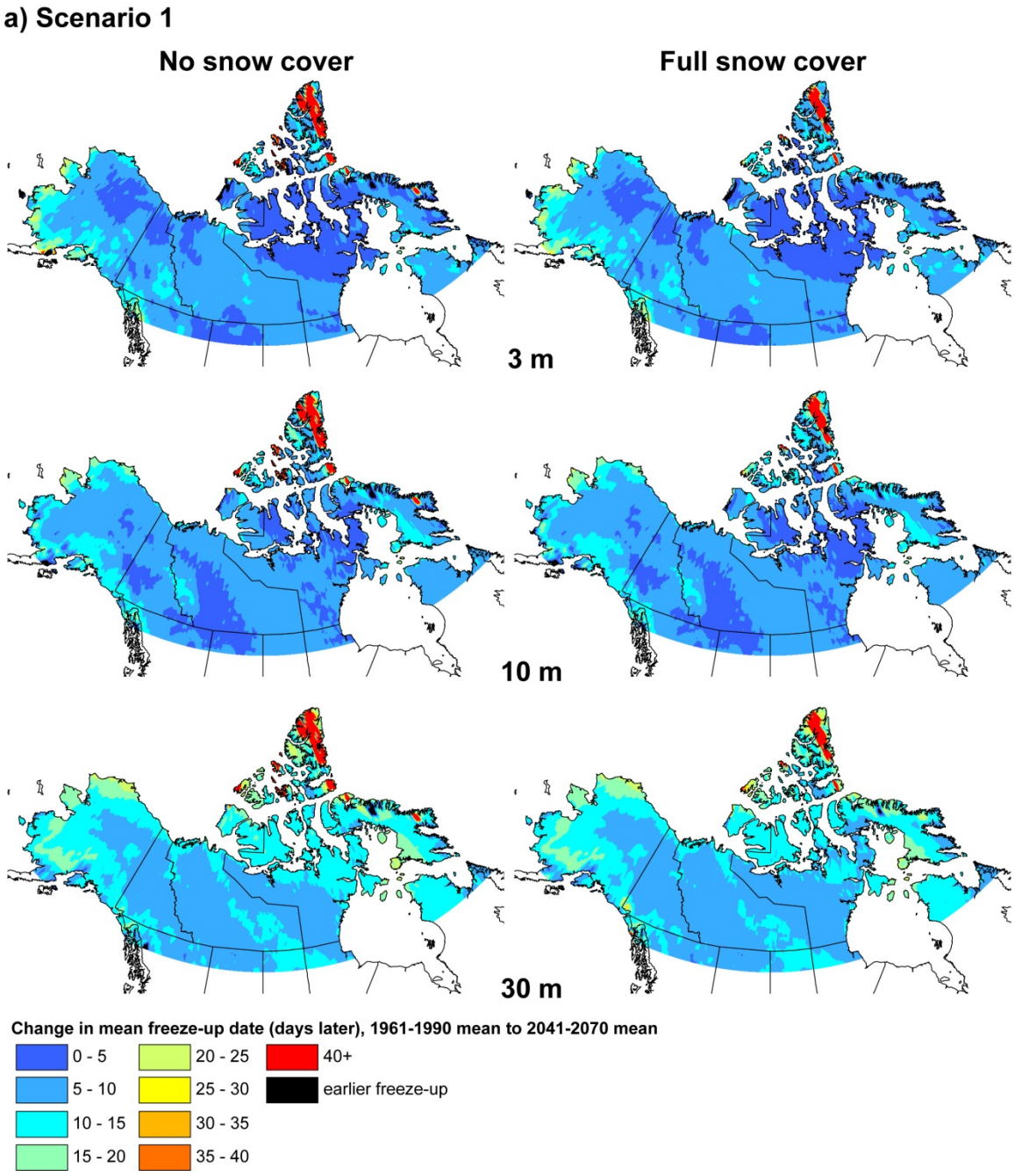

Figure 4.12. Change in mean freeze-up date from 1961-1990 to 2041-2070 for a) scenario 1; b) scenario 2; c) the difference between the scenarios for the 2041-2070 mean freeze -up dates.

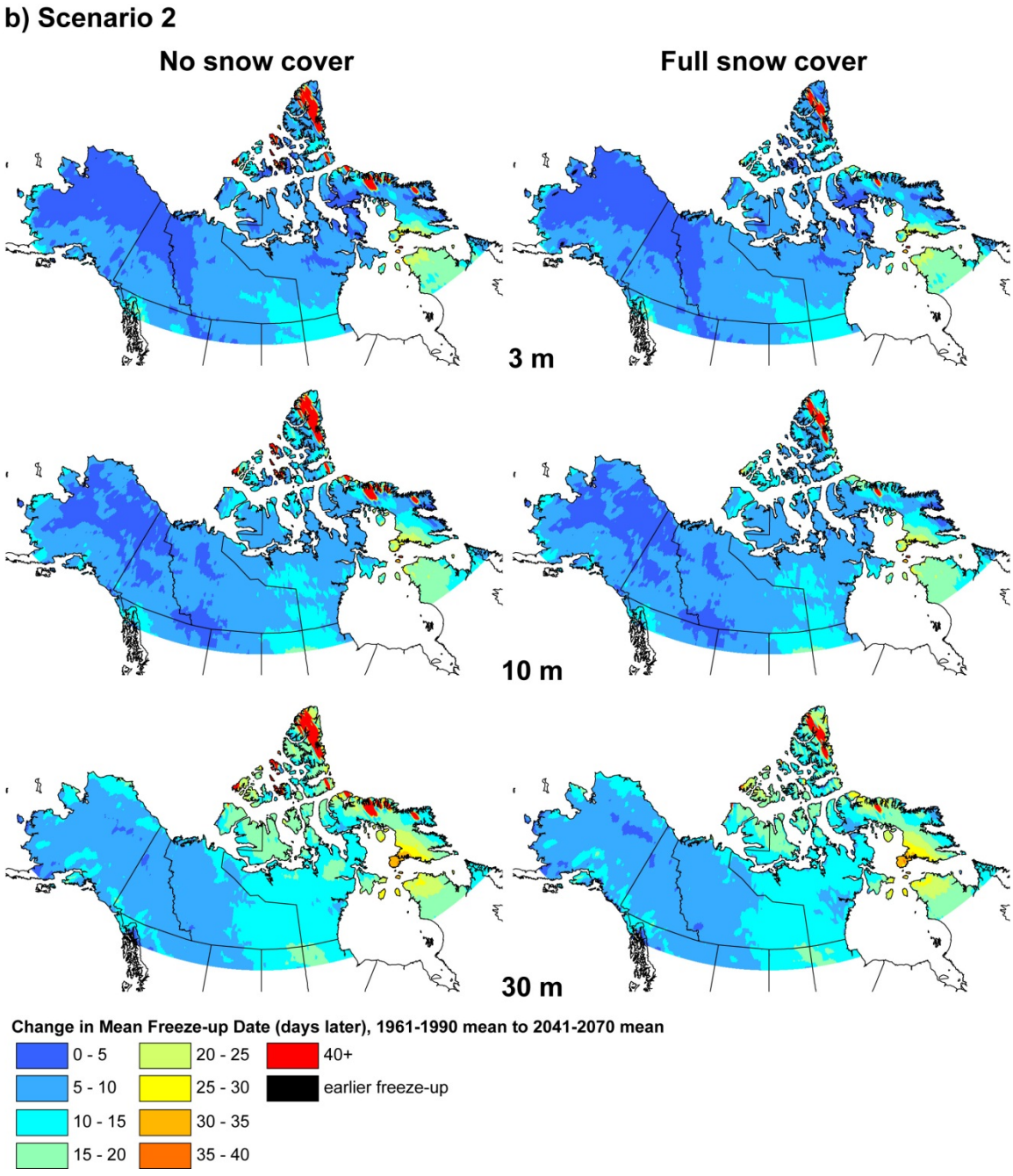

Figure 4.12. Continued.

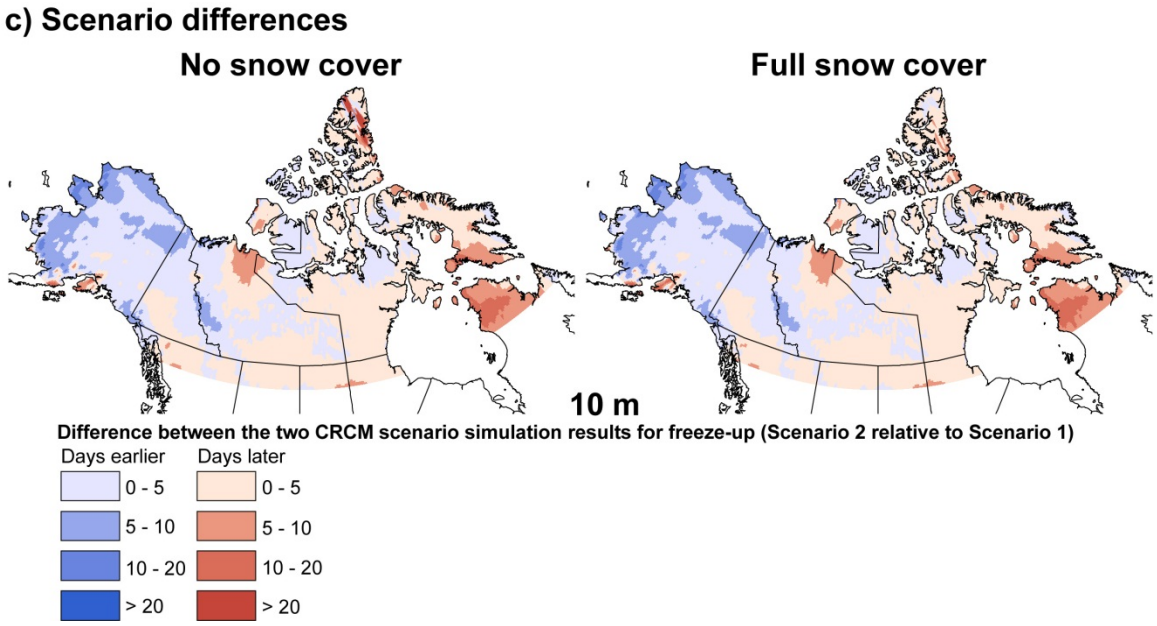

Figure 4.12. Continued.

The changes in ICD from 1961-1990 to 2041-2070 are presented in Figures 4.13a and 4.13b. Scenario 1 shows a change in ICD ranging from 10 to more than 40 days shorter by 2041-2070. The areas of the most change are the Alaska coast and the High Arctic islands (25 to >40 days shorter ICD); and northern Quebec (20-30 days shorter ICD). The ICD throughout the rest of the region is mainly 10-25 days shorter ICD and the effect of snow cover can also be seen in the simulations, with the snow-covered simulations producing slightly less change in ICD than the snow-free simulations.

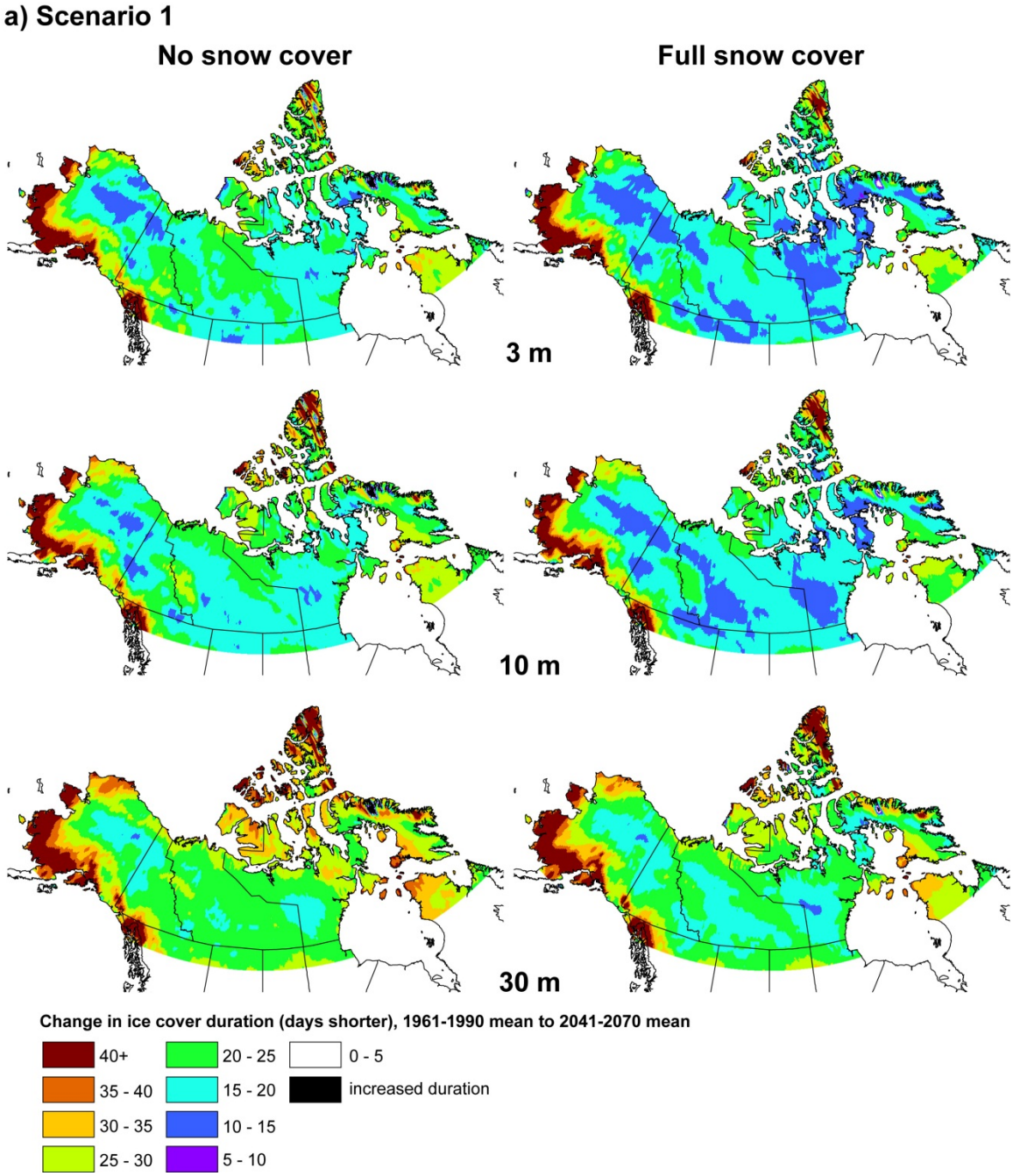

Figure 4.13. Change in mean ice cover duration from 1961-1990 to 2041-2070 for a) scenario 1; b) scenario 2; c) the difference between the scenarios for the 2041-2070 mean ice cover duration.

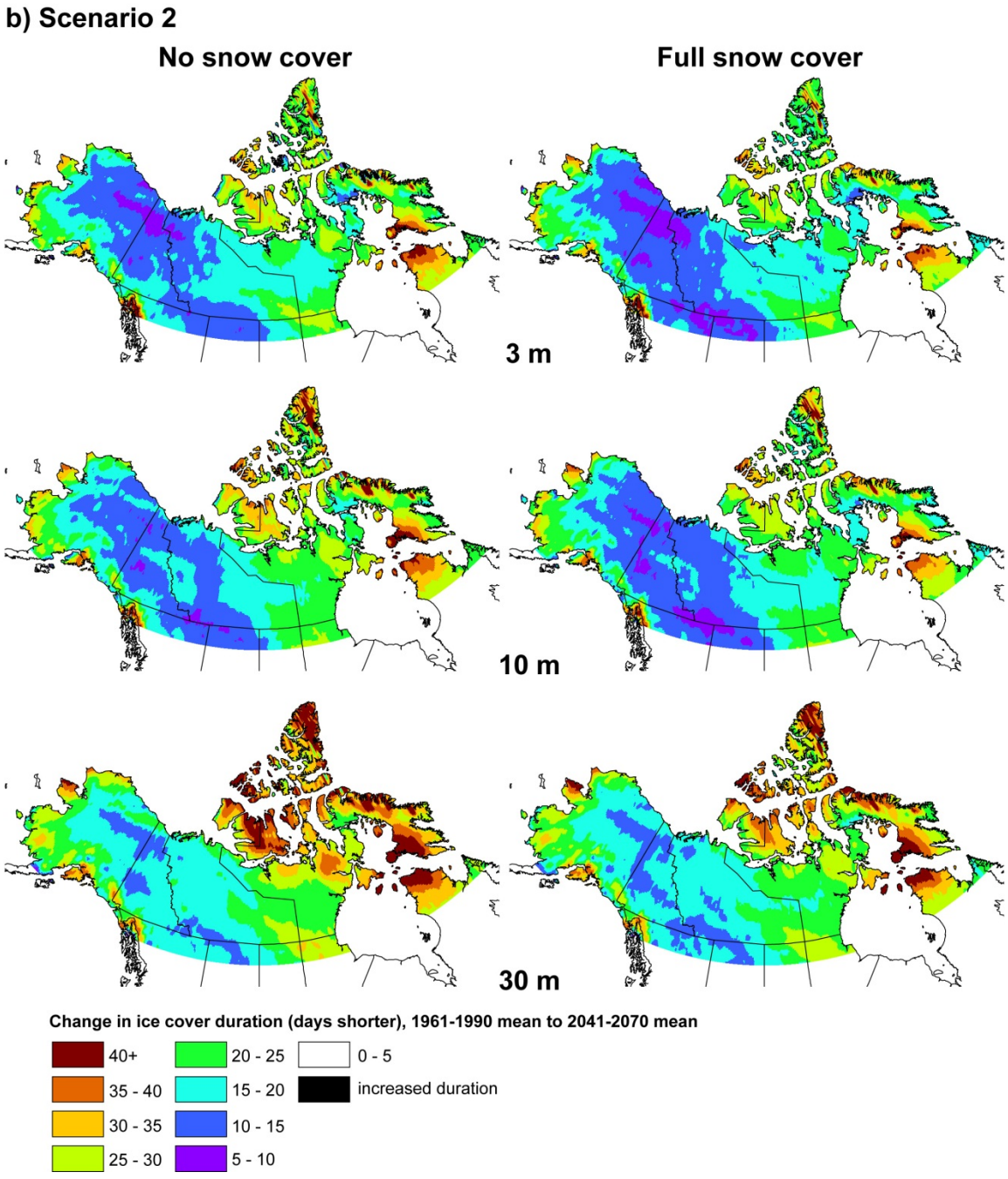

Figure 4.13. Continued.

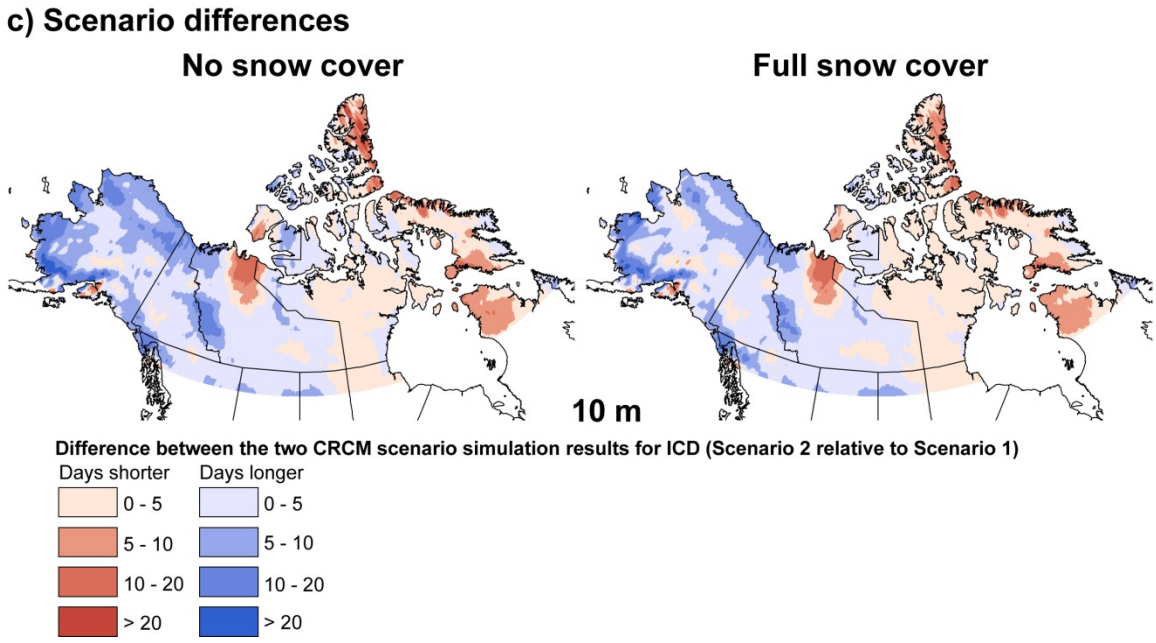

Figure 4.13. Continued.

Although scenario 1 and 2 appear quite different in terms of spatial pattern (Figures 4.13a, 4.13b) this is in part due to the broad 5 day categorization. Scenario 2 shows the same range of ICD changes as scenario 1, however, there are much larger areas with less change due to the smaller changes in break-up and freeze-up. Of note here is the areas of most change – scenario 1 focusing over the Alaskan coast and scenario 2 focusing over the Arctic islands as well as northern Quebec and southern Baffin Island rather than the Alaskan coast (as seen in scenario 1). Similar to break-up and freeze-up, the ICD differences for the two CRCM scenarios (Figure 4.13c) is mainly ± 5 days, with more areas in the 5-10 day differences from the combined effect of break-up and freeze-up differences.

Both future scenarios show a loss of perennial ice cover as well as large reductions to the area where occasional summer ice cover is predicted to occur (Figure 4.14). There is a larger reduction of grid cells where occasional summer ice occurs with the no-snow scenarios than with snow. However, a smaller area remains with occasional summer ice when snow is taken into account, reflecting the insulating effects of the snow, leading to thinner ice, leading to fewer summers where any ice persists in the lakes. Using the 10 m hypothetical lakes as an example, a reduction of 192 grid cells where perennial or occasional ice would occur (388800 km^2) was seen with no-snow and reduction of 91

grid cells (184275 km^2) was seen with snow. Also, while scenario 2 begins with slightly more occasional summer ice, due to the greater warming in the high latitude areas by the 2041-2070 mean in this scenario, a greater reduction in the summer ice cover is seen.

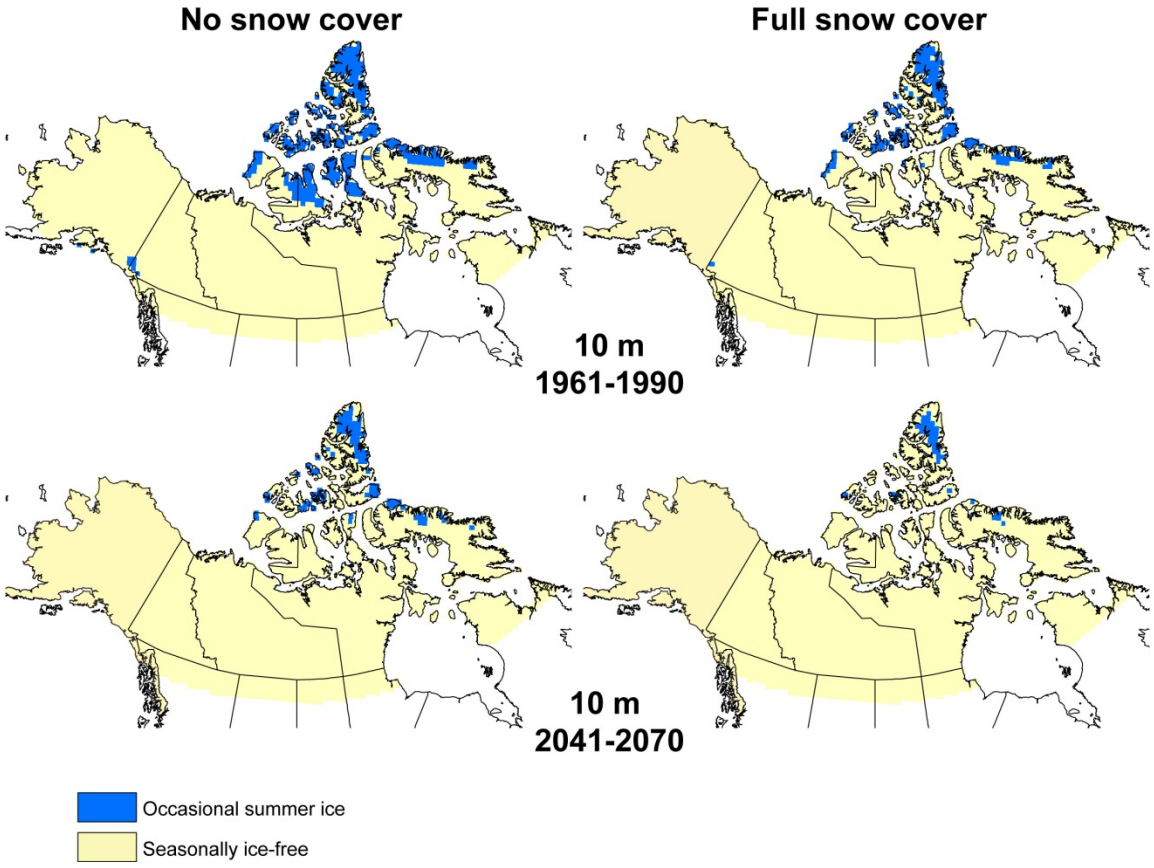

Figure 4.14. Area of occasional summer ice (including perennial ice cover) and the change from 1961-1990 to 2041-2070. Scenario 1, 10 m lakes shown.

4.3.4.2 Ice cover thickness 2041 – 2070

Along with a reduction in the ICD for the future scenarios, the mean maximum thickness of the ice cover on the lakes is also shown to decrease. Scenario 1, for the snow-free simulations, has an average of 32 cm less ice, ranging from 20 – 40 cm with up to 60 cm reduction in thickness in the northwest Alaskan coastal regions. The snow covered simulations show most of the region to have a loss of thickness ranging from 10 – 30 cm, with a few small regions reaching just over 40 cm reduction (average of 25 cm reduction in ice thickness). Spatially, the snow cover scenarios produce

quite different results (Figures 4.15a, 4.15b). With the snow-free simulations, the deeper the lake, the more change in thickness predicted (30 m lakes mainly greater than 30 cm reduction in ice thickness). With snow added on top of the ice cover however, the 10 m deep lakes show slightly less loss of thickness than the 3 m lakes, with the most change occurring in the 30 m lakes.

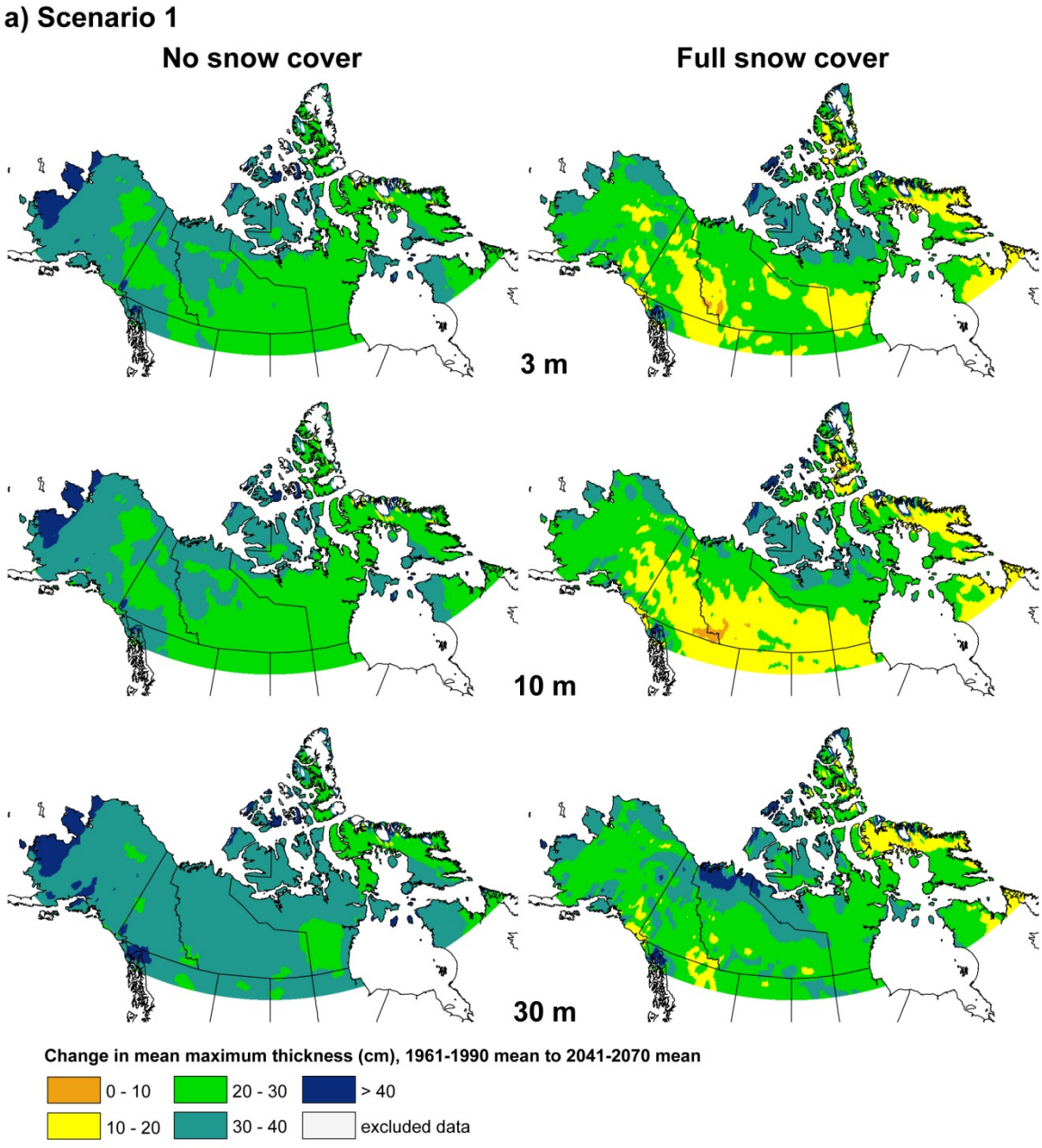

Figure 4.15. Change in mean maximum thickness 1961-1990 to 2041-2070 for a) scenario 1; b) scenario 2; c) the difference between the scenarios for the 2041-2070 mean maximum thickness.

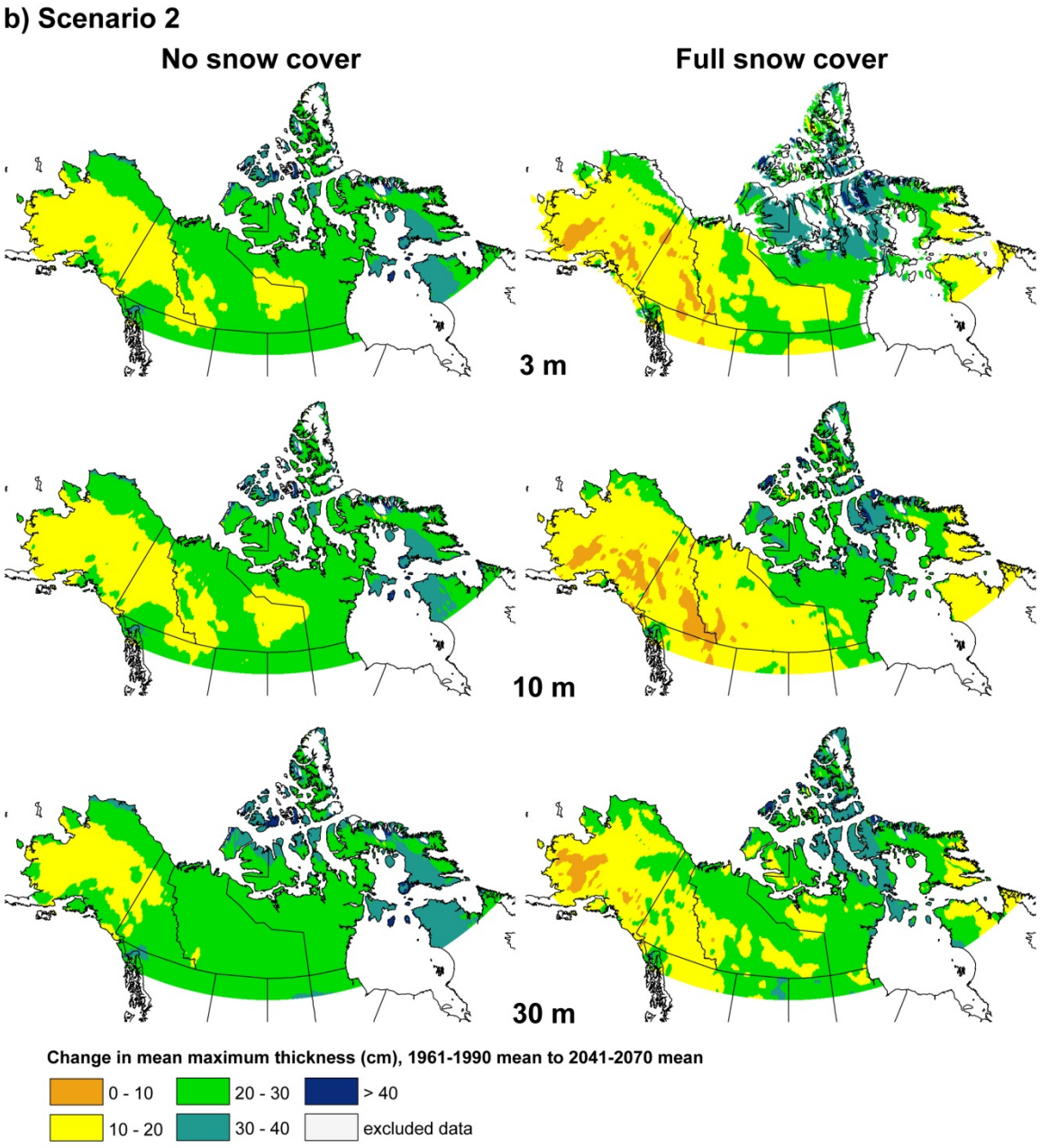

Figure 4.15. Continued.

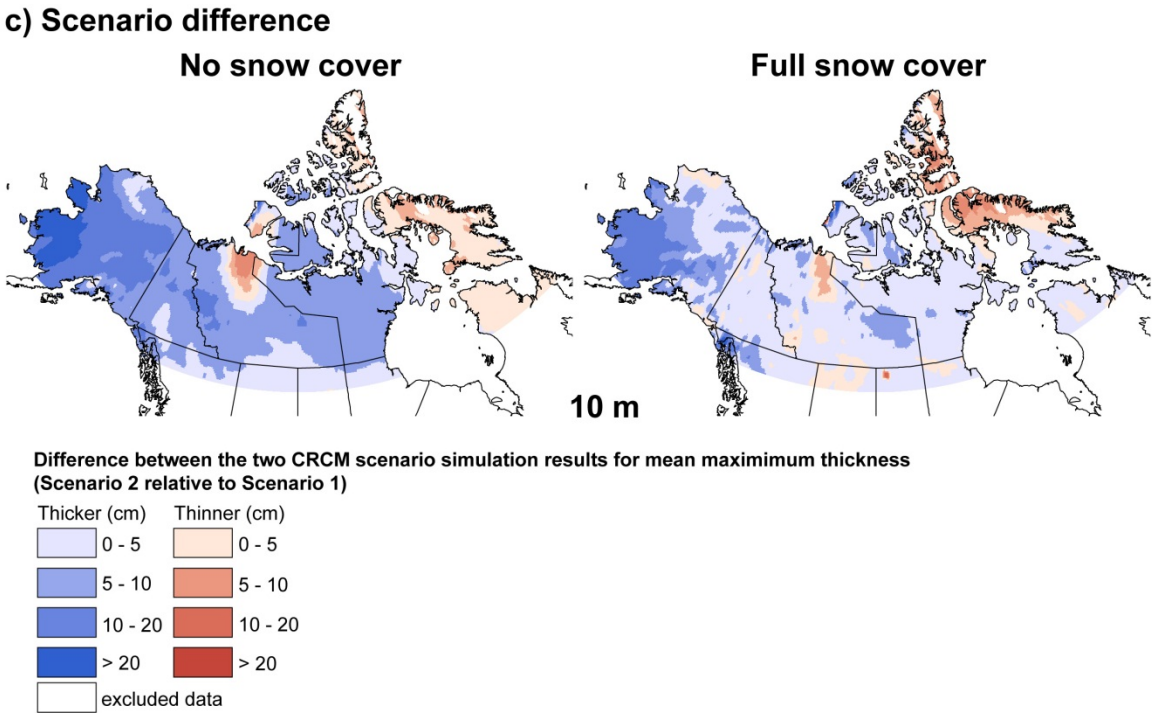

Figure 4.15. Continued.

Scenario 2, being generally cooler than scenario 1 for the majority of the study area shows less predicted loss of thickness, with 21 cm less (mean) for snow covered and 24 cm less for snow free. Again the deeper the lake, the more change in thickness seen, but less change than scenario 1. In this case, most of the changes to the ice thicknesses are in the 10 - 30 cm, except for some areas of the CAA and northern Quebec/southern Baffin Island where this increases to 30 – 40 cm.

Comparing the two scenarios (Figure 4.15c), most of the area has less than 10 cm difference between them, with the exception of the northern western Alaskan coastal areas in the same areas the differences in ICD were seen. With snow covered scenarios the difference is less than 20 cm (with scenario 2 being thicker) however with the snow free scenarios this difference increased to up to 25 cm.

Mean maximum thickness amounts include both snow ice and black ice in the total amounts. Looking at the changes in to the snow ratio ice from 1961-90 to 2041-70 most of the study area experiences some increase, though in the central regions this increase is less than 1% (Figure 4.16). Also, with the shallower lakes, increased snow ice ratios are seen around Hudson Bay and up into the

High Arctic that are not evident with the deeper 30 m lakes. Areas of decreased snow ice ratio are along the warmer coastal areas of Alaska (and a small area of northern Quebec/Labrador), corresponding to areas of decreased SWE (Figure 4.10) where increased amounts of precipitation would be expected to fall as rain rather than snow, reducing the chance for snow to accumulate on the ice surface to form snow ice.

4.4 Summary and Conclusions

Ice phenology simulations using the lake ice model CLIMo driven by climate model output from CRCM scenarios for 1961-90 had an average absolute error of less than 1 week compared to observation data at 15 validation sites across northern Canada. For three validation lakes where CLIMo was able to represent the phenology well, the mean maximum ice thickness had an average absolute error of 12 cm (6.5 %) compared to the measured ice thickness. Capturing the correct ice thickness in the simulations depends on how well the snow cover on the ice surface is represented both in terms of depth and density.

By 2041-70, the mean break-up date was shown to shift 7 days earlier with snow cover on the lakes and 14 days earlier with no snow cover. Most of the northern areas show a change in the range of 10 - 25 days earlier for break-up (excluding the areas of maximum change discussed later). Mean freeze-up for the north was shown to shift 7, 8 and 11 days later (3, 10 and 30 m depths respectively) with shifts ranging from 0 - 15 days later, a smaller change than seen in break-up. These ranges are comparable to those identified by Dibike et al., (2011), using the MyLake model (Saloranta and Anderson, 2007) to examine future changes over a broader and more southern area of North America. Ice cover durations ranged from 10 to more than 40 days shorter, with the areas of greatest change in scenario 1 located near the Alaskan coast, the far northern Arctic islands, and northern Quebec; while scenario 2 had the greatest changes in the north eastern section of the study area (the CAA and southern Baffin Island/northern Quebec). In the remainder of the study area (away from the areas of maximum change) the shallower lakes (3 and 10 m) show mainly 10 - 25 days shorter ICD (5 -25 days shorter for scenario 2), while the 30 m lakes show primarily 15 - 30 days shorter ICD (10 - 30 days shorter for scenario 2). The areas of maximum change identified in this study were more extreme than those in the results produced by Dibike et al (2011) for reduction in ICD, however the spatial patterns in their results were most similar to scenario 1.

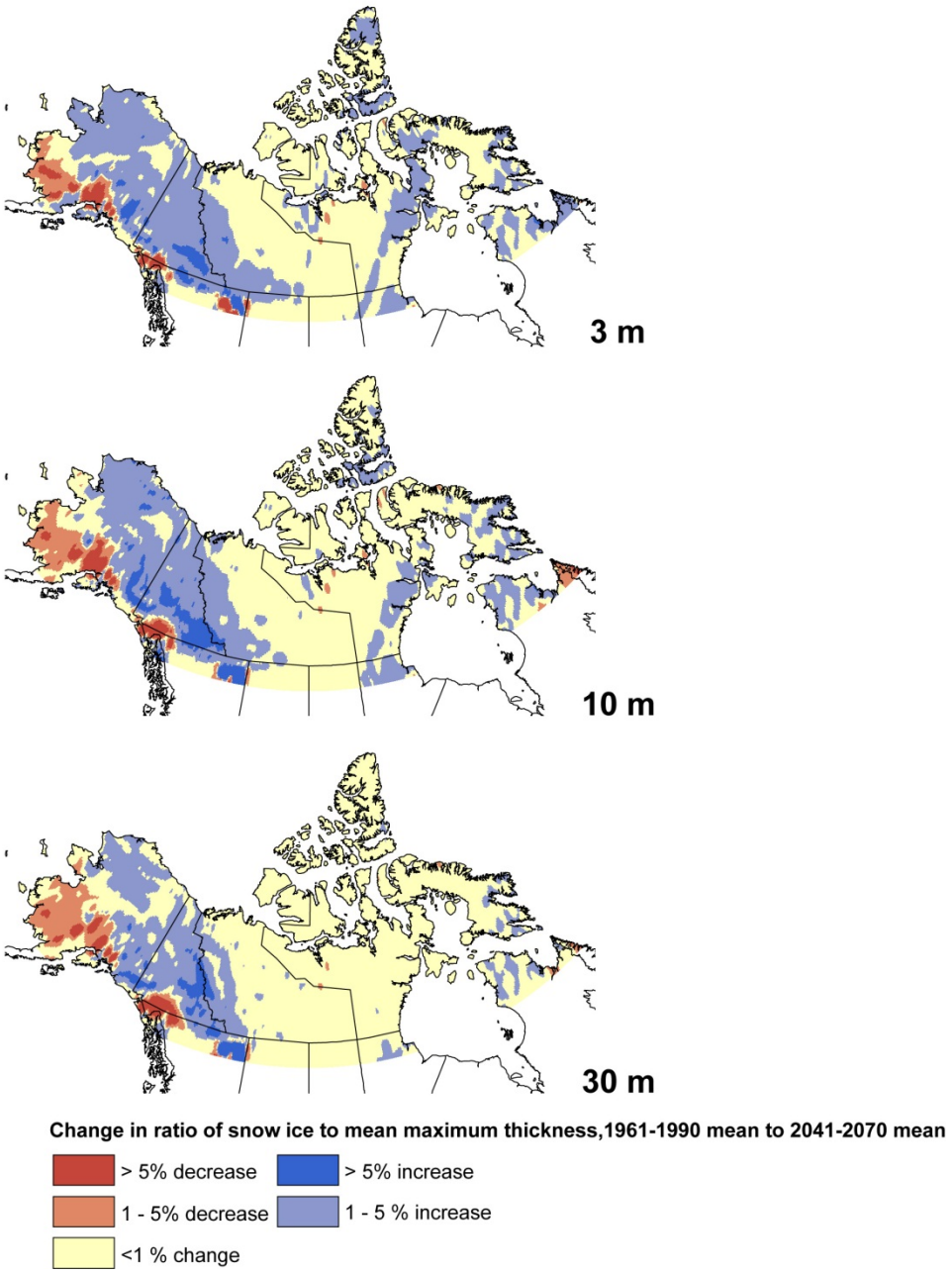

Figure 4.16. Change in snow ice thickness to total ice thickness from 1961-1990 to 2041-2070 mean.

Both scenarios show a drastic reduction in the number of grid cells with perennial ice cover, with none remaining in scenario 2. The areas of occasional summer ice cover are also reduced, with greater losses when no snow cover is on the ice (though a smaller area remains when snow cover is taken into account).

Changes to the mean maximum thickness show an average of 25 cm less ice for the snow simulations (21 cm less for scenario 2), and 32 cm (24 cm) less ice for the snow-free simulations. Overall, scenario 1 shows more reduction in ice thickness than scenario 2 with the maximum loss reaching over 40 cm in the Alaskan coast areas (scenario 1) and up to 40 cm reduction in the CAA and northern Quebec/southern Baffin Island (scenario 2). The ratio of snow ice to total maximum ice thickness was also shown to increase throughout the study area, with the exception of the Alaskan coastal areas, where a reduction in the SWE was also observed. Dibike et al. (2011) show the area with the thickness changes along the northern coast lines at the upper extent of their study area (up to 25 cm reduction), which is again, most comparable to the full snow simulations in scenario 1.

The use of two variations of the CRCM data allows for some measure of uncertainty in the range of dates produced by the simulations. Break-up and freeze-up dates were generally within 5 days for the two scenarios, except in three key areas where the most variability is seen throughout, around the coasts in: Alaska, the far north on Ellesmere Island and northern Quebec/southern Baffin Island (and to a lesser extent a localised area on the coast of the NWT). In these areas, differences between the scenarios for freeze-up range up to ± 16 days (the very large values ranging up to ~100 days in the far north are due to the different amounts of perennial ice cover). Thickness typically varied less than 10 cm between the scenarios except for Alaska, where the snow free simulations were up to 20 cm different (snow covered up to 25 cm) in the same areas of maximum differences seen in ICD. The variations in these areas are a reflection of the different patterns of temperature change between the scenarios by the time they evolve to 2041-70. Scenario 1 shows the greatest warming over the Alaska region in the fall and winter, while scenario 2 has the greatest warming in the Quebec/Baffin region in the winter and the CAA in the fall. Higher temperatures throughout in the spring for scenario 1 would affect the break-up, and the warmer winter temperatures would lead to less ice thickening and earlier spring break-up.

Changes to northern lakes as a result of a shorter ice cover season and thinner ice covers could lead to in an increase to the availability of under ice habitat, a prolonged productivity period (ACIA, 2005) and a change to the habitats and species from increased amounts of light and UV radiation reaching

the water (e.g. Reist et al., 2006). Longer open water seasons will result in changes to the stratification and circulation patterns in the lakes (ACIA, 2005), and previously stratified perennially ice covered lakes that have changed to seasonally ice free will experience wind-driven mixing, changing the water column regime (Mueller et al., 2009). Longer open water seasons will also lead to increased evaporation from lakes, and while ponds in the High Arctic are drying out as the climate warms (Smol and Douglas, 2007) the shrinking/drying of lakes and ponds will likely be mitigated in some areas by increases in precipitation (Duguay et al., 2009). A shortened ice covered season is also expected to have a detrimental effect on the duration and stability of the winter ice roads in northern Canada and Alaska. By mid-century, Canada is predicted to lose access to 13% of the northern areas currently accessible via ice roads, while Alaska is predicted to lose access to 29%, with most of the changes occurring in April and November (Stephenson et al., 2011).

Reanalysis data or climate model output specifically created for the arctic regions could be beneficial for future predictions. Alternatively, the use of model ensemble data for future ice cover simulations could be beneficial as the largest source of uncertainty can come from the section of the model used (e.g. Prudhomme and Davis, 2009). Downscaling projects to examine regional changes to the future climate are underway through programs such as CORDEX: (COordinated Regional climate Downscaling Experiment, regional climate change scenarios) and high resolution climate change scenarios are being studied at NARCCAP (North American Regional Climate Change Assessment Program) to better assess the uncertainties in the various model simulations.

The gridded phenology maps produced herein highlight the important effects that both snow cover and lake depth have on lake ice regimes, and that snow cover tends to mitigate the changes to the ice cover. As well, the use of the two scenarios suggests areas of the greatest uncertainty in the phenology and thickness changes, primarily the Alaska coastal areas, the eastern CAA and the Baffin Island/northern Quebec region.

4.5 Acknowledgments

This research was supported by a NSERC postgraduate scholarship (CGS) to L. Brown and Discovery Grant to C. Duguay. The CRCM data was generated and supplied by Ouranos. We are indebted to Ross Brown (Environment Canada at OURANOS) for valuable advice throughout the project.

Chapter 5
Modelling lake ice phenology with an examination of satellite detected sub-grid cell variability

5.1 Introduction

Lakes are a dominant part of the landscape in Canada, forming an important part of the cryosphere. Their ice cover both plays a role in and responds to climate variability and the presence (or absence) of ice cover on lakes during the winter months is known to have an effect on both regional climate and weather events (e.g. thermal moderation and lake-effect snow) (Rouse et al., 2008). Lake ice has also been shown to respond to climate variability; particularly changes in air temperature and snow accumulation. Both long-term and short-term trends have been identified in ice phenology records and are typically associated with variations in air temperatures; while trends in ice thickness tend to be associated more with changes in snow cover (Brown and Duguay, 2010).

Monitoring lake ice in vast areas such as Canada, particularly in the northern areas, is logistically challenging as many lakes are in remote regions with limited accessibility. Currently, there is a very limited surface-based network for monitoring lake ice in Canada. Volunteer-based lake ice observations have also been used for monitoring ice cover, for example Futter (2003) using data from the 'IceWatch' program – Canadian lake ice observations by citizens; Dyck (2007) discussing long term monitoring of Crazy Lake, Nunavut by Nunavut Arctic College students; and Jeffries and Morris (2006) in Alaska (USA) using data collected by teachers and students as part of the Alaska Lake Ice and Snow Observatory Network (ALISON). Digital camera imagery has been shown to be a useful tool for unattended lake ice monitoring (Brown and Duguay, 2011a) and while the imagery used for the aforementioned study was downloaded in situ, the technology is available for digital cameras to be connected to telemetry systems for real-time monitoring.

Remote sensing products can contribute towards monitoring lake ice cover where no in situ data exists. Presently the Canadian Ice Service (CIS) monitors the fractional ice cover on 135 large lakes throughout Canada on a weekly basis using visual interpretation of satellite data. Products using a combination of several remotely sensed data sources such as the Interactive Multisensor Snow and Ice Mapping System (IMS, 4km: Ramsay, 1998; Helfrich et al., 2007) provide the opportunity for detection of daily ice cover extents across the entire northern hemisphere for larger lakes (Duguay et al., 2011). The use of optical imagery is limited in the northern regions due frequent cloud cover and

polar darkness (e.g. MODIS, AVHRR). However, microwave data provides the potential for obtaining ice phenology on both large lakes (e.g. Howell et al., 2009) and small lakes (Duguay et al., 2002; Geldsetzer et al., 2010) as well as ice thickness on large lakes (Kang et al., 2010). In latitudes where polar darkness does not occur, one product of particular interest for lake ice monitoring is the MODIS daily snow product (Hall et al., 2002; Hall and Riggs, 2007). While primarily used for monitoring snow cover (e.g. Frei and Lee, 2010; Brown et al. 2010; Hall et al. 2012) this product has a wide variety of applications including both the validation and incorporation into hydrological modelling (e.g. Parajka and Blöschl, 2008; Brown et al., 2008; Roy et al., 2010). MODIS surface reflectance products (MOD09A1) combined with eight day snow cover composites (MOD10A2) (Mischra et al., 2011) and calibrated radiance images/visible composites (Reed et al., 2009) have been used for identification of lake ice on/off dates, and although lake ice and open water are identified in both IMS and the MODIS snow cover product, limited work has been done to examine the utility of extracting ice phenology from these products (Duguay et al., 2011; Kang et al., 2012; Balsamo et al., 2012).

While satellite data presents the possibility of wide scale monitoring of lake ice phenology, ice thickness and composition are not readily obtainable through current techniques. Modelling can provide the opportunity to examine ice cover regimes on lakes, including the timing of break-up/freeze-up, ice thickness and composition. Different types of models have been used to examine lake ice with varying degrees of complexity such as regression or empirical models (e.g. Palecki and Barry, 1986; Livingstone and Adrian, 2009); energy balance models (e.g. Heron and Woo, 1994; Liston and Hall, 1995); thermodynamic lake ice models (e.g. Vavrus et al., 1996; Launiainen and Chang, 1998; Duguay et al., 2003; Mironov et al., 2010). Additionally, lake ice models provide the ability to examine potential changes to the ice cover regimes through the use of future climate scenario data. Recent work using lake ice models suggests future changes in the North American Arctic ice cover could result in a 10-60 day reduction in ice cover duration – with the larger reductions found in coastal areas (Brown and Duguay, 2011b) and 15-50 days shorter ice cover duration for more southerly regions (40°N -75°N) across the Northern Hemisphere (Dibike et al., 2011).

The most suitable way to undertake wide scale lake ice modeling is to drive the models with climate model output or reanalysis data, rather than in situ meteorological stations, as in Canada, climate stations are typically confined to the relatively accessible areas of the mainland or coastal

areas in the Arctic islands. While previous work has modelled ice phenology using grid based climate data for hypothetical lakes of various depths (e.g. Brown and Duguay, 2011; Dibike et al., 2011), the one-dimensional models used would produce the same ice phenology for the entire (reanalysis or climate model) grid cell for lakes of a given depth. However, in reality, a variety of different lake morphometric conditions could exist within a given grid cell leading to different durations of ice cover within the grid cell.

The objective of this paper is to examine the spatial variability in lake ice-on/off dates present within a grid cell of forcing data, and determine how well the one-dimensional model CLIMo (Duguay et al., 2003) is able to simulate the ice cover with respect to the observed sub-grid variability. Specifically, this work aims to 1) examine the utility of both the IMS and MODIS snow products for identifying ice-on/off dates and determine the sub-grid cell variability using these products; 2) produce modelled ice cover which better represents the lake conditions within each grid cell (rather than hypothetical lakes) and; 3) create ice cover predictions based on future climate scenario data and provide an indication of the model performance in terms of the observed sub-grid cell variability.

5.2 Study Area and Methodology

5.2.1 Study Area

The area of focus for this work is the Province of Quebec, Canada (Figure 5.1). The climate in this region varies northwards from humid continental, to subarctic, to arctic, with both continuous and discontinuous permafrost located in the far northern areas. Over 90% of the province is underlain by the Canadian Shield Precambrian rock formation and there are over 8000 lakes and reservoirs ranging in size up to 2500 km2 (93 > 100 km^2, 20 > 400 km^2).

Seasonal temperature increases throughout the province have been observed over the last 50 years, particularly in the summer; with the exception of two northern stations, Kuujjuaq and Schefferville, which showed non-significant cooling trends during the winter (Vincent et al., 2007). Rainfall also shows significant increasing trends across Canada with the most pronounced increases found in the spring and fall for Quebec (Mekis and Vincent, 2011). Mixed trends were found for annual snowfall, although a notable decrease in winter snowfall was found in southern Quebec (Mekis and Vincent, 2011). Trends in snow cover typically have a north-south gradient in maximum SWE and spring snow cover duration, with significant decreases over southern Quebec and significant local increases

over north-central Quebec (Brown, 2010). Trends in the timing of lake ice formation and decay have also been identified in this region with varying degrees of strength. From 1961-1990, trends were predominantly towards later ice-on and earlier ice-off (though most were non-significant). For the 1971-2000 period, trends still show earlier ice-off but only 2 stations were available for ice-on (one with an earlier trend, the other with a later trend) (Duguay et al., 2006).

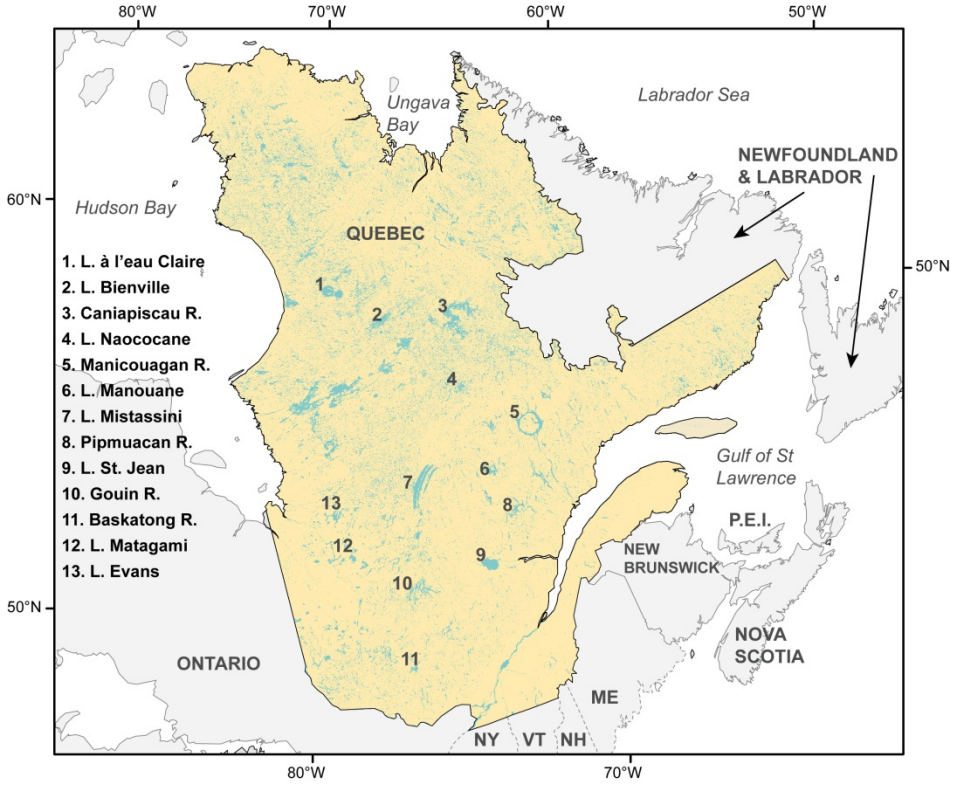

Figure 5.1. Map of the Province of Quebec, Canada, with the specific lakes (L.) and reservoirs (R.) referred to in this paper indicated.

5.2.2 Sub-grid cell lakes

The locations of lakes within the study area (including those smaller than can be resolved with satellite data used for this study) were identified using a modified version of the CanVec 1.1 files. CanVec is a digital cartographic product generated produced by Natural Resources Canada (obtained through GeoGratis), derived primarily from the National Topographic Data Base, with additional

information from the GeoBase initiative, updated with Landsat 7 or Spot imagery (Natural Resources Canada, 2010). A grid-based lake fraction (32 km resolution, based on the North American Regional Reanalysis data grid) was determined including all sizes of lakes identified using the modified CanVec files (Figure 5.2).

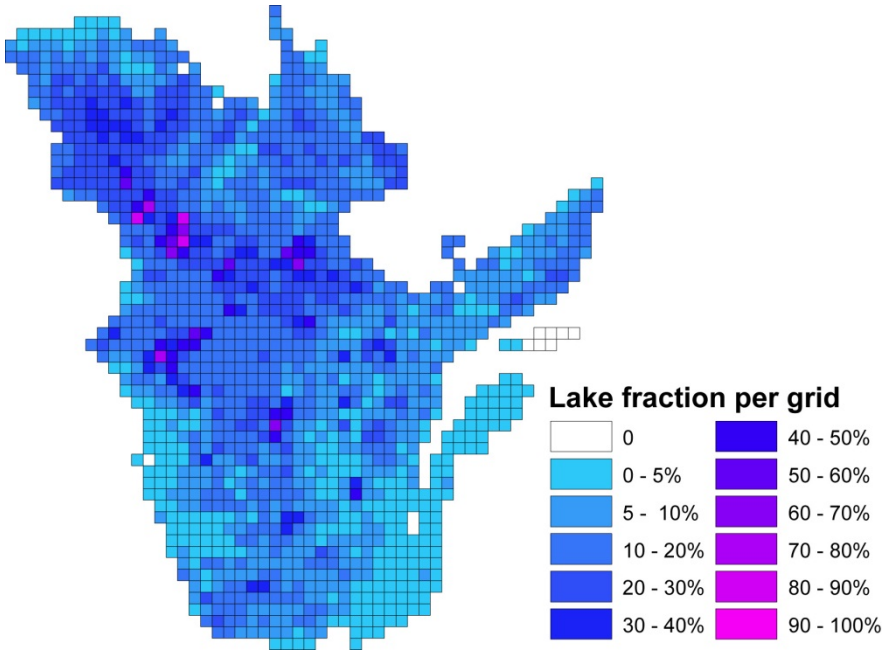

Figure 5.2. Lake fraction throughout the Province of Quebec, determined for 32 km grid cells.

5.2.3 Satellite Data

To examine the variability in ice-on/off dates of the numerous lakes throughout Quebec, two satellite-derived products were used: the Interactive Multisensor Snow and Ice Mapping System (IMS, 4 km northern hemisphere product, 2004 - present) and the MODIS snow product (MOD10A1, 500 m global product, 2000 – present) acquired through the National Snow and Ice Data Centre (NSIDC). The IMS product provides categories of ice, water, land, and snow and is produced daily by analysts from numerous remote sensing products (mainly optical but with some passive microwave data) augmented by station data (see Helfrich et al. 2007; Ramsay, 1998). The first date with open water for each lake pixel (change from ice to water) was used as the ice-off date, and vice versa for ice-on.

IMS can provide ice phenology for larger lakes (Duguay et al., 2011) however, there are numerous smaller lakes through the province that are not resolved by the 4 km pixels. The 500 m MODIS snow product was evaluated for use on these smaller lakes. The MODIS snow product (Collection 5) was obtained from the Terra sensor (MOD10A1) (2000 – 2011) with any missing days filled with the Aqua version of the snow cover product (MYD10A1). Snow cover is determined based on the algorithm Snowmap, which uses a grouped-criteria technique employing the Normalized Difference Snow Index (NDSI) and other threshold-based criterion to classify snow on a pixel-by-pixel basis (Hall et al., 2001) with an estimated accuracy of ~93%, varying with respect to snow conditions and land cover type (Hall & Riggs, 2007). Algorithm details can be found in the Algorithm Theoretical Basis Document (ATBD) (Hall et al., 2001, Riggs et al., 2006). Inland water areas are also analysed for snow-covered ice conditions based on a land/water mask developed by Boston University, which includes water bodies greater than 1 km in dimension (removing isolated pixels). The 1 km land/water mask is applied to the four corresponding 500 m pixels in the level 2 product used to generate the MOD10A1 product (MOD10_L2 swath product).

Cloud cover presents limitations in obtaining ice phenology from the daily snow product. In order to determine a 'best-estimate' date for ice-off, the first day of open water was extracted for each pixel. The actual ice-off date could therefore be earlier, depending on the persistence of the cloud cover. Ice-on was estimated as the day after the last day with open water was identified and could be later due to the precise ice-on date being obscured by cloud cover. The extracted ice-on/off dates were then filtered using a 5 x 5 mode filter to reduce erroneous pixels found throughout the data set, likely as a result of cloud/ ice confusion. Clouds are identified in the MODIS snow product using the MODIS cloud mask product and the misidentification of open water as ice may occur in situations where the water has a high turbidity, is shallow with a bright bottom, or is partially cloud obscured resulting in the NSDI falling in the range considered to be snow or lake ice (Hall et al., 2006). The IMS product does not exclude pixels with cloud; rather the analyst provides the best estimate for conditions that day based on previous imagery or, in the case of snow, carries the previous conditions forward until a cloud free day is available (Helfrich et al., 2007).

The range of ice-on/off dates obtained from the MODIS snow product (2000-2010) were compared to those obtained by using the IMS data (2004-2010) as well as visual inspection of MODIS imagery in selected areas obtained from NASA LANCE Rapid Response (http://lance.nasa.gov/imagery/rapid-response/). The MODIS snow product will be referred to simply as MODIS for the purposes of this

paper, and any other MODIS product used (e.g. reflectance imagery) will be identified as such. Both the lake-wide and grid-wide variability of ice-on/off dates were examined and mean difference in days determined between them.

5.2.4 Lake Ice Model

The Canadian Lake Ice Model (CLIMo) is a one-dimensional thermodynamic model used for freshwater ice cover studies (e.g. Ménard et al., 2002; Duguay et al., 2003; Jeffries et al., 2005, Morris et al., 2005; Brown and Duguay, 2011a,b) capable of simulating ice on and off dates, thickness and composition of the ice cover (clear or snow ice). CLIMo has been shown to perform very well at simulating lake ice phenology when using input data that well represents the climate for the lake, for example from nearby meteorological towers (Duguay et al., 2003; Jeffries et al., 2005; Brown and Duguay, 2011a; Kheyrollah Pour et al., in press).

CLIMo has been modified from the one-dimensional sea ice model of Flato and Brown (1996), which was based on the one-dimensional unsteady heat conduction equation, with penetrating solar radiation, of Maykut and Untersteiner (1971), i.e.

$$\rho C_p \frac{\partial T}{\partial t} = \frac{\partial}{\partial z} k \frac{\partial T}{\partial z} + F_{sw} I_o (1-\alpha) K e^{-kz} \quad (1)$$

where ρ (kg m^{-3}) is the density, C_p (J kg^{-1} K^{-1}) is the specific heat capacity, T (K) is the temperature, t (s) is the time, k (Wm^{-1}K^{-1}) is the thermal conductivity, z (m) is the vertical coordinate, positive downward, F_{sw} (Wm^{-2}) is the downwelling shortwave radiative energy flux, I_o (Wm^{-2}) is the fraction of shortwave radiation flux that penetrates the surface, α is the surface albedo, and K is the bulk extinction coefficient for penetrating shortwave radiation.

From this, the surface energy budget can then be calculated:

$$F_o = F_{lw} - \varepsilon \sigma T^4(0,t) + (1-\alpha)(1-I_o)F_{sw} + F_{lat} + F_{sens} \quad (2)$$

where F_o (Wm^{-2}) is the net downward heat flux absorbed at the surface, ε is the surface emissivity, σ is the Stefan–Boltzmann constant (5.67 x 10^{-8} Wm^{-2} K^{-4}), F_{lw} (Wm^{-2}) is the downwelling longwave radiative energy flux, F_{lat} (Wm^{-2}) is the downward latent heat flux, and F_{sens} (Wm^{-2}) is the downward sensible heat flux (Ménard et al., 2002, Jeffries et al., 2005).

The snow layer (if present) is represented as a single layer and CLIMo has been shown to simulate the on-ice snowpack depth and melt well compared to observations (Brown and Duguay, 2011a).

Snow ice is created by the model if there is a sufficient amount of snow to depress the ice surface below the water level. The added mass of the water filled snow pores (slush) is added to the ice thickness as snow ice. The albedo parameterization in CLIMo is based mainly on surface type (ice, snow or open water), surface temperatures (melting vs. frozen) and ice thickness, with no distinction regarding ice composition.

CLIMo includes a fixed-depth mixed layer in order to represent an annual cycle. When ice is present, the mixed layer temperature is fixed at the freezing point and when ice is absent, the mixed layer temperature is computed from the surface energy budget and hence represents a measure of the heat storage in the lake. The water column of shallow lakes is typically well-mixed and isothermal from top to bottom during the ice-free period, permitting the mixed layer depth to be a good approximation of the effect of lake depth leading to autumn freeze-up (Duguay et al., 2003). A more detailed description of CLIMo can be found in Duguay et al. (2003).

5.2.5 Forcing Data

CLIMo simulations were driven by North American Regional Reanalysis data (NARR, 32 km, 1979-2010: air temperature, relative humidity, wind speed, cloud cover, snow depth – acquired from the National Oceanic and Atmospheric Administration (NOAA)) with snow density obtained from the Canadian Snow CD (MSC, 2000). These snow densities were acquired over land and as the density of on-ice snow has been found to be 120% higher than on-land nearby (Sturm and Liston, 2003), the snow densities were adjusted accordingly.

Additionally, simulations where CLIMo was driven by future climate scenario data from the Canadian Regional Climate Model (CRCM 4.2.0, 45 km true at 60°N, provided by Consortium Ouranos) were performed. CRCM is a limited-area model, originally developed at Université du Québec à Montréal (UQAM), driven at the boundaries by GCMs or reanalysis data. For a detailed description of CRCM see Caya and Laprise (1999) and Laprise (2008). Two CRCM scenarios were used, both spanning from 1961 – 2100, driven at the boundaries with the Canadian Global Climate Model (CGCM 3.1/T47 member 4 (scenario 1) and member 5 (scenario 2)) following the SRES A2 green-house-gas scenario. The two scenarios are the same except with a slight perturbation to the initial GCM conditions which allows the climate to evolve slightly differently, providing some insight into the interannual variability in the climate simulations. CGCM data is produced by the Canadian Centre for Modelling and Analysis (CCCma). Daily data from each scenario spanned 1961-2100 and consisted of 2 m screen temperature, humidity (specific humidity converted to relative humidity

using a calculated saturated vapour pressure as a function of temperature (Beljaars et al., 1989) and a fixed air pressure of 1015 mb), wind speed, water equivalent of snow, snow density and cloud cover amounts. A cold bias has been previously identified in the CRCM temperature data (e.g., Plummer et al., 2006; Gagnon et al., 2009; Brown and Duguay, 2011b) and a temperature adjustment was performed using the mean NARR data from 1979-2010.

5.2.6 Simulations

The simulated ice cover was generated for both NARR (1981-2010) and CRCM (1961-2100) with both a full snow cover and no snow cover on the ice to account for snow redistribution across the ice surface, using a range of lake depths (3 m, 5 m, 10 m, 20 m, 30 m) to represent a variety of potential lakes within each grid cell. When the depth of the lake is known and the climate conditions are well represented, ice-on is usually simulated very well (e.g. Duguay et al., 2003; Brown and Duguay, 2011a). Lake depths are largely unknown through this region, so in order to select the most appropriate depth for each grid cell from the range of depth simulations, the mean satellite detected ice-on for each grid cell was compared to each of the depth simulations and the most common best fit over the 11 years of satellite data was selected. Since MODIS includes a wider variety of lake sizes than only the larger lakes resolved with IMS, the most common depths from MODIS were selected as best representative of each grid cell. Probabilities were determined for each grid cell to describe the model performance for the recent climate (2000-2010) with respect to the sub-grid cell variability. The relative change from the 1981 - 2010 CRCM-driven ice phenology means to the 2041 - 2070 mean and the 2071 - 2100 mean were extracted from the CRCM data at the central point of each NARR grid and applied to the 1981 - 2010 mean NARR climate data to simulate potential changes to the ice cover based on future climate scenarios. The 1981 – 2010 means for CRCM and NARR varied by an average of 3 days for ice-on, and 8 days for ice-off.

5.2.7 Definitions of terminology

Lake ice break-up and freeze-up are processes that occur over time and space as a lake may experience thaw or freeze in one area but not become completely ice-free/ice-covered for several days later. Pixel-based observations are defined as ice-on/off, while lake-wide observations are two dimensional and therefore variations in terms of timing of ice-on/off may be detected. The earliest date of open water/ice detected would be defined as the beginning of the break-up/freeze-up process, while water-clear-of-ice (WCI)/complete-freeze-over (CFO) are defined as the latest ice-off/ice-on

date for the entire lake. Conversely, the one dimensional model produces one value to represent all areas within its given area of forcing data and will be referred to as ice-on/ice-off.

5.3 Remote Sensing of Ice phenology

5.3.1 Lake ice phenology from IMS and MODIS products

A comparison of the MODIS and IMS detected WCI/CFO dates was possible for 189 lakes in the study area (lakes identified by both satellite-based methods, Figure 5.3).

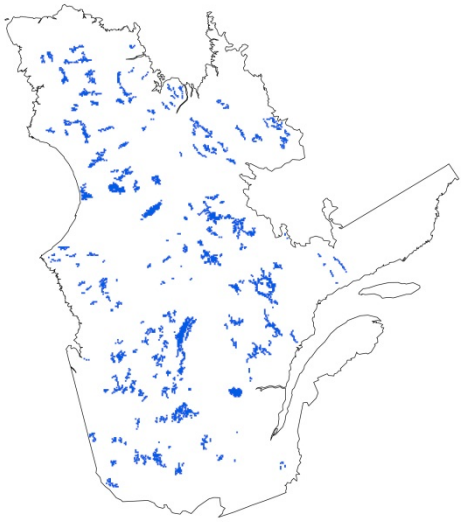

Figure 5.3. Lakes identified by both IMS and MODIS methods.

Spearman correlation values between the two products for the coinciding lakes were high, particularly for ice-off dates (Table 5.1). While ice-on dates were still significantly correlated, the lower values are indicative of not only the resolution differences between the products (with MODIS potentially identifying smaller areas remaining ice-free longer than IMS can detect) but also some suspected errors in the IMS ice-on dates (as discussed in later in this section). As the earliest and latest dates detected across the lake will be more heavily influenced by resolution, the highest correlations are typically found for comparing the mean ice-on/off values for the lakes. The coefficient of variation (CV) for each lake was determined (n=189) for each year (Table 5.2). Little variation around the mean ice-on/off dates on the lakes were detected (~2% or less), particularly with IMS (<1%).

Table 5.1. Spearman correlation (R) values for 189 lakes identified with both IMS and MODIS pixels.

	2004	2005	2006	2007	2008	2009	2010
Break-up (start)	0.84	0.91	0.91	0.95	0.85	0.91	0.92
Mean ice-off	0.89	0.92	0.92	0.97	0.93	0.95	0.97
WCI	0.87	0.91	0.86	0.96	0.91	0.94	0.95
Freeze-up (start)	0.48	0.56	0.46	0.79	0.57	0.71	0.43
Mean ice-on	0.62	0.64	0.63	0.80	0.49	0.75	0.44
CFO	0.55	0.55	0.57	0.72	0.41	0.63	0.31

Table 5.2. Mean coefficient of variation (CV) for all 189 lakes: 2000 – 2010 (MODIS), 2004-2010(IMS).

	2000	2001	2002	2003	2004	2005	2006	2007	2008	2009	2010
IMS (Ice-off)					0.012	0.007	0.007	0.005	0.003	0.003	0.004
MODIS (Ice-off)	0.016	0.014	0.013	0.016	0.013	0.017	0.016	0.013	0.019	0.013	0.021
IMS (Ice-on)					0.001	0.002	0.003	0.003	0.002	0.001	0.002
MODIS (Ice-on)	0.013	0.012	0.012	0.018	0.012	0.014	0.025	0.012	0.012	0.013	0.014

Thirteen water bodies (lakes or reservoirs) were selected for a more detailed comparison between the IMS/MODIS ice cover dates. The mean difference (MD) and overall mean absolute difference (MAD) was determined (MODIS minus IMS) for both WCI and CFO (Table 5.3). WCI had an overall MAD for all 13 lakes of three days (with the largest MD of eight days, MODIS later than IMS). Since the actual WCI date might be obscured by cloud cover a few days variation is to be expected. Also, the resolution differences with MODIS would tend towards MODIS being slightly later than IMS as small patches of ice may remain. No pattern to the direction of the difference was found for WCI (six lakes had a MD indicating later WCI with MODIS, seven with IMS - though the individual years vary with no consistency). CFO had a higher average MD of nine days (eight lakes with late CFO for MODIS, five lakes later with IMS). The cloud cover in MODIS may result in

slightly earlier CFO dates than reality based on the current extraction technique; however, the spatial resolution differences between the satellite data products would tend towards later CFO as the MODIS pixels would be able to detect smaller areas of persistent open water. The resolution difference appears to be more influential for detecting CFO than WCI as more of the lakes had a tendency for later MODIS dates than with IMS.

Table 5.3. Mean difference (MD) for 13 lakes (L.) or reservoirs (R.), 2004-2010

	Mean difference (days) MODIS minus IMS	
Water body	WCI	CFO
L. à l'eau Claire	-2	32
Caniapiscau R.	-2	-2
L. Bienville	-1	-2
L. Naococane	4	-7
Manicouagan R.	1	13
L. Manouane	-5	-11
L. Evans	2	7
L. Mistassini	2	15
L. Matagami	-5	-1
L. ST Jean	-1	10
Gouin R.	8	6
Baskatong R.	2	5
Pipmuacan R.	-4	12
Overall Mean Absolute Difference	***3***	***9***

Some of the differences between MODIS and IMS can be attributed to cloud cover and resolution. For example, at the Baskatong R., WCI was identified as April 29, 2009 with MODIS, while IMS identified WCI at May 4, 2009. Examining the MODIS reflectance imagery for the five days between the two WCI dates shows the reservoir to be obscured by cloud cover during this time. A similar scenario occurred in 2007 at L. à L'eau Claire, with IMS identifying WCI 10 days later than MODIS. MODIS reflectance data shows open water on the same day as the MODIS snow product (June 22, 2007), but cloudy days follow with only partially unobstructed views of the lake until July 2, 2007 when IMS identified ice-off. These two examples of IMS later than MODIS would not be the result of the ice cover extraction technique used (first day of open water, potentially after ice-off was obscured by clouds) but the opposite - IMS missed the WCI on both lakes and was only able to assign the ice-free designation on the next cloud-free day (four and ten days later, respectively). It is likely

that the finer resolution of MODIS provided a better 'view' of the lake through partial cloud cover and was able to assign the open water category to the pixels while IMS could not.

In some cases, erroneous pixels remain in the MODIS ice cover dates after the mode filter was run, resulting in late WCI or CFO for the lake. For example, in 2005 (not shown), MODIS reflectance imagery shows what appears to be open water well before WCI is detected with the MODIS snow product for both the Baskatong and Gouin Reservoirs leading to 51 and 18 days difference between MODIS and IMS; both as a result of 1 erroneous pixel each.

For CFO, MODIS pixels are able to detect smaller areas of persistent open water. Two examples of this are as follows: L. Mistassini (Figure 5.4a) and the Manicouagan R. (Figure 5.4b). MODIS reflectance imagery shows a small area of open water remaining on L. Mistassini for several days after IMS detected CFO (IMS CFO = Jan. 4, 2010; MODIS CFO = Jan. 20, 2010). The Manicouagan R. has the largest difference for CFO between IMS and MODIS for all years, which occurred in 2009/2010 (IMS CFO = Jan. 4, 2010; MODIS CFO = Feb. 25, 2010) where imagery shows small clusters of MODIS pixels remain open water on the east side of the reservoir that IMS is not able to resolve.

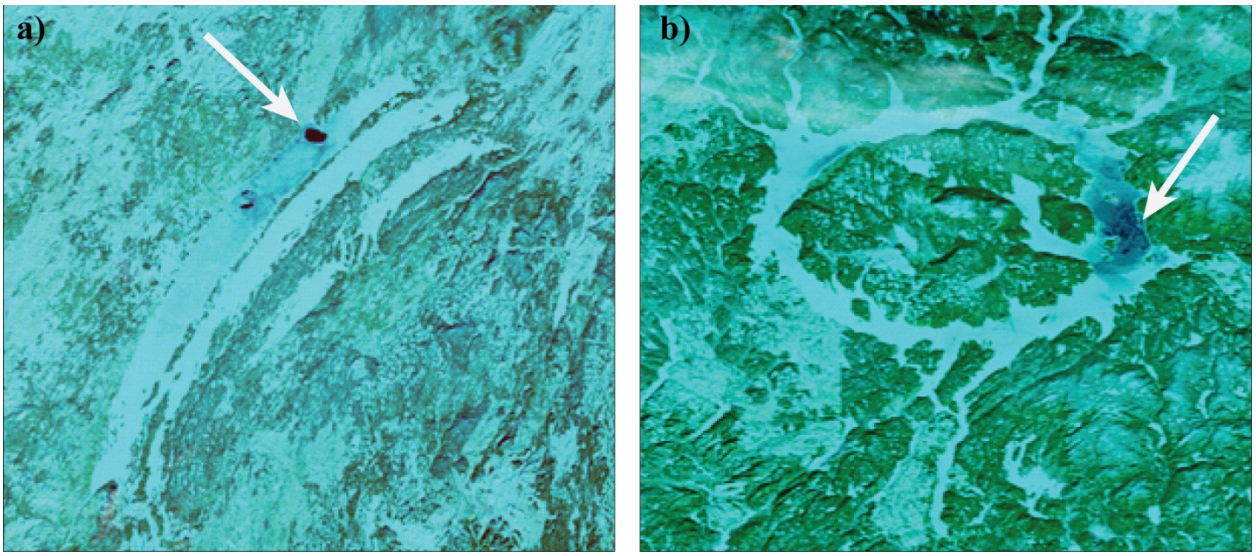

Figure 5.4. Small areas of open water detectable by MODIS but not IMS, highlighted by the white arrows for a) L. Mistassini, Jan. 8 2010 (IMS CFO = Jan. 4, MODIS CFO = Jan. 20) and b) Manicouagan R., Feb. 9, 2010 (IMS CFO = Jan. 4, MODIS CFO =Feb. 25).

Of all 13 lakes examined in detail, L. à L'eau Claire had the highest mean difference of 32 days later for MODIS compared to IMS. In 2009, a widespread problem occurred with the IMS data where the northern portion of the province all froze up on Oct. 29 or Nov. 5, including L. à L'eau Claire (MODIS CFO = Dec. 19), however, L. Bienville just to the southwest, did not freeze until Dec. 15 with IMS (MODIS = Nov. 3), 40 days later. Visible imagery (Figure 5.5) shows open water on Dec. 3, partial freeze-up on Dec. 15, and Dec. 25 appears frozen although somewhat obscured by cloud. A similar situation occurred in 2004 where a large portion of northern Quebec also experienced a uniform, early freeze-up, this time extending further southwest and including L. Bienville. Early freeze-up throughout the region again occurred in 2010/2011. While some of the discrepancy between CFO dates may be attributed to resolution, this area experiences frequent cloud cover, with more than 50% of the days in the year reported as cloud covered from 2000 - 2005 (Hachem et al., 2009). In areas with persistent cloud cover or low sun angle, IMS analysts incorporate microwave data rather than the more heavily used visible imagery (Helfrich et al., 2007). If this was the case during the years with the ice-on discrepancies the large satellite footprint for microwave data may be affecting the detection of ice cover on the lakes in this northern area.

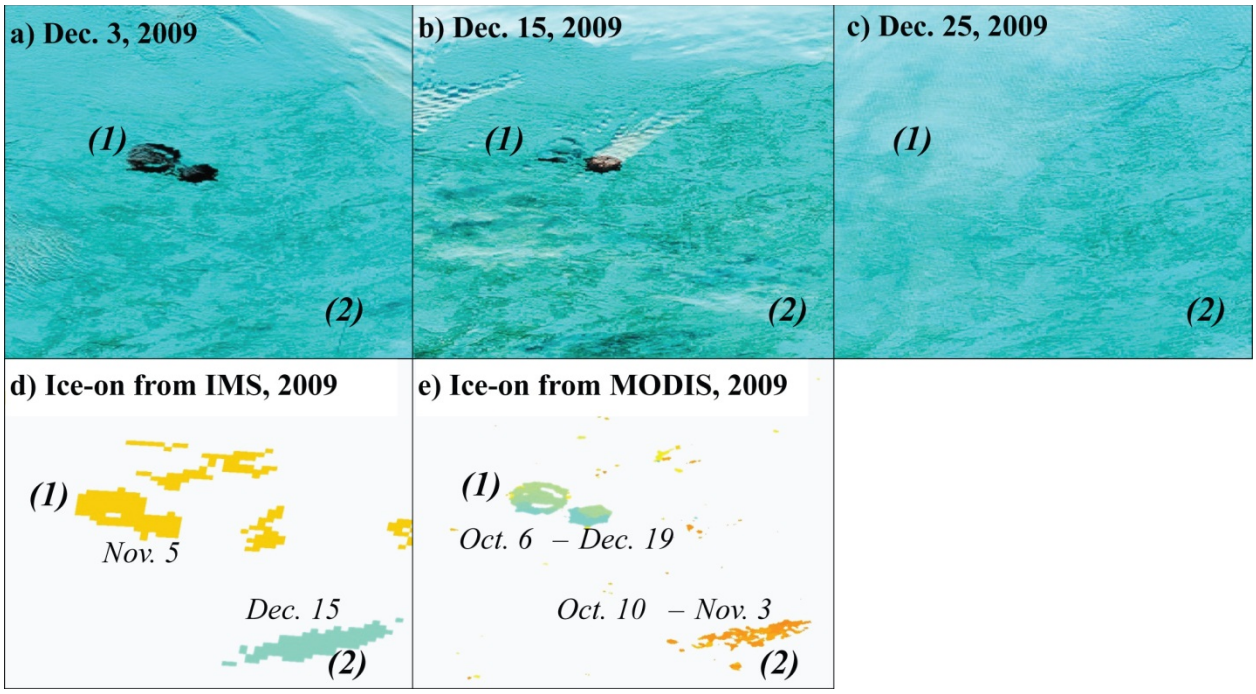

Figure 5.5. Freeze-up for L. à L'eau Claire (1) and L. Beinville (2) 2009 detected from a, b, c) MODIS bands 7,2,1 on specified dates, d) IMS detected ice-on dates, and e) MODIS snow product detected ice-on dates.

Similar to findings reported in Frei and Lee (2010) regarding numerous snow cover studies comparing MODIS and IMS, neither product is clearly better than the other. The MODIS snow product does tend to produce better results in terms of spatial detail, however, even after running a mode filter on the ice cover dates a few erroneous pixels remained. For studies interested in the break/freeze-up process rather than just WCI/CFO, the MODIS product outperforms the IMS product for spatial variability and detail on the lakes. In the Arctic region however, MODIS may not be an option for freeze-up due to polar darkness and IMS is the best option available for daily lake ice cover. For ice-off, IMS performs comparably to MODIS in the Quebec region, however ice-on was frequently too early. Early ice-on was also detected for Great Slave Lake (61°40'N, 114°W) and Great Bear Lake (66°N, 121°W) using IMS compared to ice phenology extracted from AMSR-E passive microwave data (Kang et al., 2012), suggesting that while IMS lake ice detection works well for ice-off, it experiences some limitations for the ice-on.

5.3.2 Grid-wide Ice on/off from IMS and MODIS

While the previous section compared how well MODIS and IMS detected phenology dates compared to each other for entire lakes, the forcing data for the model is 32 km grid cells, so a grid-by-grid comparison was done as well for ice-on/off occurring within each grid cell. 788 of the possible 1452 grid cells covering the province contain lakes large enough to be resolved by the filtered MODIS product and 456 grid cells have lakes resolved by IMS.

Comparison statistics were generated, similar to the previous lake-based data, for the coinciding grid cells with lakes identified by both products. Correlations between the products (Table 5.4) are lower than the lake-by-lake comparison as a result of resolution differences (with MODIS resolving more smaller lakes, and more details in the larger lakes) particularly evident in the CFO values, though all values were still significantly correlated. The mean CVs for all years (Table 5.5) were fairly similar to those found in the lake comparison, with IMS having less variability in dates than MODIS. The average CV for each grid cell was determined for all available years (2000-2010 MODIS, 2004-2010 IMS) to highlight the grid cells with the most deviation around the mean ice-on/off dates (Figure 5.6). The mean range in ice-off dates within the grids is 2 days for IMS (with a maximum of 97 days) and 14 days for MODIS (maximum of 116 days). The mean range in CFO dates within the grids is also 2 days for IMS (with a maximum of 76 days) and 7 days for MODIS (with a maximum of 81 days). Knowing the variability present at the sub-grid cell level provides

insight into the representativeness of the grid-based simulations. The following section presents the simulated ice-covers and examines the model performance with respect to the sub-grid cell variability.

Table 5.4. Correlation R values for pixels containing both IMS and MODIS lakes (456 grid cells). All values are significant at the 0.001 level.

	2004	2005	2006	2007	2008	2009	2010
Break-up (start)	0.56	0.61	0.64	0.64	0.58	0.60	0.67
Mean ice-off	0.60	0.64	0.65	0.66	0.63	0.62	0.70
WCI	0.60	0.61	0.64	0.66	0.61	0.62	0.70
Freeze-up (start)	0.31	0.28	0.34	0.49	0.37	0.51	0.24
Mean ice-on	0.39	0.36	0.42	0.53	0.37	0.54	0.26
CFO	0.36	0.32	0.39	0.47	0.34	0.46	0.19

Table 5.5. Mean coefficient of variation (CV) for all grid cells.

	2000	2001	2002	2003	2004	2005	2006	2007	2008	2009	2010
IMS (Ice-off)					0.009	0.006	0.007	0.005	0.003	0.003	0.004
MODIS (Ice-off)	0.016	0.013	0.012	0.015	0.012	0.015	0.015	0.012	0.017	0.013	0.021
IMS (Ice-on)					0.001	0.002	0.003	0.003	0.002	0.001	0.003
MODIS (ice-on)	0.012	0.012	0.012	0.016	0.011	0.012	0.012	0.011	0.012	0.014	0.014

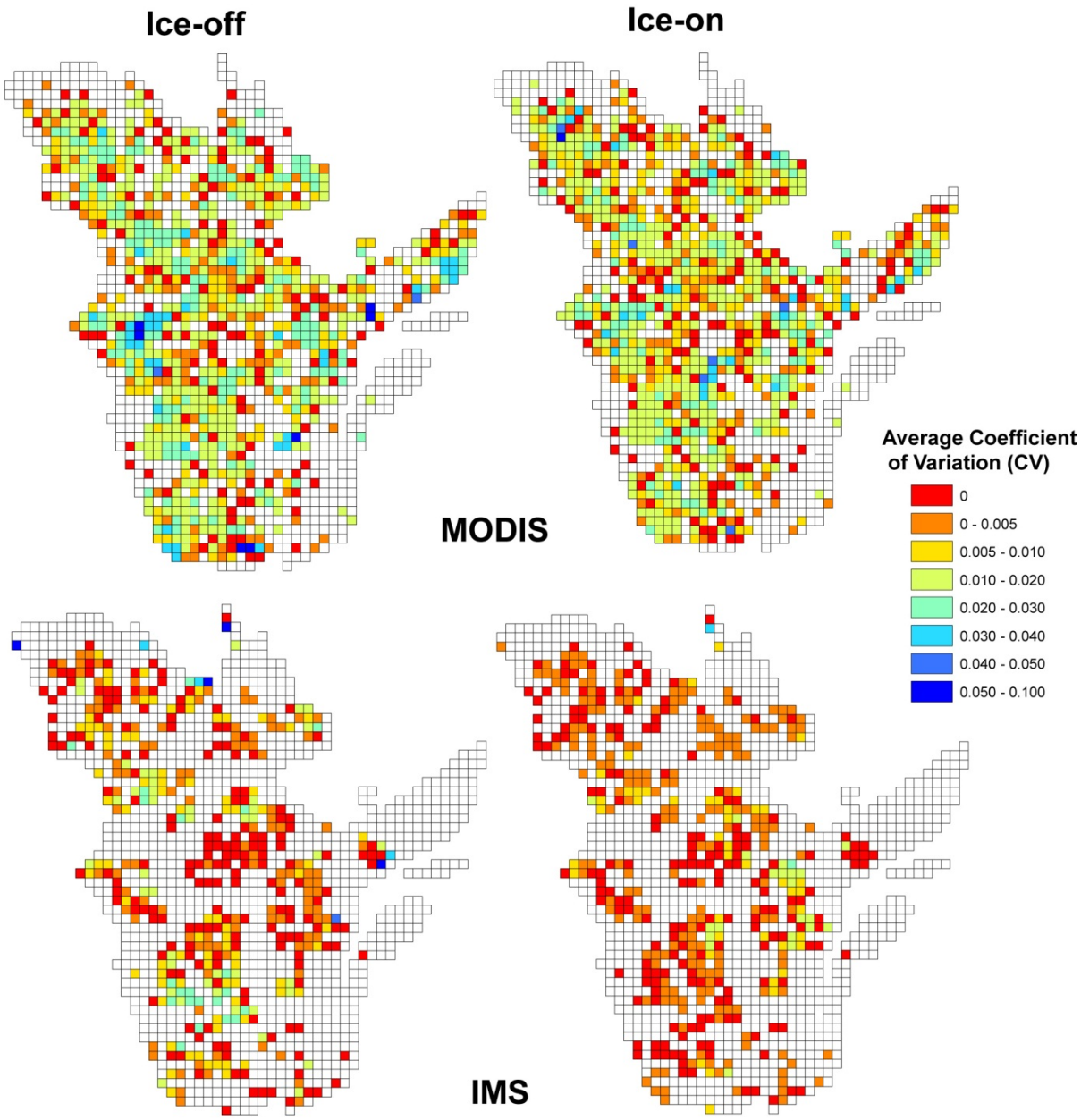

Figure 5.6. Average coefficient of variation (CV) for each grid cell for ice-on and ice-off for MODIS: 2000 - 2010 (top) and IMS: 2004-2010 (bottom).

5.4 Modelling lake ice phenology

Figure 5.7 presents the mean ice-on/off dates (1981-2010) simulated by forcing CLIMo with NARR data across Quebec. Ice-off ranged from April 13 in the south to July 1 in the north along a northwest gradient (snow-covered data shown; snow-free simulations were an average of five days earlier), while ice-on ranged from Oct. 7 to Jan. 10 mainly on a northwest gradient, but dependent on the assigned depth of each grid cell (with deeper lakes freezing over later than shallow lakes with similar climate conditions).

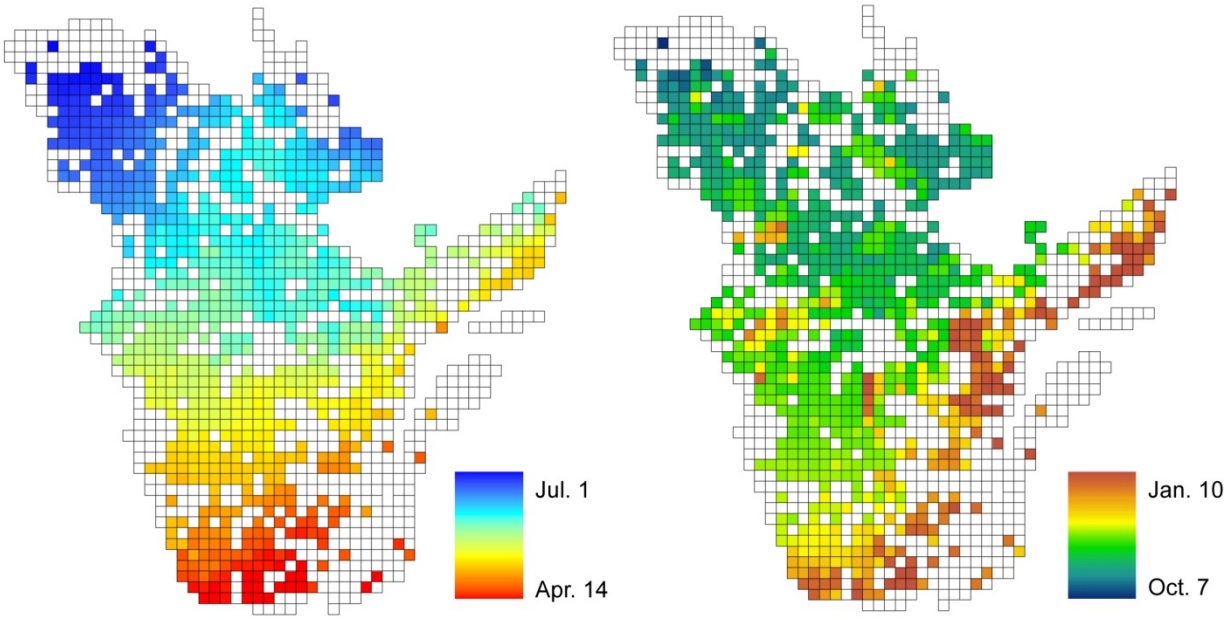

Figure 5.7. Mean simulated 1981-2010 ice-on and ice-off for the province of Quebec. Empty grid cells corresponded to areas where no lakes were identified (based on the 500 m resolution MODIS product).

The simulated ice-on/off dates were well correlated with those obtained from the satellite data, with all correlations significant at the 0.001 level (Table 5.6). Averaged over the entire region, the MD for all 11 years of MODIS data indicates that the simulated ice-off dates were only 1 day too early (5 days with no snow cover on the ice) and 1 day late for ice-on. Compared to IMS, the MD for ice-off was higher at 8 days too early (12 days too early with no snow on the ice) and 13 days early for ice-

on. Mapping the average MD for each grid cell shows a mixture of early/late grid cells for both ice-on and ice-off with MODIS (Figure 5.8). The largest difference for ice-off was found in the northern portion of Quebec (near Kuujjuaq, 58° 6′ N, 68° 24′ W). Simulations in this region range from 2 to 16 days too early.

Table 5.6. Spearman correlation (R) values for both mean MODIS and IMS detected ice-off compared to simulated ice-off (both with and without a snow cover on the ice) and ice-on dates. All values are significant at the 0.001 level.

	2000	2001	2002	2003	2004	2005	2006	2007	2008	2009	2010
MODIS											
ice-off (snow-free)	0.95	0.90	0.97	0.93	0.95	0.92	0.94	0.97	0.92	0.97	0.96
ice-off (snow)	0.97	0.87	0.96	0.92	0.94	0.92	0.94	0.97	0.87	0.95	0.96
ice-on	0.83	0.92	0.82	0.84	0.89	0.85	0.89	0.91	0.91	0.92	0.52 *
IMS											
ice-off (snow-free)					0.91	0.93	0.91	0.96	0.94	0.94	0.95
ice-off (snow)					0.90	0.93	0.90	0.95	0.92	0.93	0.96
ice-on					0.69	0.70	0.68	0.83	0.48	0.77	0.41*

* Reduced dataset for FU 2010 as lakes that froze up in 2011 were not included in the simulations.

An additional simulation was run using the Meteorological Service of Canada weather station data from Kuujjuaq to assess the NARR data for this area. Simulations from both NARR and MSC vary similarly year to year, but MSC simulations were on average four days earlier. Both reflected the early ice-off for 9 of the 11 years simulated compared to satellite detected ice-off for a lake 20 km away from the weather station (two years were represented well in the simulations). The amount of snow accumulation in the NARR input data is 1.6 times higher than at the MSC station over the 30 year simulation span, however both under-represent the normal snowfall amounts for the area (257.1 cm, 1971-2000 normal). As the MSC and NARR temperatures vary by less than 1°C average per season for this location, the difference between the simulations and the satellite detected dates here is likely attributed to the misrepresentation of the actual snow conditions on the ice surface, as increasing the snow amount and density in the simulations delays the ice-off dates and approaches the satellite detected dates. The area of larger difference towards late simulations (east-central region of the province) is not likely a reflection of snow conditions, but rather more likely indicative of

discrepancies between the NARR temperatures data compared to actual air temperature, as even with no snow cover on the ice, the simulations are still later than the observations.

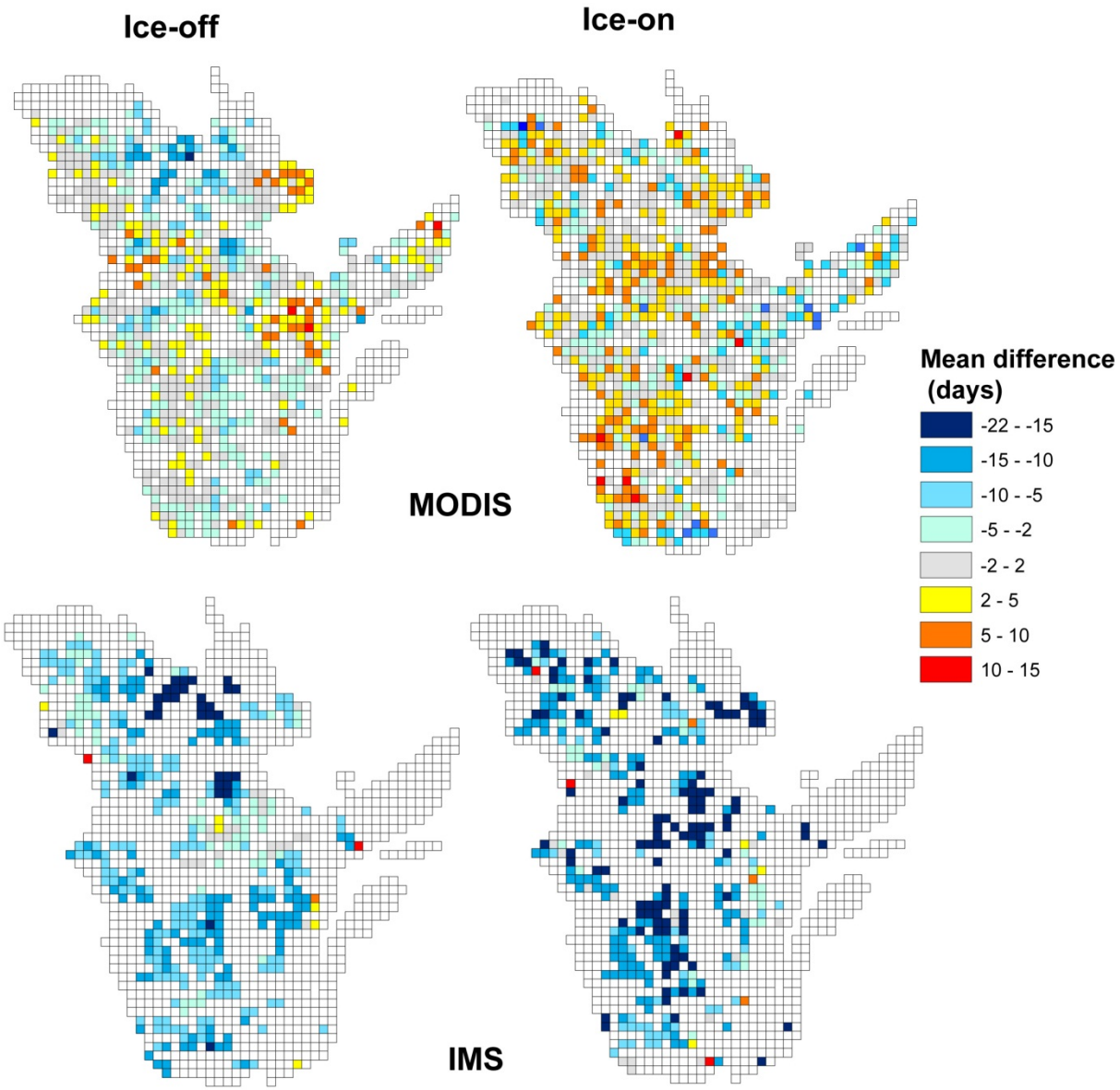

Figure 5.8. Mean difference (MD) of simulated dates relative to satellite detected dates for MODIS (11 years) and IMS (7 years) for each grid cell. Empty grid cells corresponded to areas where no lakes were identified using the stated product.

The simulations are earlier than the IMS detected ice cover dates for both ice-off and ice-on, more-so for ice-on. The depth for each grid cell in the simulations was determined using MODIS, which can resolve the smaller shallower lakes that would freeze-up earlier than the larger (and likely deeper) lakes that IMS can resolve, likely the source of the large differences for ice-on.

One lake in the study region (L. St. Jean) has a historical record of ice observations in the Canadian Ice Database (Lenormand et al., 2002) and provides the ability to compare all of the data sources. Figure 5.9 presents the long term record of ice-on/off dates from observations (near-shore), simulations driven by NARR and both IMS and MODIS satellite detected dates (mean ice-on/off for the lake). The MD for ice-on between observations and simulations is 1 day (1979-1997), while ice-off is 4 days. No observations are available to compare to the satellite detected dates, but simulations compare well for both ice-on and ice-off (MODIS 4 and 1 MD days respectively; IMS 1 and 5 days respectively MD).

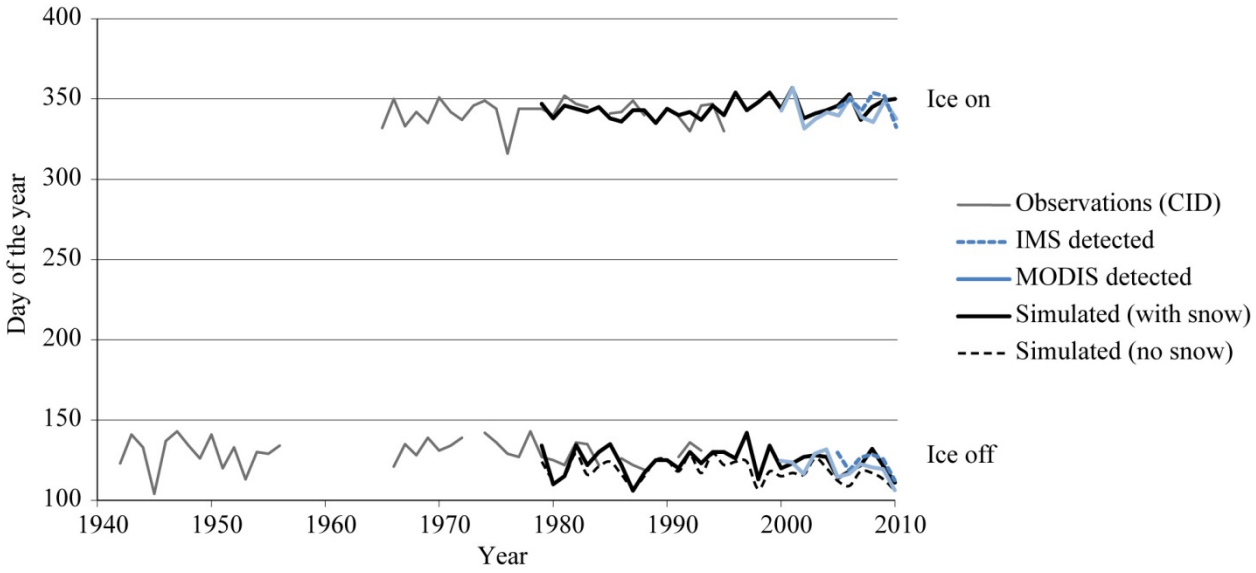

Figure 5.9. Ice-on/off dates for L. St Jean for simulations, MODIS, IMS and in situ observations.

Year-to-year variations in how well the NARR data is capturing the local climate can vary. In order to represent how well the model is performing for the current climate (2000-2010: years with available satellite data) each year was tested to see if the simulations fell within ±1 standard

deviations (σ) of the mean observations from all other years. A probability for each grid cell was then determined for the 11 years to represent the ability of the model to simulate the ice-on/off dates within the grid cell (Figure 5.10). Province-wide, the probability of the simulations for ice-off being within ±1σ of the mean observations is 62%, while ice-on is 80%. As little to no sub-grid cell variability was found with IMS, only MODIS was used to determine the probabilities. These probabilities can then be applied to the future ice cover scenarios, under the assumption that the variability captured in the 11 years of MODIS data remains the same in the future. The current data available only allows for an 11 year time series, however a long time series (20 years or more) would provide greater confidence in the probabilities.

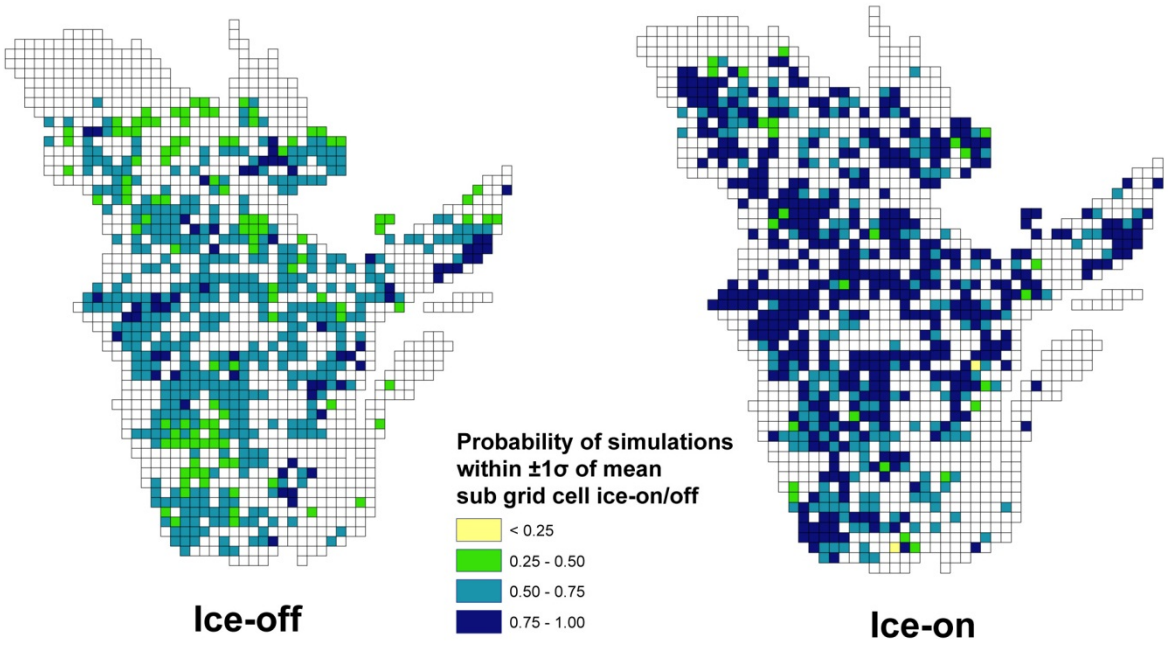

Figure 5.10. Probability of the simulations from 2000 – 2010 being within ±1 standard deviations of the mean satellite detected ice on/off dates for each grid cell. Empty grid cells corresponded to areas where either no lakes were identified using the filtered MODIS product or no probabilities were determined due to an incomplete data record (only grid cells with a complete 11 year satellite record were used).

5.4.1 Future Ice Cover

Based on the depths for each grid cell determined in the previous section, simulations were run using future climate scenario data from CRCM to investigate the potential changes for this region. Knowing

how well the model performed for each grid cell for the contemporary climate provides some insight on the representativeness of the future predictions.

5.4.1.1 1981-2010 to 2041 – 2070

Temperature changes between the 1981-2010 means and the 2041-2070 means predicted by CRCM are similar for spring, summer and fall for both scenarios ranging from 1 – 3 °C increase with greater warming in the south. The largest temperature increases are found in the winter, with the opposite pattern from the other seasons. More warning is shown in the north (3 – 4 °C increase for scenario 1 and 4 – 5 °C for scenario 2) than the south (2 – 3 °C increase) with the southeastern side of Hudson Bay experiencing the most warming in scenario 2 (up to 7 °C). The largest changes in the area are found over Hudson Bay ranging from 7 – 9 °C during the winter. Both scenarios suggest a decrease in snow water equivalent throughout most of the province, except for in the northern areas where an increase of up to 15% in the winter and spring is shown (with very small areas of < 5% increase in the fall). This is consistent with GCM simulations of winter snow accumulation for this region, with increases in the north and decreases in the south (Räisänen, 2007). Scenario 1 also indicates a region with a 5 - 10% increase around the St. Lawrence River during the winter season.

The two scenarios show slightly different amounts of change, and in different regions, for both ice-on and ice-off (Figure 5.11). Scenario 1 shows changes in ice-off ranging from 10 -15 days earlier, with a section of less than 5 days earlier in the central region of the province. Scenario 2 shows changes in ice-off from 15 - 25 days in the south to less than 5 days in the northern half of the province (excluding an area of 5 - 10 days the very north). Scenario 1 shows ice-on ranging mainly from 0 – 10 days later with a few grid cells of 10-20 days in the far southern areas. Scenario 2 shows much more pronounced change for ice-on, ranging from 20 - 25 days in the St. Lawrence region to a mixture of 5 - 15 days through the rest of the province. Combined, these changes to the ice-on/off dates result in reduced ICD of 5 – 25 days (with a few isolated pixels greater than 30 days) for scenario 1 and less than 5 up to 50 days shorter for scenario 2.

Generally, scenario 2 shows more change than scenario 1. Using the same scenarios to simulate arctic ice cover changes Brown and Duguay (2011b) showed greater change with scenario 1 in the western arctic and greater change in scenario 2 in the Baffin Island/Northern Quebec region. The areas of greater change for both ice-on and ice-off are the southern portion of the province in the St. Lawrence region. While previous research (not specifically in this region) has suggested greater changes to the ice-off dates (Brown and Duguay, 2011b, Dibike et al., 2011), in the case of scenario

2, greater change was found in ice–on dates. This is likely a reflection of the greater increase in fall temperatures experienced in this region for scenario 2 over scenario 1. The larger changes in both ice-on/off in scenario 2 lead to the larger reductions in ICD for this scenario.

5.4.1.2 1981 – 2010 to 2070 – 2100

Extending the projected changes to the 2071-2100 means shows that temperature increases for the spring season are similar between the two scenarios, ranging from 4 - 5 °C in the south, to 2 - 3 °C in the north. Summer is also similar with 4 – 5 °C increase in the south, 3-4 °C through most of central region and 2 – 3 °C in the north (with a section of 3 – 4 °C increase at the far north for scenario 1). Scenario 1 has a fall temperature increase of 3 – 4 °C throughout most of the province, while scenario 2 is again warming more in the fall with a 3-4° increase in the south and 4-5 °C in the north. Winter shows the greatest changes ranging from 1 – 6 °C from south to north for scenario 1, and 3 – 7 °C from south to north for scenario 2. Again, the greatest area of warming in the area is over Hudson Bay, with up to 11 °C warming during the winter. Similar to the 2041-2070 means, snow water equivalent is shown to decrease throughout the province except for northern regions, which show an increase of 5 -10% in the winter and up to 30% in the spring (up to 20% with scenario 1). Scenario 1 also shows a very small area of increase along the St Lawrence River during the fall.

Figure 5.12 presents the ice cover changes for this time frame. Scenario 1 ranges from 10 to 30 days earlier for ice-off and mainly 5 to 30 days later for ice-on (with a maximum of 65 days in the southern area near the St. Lawrence River). Scenario 2 ranges from 5 to more than 30 days earlier for ice-off with more pronounced changes in the St. Lawrence region than Scenario 1. Ice-on for scenario 2 also ranges from 10 to more than 30 days later (up to 42 days later), but differs spatially from scenario 1 with greater amounts of change occurring in the St. Lawrence region and in the eastern portion of the province. The resulting ICD ranges from 15 to nearly 100 days shorter, with most change occurring in the St. Lawrence region and decreasing northwards along a northwest gradient. For scenario 1, the southern-most region ranges from 60 to 94 days shorter ICD and in the St. Lawrence River region 40 to 60 days shorter. Scenario 2 has a larger area covered by large reductions in the ICD along the St. Lawrence (60 – 72 days shorter), but less change in the northern areas than scenario 1.

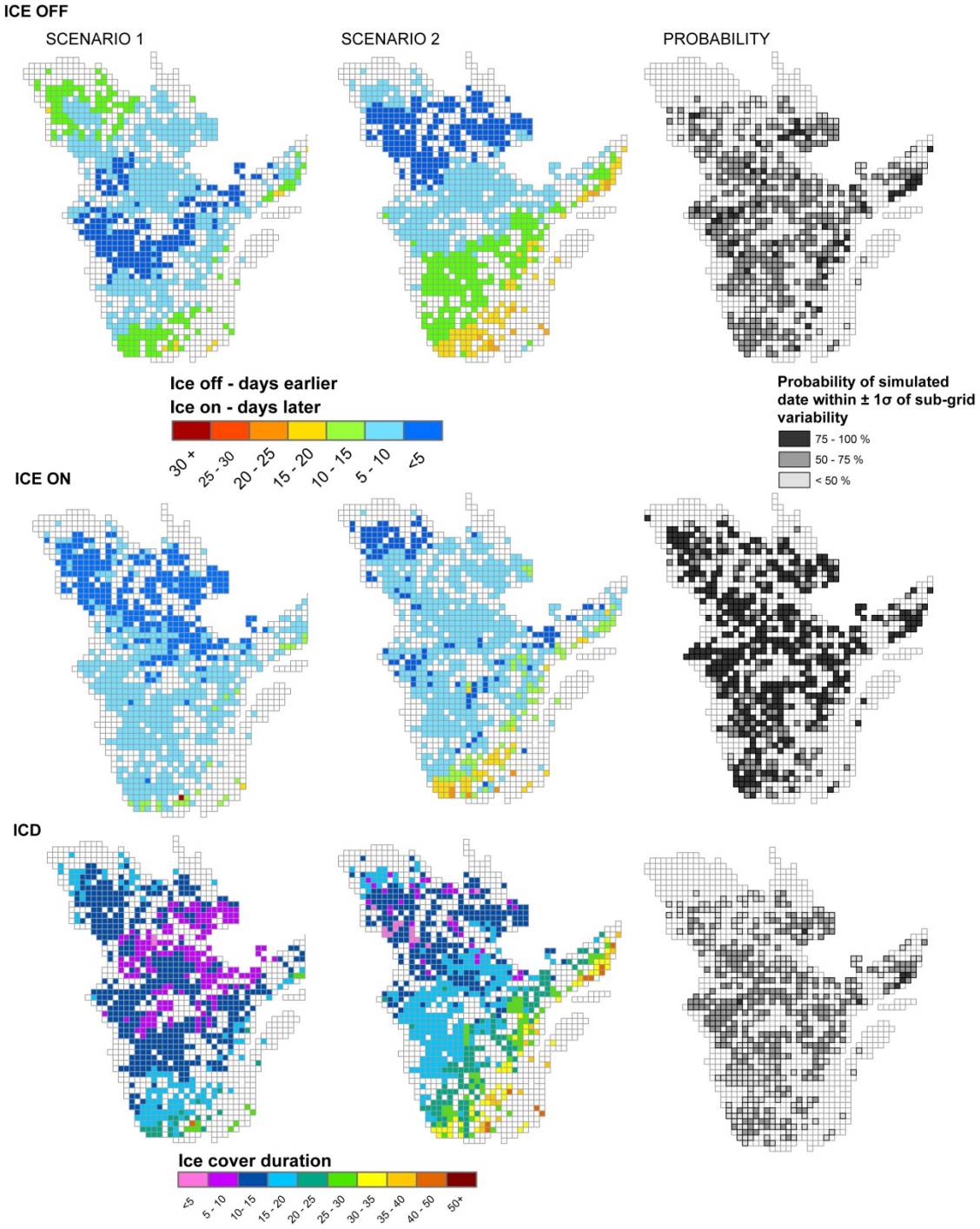

Figure 5.11. Ice-on, ice-off and ice cover duration changes from the 1981-2010 mean to the 2041-2070 mean, with the probability of the model simulating within ±1 standard deviations of the sub-grid cell variability indicated.

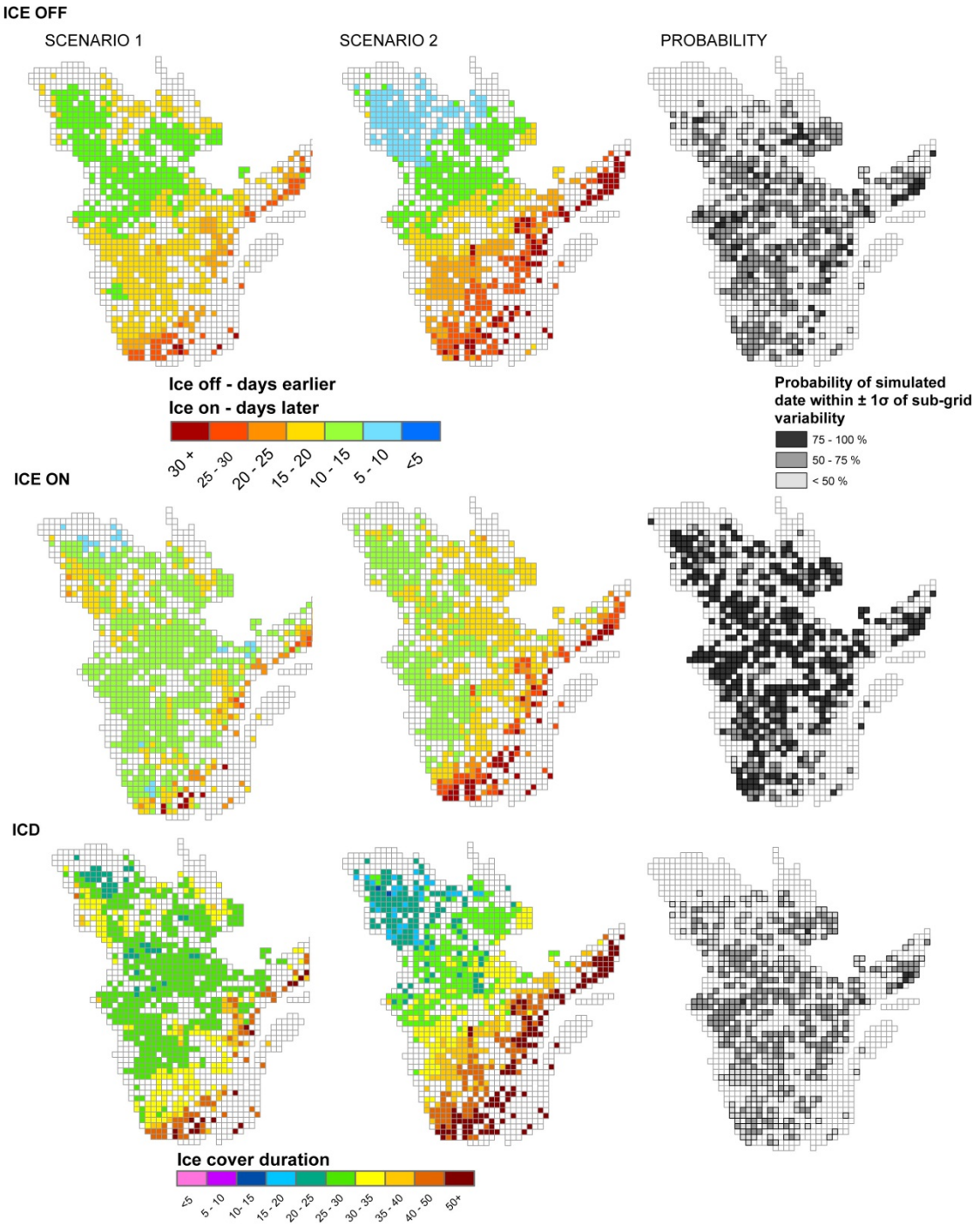

Figure 5.12. Ice-on, ice-off and ice cover duration changes from the 1981-2010 mean to the 2070-2099 mean, with the probability of the model simulating within ±1 standard deviations of the sub-grid cell variability indicated.

5.5 Summary and Conclusions

Overall, the MODIS and IMS products are useful for monitoring daily ice cover on lakes, and while both can obtain comparable ice-off dates, MODIS outperforms IMS for ice-on due to finer resolution and the tendency towards early ice-on with IMS. Ice-off dates from both products are strongly correlated and while still significantly correlated, were weaker for ice-on due predominantly to the resolution differences that allow for more spatial detail with the MODIS snow product. For the 13 relatively large lakes/reservoirs examined in detail, a mean absolute difference between MODIS and IMS of 3 days for ice-off and 9 days for ice-on was determined. The main differences between the products were a result of spatial resolution, cloud cover and different methods for assigning the ice category. Whether or not lake ice is present within a pixel is at the IMS analyst's discretion based on available data, while the MODIS algorithm is fully automated. While both MODIS and IMS have problems reported with over-represented snow cover extent during snowmelt, attributed at least partially to the confusion of lake ice and snow (Frei and Lee, 2010), the change from ice-covered to ice-free for a lake (and to a lesser extent ice-free to ice-covered) is more readily distinguishable than snow vs. lake ice. Some ice/cloud confusion does occur, leading to late WCI/CFO for some lakes, however filtering the MODIS dates removes the majority of these pixels. A new product has recently been developed to fill cloud gaps in the snow cover data (Hall et al., 2012) and this could be beneficial for reducing the cloud interference for lake ice as well.

More variability was found in the ice-on/off dates at the sub-grid cell level using the MODIS snow product rather than IMS, as the resolution differences allow for more lakes and more detail on the larger lakes to be incorporated. The sub-grid cell variation was typically less than 2%, with a maximum of 10% of the mean value of the encompassing grid. The simulations for contemporary climate conditions were more comparable to the MODIS detected ice phenologies than IMS, again due to the incorporation of the smaller lakes in the MODIS data. An indication of whether or not the simulated ice phenology is within the 11 year sub-grid cell variability was determined. Averaged over the entire province the simulations were within the sub-grid cell variability 62% of the time for ice-off and 80% of the time for ice-on. Driving the model with the future climate scenarios predicts ice cover durations throughout the region will decrease by up to 50 days from the current 1981-2010 means to the 2041-2070 means, and decrease from 15 to nearly 100 days shorter between the contemporary and 2071-2100 means.

The inclusion of lakes in numerical weather predictions (NWP) and climate modelling is an ongoing and important step in current research. Several groups are now incorporating lake models (with ice-cover) into their NWP/climate models to better represent the local climate (e.g. Balsamo, et al., 2012; Martynov et al., 2012). The incorporation of remote sensing data into modelling can contribute to advancements in the predictive abilities of lake/lake ice models by providing the ability to incorporate lakes at the sub grid cell scale. The inclusion of sub-grid cell lakes in NWP can contribute to reduced forecast errors in some regions, particular for spring and summer (Balsamo et al., 2012). The next generation of the CRCM model (version 5, version 4 was used in this study) incorporates a mosaic approach to parameterize the surface types using the CLASS 3.5 land surface scheme, with an additional surface type added to represent lakes (all land water bodies). This provides, among other improvements, the ability to distinguish between open water and ice-covered parts of a lake for calculations such as latent and sensible heat fluxes (Martynov et al., 2012).

One of the limitations in modelling ice cover is the lack of known lake depths, a problem particularly evident in Canada where numerous lakes are situated in northern or remote regions. Since lake depth is a controlling factor for ice-on, correctly representing the depth in the model is of key importance. Lake depths are often assumed in modelling at 10 m (Samuelsson et al., 2010) or accounted for by numerous depth simulations (Brown and Duguay, 2011b). In this study we used an approach whereby the best depth for each grid cell was determined based on satellite data in the absence of measured depths, which could lead to some discrepancies between the simulations and satellite-detected dates for ice-on. Deviations in the NARR data from actual climate conditions, particularly with respect to temperatures in the summer and fall seasons, may have affected the selection of depths by advancing or delaying the ice formation. A global database and raster product of lake depths has been created for use in weather forecasting and climate modelling and is being implemented in several NWP and climate models (Kourzeneva et al., 2012). A dataset of this nature could be very beneficial for lake ice modelling, however with lake depths unknown throughout many parts of Canada there is still potential for the misrepresentations of depths.

Furthermore, an accurate representation of snow on the ice is essential for lake ice simulations. Reanalysis data or climate model output may not be able to represent the local snow conditions well within a grid cell and redistribution across the lake surface is difficult to capture. Using snowfall records to represent depth of snow on the ground is sometimes necessary; but weather station records have a tendency for snow undercatch (Goodison, 1981). The ability to obtain variables such as on-ice

snow depths at fine spatial resolutions, such as that proposed by the Cold Regions Hydrology High-resolution Observatory (CoReH20) candidate satellite mission of the European Space Agency (Nagler et al., 2008), will be extremely beneficial for accurate lake ice modelling.

5.6 Acknowledgements

This research was supported by a NSERC postgraduate scholarship (CGS) to L. Brown and Discovery Grant to C. Duguay. The CRCM data was generated and supplied by Ouranos (with thanks to Ross Brown). The National Snow and Ice Data Center is acknowledged for providing access to the IMS and the MODIS snow cover products as well as NOAA for providing the NARR data (ftp://ftp.cdc.noaa.gov/).

Chapter 6
General Conclusions

6.1 Overall Summary

The overall aim of this research was to further our understanding of lake ice and climate interactions, with an emphasis on ice cover modelling. This work is not only a contribution to cryosphere research and hydrological studies in general, but also extends to other fields such as climatology, limnology and biology due to the complex interactions between the climate and the ice cover as well as the effects on the biological and limnological aspects of the water column below. The literature review (Chapter 2) offered a synthesis focusing on both the response and role of lake ice in climate. The first use of a SWIP upward looking sonar in a shallow lake was presented in Chapter 3. The results showed the promising ability of this device for model validation and for monitoring the ice phenology and thickness over the ice season. Adding the digital camera for visual monitoring of the ice cover formation/decay on the study lake showed the potential for devices such as this to be used in other locations as well to supplement the diminished lake ice monitoring network. Future predictions for lake ice cover (Chapter 4), thickness, and composition using climate model output for arctic areas, contributed towards the overall understanding of the lake ice/climate interactions in the sensitive northern areas. Examining the use of IMS and MODIS snow cover daily products for monitoring ice cover (Chapter 5) contributed a new technique which could be incorporated into the current monitoring practices for lake ice phenology. Examining the sub-grid cell variability advances research into downscaling larger grid cell data to specific lakes within an area and offers some ideas of uncertainty in the simulations at the grid cell level.

Lake ice has been shown to respond to climate variability, particularly changes in air temperature and snow accumulation. Trends have been identified throughout historical ice cover records; with trends in ice thickness associated more with changes in snow cover, while changes in phenology were typically associated with variations in air temperature. Variability in ice cover has also been related to teleconnections as they affect the overall circulation patterns influencing the local climate. As highlighted in Chapter 2, the time scales used for analysis affect the trends identified in the ice records, emphasizing the importance of the extent of the time series for interpreting trend data. Snow has a dual role on how it affects lake ice thickness. Increased snowfall can result in thicker ice cover,

mainly due to an increase in snow-ice formation. Conversely, reducing the snow cover below a certain threshold can also result in thickening of the ice cover due to less thermal resistance. Less is documented on the role of ice cover in the regional climate; however, several studies have noted the effects of increased evaporation and downwind precipitation (lake-effect snow) in the fall and winter seasons from partially ice-covered or ice-free lakes. Thermal moderation of the local/regional climate occurs in both the break-up and freeze-up seasons, with a cooling effect from ice remaining on the lake after the surrounding land has warmed, and a warming effect in the fall after the surrounding land has cooled (until the ice cover forms, stopping the turbulent exchange with the atmosphere). Including lakes and lake ice in climate modelling is an area of increased attention in recent studies. Not all RCM/NWP models parameterize lakes, though simulations that include parameterized lakes when coupled to lake models (including ice cover) have presented results that are closer to observed values.

The key findings from Chapter 3 revolve mainly around how sensitive the ice cover simulations are with respect to the on-ice snow conditions. Altering the amounts of snow cover on the ice surface to represent potential snow redistribution affected simulated freeze-up dates by a maximum of 22 days and break-up dates by a maximum of 12 days. The late season ice thickness tended to be underestimated by the simulations with break-up occurring too early, however, the evolution of the ice cover was simulated to fall between the range of the full snow and no snow scenario, with the thickness being dependent on the amount of snow cover on the ice surface. The SWIP was a useful tool for measuring the seasonal evolution of the ice thickness, and in combination with the digital camera allowed for detailed observations such as the identification of snow redistribution events, enabling a better interpretation of the model performance.

Driving CLIMo with future climate scenarios for continental-scale simulations of ice cover in the arctic areas (Chapter 4) show a projected shift in break-up and freeze-up dates from 1961-1990 to 2041-2070 for most areas ranging from 10 – 25 days earlier (break-up) and 0 – 15 days later (freeze-up). The resulting ice cover durations show mainly a 10 - 25 day reduction for the shallower lakes (3 and 10 m) and 10 – 30 day reduction for the deeper lakes (30 m). More extreme reductions of up to 60 days (excluding the loss of perennial ice cover) were shown in the coastal regions compared to the interior continental areas. Regime shifts from perennial ice cover to occasion summer ice cover to seasonally ice-free were also shown in the future predictions for the High Arctic areas. The mean maximum ice thickness was shown to decrease by 10 – 60 cm with no snow cover and 5 – 50 cm with

snow cover on the ice. Snow ice was also shown to increase through most of the study area with the exception of the Alaskan coastal areas which saw a decrease, likely as a result of the precipitation in this region occurring more frequently as rain rather than snow due to warming temperatures.

Examining the utility of remote sensing products for daily monitoring of ice cover on lakes found that both the MODIS snow cover product and IMS product are useful. While both can obtain comparable ice-off dates, MODIS outperforms IMS for ice-on due to finer resolution and the tendency towards early ice-on with IMS. The main differences between the products were a result of spatial resolution, cloud cover and different methods for assigning the ice category. The MODIS algorithm is fully automated, while the decision of whether or not lake ice is present within a pixel is at the IMS analyst's discretion based on available data. The sub-grid cell variability was typically less than 2% of the mean, although it ranged as high as 10% for some grid cells. Simulations were conducted for the ice cover throughout Quebec based on contemporary NARR data as well as future scenario data from CRCM. An indication of whether or not the simulated ice-on/off dates were within the sub-grid cell variability observed in the remote sensing products was determined based on the contemporary climate data and, on average across the entire province, were found to be within the sub-grid variability 62% of the time for ice-off and 80% of the time for ice-on. Projections for ice cover durations throughout the region show decreases of up to 50 days from the current 1981-2010 means to the 2041-2070 means, and decreases from 15 to nearly 100 days shorter between the contemporary and 2071-2100 means.

6.2 Limitations

The most prominent limitation throughout this work is the lack of in situ data for model validation. Ice cover observations exist for some locations until the early 1990s, however these locations are sparse and typically only include ice-on/off dates with few ice thickness records. Climate data to drive local-scale lake ice simulations is also sparse throughout the northern regions and typically confined to coastal and easy accessible locations. The use of remote sensing can help remedy this, however cloud cover and spatial/temporal resolution limitations exist. The use of an automated digital camera to monitor ice cover as discussed previously presents a promising solution to supplement the lost in situ monitoring network.

The use of a one-dimensional lake ice model does have some limitations with respect to the ability of capturing locally-specific spatial processes, such as additions of heat from river inflows, snow redistribution or local topographic effects (such as persistent ice cover in shade-dominated areas of a lake). The best results from ice cover simulations using CLIMo are found when using local climate data, especially when the snow conditions are well represented. Using climate model output and reanalysis data is the only realistic way to produce wide-scale simulations; however these grid cells may not always capture the local variations in the climate. Although driving lake ice models with this type of data may not always simulate the ice cover precisely for specific lakes, at the macro-scale and above some loss of detail is to be expected.

Climate projections come with their own set of inherent limitations and one must be careful to note that each projection is only one possible realization of the future climate. The use of two initially similar climate scenarios to drive the lake ice model, with rather different realizations of the climate by 2100, highlights this by the differing amounts of ice cover change they show.

6.3 Future Directions

Moving forward, an important step in improving predictions of ice conditions could be the incorporation of remote sensing data into the models, both as forcing data, and/or as an ongoing validation (adjustments) similar to how climate reanalysis data incorporates observations for continual adjustments. As forcing data, remote sensing can provide a time series of input parameters (e.g. temperature, snow conditions, albedo, cloud cover) in areas where local data is not available, or at a finer resolution than reanalysis data. The inclusion of variability from sub-grid cell lakes is also a useful benefit achieved through the use of remote sensing. A value of representativeness attached to phenology simulations allows for a better understanding of the effects of the lake morphometry present in at the sub-grid cell level.

Continued improvements to the coupling of lake/lake ice models with RCM/NWPs is needed, especially as the resolution of atmospheric models increases and more of the smaller lakes are resolved. The inclusion of lakes is important to capture the regional climate correctly, and a key factor is the correct representation of the lake surface temperature (LST). Current work involving the assimilation of MODIS-derived LST data into NWP models presents promising advances (H. Kheyrollah Pour, personal communication). Ongoing work with the CRCM version 5 also involves

the incorporation of lake ice models (Hostetler Model and FLake were tested) and the recent inclusion of lakes into the CLASS land surface scheme (Martynov et al. 2012) can lead to better surface layer representations in RCMs.

With respect to CLIMo, both the albedo parameterization and the representation of snow ice could be improved. Since the surface albedo will change depending on the snow cover or ice type (snow/black) a parameterization method that accounts for ice composition could result in a more realistic albedo (Jeffries *et al.* 2005; Morris *et al.* 2005). Incorporating remote sensing albedo data into ice cover simulations for larger lakes could be beneficial (e.g. MODIS) to capture daily changes (Svacina and Duguay, unpublished work). However, snow redistribution will also affect albedo values, so large remote sensing pixels may not offer much improvement for modelling small lakes. Rather, some empirical values based on ice composition and temperature (rather than only temperature as in the current parameterization scheme) could be used or an albedo model incorporated (Henneman and Stefan, 1999).

The results presented in chapter 3 showed the over-representation of snow ice with the full snow scenario compared to field sampling, and a full validation of snow-ice simulations has yet to take place. This work is planned for Fall 2012 and will be done using in situ measurements of ice thickness (including snow ice measurements) and from multiple locations in Finland with additional sites in Canada. Local climate station data will be used to run CLIMo, and validation of the simulated snow ice will be undertaken in a variety of different climate and snow cover conditions (e.g. colder vs. warmer snow conditions; wind swept vs. sheltered lakes).

The climate data used in this thesis was not specifically created for the arctic regions, and current work with downscaling over the pan-arctic domain is underway as part of the CORDEX (COordinated Regional climate Downscaling Experiment). This area-specific downscaling will use multiple GCMs, with newer green-house-gas emission scenarios to produce future projections. This could lead to improved ice cover simulations for the high latitude areas through the use of multiple scenarios to drive the lake ice model. As shown with the two scenarios used in this work, uncertainty in the simulated ice cover exists between the future projections, particularly in the coastal regions. The incorporation of an increased number of future projections can be used to create multiple ice cover predictions and develop a more detailed measure of uncertainty to attach to the simulations.

Multiple CORDEX pan-arctic data sets are expected to be ready for use by summer 2012 and simulations of future ice cover will then take place.

Additionally, relationships between lake ice cover and atmospheric teleconnections have been observed in the historical ice cover records. Throughout this thesis, 30-year climate normals were used for comparisons and identification of change, however, the year-to-year simulations using the climate model output data were not examined in detail. Using climate model data to produce ice cover simulations may not capture the inter-annual or inter-decadal patterns observed in the ice records as a result of atmospheric teleconnections as the various oscillations are not well represented in climate models. Future work will also focus on identifying if the observed relationships between teleconnections and ice cover are present in the modelled data, and how this may impact the ice cover simulations.

References

ACIA. 2005. Arctic Climate Impact Assessment: Cambridge University Press, New York, 1042pp.

Adams, W.P .1976a. Diversity of lake cover and its implications. *Musk-Ox* 18: 86-98.

Adams, W.P. 1976b. A classification of freshwater ice. *Musk-Ox* 18: 99 – 102.

Adams, W.P. and Jones, J.A.A.A. 1970. *Crystallography of black ice and white ice with notes on terminology*. Montreal, McGill University. McGill Sub-Arctic Research Paper 25: 161-172.

Adams, W.P. and Roulet, N.T. 1980. Illustration of the roles of snow in the evolution of the winter cover of a lake. *Arctic* 33: 100-116.

Anderson, W.L., Robertson, D.M., and Magnuson, J.J. 1996. Evidence of climatic change and projected future change. *Limnology and Oceanography* 41(5): 815-821.

Ashton, G.D. 1986. *River and lake ice engineering*. Littleton, CO: Water Resources Publications, 485p.

Assel, R.A. 1998. The 1997 ENSO event and implication for North American Laurentian Great Lakes winter severity and ice cover. *Geophysical Research Letters* 25: 1031-1033.

Assel R.A., Cronk, K. and Norton, D. 2003. Recent trends in Laurentian Great Lakes ice cover. *Climatic Change* 57: 185–204.

Assel, R.A. and Robertson, D.M. 1995. Changes in winter air temperature near Lake Michigan, 1851–1993, as determined from regional lake-ice records. *Limnology and Oceanography* 40: 165–176.

Atkinson, D., Brown, R., Alt, B., Agnew, T., Bourgeois, J., Burgess, M., Duguay, C., Henry, G., Jeffers, S., Koerner, R. , Lewkowicz, A.G., McCourt, S., Melling, H., Sharp, M., Smith, S., Walker,

A., Wilson, K., Wolfe, S., Woo, M.k. and Young, K.L. 2006. Canadian cryospheric response to an anomalous warm summer. *Atmosphere–Ocean* 44: 347−375

Austin, J.A. and Colman, S.M. 2007. Lake Superior summer water temperatures are increasing more rapidly than regional air temperatures: A positive ice-albedo feedback. *Geophysical Research Letters* Vol. 34: L06604, doi:10.1029/2006GL029021.

Balsamo, G., Salgado, R., Dutra, E., Boussetta S., and Stockdale, T. 2012. On the contribution of lakes in predicting near-surface temperature in global weather forecasting model. *Tellus A*, 64, 15829, DOI: 10.3402/tellusa.v64i0.15829.

Bates, G.T., Giorgi, F. and Hostetler, S.W. 1993. Toward the simulation of the effect of the Great Lakes on regional climate. *Monthly Weather Review* 121: 1373- 1387.

Beljaars, A.C.M., Holtslag, A.A.M., and van Westrhenen, R.M. 1989. Description of a software library for the calculation of surface fluxes. KNMI Technical Report; TR-112, Royal Netherlands Meteorological Institute (KNMI), Netherlands.

Beltaos, S., Prowse, T., Bonsal, B., MacKay, R., Romolo, L., Pietroniro, A. and Toth, B. 2006. Climatic effects on ice-jam flooding of the Peace-Athabasca Delta. *Hydrological Processes* 20: 4031–4050, DOI: 10.1002/hyp.6418.

Bengtsson, L. 1986. Spatial Variability of Lake Ice Covers. *Geografiska Annaler* 58A,1-2: 113 – 121.

Benson, B.J., Magnuson, J.J., Jacob, R.L., and Fuenger, S.L. 2000. Response of lake ice breakup in the Northern Hemisphere to the 1976 interdecadal shift in the north Pacific. *Verhandlungen der Internationalen Vereinigung fur Theoretische und Angewandte Liminologie* 27: 2770-2774.

Besonen, M.R., Patridge, W., Bradley, R.S., Francus, P., Stoner, J.S. and Abbott, M.B. 2008. A record of climate over the last millennium based on varved lake sediments from the Canadian High Arctic. *The Holocene* 18: 169-180

Bilello, M.A. 1980. Maximum thickness and subsequent decay of like, river and fast sea ice in Canada and Alaska. U.S. Army Cold Regions Research and Engineering Laboratory, Hanover, New Hampshire, CRREL, Rep.80-6.

Blenckner, T., Jarvinen, M., and Weyhenmeyer, G.A. 2004. Atmospheric circulation and its impact on ice phenology in Scandinavia. *Boreal Environment Research* 9: 371-380.

Bonsal, B. R. and Kochtubajda, B. 2009. An assessment of present and future climate in the Mackenzie Delta and the near-shore Beaufort Sea region of Canada. *International Journal of* Climatology 29: 1780–1795, DOI: 10.1002/joc.1812.

Bonsal, B.R., Prowse, T.D., Duguay, C.R., and Lacroix, M.P. 2006. Impacts of large-scale teleconnections on freshwater-ice duration over Canada. *Journal of Hydrology* 330: 340-353.

Bonsal, B.R. and Prowse, T.D. 2003. Trends and variability in spring and autumn 0°C-isotherm dates over Canada. *Climatic Change* 57: 341-358.

Brown, L.C. and Duguay, C.R. 2010. The response and role of ice cover in lake-climate interactions. *Progress in Physical Geography* 34(5):671-704.

Brown, L.C. and Duguay, C.R. 2011a. A comparison of simulated and measured lake ice thickness using a Shallow Water Ice Profiler. *Hydrological Processes* 25: 2932-2941, doi: 10.1002/hyp.8087.

Brown, L.C. and Duguay C.R. 2011b. The fate of lake ice in the North American Arctic. *The Cryosphere*, 5: 869-892, www.the-cryosphere.net/5/869/2011, doi:10.5194/tc-5-869-2011.

Brown, L., Thorne, R., and Woo, Mk. 2008. Using Satellite Imagery to Validate Simulated Snow Distribution in Large Northern Basins. *Hydrologic Processes* 22: 2777- 2787.

Brown, R.D. and Braaten, R.O. 1998. Spatial and temporal variability of Canadian monthly snow depths, 1946-1995. *Atmosphere-Ocean* 36: 37-45.

Brown, R.D. and Mote, P. 2009. The response of Northern Hemisphere snow cover to a changing climate. *Journal of Climate* 22: 2124–2145.

Brown, R.D. Analysis of snow cover variability and change in Quebec, 1948-2005. 2010. *Hydrological Processes* 24: 1929-1954.

Brown, R., Derksen, C. and Wang, L. 2010. A multi-data set analysis of variability and change in Arctic spring snow cover extent, 1967–2008. *Journal of Geophysical Research* 115: D16111, doi:10.1029/2010JD013975.

Busuioc, A., Chen , D., and Hellström, C. 2001. Temporal and spatial variability of precipitation in Sweden and its link with large scale atmospheric circulation. *Tellus* 53: 348-367.

Canadian Ice Thickness Program: http://www.ec.gc.ca/glaces-ice/default.asp?lang=En&n=E1B3129D-1, last accessed: 2010.

Caya, D. and Laprise, R. 1999. A semi-Lagrangian semi-implicit regional climate model: the Canadian RCM. *Monthly Weather Review* 127 (3): 341–362.

Chung, Y. C., Belair, S., and Mailhot, J. 2010. Simulation of Snow on Arctic Sea Ice Using a Coupled Snow–Ice Model. *Journal of Hydrometeorology* 11: 199-210.

Cole, J.J., Caraco, N.F., Kling, G.W. and Kratz, T.K. 1994. Carbon dioxide supersaturation in the surface water of lakes. *Science* 265: 1568-1570.

Cordeira, J.M. and Laird, N.F. 2008. The influence of ice cover on two lake-effect snow events over Lake Erie. *Monthly Weather Review* 139: 2747- 2763

Croley, T.E. and Assel, R.A. 1994. A one-dimensional ice thermodynamics model for the Laurentian Great Lakes. *Water Resources Research* 30: 625-639.

Croll, J. 1875. *Climate and Time in their Geological Relations, a Theory of Secular Change of the Earth's Climate*, D.Appleton and Company, New York pp. 577

Curry, J.A., Schramm, J.L. and Ebert E.E. 1993. Impact of clouds on the surface radiation budget of the Arctic Ocean. *Meteorology and Atmospheric Physics* 51: 197–217.

de Elía, R., Caya, D., Côté, H., Frignon, A., Biner, S., Giguère, M., Paquin, D., Harvey, R. and Plummer, D. 2008. Evaluation of uncertainties in the CRCM-simulated North American climate. *Climate Dynamics* 30: 113-132.

Dibike, Y., Prowse, T., Bonsal, B., de Rham, L. and Saloranta, T. 2011. Simulation of North American lake-ice cover characteristics under contemporary and future climate conditions. *International Journal of Climatology,* Article first published online: 9 FEB 2011, DOI: 10.1002/joc.2300.

Dibike, Y., Prowse, T., Saloranta, T., and Ahmed, R. 2011. Response of Northern Hemisphere lake-ice cover and lake-water thermal structure patterns to a changing climate. *Hydrological Processes* 25:2942-2953, DOI: 10.1002/hyp.8068.

Douglas, M.S.V. and Smol, J.P. 1999. Freshwater diatoms as indicators of environmental change in the High Arctic. In Stoermer, E.F. ad Smol, J.P. (eds.) *The Diatoms: Applications for the Environmental and Earth Sciences*. Cambridge, Cambridge University press: 227-244.

Duguay, C.R., Pultz, T.J., Lafleur, P.M. and Drai, D. 2002. RADARSAT backscatter characteristics of ice growing on shallow sub-arctic lakes, Churchill, Manitoba, Canada. *Hydrological Processes* 16, 1631-1644.

Duguay, C.R., Flato, G.M., Jeffires, M.O., Ménard, P., Morris, K. and Rouse, W.R. 2003. Ice-cover variability on shallow lakes at high latitudes: model simulations and observations. *Hydrological Processes* 17: 3465-3483.

Duguay, C.R., Prowse, T.D., Bonsal, B.R., Brown, R.D., Lacroix, M.P. and Ménard, P. 2006. Recent trends in Canadian lake ice cover. *Hydrological Processes* 20: 781-801.

Duguay, C.R., Pivot, F.C., Brown, R.D. and Flato, G.M. 2007. Continental-scale simulation of lake ice cover phenology, thickness and composition in Canada. CMOS-CGU-AMS Congress. St. Johns, Newfoundland, Canada, May 28 – June 1, 2007, Abstract ID: 1908.

Duguay, C.R., Macrae, M.L., Parrott, J.A., Brown, L.C. and Svacina, N. 2009. Response of shallow lakes and ponds to contemporary climate change in the Hudson Bay Lowland near Churchill, Manitoba, American Geophysical Union Fall Meeting, San Francisco, California, USA, December 14-18, 2009, C42A-03.

Duguay, C.R., Brown, L.C., Kang, K.K, Kheyrollah Pour, H. 2011. Lake Ice. In : Arctic Report Card 2011. http://www.arctic.noaa.gov/reportcard/lake_ice.html

Dyck, M.G. 2007. Community monitoring of environmental change: college-based limnological studies at Crazy Lake (Tasirluk), Nunavut. *Arctic* 60: 55-61.

Ebert, E. and Curry, J. 1993. An intermediate one-dimensional thermodynamic sea ice model for investigating ice-atmosphere interactions. *Journal of Geophysical Research* 98(C6): 10085-10109.

Eerola, K., Rontu, L., Kourzeneva, E. and Shcherbak, E. 2010. A study on effects of lake temperature and ice cover in HIRLAM. *Boreal Environment Research* 15: 130–142.

Ellis, A.W. and Johnson, J.J., 2004. Hydroclimatic analysis of snowfall trends associated with the North American Great Lakes. *Journal of Hydrometeorology* 5: 471–486.

Elo, A.R. 2006. Long-term modeling of winter ice periods for morphologically different lakes. *Nordic Hydrology* 37: 107-119.

Elo, A.R. and Vavrus, S. 2000. Ice modelling calculations, comparison of the PROBE and LIMNOS models. *Verhandlungen der Internationalen Vereinigung fur Theoretische und Angewandte Liminologie* 27: 2816-2819.

ESA, 2008: Candidate Earth Explorer Core Mission: CoReH2O – cold regions hydrology high-resolution observatory. Report for Assessment, November 2008 SP-1313/3, European Space Agency, 114p. www.esa.int.

Fang, X., Ellis, C.R. and Stefan, H.G. 1996. Simulation and observation of ice formation (freeze-over) on a lake. *Cold Regions Science and Technology* 24: 129-145.

Flato, G.M. and Brown, R.D. 1996. Variability and climate sensitivity of landfast Arctic sea ice. *Journal of Geophysical Research* 101(C10): 25767-25777.

Francus, P., Bradley, R.S., Lewis, T., Abbott, M.B., Retelle, M. and Stoner, J.S. 2008. Limnological and sedimentary processes at Sawtooth Lake, Canadian High Arctic, and their influence on varve formation. *Journal of Paleolimnology* 40: 963-985.

Frei, A. and Lee, S. 2010. A comparison of optical-band based snow extent products during spring over North America. *Remote Sensing of Environment* 114: 1940–1948.

Futter, M.N. 2003. Patterns and trends in southern Ontario lake ice phenology. *Environmental Monitoring and Assessment* 88: 431–444.

Ghanbari, R.N., Bravo, H.R., Magnuson, J.J., Hyzer, W.G. and Benson, B.J. 2009. Coherence between lake ice cover, local climate and teleconnections (Lake Mendota, Wisconsin). *Journal of Hydrology* 374: 282-293.

Gagnon, P., Konan, B., Rousseau, A.N., and Slivitzky, M. 2009. Hydrometeorological validation of a Canadian Regional Climate Model simulation within the Chaudière and Châteauguay watersheds (Québec, Canada). *Canandian Journal of Civil Engineering* 36: 253-266.

Gao, S. and Stefan, H.G. 2004. Potential climate change effects on ice covers of five freshwater lakes. *Journal of Hydrologic Engineering* 9: 226 – 234.

Gao, S. and Stefan, H.G. 1999. Multiple linear regression for lake ice and lake temperature characteristics. *Journal of Cold Region Engineering* 13: 59-77.

George, D.G. 2007. The impact of the North Atlantic Oscillation on the development of ice on Lake Windermere. *Climatic Change* 81: 455-468.

Geldsetzer, T., van der Sanden, J., and Brisco, B. 2010. Monitoring lake ice during spring melt using RADARSAT-2 SAR. *Canadian Journal of Remote Sensing*, 36 S2, S391-S400.

Goyette, S., McFarlane, N.A., and Flato, G.M. 2000. Application of the Canadian Regional Climate model to the Laurentain Great Lakes region: implementation of a lake model. *Atmosphere-Ocean* 38: 481-605.

Gerbush, M.R., Kristovich, D.A.R. and Laird, N.F. 2008. Mesoscale boundary layer and heat fluxes variations over pack-ice covered Lake Erie. *Journal of Applied Meteorology and Climatology* 47: 668-682.

Goodison, B.E. 1981. Compatibility of Canadian snowfall and snow cover data. *Water Resources Research* 17: 893-900.

Hachem, S., Allard, M., Duguay, C. 2009. Using the MODIS Land Surface Temperature Product for Mapping Permafrost: An Application to Northern Quebec and Labrador, Canada. Permafrost and Periglacial Processes 20: 407–416.

Hall, D.K., Riggs, G.A. and Salomonson, V.V. 2001. Algorithm Theoretical Basis Document (ATBD) for the MODIS Snow and Sea Ice-Mapping Algorithms. http://modis-snow-ice.gsfc.nasa.gov/atbd.html.

Hall, D.K., Riggs, G.A., Salomonson, V.V., DiGirolamo, N.E. and Bayr, K.J. 2002a. MODIS snowcover products. *Remote Sensing of Environment* 83:181–194.

Hall, D.K., Riggs, G.A. and Salomonson, V.V. 2006. Updated daily. MODIS/Terra Snow Cover Daily L3 Global 500m Grid V005, 2000 - 2011. National Snow and Ice Data Center: Boulder, CO, Digital media.

Hall, D.K. and Riggs, G.A. 2007. Accuracy assessment of the MODIS snow products. *Hydrological Processes*, 21: 1534−1547. doi:10.1002/hyp.6715.

Hall, D.K., Foster, J.L., DiGirolamo, and Riggs, G.A., Snow cover, snowmelt timing and stream power in the Wind River Range, Wyoming, *Geomorphology* 137: 87-93.

Hamilton, D.P., Spillman, C.M., Prescott, K.L., Kratz, T.K., and Magnuson, J.J. 2002. Effects of atmospheric nutrient inputs and climate change on the trophic status of Crystal Lake, Wisconsin. *Verhandlungen der Internationalen Vereinigung fur Theoretische und Angewandte Liminologie* 28: 467 – 470.

Helfrich, S.R., McNamara, D., Ramsay, B.H., Baldwin, T., and Kasheta, T. (2007). Enhancements to, and forthcoming developments in the Interactive Multisensor Snow and Ice Mapping System (IMS). *Hydrological Processes* 21: 1576−1586. doi:10.1002/HYP.6720.

Henneman, H.E. and Stefan, H.G. 1999. Albedo models for snow and ice on a freshwater lake. *Cold Regions Science and Technology* 29: 31–48.

Heron, R., Woo, Mk. 1994. Decay of a High Arctic lake-ice cover: observations and modeling. *Journal of Glaciology* 40: 283-292.

Hinzman, L.D., Bettez, N.D., Bolton, W.R., Chapin, F.S., Dyurgerov, M.B., Fastie, C.L., Griffith, B., Hollister, R.D., Hope, A., Huntington, H.P., Jensen, A.M., Jia, G.J., Jorgenson, T., Kane, D.L., Klein, D.R., Kofinas, G., Lynch, A.H., Lloyd, A.H., McGuire, A.D., Nelson, F.E., Oechel, W.C., Osterkamp, T.E., Racine, C.H., Romanovsky, V.E., Stone, R.S., Stow, D.A., Sturm, M., Tweedie,

C.E., Vourlitis, G.L., Walker, M.D., Walker, D.A., Webber, P.J., Welker, J.M., Winker, K.S. and Yoshikawa, K. 2005. Evidence and implications of recent climate change in northern Alaska and other Arctic regions. *Climatic Change* 72: 251-298.

Holland, M.M., Bitz, C.M. and Tremblay, B. 2006. Future abrupt reductions in the summer Arctic sea ice. *Geophysical Research Letters* 33: L23503, doi:10.1029/2006GL028024.

Hostetler, S.W., Bates, G.T. and Giorgi, F. 1993. Interactive coupling of a lake thermal model with a regional climate model. *Journal of Geophysical Research* 98(D3): 5045–5057.

Howell, S.E.L., Brown, L.C., Kang, K.K. and Duguay, C.R. 2009. Variability in Ice Phenology on Great Bear Lake and Great Slave Lake, Northwest Territories, from SeaWinds/QuikSCAT: 2000-2006. *Remote Sensing of Environment* 113: 816-834.

Hurrell, J.W. 1996. Influence of variations in extratropical wintertime teleconnections on Northern Hemisphere temperatures. *Geophysical Research Letters* 23: 665-668.

Huttunen, J.T., Hammar, T., Manninen, P., Servomaa, K., and Martikainen, P.J. 2001. Potential springtime greenhouse gas emissions from a small southern boreal lake (Keihäsjärvi, Finland). *Boreal Environment Research* 9: 421-427.

Huttunen, J.T., Hammar, T., Alm, J., Silvola, J. and Martikainen, P.J. 2001. Greenhouse gases in non-oxygenated and artificially oxygenated eutrophied lakes during winter stratification. *Journal of Environmental Quality* 30: 387–394.

IPCC, 2007. Chapter 10 supplementary figures: http://www.ipcc.ch/publications_and_data/ar4/wg1/en/en/chapter10/Ch10_indiv-maps.html last accessed: Sept., 2011.

Jakkila, J., Leppäranta, M., Kawamura, T., Shirasawa, K., and Salonen, K. 2009. Radiation transfer and heat budget during the ice season in Lake Pääjärvi, Finland. *Aquatic Ecology* 43: 681-692.

Jasek, M., Marko, J.R., Fissel, D., Clarke, M., Buermans,J. and Paslawski, K. 2005. In: Proceedings from the 13th Workshop on the Hydraulics of Ice-Covered Rivers (sponsored by CGU HS Committee on River Ice Processes and the Environment) Hanover, NH, 34p.

Jeffries, M.O., Morris, K. and Duguay, C.R. 2005a. Lake ice growth and decay in central Alaska, USA: observations and computer simulations compared. *Annals of Glaciology*, 40: 195-199.

Jeffries, M.O., Morris, K. and Kozlenko, N. 2005b. Ice characteristics and processes, and remote sensing of frozen rivers and lakes. In: *Remote Sensing in Northern Hydrology: measuring environmental change*. Duguay, C.R and Pietroniro (eds.), Geophysical Monograph 163, American Geophysical Union, Washington DC, USA. p 63-90.

Jeffries, M.O. and Morris, K. 2006. Instantaneous daytime conductive heat flow through snow on lake ice in Alaska. *Hydrological Processes* 20: 803-815.

Jeffries, M.O. and Morris, K. 2007. Some aspects of ice phenology on ponds in central Alaska, USA. *Annals of Glaciology* 46: 397-403.

Jeffries, M.O., Morris, K., Weeks, W.F., and Wakabayashi, H. 1994. Structural and statigraphic features and ERS1 synthetic aperture radar backscatter characteristics of ice growing on shallow lakes in NW Alaska, winter 1991-1992. *Journal of Geophysical Research* 99: 22459 – 22471.

Jensen, O.P., Benson, B.J., Magnuson, J.J., Card, V.M., Futter, M.N., Soranno, P.A. and Stewart, K.M. 2007. Spatial analysis of ice phenology trends across the Laurentian Great Lakes region during a recent warming period. *Limnology and Oceanography* 52: 2013-2026.

Johnson, S.L., and Stefan, H.G. 2006. Indicators of climate warming in Minnesota: Lake ice covers and snowmelt run off. *Climatic Change* 75: 421-453.

Kang, K.K, Duguay, C.R., Howell, S.E.L., Derksen, C.P., Kelly, R.E.J. 2010. Sensitivity of AMSR-E Brightness Temperatures to the Seasonal Evolution of Lake Ice Thickness. *IEEE Geoscience and Remote Sensing Letters* 7(4): 751-755, doi:10.1109/LGRS.2010.2044742.

Kang, K.K., Duguay C.R, Howell, S.E.L. 2012. Estimating ice phenology on large northern lakes from AMSR-E: algorithm development and application to Great Bear Lake and Great Slave Lake, Canada. *The Cryosphere* 6:235-254, doi:10.5194/tc-6-1-2012.

Karetnikov, S.G. and Naumenko, M.A. 2008. Recent trends in Lake Ladoga ice cover. *Hydrobiologia* 599: 41-48.

Kaufman, D.S., Schneider, D.P., McKay, N.P., Ammann, C.M., Bradley, R.S., Briffa, K.R., Miller, G.H., Otto-Bliesner, B.L., Overpeck, J.T., Vinther, B.M., Arctic Lakes 2k Project Members. 2009. Recent Warming Reverses Long-Term Arctic Cooling. *Science* 325: 1236, doi: 10.1126/science.1173983.

Keatley, B.E., Douglas, M.S.V. and Smol, J.P. 2008. Prolonged ice cover dampens diatom community response to recent change in high arctic lakes. *Arctic, Antarctic and Alpine Research* 40, 364-372.

Kheyrollah Pour, H., Duguay, C. R. , Martynov, A., and Brown, L. C. in press. Simulation of surface temperature and ice cover of large northern lakes with 1-D models: A comparison with MODIS satellite data and in situ measurements. *Tellus Series A: Dynamic Meteorology and Oceanography*, 64.

Knight, C.A. 1962. Studies of arctic lake ice. *Journal of Glaciology* 4: 319-336.

Korhonen, J. 2006. Long-term changes in lake ice cover in Finland. *Nordic Hydrology* 4–5: 347–363.

Kouraev, A.V., Semovski, S.V., Shimaraev, M.N., Mognard, N.M., Legrésy, B., and Rémy, F. 2007. The ice regime of Lake Baikal from historical and satellite data: Relationship to air temperature, dynamical and other factors. *Limnology and Oceanography* 52:1268-1286.

Kourzeneva, E., Asensio, H., Martin, E. and Faroux, S. 2012. Global gridded dataset of lake coverage and lake depth for use in numerical weather prediction and climate modelling. *Tellus A,* 64,15640, DOI: 10.3402/tellusa.v64i0.15640.

Kunkel, K.E., Ensor, L., Palecki, M., Easterling, D., Robinson, D., Hubbard, K.G. and Redmond, K. 2009a. A new look at lake-effect snowfall trends in the Laurentian Great Lakes using a temporally homogeneous data set. *Journal of Great Lakes Research* 35: 23-29.

Kunkel, K.E., Palecki, M., Ensor, L., Hubbard, K.G., Robinson, D., Redmond, K. and Easterling, D. 2009b. Trends in 20th Century U.S. snowfall using a quality-controlled data set. *Journal of Atmospheric and Oceanic Technology* 26: 33–44.

Latifovic, R., and Pouliot, D. 2007. Analysis of climate change impacts on lake ice phenology in Canada using the historical satellite data record. *Remote Sensing of Environment* 106: 492-507.

Kvambekk, A.S. and Melvold, K. 2010. Long-term trends in water temperature and ice cover in the subalpine lake, Øvre Heimdalsvatn, and nearby lakes and rivers. *Hydrobiologia* 642: 47–60, DOI 10.1007/s10750-010-0158-2.

Laprise, R. 2008. Regional climate modeling. *Journal of Computational Physics* 227: 3641-3666.

Latifovic, R. and Pouliot, D. 2007. Analysis of climate change impacts on lake ice phenology in Canada using the historical satellite data record. *Remote Sensing of Environment* 106: 492–507.

Launiainen, J. and Cheng, B. 1998. Modelling of ice thermodynamics in natural water bodies. *Cold Regions Science and Technology* 27: 153–178.

Lenormand, F., Duguay, C.R. and Gauthier, R. 2002. Development of a historical ice database for the study of climate change in Canada. *Hydrological Processes* 16: 3707-3722.

León, L.F., Lam, D., Schertzer, W.M. and Swayne, D.A. 2005. Lake and climate models linkage: a 3-D hydrodynamic contribution. *Advances in Geosciences* 4: 57-62.

Liston G.E, and Hall, D.K. 1995a. Sensitivity of lake freeze-up and break-up to climate change: a physically based modeling study. *Annals of Glaciology* 21: 387–393.

Livingstone, D.M. 1997. Break-up dates of alpine lakes as proxy data for local and regional mean surface air temperatures. *Climatic Change* 37: 407–439.

Livingstone, D.M. 1999. Ice break-up on southern Lake Baikal and its relationship to local and regional air temperatures in Siberia and to the North Atlantic Oscillation. *Limnology and Oceanography* 44: 1486-1497.

Livingstone, D.M. 2000. Large-scale climatic forcing detected in historical observations of lake ice break-up. *Verhandlungen der Internationalen Vereinigung fur Theoretische und Angewandte Liminologie* 27: 2775-2783.

Livingstone, D.M. and Adrian, R. 2009. Modeling the duration of intermittent ice cover on a lake for climate change studies. *Limnology and Oceanography* 54: 1709-1722.

Livingstone, D.M., Adrian, R., Blenckner, T., George, D.G. and Weyhenmeyer, G.A. 2009. Lake ice phenology. In: *The impact of climate change on European lakes*. Ed.: D. G. George. Aquatic Ecology Series. Springer: 51-61.

Lofgren, B.M. 1997. Simulated effects of idealized Laurentian Great Lakes on regional and large-scale climate. *Journal of Climate* 10: 2847-2858.

Long, Z., Perrie, W., Gyakum, J., Caya, D. and Laprise, R. 2007. Northern lake impacts on local seasonal climate. *Journal of Hydrometeorology* 8: 881-896.

MacKay, M.D., Neale, P.J., Arp, C.D., De Senerpont Domis, L.N., Fang, X., Gal, G., Jöhnk, K.D., Kirillin, G., Lenters, J. D., Litchman, E., MacIntyre, S., Marsh, P., Melack, J., Mooij, W.M., Peeters, F., Quesada, A., Schladow, S. G., Schmid, M., Spence, C., and Stokes, S.L. 2009. Modeling lakes and reservoirs in the climate system. *Limnology and Oceanography* 54: 2315-2329.

Magnuson, J.J, Robertson, D.M., Benson, B.J., Wynne, R.H., Livingstone, D.M., Arai, T., Assel, R.A., Barry, R.G., Card, V., Kuusisto, E., Granin, N.G, Prowse, T.D., Stewart, K.M. and Vuglinski, V.S. 2000. Historical trends in lake and river ice cover in the Northern Hemisphere. *Science* 289: 1743–1746. errata 2001. *Science* 291: 254.

Magnuson, J.J., Wynne, R.H., Benson, B.J. and Robertson, D.M. 2001. Lake and river ice as a powerful indicator of past and present climates. *Verhandlungen der Internationalen Vereinigung fur Theoretische und Angewandte Liminologie* 27: 2749-2756.

Magnuson, J.J., Benson, B. J., and Kratz, T. K. 2004. Patterns of coherent dynamics within and between lake districts at local to intercontinental scales. *Boreal Environment Research* 9: 359-369.

Magnuson, J.J., Benson, B.J., Jensen, O.P., Clark, T.B., Card, V., Futter, M.N., Soranno, P.A., and Stewart, K.M. 2005. Persistence of coherence of ice-off dates for inland lakes across the Laurentian Great Lakes region. *Verhandlungen der Internationalen Vereinigung fur Theoretische und Angewandte Liminologie* 29: 521-527.

Magnuson, J.J., Benson, B.J., Lenters, J.D., and Robertson, D.M. 2006. Climate driven variability and change. In: Magnuson, J.J., T.K. Kratz, and B.J. Benson, eds. *Long-Term Dynamics of Lakes in the Landscape: Long-Term Ecological Research on North Temperate Lakes*. Oxford University Press: 123-150.

Marko, J.R. and Fissel, D.B. 2006. Marine Ice profiling: future directions. In: Proceedings from ICETECH 2006, Banff, Canada, 6p.

Marko, J.R., Fissel, D.B. and Jasek, M. 2006. Recent developments in ice and water column profiling technology. In: Proceedings from the 18th IAHR Ice Symposium 2006, Sapporo Japan, 8p.

Marszelewski, W. and Skowron, R. 2006. Ice cover as in indication of winter air temperature changes: case study of the Polish Lowland lakes. *Hydrological Sciences* 51: 336-349.

Martynov, A., Sushama, L. and Laprise, R. 2010. Simulation of temperate freezing lakes by one-dimensional lake models: performance assessment for interactive coupling with regional climate models. *Boreal Environment Research* 15: 143–164.

Martynov, A., Sushama, L., Laprise, R. and Winger, K. 2012. Interactive lakes in the Canadian Regional Climate Model, version 5: the role of lakes in the regional climate of North America. *Tellus A* 2012, 64, 16226, DOI: 10.3402/tellusa.v64i0.16226.

Maykut, G.A. 1978. Energy exchange over young sea ice. *Journal of Geophysical Research* 83(C7): 3646-3658.

Maykut, G.A. and Untersteiner, N. 1971. Some results from a time-dependent thermodynamic model of sea ice. *Journal of Geophysical Research* 76: 1550-1575.

Meehl, G.A., Stocker, T.F., Collins, W.D., Friedlingstein, P., Gaye, A.T., Gregory, J.M., Kitoh, A., Knutti, R., Murphy, J.M., Noda, A., Raper, S.C.B., Watterson, I.G., Weaver, A.J. and Zhao, Z.-C.: Global Climate Projections. 2007. In: *Climate Change 2007*: The Physical Science Basis. Contribution of Working Group I to the Fourth Assessment Report of the Intergovernmental Panel on Climate Change, edited by: Solomon, S., Qin, D., Manning, M., Chen, Z., Marquis, M., Averyt, K.B., Tignor, M., Miller, H.L., Cambridge University Press: Cambridge, United Kingdom and New York, NY, USA.

Mekis, E. & Lucie A. Vincent, L. A. 2011. An Overview of the Second Generation Adjusted Daily Precipitation Dataset for Trend Analysis in Canada, *Atmosphere-Ocean*, 49(2): 163-177.

Melling, H. and Johnston, P.H. and Riedel, D.A. 1995. Measurements of the underside topography of sea ice by moored subsea sonar. *Journal of Atmospheric and Oceanic Technology* 12: 589-602.

Ménard, P., Duguay, C.R., Pivot, F.C., Flato, G.M. and Rouse, W.R. 2003. Sensitivity of Great Slave Lake ice cover to climate variability and climatic change. Proceedings of the 16th International Symposium on Ice, Dunedin, New Zealand, 2-6 December 2002, Vol. 3, pp. 57-63.

Ménard, P., Duguay, C.R., Flato, G.M., Rouse, W.R. 2002. Simulation of ice phenology on Great Slave Lake, Northwest Territories, Canada. *Hydrological Processes* 16: 3691-3706.

Ménard, P., Duguay, C.R., Pivot, F.C., Flato, G.M., Rouse, W.R. 2003. Sensitivity of Great Slave Lake ice cover to climate variability and climatic change. In: Proceedings of the 16th International Symposium on Ice. Dunedin, New Zealand, 2–6 December 2002, Volume 3: 57–63.

Michel, B., Ashton, G.D., Beltaos, S., Davar, K., Frederking, R., Gerard, R.L., Pratte, B., Tsang, G. and Williams, G.1986. Chapter 5 - Hydraulics. In Ashton, G.D. ed. *River and lake ice engineering*. Littleton, CO: Water Resources Publications: 261 – 372.

Mironov, D., Heise, E., Kourzeneva, E., Ritter, B., Schneider, N. and Terzhevik, A. 2010. Implementation of the lake parameterisation scheme FLake into the numerical weather prediction model COSMO. *Boreal Environment Research* 15: 218–230.

Mironov, D. 2008. Parameterization of lakes in numerical weather prediction, Part 1: Description of a lake model, Offenbach: Consortium for Small-scale Modeling, Technical Report 11, Deutscher Wetterdienst, Offenbach am Main, Germany, 41 pp.

Mironov, D., Heise, E., Kourzeneva, E., Ritter B. and Schneider, N. 2007. Parameterisation of lakes in numerical weather prediction and climate models. Proceedings of the 11th Workshop on Physical Processes in Natural Waters, L. Umlauf and G. Kirillin, Eds., Berichte des IGB, Vol. 25, Berlin, Germany: 101-108.

Mishra, V., Cherkauer, K.A., Bowling, L.C. and Huber, M. 2011. Lake ice phenology of small lakes: Impacts of climate variability in the Great Lakes region. *Global and Planetary Change* 76: 166-185.

Morris, K., Jeffries, M. and Duguay, C. 2005. Model simulation of the effects of climate variability and change on lake ice in central Alaska, USA. *Annals of Glaciology* 40: 113-118.

Morris, K., Jeffries, M.O. and Weeks, W.F. 1995. Ice processes and growth history on arctic and sub-Arctic lakes using ERS-1 SAR data. *Polar Record* 31: 115–128.

MSC: Canadian Snow Data CD-ROM, CRYSYS Project, Climate Processes and Earth Observation Division, Meteorological Service of Canada, Downsview, Ontario, January, 2000

Mueller, D.R., Van Hove, P., Antoniades, D., Jeffries, M.O. and Vincent, W.F. 2009. High Arctic lakes as sentinel ecosystems: Cascading regime shifts in climate, ice cover, and mixing. *Limnology and Oceanography* 54: 2371–2385.

Music, B. and Caya, D. 2007. Evaluation of the hydrological cycle over the Mississippi River Basin as simulated by the Canadian Regional Climate Model (CRCM). *Journal of Hydrometeorology* 8: 969-988.

Nagler, T., Rott, H., Heidinger, M., Malcher, P., Macelloni, G., Pettinato, S., Santi, E., Pulliainen, J., Takala, M., Malnes, E., Storvold, R., Johnsen, H., Haas, C., and Duguay, C. 2008. Retrieval of physical snow properties from SAR observations at Ku- and X-band frequencies. European Space Agency Study Contract Report, ESTEC Contract 20756/07/NL/CB, Final Report, 346 p.

National Ice Center. 2008, updated daily. IMS daily Northern Hemisphere snow and ice analysis at 4 km and 24 km resolution. Boulder, CO: National Snow and Ice Data Center. Digital media.

Norton, D.C. and Bolsegna, S.J., 1993. Spatiotemporal trends in lake effect and continental snowfall in the Laurentian Great Lakes, 1951-1980. *Journal of Climate* 6: 1943-1956.

North American Regional Climate Change Assessment Program: http://www.narccap.ucar.edu/results/crcm-cgcm3-results.html, last accessed: 2011.

Natural Resources Canada, 2010. CanVec, Canada ed. 1,1. Government of Canada, Natural Resources Canada, Earth Sciences Sector, Centre for Topographic Information: ftp://ftp2.cits.rncan.gc.ca/pub/canvec/

Palecki, M.A. and Barry, R.G. 1986. Freeze-up and break-up of lakes as an index of temperature changes during the transition seasons: a case study for Finland. *Journal of Climate and Applied Climatology* 25: 893–902.

Parajka, J and Bloschl, G. 2008. The value of MODIS snow cover data in validation and calibrating conceptual hydrologic models. *Journal of Hydrology* 358: 240-258.

Perroud, M., Goyette, S., Martynov, A., Beniston, M. and Anneville, O. 2009. Simulation of multiannual thermal profiles in deep Lake Geneva: a comparison of one-dimensional lake models. *Limnology and Oceanography* 54: 1574–1594.

Peters, D. L. and Buttle, J. M. 2010. The effects of flow regulation and climatic variability on obstructed drainage and reverse flow contribution in a northern river–lake–delta complex, Mackenzie Basin headwaters. *River Research and Applications* 26: 1065–1089.

Petrov, M.P., Terzhevik, A.Yu. Palshin, N.I., Zdorovennov, R.E. and Zdorovennova, G.E. 2005. Absorption of solar radiation by snow-and-ice cover of lakes. *Water Resources* 32: 496-504.

Plummer, D.A., Caya, D., Frigon, A., Côté, H., Giguère, M., Paquin, D., Biner, S., Harvey, R., De Elia, R. 2006. Climate and climate change over North America as simulated by the Canadian RCM. *Journal of Climate* 19: 3112–3132.

Pohl, S., Marsh, P. and Bonsal, B. R. 2007. Modeling the impact of climate change on runoff and annual water balance of an Arctic headwater basin. *Arctic* 60(2):173-186.

Prowse, T.D., Bonsal, B.R., Duguay, C.R., and Lacroix, M.P. 2007. River-ice break-up/freeze-up: A review of climatic drivers, historical trends, and future predictions. *Annals of Glaciology* 46: 443-451.

Prowse, T.D. and Beltaos, S. 2002. Climatic control of river-ice hydrology: a review. *Hydrological Processes* 16(4): 805–822.

Prudhomme, C. and Davies, H. 2009. Assessing uncertainties in climate change impact analyses on the river flow regimes in the UK, Part 2: future climate. *Climatic Change* 93: 197–222.

Räisänen, J. 2007. Warmer climate: less or more snow? *Climate Dynamics* 30: 307-319, doi:10.1007/s00382-007-0289-y.

Ramsay, B. H. 1998. The interactive multisensor snow and ice mapping system. *Hydrological Processes* 12: 1537−1546.

Reed, B., Budde, M., Spencer, P. and Miller, A.E. 2009. Integration of MODIS-derived metrics to assess interannual variability in snowpack, lake ice, and NDVI in southwest Alaska. *Remote Sensing of Environment*, 113: 1443–1452.

Reist, J. D., Wrona, F. J., Prowse, T. D., Dempson, J B., Power, M., Köck, G., Carmichael, T.J., Sawatzky, C.D., Lehtonen, H., and Tallman, R.F. 2006. Effects of climate change and UV Radiation on fisheries for Arctic freshwater and anadromous species. *Ambio* 35(7): 402-410, DOI: 10.1579/0044-7447.

Riggs, G.A., Hall, D.K., Salomonson, V.V. 2006. MODIS Snow Products User Guide to Collection 5. Available online: modis-snow-ice.gsfc.nasa.gov/uploads/sug_c5.pdf.

Robertson, D M., Wynne, R.H. and Chang, W.Y.B. 2000. Influence of El Nino on lake and river ice cover in the Northern Hemisphere from 1900 to 1995. *Verhandlungen der Internationalen Vereinigung fur Theoretische und Angewandte Liminologie* 27: 2784-2788.

Robertson, D.M, Ragotzkie, R.A., and Magnuson, J.J. 1992. Lake ice records used to detect historical and future climatic changes. *Climatic Change* 21: 407–427.

Rodinov, S., and Assel, R. 2003. Winter severity in the Great Lakes region: a tale of two oscillations. *Climate Research* 24: 19-31.

Rodinov, S., and Assel, R 2000. Atmospheric teleconnection patterns and severity of winters in the Laurentian Great Lakes Basin. *Atmosphere-Ocean* 38: 601-635.

Rouse, W.R., Blanken, P.D., Eaton, A.K, Petrone, R.M., Schertzer, W.M., and Spence, C. 2000. Energy and water balance of high latitude surfaces. MAGS: Final Reports and Proceedings, 6th Scientific Workshop for MAGS, 15-17 November, 2000, pp. 81-98.

Rouse, W.R., Oswald, C.J., Binyamin, J., Blanken, P.D., Schertzer, W.M., Spence, C. 2003. Interannual and seasonal variability of the surface energy balance and temperature of central Great Slave Lake. *Journal of Hydrometeorology* 4: 720-730.

Rouse, W.R., Blanken, P.D., Duguay, C.R., Oswald, C.J. and Schertzer, W.M. 2008a. Climate-Lake interactions. Chapter 8 in *Cold Region Atmospheric and Hydrologic Studies: The Mackenzie GEWEX Experience* Vol 2: 139-160.

Rouse, W.R., Binyamin, J., Blanker, P.D., Bussières, N., Duguay, C.R., Oswald, C.J., Schertzer, W.M. and Spence, C. 2008b. The influence of lakes on the regional energy and water balance of the central Mackenzie. Chapter 18 in *Cold Region Atmospheric and Hydrologic Studies: The Mackenzie GEWEX Experience* Vol 1: 309-325.

Roy, A., Royer, A. and Turcotte, R. 2010. Improvement of springtime streamflow simulations in a boreal environment by incorporating snow-covered area derived from remote sensing data. *Journal of Hydrology* 390: 35-44.

Saloranta, T. M. and Anderson, T. 2007. MyLake—A multi-year lake simulation model code suitable for uncertainty and sensitivity analysis simulations. *Ecological Modelling* 207: 45-60.

Samuelsson, P., Kourzeneva, E., and Mironov, D. 2010. The impact of lakes on the European climate as simulated by a regional climate model. *Boreal Environment Research* 15: 113-129.

Schertzer, W.M., Rouse, W.R., Blanken, P.D. and Walker, A.E. 2000. Over-Lake meteorology and estimated bulk heat exchange of Great Slave Lake in 1998 and 1999. *Journal of Hydrometeorology* 4: 649-659.

Schindler, D.W. Beaty, K.G., Fee, E.J., Cruikshank, D.R., DeBruyn, E.R., Findlay, D.L., Linsey, G.A., Shearer, J.A., Stainton, M.P. and Turner, M.A. 1990. Effects of climate warming on lakes of the central boreal forest. *Science* 250: 967-970.

Seidou, O., Ouarda, T.B.M.J., Bilodeau, L., Hessami, M., St-Hilaire, A. and Bruneau, P. 2006. Modelling ice growth on Canadian lakes using artificial neural networks. *Water Resources Research* 42, W11407, doi:10.1029/2005WR004622.

Serreze, M.C., Walsh, J.E., Chapin III, F., Osterkamp, T., Dyurgerov, M., Romanovsky, V., Oechel, W.C., Morison, J., Zhang, T. and Barry, R.G. 2000. Observational evidence of recent change in the northern high-latitude environment. *Climatic Change* 46: 159– 207.

Smol, J.P. 1983. Paleophycology of a High Arctic lake near Cape Herschel, Ellesmere Island. *Canadian Journal of Botany* 61: 2195–2204.

Smol, J.P. 1988. Paleoclimate proxy data from freshwater Arctic diatoms. *Verhandlungen der Internationalen Vereinigung fur Theoretische und Angewandte Liminologie* 23: 837-844.

Smol, J.P., Wolfe, A.P., Birks, H.H., Douglas, M.S.V., Jones, V., Korhola, A., Pienitz, R., Rühland, K., Sorvari, S., Antoniades, D., Brooks, S.J., Fallu, M.A., Hughes, M., Keatley, B.E., Laing, T.E., Michelutti, N., Nazarova, L., Nyman, M., Paterson, A.M., Perren, B., Quinlan, R., Rautio, M., Saulnier-Talbot, E., Siitonen, S., Solovieva, N., and Weckström, J., 2005. Climate-driven regime shifts in the biological communities of Arctic lakes. Proceedings of the National Academy of Sciences USA 102: 4397–4402

Sou, T. and Flato, G. 2009. Sea Ice in the Canadian Arctic Archipelago: Modeling the Past (1950–2004) and the Future (2041–60). *Journal of Climate* 22: 2181-2198.

Stefan, H.G. and Fang, X. 1997. Simulated climate change effects on ice and snow covers on lakes in a temperate region. *Cold Regions Science and Technology* 25: 137-152.

Stepanenko, V.M., Goyette, S., Martynov, A., Perroud, M., Fang, X. and Mironov, D. 2010. First steps of a Lake Model Intercomparison Project: LakeMIP. *Boreal Environment Research* 15: 191–202.

Stephenson, S.R., Smith, L.C. and Agnew, J.A. 2011. Divergent long-term trajectories of human access to the Arctic. *Nature Climate Change* 1: 156-160, doi:10.1038/NCLIMATE1120.

Stewart, K.M. and Magnuson, J.J. 2009. Ice. G. Likens [ed*.] Encyclopedia of Inland waters*. Elsivier, p. 664 – 670.

Striegl, R.G., Kortelainen, P., Chanton, J.P., Wickland, K.P., Bugna, G.C., and Rantakari, M. 2001. Carbon dioxide partial pressure and 13C content of north temperate and boreal lakes at spring ice melt. *Limnology and Oceanography* 46: 941-945.

Sturm , M., Holmgren, J., König, M. and Morris, K. 1997. The thermal conductivity of seasonal snow. *Journal of Glaciology* 43: 26–41.

Sturm, M. and Liston, G.E. 2003. The snow cover on lakes of the Arctic Coastal Plain of Alaska, U.S.A. *Journal of Glaciology* 49(166): 370-380.

Swayne, D., Lam, D., MacKay, M., Rouse, W. and Schertzer, W. 2005. Assessment of the interaction between the Canadian Regional Climate Model and lake thermal-hydrodynamic models. *Environmental Modelling & Software* 20: 1505-1513.

Thorne, R. 2011. Uncertainty in the impacts of projected climate change on the hydrology of a subarctic environment: Liard River Basin. *Hydrological Earth Systems Science* 15: 1483-1492, doi:10.5194/hess-15-1483-2011.

Tomkins, J.D., Lamoureux, S.F., Antoniades, D., and Vincent, W.F. 2009. Sedimentary pellets as an ice-cover proxy in a High Arctic ice-covered lake. *Journal of Paleolimnology* 41: 225-242.

Vavrus, S.J., Wynne, R.H. and Foley, J.A. 1996. Measuring the sensitivity of southern Wisconsin lake ice to climate variations and lake depth using a numerical model. *Limnology and Oceanography* 41: 822-831.

Verseghy, D. L. 1991. CLASS – A Canadian land surface scheme for GCMs. Part I: Soil model. *International Journal of Climatology* 11(2): 111–133.

Verseghy, D. L., McFarlane, N. A., and Lazare, M. 1993. CLASS – A Canadian land surface scheme for GCMs. Part II: Vegetation model and coupled runs. *International Journal of Climatology* 13(4): 347–370.

Vincent, L. A. 1998. A technique for the identification of inhomogeneities in Canadian temperature series. *Journal of Climate* 11: 1094–1104.

Vincent, L. A., and Gullet, D. W. 1999. Canadian historical and homogeneous temperature datasets for climate change analyses. *International Journal of Climatology* 19: 1375–1388.

Vincent, L. A., Zhang, X., Bonsal, B. R. and Hogg, W. D. 2002. Homogenization of daily temperatures over Canada. *Journal of Climate* 15: 1322-1334.

Vincent, L. A., van Wijngaarden, W. A., and Hopkinson, R. Surface temperature and humidity trends in Canada for 1953-2005. Journal of Climate, 20: 5100 - 5113. DOI: 10.1175/JCLI4293.1.

Walsh, S.E, Vavrus, S.J., Foley, J.A., Fisher, V.A., Wynne, R.H. and Lenters, J.D. 1998. Global pattern of lake ice phenology and climate: model simulation and observations. *Journal of Geophysical Research* 103(D22): 28825–28837.

Walter, K.M., Zimov, S.A., Chanton, J.P., Verbyla, D. and Chapin III, F.S. 2006. Methane bubbling from Siberian thaw lakes as a positive feedback to climate warming. *Nature* 443:71-75.

Walter, K.M., Smith L.C., Chapin III, F.S. 2007. Methane bubbling from northern lakes: present and future contributions to the global methane budget. *Philosophical Transactions of the Royal Society A* 365: 1657–1676.

Walter, K.M., Engram, M., Duguay, C.R., Jeffries, M.O., Chaplin III, F.S. 2008. The potential use of synthetic aperture radar for estimating methane ebullition from arctic lakes. *Journal of the American Water Resources Association* 44: 305-315.

Wang, X. and Key, J.R., 2005. Arctic surface, cloud, and radiation properties based on the AVHRR Polar Pathfinder dataset. Part I: spatial and temporal characteristics. *Journal of Climate* 18: 2558–2574.

Weyhenmeyer, G.A., Meili, A.M. and Livingstone, D.M. 2004. Nonlinear temperature response of lake ice breakup. *Geophysical Research Letters* 31:L07203 doi:10.1029/2004GL019530.

Williams, G.P. 1965. Correlating freeze-up and break-up with weather conditions. *Canadian Geotechnical Journal* 2: 313-326.

Williams, G., Layman, K.L. and Stefan, H.G. 2004. Dependence of lake ice covers on climatic, geographic and bathymetric variables. *Cold Regions Science and Technology* 40, 145– 164.

Williams, S.G. and Stefan, H.G. 2006. Modeling of lake ice characteristics in North America using climate, geography, and lake bathymetry. *Journal of Cold Regions Engineering* 20: 140-167.

Weyhenmeyer, G.A., Livingstone, D.M., Meili, M., Jensen, O., Benson, B. and Magnuson, J.J. 2010. Large geographical differences in the sensitivity of ice-covered lakes and rivers in the Northern Hemisphere to temperature changes. *Global Change Biology* 17:268-275, doi: 10.1111/j.1365-2486.2010.02249.x.

Woo, M.K. and Heron, R. 1989. Freeze-up and break-up of ice cover on small arctic lakes. In *Northern Lakes and Rivers*. Mackay WC (ed.), Boreal Institute for Northern Studies Occasional Publication 22, Edmonton: 56–62.

Woo, M.K., Thorne, R., Szeto, K. and Yang, D. 2008. Streamflow hydrology in the boreal region under the influences of climate and human interference, *Philosophical Transactions of the Royal Society B*, 363: 2251–2260, doi:10.1098/rstb.2007.2197.

Woo, M.K. 2012. *Permafrost Hydrology*. Springer, 575p.

Wynne, R.H. and Lillesand, T.M. 1993. Satellite observation of lake ice as a climate indicator: initial results from statewide monitoring in Wisconsin. *Photogrammetric Engineering and Remote Sensing* 59: 1023-31.

Wynne, R.H., Magnuson, J.J., Clayton, M.K., Lillesand, T.M., and Rodman, D.C. 1996. Determinants of temporal coherence in the satellite-derived 1987-1994 ice breakup dates of lakes on the Laurentian Shield. *Limnology and Oceanography* 41: 832-838.

Zaier, I., Shu, C., Ouarda, T.B.M.J., Seidou, O. and Chebana, F. 2010. Estimation of ice thickness on lakes using artificial neural network ensembles. *Journal of Hydrology* 383: 330-340.

Zhang, X., Zwiers, F. W., Hegerl, G. C., Lambert, F. H., Gillett, N. P., Solomon, S., Stott, P. A. and Nozawa, T. 2007. Detection of human influence on twentieth-century precipitation trends. *Nature*, 448: 461-466, doi:10.1038/nature06025.